

Advances

in Clinical and Experimental Medicine

MONTHLY ISSN 1899-5276 (PRINT) ISSN 2451-2680 (ONLINE)

advances.umw.edu.pl

2024, Vol. 33, No. 2 (February)

Impact Factor (IF) – 2.1
Ministry of Science and Higher Education – 70 pts
Index Copernicus (ICV) – 161.11 pts



WROCLAW
MEDICAL UNIVERSITY

Advances
in Clinical and Experimental
Medicine



Advances in Clinical and Experimental Medicine

ISSN 1899-5276 (PRINT)

ISSN 2451-2680 (ONLINE)

advances.umw.edu.pl

MONTHLY 2024
Vol. 33, No. 2
(February)

Advances in Clinical and Experimental Medicine (*Adv Clin Exp Med*) publishes high-quality original articles, research-in-progress, research letters and systematic reviews and meta-analyses of recognized scientists that deal with all clinical and experimental medicine.

Editorial Office

ul. Marcinkowskiego 2–6
50-368 Wrocław, Poland
Tel.: +48 71 784 12 05
E-mail: redakcja@umw.edu.pl

Editor-in-Chief

Prof. Donata Kurpas

Deputy Editor

Prof. Wojciech Kosmala

Managing Editor

Marek Misiak, MA

Statistical Editors

Wojciech Bombała, MSc

Łucja Janek, MSc

Anna Kopszak, MSc

Dr. Krzysztof Kujawa

Jakub Wronowicz, MSc

Manuscript editing

Marek Misiak, MA

Paulina Piątkowska, MA

Jolanta Prazeres, MA

Publisher

Wrocław Medical University
Wybrzeże L. Pasteura 1
50-367 Wrocław, Poland

Online edition is the original version
of the journal

Scientific Committee

Prof. Sandra Maria Barbalho

Prof. Antonio Cano

Prof. Chong Chen

Prof. Breno Diniz

Prof. Erwan Donal

Prof. Chris Fox

Prof. Yuko Hakamata

Prof. Carol Holland

Prof. Sabine Bährer-Kohler

Prof. Markku Kurkinen

Prof. Christos Lionis

Prof. Raimundo Mateos

Prof. Zbigniew W. Raś

Prof. Jerzy W. Rozenblit

Prof. Silvina Santana

Prof. Sajee Sattayut

Prof. James Sharman

Prof. Jamil Shibli

Prof. Michał J. Toborek

Prof. László Vécsei

Prof. Cristiana Vitale

Prof. Hao Zhang

Section Editors

Basic Sciences

Prof. Iwona Bil-Lula

Prof. Bartosz Kempisty

Dr. Wiesława Kranc

Dr. Anna Lebedeva

Clinical Anatomy, Legal Medicine, Innovative Technologies

Prof. Rafael Boscolo-Berto

Dentistry

Prof. Marzena Dominiak

Prof. Tomasz Gedrange

Prof. Jamil Shibli

Laser Dentistry

Assoc. Prof. Kinga Grzech-Leśniak

Dermatology

Prof. Jacek Szepietowski

Emergency Medicine, Innovative Technologies

Prof. Jacek Smereka

Gynecology and Obstetrics

Prof. Olimpia Sipak-Szmigiel

Histology and Embryology

Dr. Mateusz Olbromski

Internal Medicine

Angiology

Dr. Angelika Chachaj

Cardiology

Prof. Wojciech Kosmala

Dr. Daniel Morris

Endocrinology

Prof. Marek Bolanowski

Gastroenterology

Assoc. Prof. Katarzyna Neubauer

Hematology

Prof. Andrzej Deptała
Prof. Dariusz Wołowicz

Nephrology and Transplantology

Assoc. Prof. Dorota Kamińska
Prof. Krzysztof Letachowicz

Pulmonology

Prof. Anna Brzecka

Microbiology

Prof. Marzenna Bartoszewicz
Assoc. Prof. Adam Junka

Molecular Biology

Dr. Monika Bielecka

Prof. Jolanta Saczko

Neurology

Assoc. Prof. Magdalena Koszewicz
Assoc. Prof. Anna Pokryszko-Dragan

Dr. Masaru Tanaka

Neuroscience

Dr. Simone Battaglia
Dr. Francesco Di Gregorio

Oncology

Prof. Andrzej Deptała
Prof. Adam Maciejczyk

Gynecological Oncology

Dr. Marcin Jędryka

Ophthalmology

Dr. Małgorzata Gajdzis

Orthopedics

Prof. Paweł Reichert

Otolaryngology

Assoc. Prof. Tomasz Zatoński

Pediatrics

Pediatrics, Metabolic Pediatrics, Clinical Genetics, Neonatology, Rare Disorders

Prof. Robert Śmigiel

Pediatric Nephrology

Prof. Katarzyna Kiliś-Pstrusińska

Pediatric Oncology and Hematology

Assoc. Prof. Marek Ussowicz

Pharmaceutical Sciences

Assoc. Prof. Marta Kepińska
Prof. Adam Matkowski

Pharmacoeconomics, Rheumatology

Dr. Sylwia Szafraniec-Buryło

Psychiatry

Dr. Melike Küçükkarapınar
Prof. Jerzy Leszek
Assoc. Prof. Bartłomiej Stańczykiewicz

Public Health

Prof. Monika Sawhney
Prof. Izabella Uchmanowicz

Qualitative Studies, Quality of Care

Prof. Ludmiła Marcinowicz

Radiology

Prof. Marek Szaśiadek

Rehabilitation

Dr. Elżbieta Rajkowska-Labon

Surgery

Assoc. Prof. Mariusz Chabowski
Assoc. Prof. Mirosław Kozłowski
Prof. Renata Taboła

Telemedicine, Geriatrics, Multimorbidity

Assoc. Prof. Maria Magdalena
Bujnowska-Fedak

Editorial Policy

Advances in Clinical and Experimental Medicine (Adv Clin Exp Med) is an independent multidisciplinary forum for exchange of scientific and clinical information, publishing original research and news encompassing all aspects of medicine, including molecular biology, biochemistry, genetics, biotechnology and other areas. During the review process, the Editorial Board conforms to the "Uniform Requirements for Manuscripts Submitted to Biomedical Journals: Writing and Editing for Biomedical Publication" approved by the International Committee of Medical Journal Editors (www.ICMJE.org). The journal publishes (in English only) original papers and reviews. Short works considered original, novel and significant are given priority. Experimental studies must include a statement that the experimental protocol and informed consent procedure were in compliance with the Helsinki Convention and were approved by an ethics committee.

For all subscription-related queries please contact our Editorial Office: redakcja@umw.edu.pl

For more information visit the journal's website: advances.umw.edu.pl

Pursuant to the ordinance of the Rector of Wrocław Medical University No. 12/XVI R/2023, from February 1, 2023, authors are required to pay a fee for each manuscript accepted for publication in the journal Advances in Clinical and Experimental Medicine. The fee amounts to 990 EUR for original papers and meta-analyses, 700 EUR for reviews, and 350 EUR for research-in-progress (RIP) papers and research letters.

Advances in Clinical and Experimental Medicine has received financial support from the resources of Ministry of Science and Higher Education within the "Social Responsibility of Science – Support for Academic Publishing" project based on agreement No. RCN/SP/0584/2021.



Ministry of Education and Science
Republic of Poland

Czasopismo Advances in Clinical and Experimental Medicine korzysta ze wsparcia finansowego ze środków Ministerstwa Edukacji i Nauki w ramach programu „Społeczna Odpowiedzialność Nauki – Rozwój Czasopism Naukowych” na podstawie umowy nr RCN/SP/0584/2021.



Ministerstwo
Edukacji i Nauki

Indexed in: MEDLINE, Science Citation Index Expanded, Journal Citation Reports/Science Edition, Scopus, EMBASE/Excerpta Medica, Ulrich's™ International Periodicals Directory, Index Copernicus

Typographic design: Piotr Gil, Monika Kołęda

DTP: Wydawnictwo UMW

Cover: Monika Kołęda

Printing and binding: PRINT PROFIT Sp. z o.o., Koźmin 27, 59-900 Żgorzelec

Contents

Original papers

- 103 Hongji Cheng, Weijun Huang, Xiaohui Huang, Wang Miao, Yuli Huang, Yunzhao Hu
The triglyceride glucose index predicts short-term mortality in non-diabetic patients with acute heart failure
- 111 Handan Duman, Hakan Duman, Meltem Puşuroğlu, Ahmet Seyda Yılmaz
Anxiety disorders and depression are associated with resistant hypertension
- 119 Krzysztof Cieślak, Anna Rogowska, Małgorzata Danowska, Wojciech Hautz
Efficacy of intravitreal injections of melphalan in the treatment of retinoblastoma vitreous seeding
- 127 Kajetan Karaszewski, Marcin Jasiński, Anna Waszczuk-Gajda, Anna Rodziewicz-Lurzyńska, Olga Ciepela, Wiesław Wiktor Jędrzejczak
Oligoclonal gammopathy: An analysis of 253 cases
- 135 Bartosz Radosław Wnuk, Damian Ziąja, Michał Buczek, Krzysztof Ziąja, Marcin Banyś
Effect of passive ankle movement in the sitting position on the symptoms of chronic venous insufficiency with long-term observation
- 143 Katarzyna Resler, Anna Oleszkiewicz, Marcin Frączek, Monika Morawska-Kochman, Anna Resler, Tomasz Zatoński, Thomas Hummel
Olfaction-associated quality of life: Polish adaptation and validation of a Questionnaire of Olfactory Disorders (QOD-PL) in patients with chronic rhinosinusitis
- 151 Ying Lin, Ya-Qiong Liu, Ke-An Zhu, Meng-Qi Hu, Zhao Li, Xiao-Jia Min
Tasquinimod enhances the sensitivity of ovarian cancer cells to cisplatin by regulating the Nur77-Bcl-2 apoptotic pathway
- 163 Weiwei Wang, Dan Ming
Oridonin attenuates apoptosis and NLRP3 inflammasome activation in IL-4-stimulated human bronchial epithelial cells in an in vitro pediatric asthma model
- 171 Ming Li, Zhao Huang, Yuxiang Zhou
Serabelisib regulates GSDMD-mediated pyroptosis, apoptosis and migration of hepatoma cells via the PI3K/Akt/E-cadherin signaling pathway

Reviews

- 183 Aleksandra Janecka, Joanna Stefanowicz
Use of salusin β for predicting atherosclerosis and components of the metabolic syndrome

The triglyceride glucose index predicts short-term mortality in non-diabetic patients with acute heart failure

Hongji Cheng^{1,2,D}, Weijun Huang^{1,A}, Xiaohui Huang^{1,B}, Wang Miao^{1,C}, Yuli Huang^{1,E}, Yunzhao Hu^{1,F}

¹ Department of Cardiology, Shunde Hospital, Southern Medical University (The First People's Hospital of Shunde), Foshan, China

² Department of Cardiology, Panyu District He Xian Memorial Hospital, Guangzhou, China

A – research concept and design; B – collection and/or assembly of data; C – data analysis and interpretation;

D – writing the article; E – critical revision of the article; F – final approval of the article

Advances in Clinical and Experimental Medicine, ISSN 1899–5276 (print), ISSN 2451–2680 (online)

Adv Clin Exp Med. 2024;33(2):103–110

Address for correspondence

Yunzhao Hu

E-mail: huyunzhao4406@163.com

Funding sources

This study was supported by the Science and Technology Innovation Project from Foshan, Guangdong (grant No. FS0AA-KJ218-1301-0006 and No. FS0AA-KJ218-1301-0010) and by Panyu District Key Discipline (Specialty) Medical and Health Project (grant No. 2021-Z04-008).

Conflict of interest

None declared

Received on February 28, 2023

Reviewed on April 23, 2023

Accepted on May 9, 2023

Published online on June 16, 2023

Cite as

Cheng H, Huang W, Huang X, Miao W, Huang Y, Hu Y.

The triglyceride glucose index predicts short-term mortality in non-diabetic patients with acute heart failure.

Adv Clin Exp Med. 2024;33(2):103–110.

doi:10.17219/acem/166043

DOI

10.17219/acem/166043

Copyright

Copyright by Author(s)

This is an article distributed under the terms of the Creative Commons Attribution 3.0 Unported (CC BY 3.0)

(<https://creativecommons.org/licenses/by/3.0/>)

Abstract

Background. The triglyceride glucose index (TyG) has previously been considered a reliable indicator of insulin resistance (IR) and an independent prognostic predictor in heart failure (HF).

Objectives. To clarify the association between the TyG and short-term death in non-diabetic patients admitted for acute heart failure (AHF).

Materials and methods. We examined 886 out of 1620 consecutive AHF patients who were admitted to Shunde Hospital, Southern Medical University, Foshan, China, from June 1, 2014, to June 1, 2022. The median of the patients' TyG values was used to divide them into 2 groups. The following formula was used to calculate the TyG: \ln [fasting triglycerides (mg/dL) \times fasting glucose (mg/dL)/2]. The data on all-cause mortality of AHF patients during their hospital stay were collected. The 30-day Enhanced Feedback for Effective Cardiac Treatment (EFFECT) death risk score was used to assess the risk of death.

Results. The TyG level was positively correlated with a poor AHF prognostic marker (N-terminal B-type natriuretic peptide (NT-proBNP)) ($p = 0.207$, $p < 0.001$) and negatively correlated with a protective marker (serum albumin) ($p = -0.43$, $p < 0.001$). Higher TyG values were associated with an elevated EFFECT score and hospital mortality ($p < 0.001$). According to multivariate logistic regression analysis, higher TyG levels raised the risk of death in hospital (odds ratio (OR) = 1.73; 95% confidence interval (95% CI): 1.03–3.27; $p = 0.031$) after adjusting for multiple variables, including age, EFFECT score and NT-proBNP. The TyG had a greater area under the receiver operating characteristic (ROC) curve (AUC: 0.688) for predicting hospital death compared to NT-proBNP (AUC: 0.506).

Conclusions. Our findings show that the TyG is associated with the short-term mortality rate of non-diabetic patients admitted to the hospital for AHF. The TyG testing could be a useful prognostic indicator for these patients.

Key words: acute heart failure, all-cause mortality, triglyceride glucose index, non-diabetics, prognostic value

Background

Acute heart failure (AHF) is a severe form of cardiovascular disease with a high mortality rate. Short-term mortality rates in clinical research patients vary from 12% to 18%.^{1–4} To improve the effectiveness and safety of clinical decision-making, multivariate risk models using demographic information, visible symptoms and lab testing have been found to estimate the risk of AHF mortality.^{5–8} Identifying AHF indicators for risk prediction and medical guidance may enhance AHF treatment overall.

It is recognized that insulin resistance (IR) and cardiac incidents in non-diabetics are associated.⁹ Heart failure (HF) can either trigger new-onset IR or worsen a pre-existing one.^{10,11} It is generally believed that neurohormonal alterations, elevated oxygen consumption and fundamental muscular tissue alterations in HF may reduce the efficiency of insulin in promoting glucose uptake and utilization, so these deviations may be related to IR.^{12–15} However, the relationship between IR and short-term prognosis has yet to be investigated in non-diabetic patients with AHF.

The triglyceride glucose index (TyG) has previously been considered a straightforward and dependable method for IR measurement.^{12,16,17} Numerous investigations have demonstrated that the TyG is more effective than the Homeostasis Model Assessment of IR (HOMA-IR) test.^{13–15} The incidence of hypertension (HTN), arterial atherosclerosis, cardiac arterial disease, and various cardiac disorders are all closely related to the TyG.^{18–22} Furthermore, the TyG is a trustworthy and practical indicator of a poor prognosis in individuals with cardiac illnesses.^{23–25}

Objectives

We conducted a retrospective cohort study to ascertain the connection between the TyG and short-term prognosis in AHF patients without diabetes.

Materials and methods

Study design and participants

A total of 1620 consecutive AHF patients admitted to Shunde Hospital, Southern Medical University, Foshan, China, from June 1, 2014, to June 1, 2022, were considered for inclusion in the study. Acute heart failure was defined according to the 2021 European Society of Cardiology (ESC) Guidelines.²⁶ A total of 734 of the 1620 patients were excluded because they met one or more exclusion criteria, such as: 1) diabetes; 2) acute coronary syndrome; 3) age <18 years; 4) lost to follow-up; and 5) lack of data upon admission. Thus, this investigation ultimately included 886 patients (Fig. 1). The research was carried out in accordance with the Declaration of Helsinki and with the permission

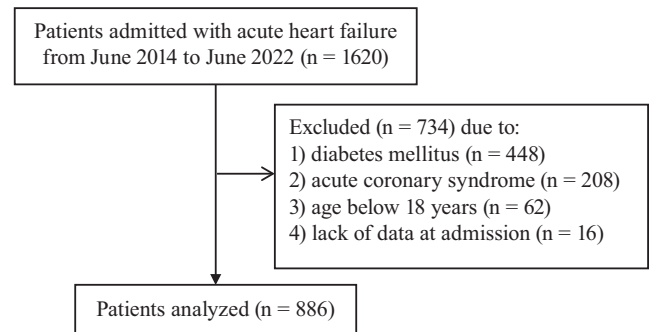


Fig. 1. Flowchart of patient selection

of Shunde Hospital, Southern Medical University (approval No. 20190906). All study participants were provided with information about the study and signed relevant consent forms.

Setting and variables

The electronic health record system was used to collect patient demographic data, health history, lab testing results, and echocardiographic metrics. In addition, we collected the medication status of patients upon admission, including vasoactive drugs (norepinephrine, phentolamine, dopamine, dobutamine, and nitroglycerin), angiotensin-converting enzyme inhibitors/angiotensin receptor antagonists (i.e., renin–angiotensin system inhibitors (RASIs)), β -blockers, statins, diuretics, and mineralocorticoid receptor antagonists (MRAs). Moreover, we collected compliance with recommended doses of RASIs, β -blockers and MRAs at discharge.

After overnight fasting (>8 h) at admission, the first sample of peripheral venous blood was drawn and measured in the lab. Hypertension was defined as systolic blood pressure (SBP) higher than 140 mm Hg and/or diastolic blood pressure (DBP) higher than 90 mm Hg, the use of any antihypertensive therapy, or previously diagnosed HTN.

N-terminal B-type natriuretic peptide (NT-proBNP), hemoglobin A1c (HbA1c), total cholesterol (TC), glucose, C-reactive protein (CRP), creatinine, blood urea nitrogen (BUN), serum sodium (Na), hemoglobin (Hb), triglycerides (TG), serum albumin, low-density lipoprotein cholesterol (LDL-C), alanine aminotransferase (ALT), aspartate transaminase (AST), serum bilirubin, lactate, high sensitivity cardiac troponin (hs-cTn), and gamma-glutamyl transpeptidase (GGT) were measured.

Data sources and measurements

Estimated glomerular filtration rate (eGFR) levels were calculated using the Chronic Kidney Disease Epidemiology Cooperation (CKD-EPI) algorithm.²⁷ The Enhanced Feedback for Effective Cardiac Treatment (EFFECT) mortality risk score was used to calculate the risk of death. This risk prediction method is meant for patients who present with HF

in a hospital setting, and it can stratify the risk within hours of hospital presentation. Risk scores are divided into 5 categories: extremely low risk (≤ 60), low risk (61–90), moderate risk (91–120), high risk (121–150), and very high risk (>150).⁸ The following formula was used to calculate the TyG: \ln [fasting triglyceride (mg/dL) \times fasting plasma glucose (mg/dL)/2].

Bias management

In order to avoid the potential of diabetes mellitus (DM) contributing to bias in the results, we routinely performed oral glucose tolerance tests (OGTTs) in patients with a predisposition to DM; OGTT results or a self-reported history of DM were used to identify DM.

Statistical analyses

The mean \pm standard deviation (M \pm SD) and median (Me) (interquartile range (IQR)) of continuous variables with normal and skewed distributions, respectively, were determined. Categorical variables were expressed using numbers.

According to the median of the TyG, patients were divided into 2 groups: D1: low-TyG group (TyG ≤ 9.44) and D2: high-TyG group (TyG > 9.44). Among the 2 groups, continuous variables were compared using analysis of variance (ANOVA) or the Kruskal–Wallis test. The χ^2 test was used to compare categorical variables among the groups.

To evaluate the connections between the 2 variables, Spearman’s correlation coefficient (ρ) was used. To examine the link between the TyG and in-hospital mortality, variables were selected using the univariate analysis accompanied by multivariate logistic regression models. With a variance inflation factor cutoff of 10, the multicollinearity of multivariate models was examined. The adjusted variables were chosen in an “enter” fashion for

the various multivariate models according to the single-factor analysis results and clinical parameters, including age, cardiogenic shock, atrial fibrillation (AF), use of vasoactive drugs, HF etiologies (including coronary heart disease (CHD), hypertensive heart disease, any cardiomyopathy, and any valvular heart disease), chronic obstructive pulmonary disease (COPD), HbA1c, NT-proBNP, and EFFECT score. Four multivariable regression models remained in the end: Model 1 – age; Model 2 – age adjustment in addition to the comorbidities of cardiogenic shock, AF, COPD, and the use of vasoactive drugs; Model 3 – adjustment for variables involved in Model 2 + HF etiologies, including CHD, hypertensive heart disease, any cardiomyopathy, and any valvular heart disease; Model 4 – adjustment for variables involved in Model 3 + HbA1c, EFFECT score, NT-proBNP, ALT, serum bilirubin, and hs-cTn. Finally, an additional model (Model 5) was constructed, adjusted for all the variables that differed between the groups, as shown in Table 1. Additionally, we calculated odds ratios (ORs) and 95% confidence intervals (95% CIs). A receiver operating characteristic (ROC) curve was drawn to show the predictive value of TyG on mortality. The area under the ROC curve (AUC) was determined through calculations.

All data were analyzed using IBM SPSS Statistics for Windows v. 26.0 (IBM Corp., Armonk, USA). A p-value <0.05 was used to indicate statistical significance.

Results

General characteristics of the patients

A total of 886 AHF candidate patients from an initial sample of 1620 were included in the research. Table 1 shows the participants’ baseline information after being

Table 1. Baseline characteristics according to TyG group

Categories	Overall (n = 886)	D1 (lower TyG) (n = 443, TyG ≤ 9.44)	D2 (higher TyG) (n = 443, TyG > 9.44)	p-value
Age, Me (P ₂₅ , P ₇₅) [years]	71.0 (58.0, 78.0)	68.0 (55.0, 78.0)	73.0 (61.5, 78.0)	0.003
Male sex, n (%)	492 (55.5)	244 (55.1)	248 (56)	0.787
Smoking, n (%)	292 (33.0)	151 (34.1)	141 (31.8)	0.475
Vital signs				
SBP, Me (P ₂₅ , P ₇₅) [mm Hg]	146.0 (123.0, 166.0)	145.0 (122.0, 165.0)	147.0 (124.0, 167.0)	0.507
DBP, Me (P ₂₅ , P ₇₅) [mm Hg]	86.0 (75.2, 97.0)	87.0 (76.0, 96.5)	85.0 (75.0, 98.0)	0.629
HR, Me (P ₂₅ , P ₇₅) [bpm]	96.0 (84.0, 113.8)	96.0 (87.0, 114.5)	96.0 (80.0, 112.0)	0.078
Cardiogenic shock, n (%)	70 (7.9)	20 (4.5)	50 (11.3)	<0.001
Heart failure etiology				
CHD	518 (58.5)	257 (58)	261 (58.9)	0.785
Hypertensive heart disease	357 (40.3)	180 (40.6)	177 (40)	0.837
Any cardiomyopathy	193 (21.8)	93 (21)	100 (22.6)	0.569
Any valvular heart disease	245 (27.7)	111 (25.1)	134 (30.2)	0.084

Table 1. Baseline characteristics according to TyG group – cont.

Categories	Overall (n = 886)	D1 (lower TyG) (n = 443, TyG ≤ 9.44)	D2 (higher TyG) (n = 443, TyG > 9.44)	p-value
Laboratory tests				
Glucose, M ±SD [mmol/L]	8.5 ±2.3	6.6 ±1.2	10.4 ±1.3	<0.001
eGFR, Me (P ₂₅ , P ₇₅) [mL/min/1.73 m ²]	94.0 (73.0, 108.0)	92.5 (73.2, 105.8)	95.4 (72.9, 109.8)	0.422
NT-proBNP, Me (P ₂₅ , P ₇₅) [pg/mL]	1362 (734, 4924)	1089 (695, 4725)	1852 (857, 5017)	0.003
CRP, Me (P ₂₅ , P ₇₅) [mg/L]	39.6 (18.8, 58.0)	40.7 (20.1, 48.0)	39.4 (15.4, 68.9)	0.518
Serum albumin, Me (P ₂₅ , P ₇₅) [g/L]	35.0 (28.0, 39.0)	39.0 (37.0, 45.0)	28.0 (28.0, 32.0)	<0.001
TC, Me (P ₂₅ , P ₇₅) [mmol/L]	3.5 (2.4, 4.1)	2.4 (1.9, 3.0)	4.1 (3.8, 4.2)	<0.001
TG, Me (P ₂₅ , P ₇₅) [mmol/L]	1.8 (1.1, 4.4)	1.1 (0.8, 1.2)	4.5 (3.0, 5.5)	<0.001
LDL-C, M ±SD [mmol/L]	2.1 ±0.9	1.5 ±0.6	2.8 ±0.5	<0.001
BUN, Me (P ₂₅ , P ₇₅) [mmol/L]	12.6 (5.9, 22.2)	12.7 (6.2, 21.5)	12.5 (4.8, 22.9)	0.38
Na, Me (P ₂₅ , P ₇₅) [mmol/L]	138 (135, 141)	138 (135, 141)	138.4 (135.4, 141.0)	0.811
Hb, Me (P ₂₅ , P ₇₅) [g/L]	95.5 (80.0, 117.0)	94.0 (83.0, 117.0)	97.0 (79.0, 117.0)	0.898
TyG, Me (P ₂₅ , P ₇₅)	9.4 (8.7, 10.5)	8.7 (8.2, 8.9)	10.5 (10.0, 10.8)	<0.001
HbA1c, Me (P ₂₅ , P ₇₅) [%]	5.4 (4.9, 6.0)	5.5 (4.8, 5.9)	5.4 (4.9, 6.0)	0.419
ALT, Me (P ₂₅ , P ₇₅) [U/L]	23.1 (13.9, 34.5)	21.5 (13.1, 31.9)	28.6 (14.1, 38.9)	0.033
AST, Me (P ₂₅ , P ₇₅) [U/L]	23.2 (17.3, 33.6)	22.6 (17.1, 35.4)	24.0 (17.5, 33.0)	0.568
Lactate, Me (P ₂₅ , P ₇₅) [mmol/L]	0.9 (0.8, 1.1)	0.9 (0.8, 1.0)	0.9 (0.8, 1.1)	0.375
Serum bilirubin, Me (P ₂₅ , P ₇₅) [μmol/L]	14.7 (6.1, 23.5)	12.8 (6.7, 22.1)	16.9 (4.8, 27.8)	0.037
hs-cTn, Me (P ₂₅ , P ₇₅) [ng/mL]	20.42 (10.34, 39.53)	19.20 (10.80, 36.50)	21.65 (9.62, 43.83)	0.053
GGPT, Me (P ₂₅ , P ₇₅) [U/L]	28.2 (22.5, 38.7)	27.9 (22.1, 40.7)	29.0 (23.7, 38.1)	0.416
Comorbidities				
HTN, n (%)	585 (66.0)	266 (60)	319 (72)	<0.001
CHD, n (%)	651 (73.5)	301 (67.9)	350 (79)	<0.001
AF, n (%)	248 (28.0)	77 (17.4)	171 (38.6)	<0.001
CVA, n (%)	305 (34.4)	128 (28.9)	177 (40)	<0.001
COPD, n (%)	124 (14.0)	36 (8.1)	88 (19.9)	<0.001
Echocardiographic characteristics				
LVEDD, Me (P ₂₅ , P ₇₅) [mm]	60.0 (58.0, 63.0)	58.0 (55.0, 59.0)	63.0 (61.0, 65.0)	<0.001
LAD, Me (P ₂₅ , P ₇₅) [mm]	48.0 (47.0, 50.8)	47.0 (44.0, 48.0)	51.0 (49.0, 53.0)	<0.001
LVEF, Me (P ₂₅ , P ₇₅) [%]	44.0 (36.0, 50.0)	44.0 (36.0, 54.0)	44.0 (36.0, 48.0)	0.169
Drug therapy at admission				
Vasoactive drugs, n (%)	552 (62.3)	222 (50.1)	330 (74.5)	<0.001
RASI, n (%)	685 (77.3)	339 (76.5)	346 (78.1)	0.574
β-blocker, n (%)	611 (69.0)	301 (67.9)	310 (70)	0.513
Statins, n (%)	548 (61.9)	278 (62.8)	270 (60.9)	0.58
Diuretics, n (%)	788 (88.9)	398 (89.8)	390 (88.0)	0.547
MRA, n (%)	354 (40.0)	173 (39.1)	181 (40.9)	0.431
Achieved recommended dose				
MRA, n (%)	310 (35.0)	151 (34.1)	159 (35.9)	0.656
RASI, n (%)	334 (37.7)	171 (38.6)	163 (36.8)	0.425
β-blocker, n (%)	265 (29.9)	128 (28.9)	137 (30.9)	0.534
EFFECT mortality risk score				
30-day	90.0 (63.0, 118.0)	63.0 (47.5, 75.0)	118.0 (100.0, 125.0)	<0.001
Events				
In-hospital mortality, n (%)	81 (9.1)	25 (5.6)	56 (12.6)	<0.001

Values are presented as mean (standard deviation (SD)), n (percentages (%)), or median (Me) (interquartile range (IQR)). TyG – triglyceride glucose index; SBP – systolic blood pressure; DBP – diastolic blood pressure; HR – heart rate; eGFR – estimated glomerular filtration rate; NT-proBNP – N-terminal B-type natriuretic peptide; CRP – C-reactive protein; TC – total cholesterol; TG – triglyceride; LDL-C – low-density lipoprotein cholesterol; BUN – blood urea nitrogen; Na – sodium; Hb – hemoglobin; HbA1c – hemoglobin A1c; ALT – alanine aminotransferase; AST – aspartate transaminase; hs-cTn – high sensitivity cardiac troponin; GGPT – gamma-glutamyl transpeptidase; HTN – hypertension; CHD – coronary heart disease; AF – atrial fibrillation; CVA – cerebrovascular accident; COPD – chronic obstructive pulmonary disease; LVEDD – left ventricular end-diastolic diameter; LAD – left atrial diameter; LVEF – left ventricular ejection fraction; RASI – angiotensin-converting enzyme inhibitor/angiotensin receptor antagonist; MRA – mineralocorticoid receptor antagonist; EFFECT – Enhanced Feedback for Effective Cardiac Treatment.

divided into 2 groups according to the median of their TyG values. The high-TyG group patients were older, had lower serum albumin levels and higher EFFECT mortality risk scores (all $p < 0.05$). Furthermore, more patients in the high-TyG group suffered from cardiogenic shock and required vasoactive drugs (all $p < 0.001$). In addition, the high-TyG group patients had consistently higher hospital all-cause mortality rates ($p < 0.001$).

The mean age of all patients was 71 years, and 55.5% were male.

The ratios of patients with HTN, cardiogenic shock, CHD, COPD, cerebrovascular accident (CVA), and AF, as well as NT-proBNP, glucose, TC, TG, LDL-C, left ventricular end-diastolic diameter (LVEDD), left atrial diameter (LAD), ALT, and serum bilirubin were significantly higher in the high-TyG group compared to the low-TyG group (all $p < 0.05$) (Table 1).

Correlation between the TyG and major clinical indicators

The TyG level was found to be positively correlated with the EFFECT score and NT-proBNP, and negatively correlated with serum albumin (Table 2).

Short-term mortality risk scores for patients with elevated TyG levels

The EFFECT mortality risk scores of patients with high TyG levels were higher than those in the low-TyG group (Fig. 2A). Higher TyG levels were correlated with higher EFFECT mortality risk scores (Fig. 2B).

Association between the TyG and mortality risk

To further examine the predictive value of the TyG on in-hospital mortality, multi- and univariate logistic regression analyses were performed. In Model 1, after adjusting for age, in-hospital mortality was strongly correlated with high TyG when compared to low TyG (OR = 2.15; 95% CI: 1.47–3.16; $p = 0.013$). In Models 2 and 3, the association between in-hospital mortality and high TyG remained significant (Model 2: OR = 1.59; 95% CI: 1.18–2.24; $p = 0.039$; Model 3: OR = 1.89; 95% CI:

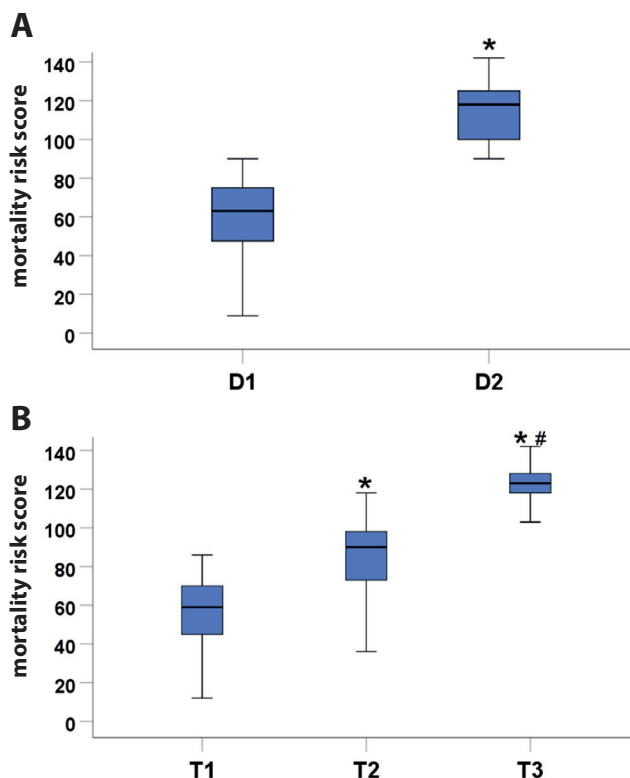


Fig. 2. Triglyceride glucose index (TyG) and mortality risk score using the Enhanced Feedback for Effective Cardiac Treatment (EFFECT) score system to assess the 30-day mortality risk for patients with acute heart failure (AHF). The results are shown as box-whisker plots. The horizontal lines denote the 10th, 25th, 50th, 75th, and 90th percentiles. The differences between the 2 groups were compared using independent samples Mann-Whitney U testing. A. According to the median of the TyG, patients were divided into 2 groups: D1 (TyG ≤ 9.44) and D2 (TyG > 9.44). The mortality risk scores of the patients in D2 were higher than those of the D1 patients (D1 compared to D2, * $p < 0.001$); B. Based on TyG levels, participants were grouped into tertiles: tertile 1 (T1): TyG ≤ 8.81; tertile 2 (T2): TyG > 8.81 and ≤ 10.27; tertile 3 (T3): TyG ≥ 10.27. The mortality risk score increased with the TyG (compared with T1, * $p < 0.001$; T2 compared to T3, # $p < 0.001$)

1.13–3.47; $p = 0.023$). A similar result was observed in Model 4 after additional adjustments for clinical factors that were found to be significantly connected with in-hospital mortality in a single-factor analysis (OR = 1.51; 95% CI: 1.06–3.21; $p = 0.042$). In Model 5, after adjusting for all variables that differed between the groups in Table 1 ($p < 0.05$), the TyG had no predictive value for in-hospital mortality (OR = 2.56; 95% CI: 1.87–4.17; $p = 0.651$) (Table 3).

Table 2. Correlation between the degrees of TyG and major clinical indicators

Parameter	Serum albumin	NT-proBNP	CRP	LVEF	EFFECT score
ρ value	-0.43	0.207	-0.034	-0.014	0.514
p-value	<0.001	<0.001	0.309	0.671	<0.001

TyG – triglyceride glucose index; NT-proBNP – N-terminal B-type natriuretic peptide; CRP – C-reactive protein; LVEF – left ventricular ejection fraction; EFFECT – Enhanced Feedback for Effective Cardiac Treatment. The Spearman’s correlation coefficient (ρ) was used to assess the correlations between the TyG and the other variables.

Table 3. Correlation between the higher TyG and in-hospital mortality

Models	OR	95% CI	p-value
Unadjusted	2.42	1.48–3.95	<0.001
Model 1	2.15	1.47–3.16	0.013
Model 2	1.59	1.18–2.24	0.039
Model 3	1.89	1.13–3.47	0.023
Model 4	1.51	1.06–3.21	0.042
Model 5	2.56	1.87–4.17	0.651

OR – odds ratio; 95% CI – 95% confidence interval; TyG – triglyceride glucose index; Model 1: adjusted for age; Model 2: adjusted for Model 1 + comorbidities of cardiogenic shock, atrial fibrillation (AF), chronic obstructive pulmonary disease (COPD), and use of vasoactive drugs; Model 3: adjusted for Model 2 + heart failure (HF) etiologies including coronary heart disease (CHD), hypertensive heart disease, any cardiomyopathy, and any valvular heart disease; Model 4: adjusted for Model 3 + hemoglobin A1c, 30-day Enhanced Feedback for Effective Cardiac Treatment (EFFECT) score, N-terminal B-type natriuretic peptide (NT-proBNP), alanine aminotransferase (ALT), serum bilirubin, and high sensitivity cardiac troponin; Model 5: adjusted for age, cardiogenic shock, NT-proBNP, serum albumin, total cholesterol, low-density lipoprotein cholesterol, serum bilirubin, ALT, comorbidities of hypertension, CHD, AF, cerebrovascular accident, COPD, and left ventricular end-diastolic diameter, left atrial diameter, EFFECT score, and use of vasoactive drugs.

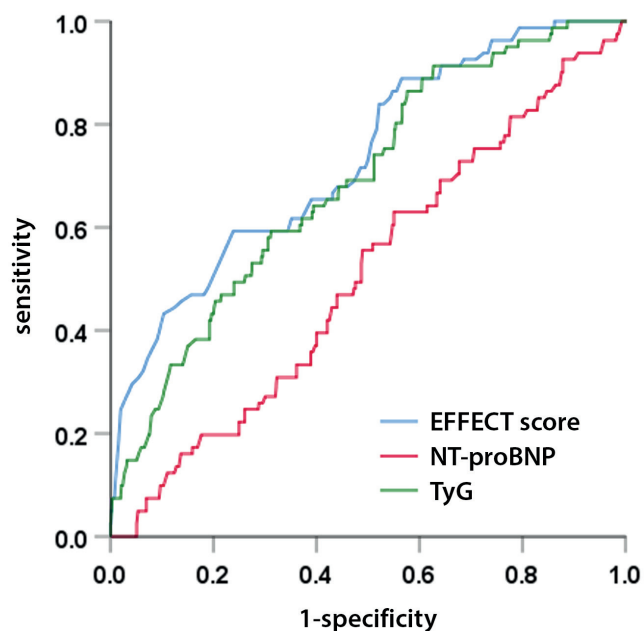


Fig. 3. Assessment of the clinical value of triglyceride glucose index (TyG) for predicting in-hospital mortality using a receiver operating characteristic (ROC) curve. The TyG, Enhanced Feedback for Effective Cardiac Treatment (EFFECT) score and N-terminal B-type natriuretic peptide (NT-proBNP) yielded areas under the ROC curve (AUC) of 0.688 (95% confidence interval (95% CI): 0.631–0.745), 0.732 (95% CI: 0.674–0.789) and 0.506 (95% CI: 0.442–0.570), respectively

The TyG has practical significance in predicting in-hospital all-cause mortality

The clinical value of the TyG for predicting in-hospital mortality of AHF patients was evaluated using ROC curve analysis. Even though the TyG value for predicting in-hospital mortality did not exceed that of the EFFECT

mortality risk score, which included 10 conditions, this variable outperformed NT-proBNP (Fig. 3).

Discussion

We initially proved a connection between the TyG and the risk of in-hospital all-cause mortality in non-diabetic AHF patients. Patients with increased TyG levels were found to be more likely to die in hospital. According to the findings, the TyG was an independent predictor of in-hospital mortality in AHF patients. Most importantly, this study suggests a simple but efficient approach for assessing IR in non-diabetic patients with AHF to enhance the risk stratification of in-hospital mortality rates.

Acute heart failure is a common and severe disease with high mortality and morbidity that is placing an increasing burden on the world's public healthcare system.²⁸ There is an urgent need for new biological markers, mechanisms and treatments for AHF. Previous research has demonstrated that IR is common in HF patients and accelerates the advancement of the disease.²⁹

Insulin resistance is linked to heart disease risk in diverse demographics, as it changes substrate metabolic activity and leads to ineffective energy metabolism, inducing subcellular component abnormalities, promoting improper initiation of the sympathetic nervous system and the renin–angiotensin–aldosterone system, and touching off innate immune infiltration and phagocytosis.³⁰ The HOMA-IR is a relatively comprehensive approach for evaluating IR.³¹ The TyG correlates strongly with HOMA-IR and the hyperinsulinemic–euglycemic clamp (HIEC), even outperforming HOMA-IR.^{20,21}

Significant recent clinical research has shown that the TyG is related to the prognosis in HF. According to a retrospective study, the TyG is associated with the prognosis of individuals with CHF and type 2 DM.³² Another study in 132 hospitalized patients with HF found the TyG to be a novel marker of myocardial injury and a useful risk prediction metric in HF.³³ The findings of this study are similar. Nevertheless, the prognostic value of the TyG in the short-term prognosis of non-diabetic AHF patients is not fully appreciated. In this research, we examined the TyG and its relationship to in-hospital mortality rates in non-diabetic patients with AHF.

Currently, there is no established cutoff point for the TyG. To avoid the influence of setting the cutoff point based on the statistical analysis, the median was used as the cutoff point in this study and cases were divided into a high-TyG group and a low-TyG group. Our study found that the high-TyG group patients had lower serum albumin levels, as well as larger left atrial and left ventricle sizes. Moreover, the degree of the TyG was found to be positively correlated with a poor prognostic indicator of AHF (i.e., NT-proBNP), and it was negatively correlated with a protective indicator (i.e., serum albumin).^{34,35}

These relationships indicate that IR (as determined using the TyG) is a multifunctional indicator that mirrors acute and chronic pathophysiological circumstances, such as abnormal glucose uptake and utilization, nutrition, and cardiac function.

One of North America's largest projects to assess and enhance cardiovascular care quality, the EFFECT study, involved 86 hospital corporate entities in the Ontario province, Canada.³⁶ Based on this research, the EFFECT score was created to stratify the risk of mortality in patients with HF.⁸ In our study, it was demonstrated that patients with high TyG levels also had high EFFECT scores. In addition, the TyG was positively correlated with EFFECT score, and both of them had similar areas under the ROC curve for the prediction of in-hospital mortality. These findings suggest that IR reflected by the TyG has significant clinical value for predicting in-hospital mortality.

Furthermore, our study showed that high TyG levels were accompanied by higher in-hospital mortality rates. According to the multivariate logistic regression analysis, the TyG was an independent risk factor for hospital death. Moreover, when compared to NT-proBNP, an indicator highly apt for AHF patients,³⁷ the TyG achieved a greater AUC for predicting hospital death, proving the clinical relevance of this indicator. To the best of our knowledge, this is the first study to demonstrate that the TyG can be utilized as a predictor of short-term mortality in AHF.

According to Park et al., the TyG is an independent predictor for the development of coronary artery calcification.³⁸ Further studies have revealed that the TyG is more strongly linked to arterial stiffness and atherosclerosis than HOMA-IR.^{13,18,39} Two studies found that individuals with elevated TyG levels are more susceptible to developing hypertension.^{20,40} Tang et al. observed that IR was prevalent in patients without DM and was linked to epicardial fat deposition and vulnerability to AF. Insulin resistance can cause AF by continuing to increase left atrial volume or by hampering left ventricular diastolic function.⁴¹ Zaigham et al. showed that an elevated TyG is a novel risk indicator of prospective COPD events in women in a cross-sectional investigation.⁴² According to these findings, it is more probable that high TyG levels are linked to CHD, AF, CVA, HTN, COPD, and other diseases. Our results are consistent with the conclusions of the above studies.

Our study found that patients with elevated TyG levels had low serum albumin and high ALT and serum bilirubin. A study by Biegus et al. showed that abnormal liver function tests (including serum bilirubin, AST, ALT, and albumin) are common in AHF patients,⁴³ which is similar to our study. In addition, AHF patients with impaired liver function exhibited more severe clinical conditions on admission.⁴⁴ This also partly explains why the high-TyG group of patients in our study had higher rates of cardiogenic shock and use of vasoactive drugs. Moreover, age as well as TC and LDL-C levels were higher in the high-TyG group. Therefore,

in addition to affecting TyG levels, the above distinctions may result in a variety of poor outcomes in the 2 groups of patients. After controlling for all clinical factors, high TyG was found to be a significant predictive marker in AHF.

Limitations of the study

This study has several limitations. First, because of its retrospective study design, we were not able to continuously assess the TyG in individuals over the course of the study. Second, as this study has limitations inherent in single-center studies and small sample studies, we could not manage to avoid data bias, even after controlling for multiple confounders. Third, due to the scarcity of clinical data, distinctions in the prognosis of AHF between the TyG and other IR measurements, such as HOMA-IR and HIEC, were not investigated. Fourth, some indicators that are recognized to affect the prognosis of patients with HF, such as serum ferritin, have not been routinely measured in clinical practice. We were not able to obtain data on these variables because of the limitations of the study's retrospective design. Therefore, it was also not possible for us to adjust for the effect of these variables on the conclusions of the study. Prospective cohort research is needed to confirm our results.

Conclusions

In summary, we discovered that the TyG is an independent predictor of short-term mortality in hospitalized AHF patients without diabetes. The TyG may be a hopeful prognostic indicator for AHF patients, given the ease and low price of IR testing.

ORCID iDs

Hongji Cheng  <https://orcid.org/0000-0002-5092-6560>
 Weijun Huang  <https://orcid.org/0000-0002-4028-2757>
 Xiaohui Huang  <https://orcid.org/0000-0001-5689-7089>
 Wang Miao  <https://orcid.org/0000-0003-0072-0107>
 Yuli Huang  <https://orcid.org/0000-0001-5423-5487>
 Yunzhao Hu  <https://orcid.org/0000-0003-2299-3560>

References

1. Naseem M, Alkassas A, Alaarag A. Tricuspid annular plane systolic excursion/pulmonary arterial systolic pressure ratio as a predictor of in-hospital mortality for acute heart failure. *BMC Cardiovasc Disord.* 2022;22(1):414. doi:10.1186/s12872-022-02857-6
2. De Matteis G, Covino M, Burzo ML, et al. Clinical characteristics and predictors of in-hospital mortality among older patients with acute heart failure. *J Clin Med.* 2022;11(2):439. doi:10.3390/jcm11020439
3. Kobayashi M, Douair A, Coiro S, et al. A combination of chest radiography and estimated plasma volume may predict in-hospital mortality in acute heart failure. *Front Cardiovasc Med.* 2022;8:752915. doi:10.3389/fcvm.2021.752915
4. Kawata T, Ikeda A, Masuda H, Komatsu S. Association between albumin-bilirubin score at admission and in-hospital mortality in patients with acute heart failure. *Int Heart J.* 2021;62(4):829–836. doi:10.1536/ihj.21-080
5. Gao L, Bian Y, Cao S, et al. Development and validation of a simple-to-use nomogram for predicting in-hospital mortality in patients with acute heart failure undergoing continuous renal replacement therapy. *Front Med.* 2021;8:678252. doi:10.3389/fmed.2021.678252

6. Shiraishi Y, Kohsaka S, Abe T, et al. Validation of the Get With The Guideline–Heart Failure risk score in Japanese patients and the potential improvement of its discrimination ability by the inclusion of B-type natriuretic peptide level. *Am Heart J*. 2016;171(1):33–39. doi:10.1016/j.ahj.2015.10.008
7. Alba AC, Agoritsas T, Jankowski M, et al. Risk prediction models for mortality in ambulatory patients with heart failure: A systematic review. *Circ Heart Failure*. 2013;6(5):881–889. doi:10.1161/CIRCHEARTFAILURE.112.000043
8. Lee DS, Austin PC, Rouleau JL, Liu PP, Naimark D, Tu JV. Predicting mortality among patients hospitalized for heart failure: Derivation and validation of a clinical model. *JAMA*. 2003;290(19):2581. doi:10.1001/jama.290.19.2581
9. Banovic M, Vasiljevic-Pokrajcic Z, Vujisic-Tesic B, et al. Are de novo acute heart failure and acutely worsened chronic heart failure two subgroups of the same syndrome? *Srp Arh Celok Lek*. 2010;138(3–4):162–169. doi:10.2298/SARH1004162B
10. Scherbakov N, Bauer M, Sandek A, et al. Insulin resistance in heart failure: Differences between patients with reduced and preserved left ventricular ejection fraction. *Eur J Heart Fail*. 2015;17(10):1015–1021. doi:10.1002/ehf.317
11. Fu F, Zhao K, Li J, et al. Direct evidence that myocardial insulin resistance following myocardial ischemia contributes to post-ischemic heart failure. *Sci Rep*. 2015;5(1):17927. doi:10.1038/srep17927
12. Liao Y, Zhang R, Shi S, et al. Triglyceride–glucose index linked to all-cause mortality in critically ill patients: A cohort of 3026 patients. *Cardiovasc Diabetol*. 2022;21(1):128. doi:10.1186/s12933-022-01563-z
13. Irace C, Carallo C, Scavelli FB, et al. Markers of insulin resistance and carotid atherosclerosis: A comparison of the homeostasis model assessment and triglyceride glucose index. *Int J Clin Pract*. 2013;67(7):665–672. doi:10.1111/ijcp.12124
14. Guerrero-Romero F, Simental-Mendía LE, González-Ortiz M, et al. The product of triglycerides and glucose, a simple measure of insulin sensitivity: Comparison with the euglycemic-hyperinsulinemic clamp. *J Clin Endocrinol Metab*. 2010;95(7):3347–3351. doi:10.1210/jc.2010-0288
15. Vasques ACJ, Novaes FS, De Oliveira MDS, et al. TyG index performs better than HOMA in a Brazilian population: A hyperglycemic clamp validated study. *Diabetes Res Clin Pract*. 2011;93(3):e98–e100. doi:10.1016/j.diabres.2011.05.030
16. Unger G, Benozzi SF, Perruzza F, Pennacchiotti GL. Triglycerides and glucose index: A useful indicator of insulin resistance. *Endocrinol Nutr*. 2014;61(10):533–540. doi:10.1016/j.endonu.2014.06.009
17. Du T, Yuan G, Zhang M, Zhou X, Sun X, Yu X. Clinical usefulness of lipid ratios, visceral adiposity indicators, and the triglycerides and glucose index as risk markers of insulin resistance. *Cardiovasc Diabetol*. 2014;13(1):146. doi:10.1186/s12933-014-0146-3
18. Kim MK, Ahn CW, Kang S, Nam JS, Kim KR, Park JS. Relationship between the triglyceride glucose index and coronary artery calcification in Korean adults. *Cardiovasc Diabetol*. 2017;16(1):108. doi:10.1186/s12933-017-0589-4
19. Li S, Guo B, Chen H, et al. The role of the triglyceride (triacylglycerol) glucose index in the development of cardiovascular events: A retrospective cohort analysis. *Sci Rep*. 2019;9(1):7320. doi:10.1038/s41598-019-43776-5
20. Zheng R, Mao Y. Triglyceride and glucose (TyG) index as a predictor of incident hypertension: A 9-year longitudinal population-based study. *Lipids Health Dis*. 2017;16(1):175. doi:10.1186/s12944-017-0562-y
21. Thai PV, Tien HA, Van Minh H, Valensi P. Triglyceride glucose index for the detection of asymptomatic coronary artery stenosis in patients with type 2 diabetes. *Cardiovasc Diabetol*. 2020;19(1):137. doi:10.1186/s12933-020-01108-2
22. Sánchez-Íñigo L, Navarro-González D, Fernández-Montero A, Pastrana-Delgado J, Martínez JA. The TyG index may predict the development of cardiovascular events. *Eur J Clin Invest*. 2016;46(2):189–197. doi:10.1111/eci.12583
23. Ma X, Dong L, Shao Q, et al. Triglyceride glucose index for predicting cardiovascular outcomes after percutaneous coronary intervention in patients with type 2 diabetes mellitus and acute coronary syndrome. *Cardiovasc Diabetol*. 2020;19(1):31. doi:10.1186/s12933-020-01006-7
24. Wang L, Cong HL, Zhang JX, et al. Triglyceride–glucose index predicts adverse cardiovascular events in patients with diabetes and acute coronary syndrome. *Cardiovasc Diabetol*. 2020;19(1):80. doi:10.1186/s12933-020-01054-z
25. Hu C, Zhang J, Liu J, et al. Discordance between the triglyceride glucose index and fasting plasma glucose or HbA1C in patients with acute coronary syndrome undergoing percutaneous coronary intervention predicts cardiovascular events: A cohort study from China. *Cardiovasc Diabetol*. 2020;19(1):116. doi:10.1186/s12933-020-01091-8
26. McDonagh TA, Metra M, Adamo M, et al. 2021 ESC Guidelines for the diagnosis and treatment of acute and chronic heart failure. *Eur Heart J*. 2021;42(36):3599–3726. doi:10.1093/eurheartj/ehab368
27. Levey AS, Stevens LA, Schmid CH, et al. A new equation to estimate glomerular filtration rate. *Ann Intern Med*. 2009;150(9):604. doi:10.7326/0003-4819-150-9-200905050-00006
28. Rider I, Sorensen M, Brady WJ, et al. Disposition of acute decompensated heart failure from the emergency department: An evidence-based review. *Am J Emerg Med*. 2021;50:459–465. doi:10.1016/j.ajem.2021.08.070
29. Witteles RM, Fowler MB. Insulin-resistant cardiomyopathy. *J Am Coll Cardiol*. 2008;51(2):93–102. doi:10.1016/j.jacc.2007.10.021
30. Huang R, Wang Z, Chen J, et al. Prognostic value of triglyceride glucose (TyG) index in patients with acute decompensated heart failure. *Cardiovasc Diabetol*. 2022;21(1):88. doi:10.1186/s12933-022-01507-7
31. Bonora E, Targher G, Alberiche M, et al. Homeostasis model assessment closely mirrors the glucose clamp technique in the assessment of insulin sensitivity: Studies in subjects with various degrees of glucose tolerance and insulin sensitivity. *Diabetes Care*. 2000;23(1):57–63. doi:10.2337/diacare.23.1.57
32. Guo W, Zhao L, Mo F, et al. The prognostic value of the triglyceride glucose index in patients with chronic heart failure and type 2 diabetes: A retrospective cohort study. *Diabetes Res Clin Pract*. 2021;177:108786. doi:10.1016/j.diabres.2021.108786
33. Yang S, Du Y, Liu Z, et al. Triglyceride–glucose index and extracellular volume fraction in patients with heart failure. *Front Cardiovasc Med*. 2021;8:704462. doi:10.3389/fcvm.2021.704462
34. Lorlowhakarn K, Arayakarnkul S, Trongtorsak A, et al. Outcomes and predictors of one-year mortality in patients hospitalized with acute heart failure. *Int J Cardiol Heart Vasc*. 2022;43:101159. doi:10.1016/j.ijcha.2022.101159
35. Çınar T, Hayiroğlu Mİ, Çiçek V, Orhan AL. A simple parameter for long-term mortality in acute heart failure patients: Serum albumin. *Acta Cardiol*. 2021;76(1):106. doi:10.1080/00015385.2019.1699280
36. Tu JV, Donovan LR, Lee DS, et al. Effectiveness of public report cards for improving the quality of cardiac care: The EFFECT study. A randomized trial. *JAMA*. 2009;302(21):2330. doi:10.1001/jama.2009.1731
37. Scrutinio D, Ammirati E, Guida P, et al. Clinical utility of N-terminal pro-B-type natriuretic peptide for risk stratification of patients with acute decompensated heart failure: Derivation and validation of the ADHF/NT-proBNP risk score. *Int J Cardiol*. 2013;168(3):2120–2126. doi:10.1016/j.ijcard.2013.01.005
38. Park K, Ahn CW, Lee SB, et al. Elevated TyG index predicts progression of coronary artery calcification. *Diabetes Care*. 2019;42(8):1569–1573. doi:10.2337/dc18-1920
39. Lee SB, Ahn CW, Lee BK, et al. Association between triglyceride glucose index and arterial stiffness in Korean adults. *Cardiovasc Diabetol*. 2018;17(1):41. doi:10.1186/s12933-018-0692-1
40. Sánchez-Íñigo L, Navarro-González D, Pastrana-Delgado J, Fernández-Montero A, Martínez JA. Association of triglycerides and new lipid markers with the incidence of hypertension in a Spanish cohort. *J Hypertens*. 2016;34(7):1257–1265. doi:10.1097/HJH.0000000000000941
41. Tang Q, Guo XG, Sun Q, Ma J. The pre-ablation triglyceride–glucose index predicts late recurrence of atrial fibrillation after radiofrequency ablation in non-diabetic adults. *BMC Cardiovasc Disord*. 2022;22(1):219. doi:10.1186/s12872-022-02657-y
42. Zaigham S, Tanash H, Nilsson PM, Muhammad IF. Triglyceride–glucose index is a risk marker of incident COPD events in women. *Int J Chron Obstruct Pulmon Dis*. 2022;17:1393–1401. doi:10.2147/COPD.S360793
43. Biegus J, Zymliński R, Sokolski M, et al. Liver function tests in patients with acute heart failure. *Pol Arch Intern Med*. 2012;122(10):471–479. doi:10.20452/pamw.1413
44. Biegus J, Demissei B, Postmus D, et al. Hepatorenal dysfunction identifies high-risk patients with acute heart failure: Insights from the RELAX-AHF trial. *ESC Heart Fail*. 2019;6(6):1188–1198. doi:10.1002/ehf2.12477

Anxiety disorders and depression are associated with resistant hypertension

Handan Duman^{1,A,D,F}, Hakan Duman^{2,C-F}, Meltem Puşuroğlu^{3,A,C}, Ahmet Seyda Yılmaz^{2,E}

¹ Department of Family Medicine, Faculty of Medicine, Recep Tayyip Erdoğan University, Rize, Turkey

² Department of Cardiology, Recep Tayyip Erdoğan University, Rize, Turkey

³ Department of Psychiatry, Faculty of Medicine, Recep Tayyip Erdoğan University, Rize, Turkey

A – research concept and design; B – collection and/or assembly of data; C – data analysis and interpretation;

D – writing the article; E – critical revision of the article; F – final approval of the article

Advances in Clinical and Experimental Medicine, ISSN 1899–5276 (print), ISSN 2451–2680 (online)

Adv Clin Exp Med. 2024;33(2):111–118

Address for correspondence

Hakan Duman

E-mail: drhakanduman@hotmail.com

Funding sources

None declared

Conflict of interest

None declared

Acknowledgements

We would like to thank Dr. Ibrahim Ezberci from Rize Center Family Health Center No. 1 for his contributions.

Received on December 12, 2022

Reviewed on February 12, 2023

Accepted on May 18, 2023

Published online on June 30, 2023

Cite as

Duman H, Duman H, Puşuroğlu M, Yılmaz AS. Anxiety disorders and depression are associated with resistant hypertension. *Adv Clin Exp Med*. 2024;33(2):111–118. doi:10.17219/acem/163409

DOI

10.17219/acem/166304

Copyright

Copyright by Author(s)

This is an article distributed under the terms of the Creative Commons Attribution 3.0 Unported (CC BY 3.0) (<https://creativecommons.org/licenses/by/3.0/>)

Abstract

Background. Anxiety and depression can adversely affect the prognosis following cardiovascular diseases (CVDs) and may be associated with resistance to hypertension (HT) treatment. A better understanding of the complex biological substratum of resistant HT complicated by depression and anxiety is crucial for designing future primary care strategies.

Objectives. To evaluate the relationship between anxiety and depression and resistant HT, which will help to look at resistant HT from a broader perspective and aid the development of new strategies for diagnosis and treatment.

Materials and methods. We used a stratified random sampling method to select HT patients aged 18 and older in primary care setting. A total of 300 consecutive patients with persistent HT who were diagnosed with essential HT and uncontrolled blood pressure (BP) despite antihypertensive therapy were prospectively included in the study. Anxiety and depression were investigated, and scoring was evaluated using the Hospital Anxiety and Depression Scale (HADS).

Results. The study included 108 controlled and 91 uncontrolled HT patients. The HADS scales were higher in the controlled HT group compared to the uncontrolled HT group (6 (0–18) compared to 9 (0–20), $p = 0.001$; 5 (0–17) compared to 7 (0–16), $p < 0.001$, respectively). Body mass index (BMI) and C-reactive protein (CRP) were also significantly higher in the uncontrolled HT patients compared to the normotensive group. Anxiety was associated with a 2.18 times increased risk of HT and a 1.99 times increased risk of depression. Thus, anxiety and depression predicted resistant HT in both univariate and multivariate analyses.

Conclusions. During the treatment of HT, efforts should be made to improve the psychological and social functions of the patients beyond the primary therapy for control of the disease. As such, we hope to draw attention to the importance of psychological factors, especially anxiety and depression, in any field of medicine related to managing resistant HT.

Key words: depression, resistant hypertension, anxiety, hypertension, high blood pressure

Background

Hypertension (HT) is one of the most preventable risk factors for premature death and disability. Also, it has a high prevalence and serious adverse cardiovascular and renal effects, and is a current global health problem.¹ Despite numerous pharmacological treatment options, HT therapy does not always result in optimal blood pressure (BP) control. This observation led to the definition of resistant or refractory HT decades ago, a form of high BP that persists despite drug usage.² Although HT is one of the treatable diseases in primary care, chronic disease remains uncontrolled in many patients.³ There are differences in the definition of HT; thus, studies on the prevalence of resistant HT are limited, though it is estimated to be approx. 5–30%. However, the prevalence of resistant HT is almost less than 10% among treated patients when using a precise definition and excluding pseudo-resistant causes.⁴ A study in Turkey determined that the number of people with uncontrolled HT has decreased, though around 11 million people suffer from uncontrolled HT worldwide.⁵ Patients with resistant HT are at risk of chronic renal disease and early cardiovascular disease (CVD).⁶ Considering the end-organ damage in uncontrolled HT patients, the importance of visits and compliance with treatment draws attention. Therefore, patient management is crucial at all stages, from patient and clinician awareness, through treatment modalities and diagnosis, to invasive treatment strategies.^{7,8}

The pathophysiology of neurocognitive disorders is complex.^{9–11} Emotions play an important role as they motivate action in response to environmental changes and trigger adaptive behaviors to achieve variable goals. Moreover, the evidence shows that emotions affect metabolic processes and numerous cognitive abilities. It is vital to understand the central role of the prefrontal cortex to better comprehend how its impaired function can contribute to dysregulated behavioral responses and the development of mental dysfunctions, commonly associated with anxiety and depression.^{12,13} Chronic diseases can cause anxiety and depression, and also be caused by them, leading to a more severe disease course.^{14,15} Depression is quite common in patients with CVD, and leads to adverse cardiovascular outcomes and increased healthcare costs.^{16–18} Furthermore, the presence of anxiety disorders in HT individuals significantly affects the patient's response to treatment and increases the number of drugs used.¹⁹ In addition, the incidence of depression is higher in patients with coronary artery disease (CAD) and heart failure (HF) than in the general population.²⁰

There is a causative relationship between human mood and physical diseases such as HT. Patients with CVD commonly have anxiety and depression, both of which cause negative adverse cardiovascular outcomes and increased healthcare costs.⁸ A previous study in a heterogeneous

population of all ages showed that anxiety, depression and HT are clearly related.^{21,22} In the pathophysiological background of HT, at the molecular level, dynamic changes in the mitochondrial cycle may be linked to HT development, left ventricular hypertrophy, insulin resistance, obesity, and type 2 diabetes mellitus (T2DM).²³ Mitochondrial dynamics and factors involved in its regulation are critical for neuronal development, survival and optimal cell function. Moreover, mitochondrial dysfunction may be related to psychiatric symptoms such as depression, cognitive impairment, psychosis, and anxiety.²⁴ Endothelial dysfunction and inflammation also co-occur in HT. Accordingly, inflammatory cytokines are increased in depression, which may explain the serotonergic, noradrenergic and dopaminergic dysfunction of depression.^{25–28}

Hypertension, accompanied by anxiety and depression, was associated with adverse conditions such as lower treatment adherence, lower levels of daily functioning, poor health-related quality of life, and lower employment rate.²⁹ The relationship between depression and uncontrolled HT is still controversial. Data on this relationship are insufficient, especially those obtained from primary healthcare institutions.³⁰

The Hospital Anxiety and Depression Scale (HADS) is a readily obtainable anxiety-depression assessment instrument consisting of 14 items, with 7 items related to anxiety (HADS-A) and 7 items to depression (HADS-D). Although the score has been used to test compliance with treatment in CVDs, studies on patients with resistant HT did not demonstrate the impact of emotional status on the HT course.^{14,16} Therefore, this study aimed to assess the relationship between depression, HT and uncontrolled HT by evaluating the HADS in patients with resistant HT.

Objectives

This study was designed to investigate whether there is a relationship between resistant HT and anxiety and depression. As such, the study aimed to investigate the lack of BP control despite receiving optimal treatment, and reveal a relationship that may contribute to patient treatment and quality of life using an easily applicable test.

Materials and methods

Study population

This cross-sectional study included patients aged ≥ 18 who attended the family medicine and cardiology outpatient clinic at the Recep Tayyip Erdoğan University hospital (Rize, Turkey) between November 2021 and August 2022, and who completed the survey, which had a response

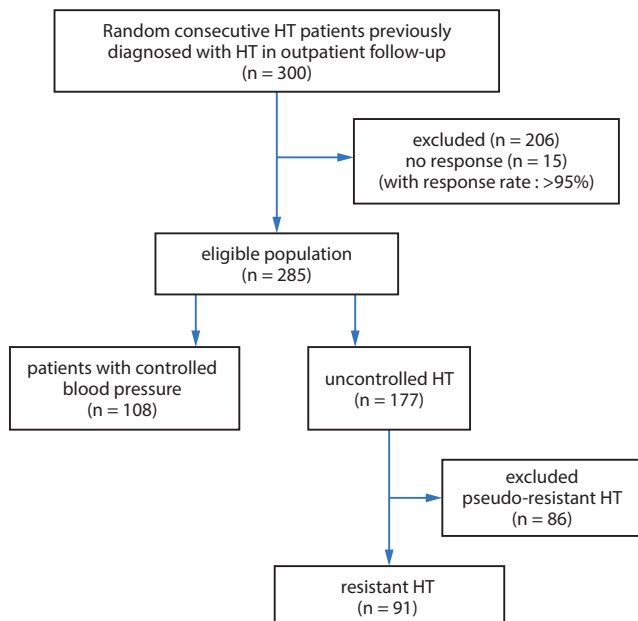


Fig. 1. The flowchart used for the screening and inclusion of patients
HT – hypertension.

rate >95%. Each patient had sociodemographic data and medical history recorded on admission. A cardiologist performed a detailed physical examination, and patients were referred to a psychiatric clinic for evaluation of anxiety and depression scores. A total of 300 patients with resistant HT diagnoses were prospectively included in this study. The control group comprised normotensive patients diagnosed with HT who received regular treatment. Patients with uncontrolled BP who did not use medication or used it tentatively were classified as pseudo-HT and excluded from the study (Fig. 1). Other information on comorbidities, demographics, behavioral lifestyle factors, and metabolic diseases such as dyslipidemia, diabetes, and CVDs and their complications, including stroke and CAD, was also obtained. This study was carried out in accordance with the Declaration of Helsinki and approved by Recep Tayyip Erdoğan University Ethical Committee (decision No. 2022/41).

Exclusion criteria

The study included patients diagnosed with essential HT who had uncontrolled BP despite antihypertensive therapy. Patients who did not want to fill out the questionnaire, those with dementia, and those receiving treatment for depression, anxiety or other psychiatric disorders, were not included in this study. Secondary HT, history of CAD, history of cerebrovascular disease, acute or chronic renal failure (estimated glomerular filtration rate (eGFR) <30 mL/1.7 m²/min), end-stage liver disease, malignancy, active inflammatory disease, endocrine diseases, and electrolyte disturbances were determined as exclusion criteria.

Blood pressure, plasma glucose and lipid measurements

An automatic sphygmomanometer (OMRON HBP-1300; OMRON, Kyoto, Japan) measured each patient's BP, with 3 measurements taken at 30-second intervals and the mean value of the 3 measurements used for the analysis. Also, trained professional healthcare providers measured each patient's height, weight and waist circumference. Body mass index (BMI) was calculated by dividing weight by the square of height (kg/m²). All patients fasted for ≥8 h, and 5-milliliter fasting blood samples were obtained and tested for fasting plasma glucose (FPG), triglycerides (TG), total cholesterol (TC), low-density lipoprotein cholesterol (LDL-C), and high-density lipoprotein cholesterol (HDL-C) using standard methods.

Hypertension was defined as systolic BP (SBP) ≥ 140 mm Hg, diastolic BP (DBP) ≥ 90 mm Hg, and/or the use of antihypertensive agents within 2 weeks.⁴ Hypertensive patients receiving antihypertensive treatment and whose SBP/DBP was <140/90 mm Hg were identified and assigned to the control group. Resistant HT was diagnosed using the guidelines of the European Society of Cardiology (ESC).⁴ Treatment-resistant HT was diagnosed if lifestyle changes and recommended combination therapy did not reduce BP values under 140/90 mm Hg. Meanwhile, true resistant HT was defined when SBP was ≥140 mm Hg and/or DBP was ≥90 mm Hg while receiving treatment with the optimal or most tolerable doses of 3 or more drugs, including a diuretic, β-blocker, calcium channel blocker, and a renin-angiotensin-aldosterone antagonist.^{31,32} Uncontrolled BP was measured using ambulatory or home monitoring in all patients. We identified pseudo-resistant HT patients after classifying true resistant HT patients.^{33,34}

Evaluation and definition of anxiety and depression

Each subject completed the HADS questionnaire alone in a quiet environment. The HADS consists of 14 items, including 7 HADS-A and 7 HADS-D items.^{35–38} Each item was scored using a scale that separately evaluates anxiety and depression from 0 to 3 points to give a total score between 0 and 21. The scale classified patients as normal (0–7 points), borderline abnormal (8–10 points) or abnormal (11–21 points).

Statistical analyses

The Shapiro–Wilk test was used to evaluate the distribution normality of continuous variables, and continuous and categorical variables were expressed as mean ± standard deviation (M ±SD) and percentage (%), respectively. In addition, median values (Me) and interquartile ranges (IQRs) were used for non-normally distributed parameters. The Student's t-test compared continuous data with

a normal distribution, and a χ^2 test or Fisher's exact test were employed to compare categorical variables. Continuous variables without a normal distribution were evaluated using the Mann–Whitney U test, while logistic regression was employed to assess the relationship between HT groups (resistance compared to nonresistance) and anxiety and depression scores. The relationship between the predictors and HT groups was determined using odds ratio (OR) and 95% confidence intervals (95% CIs). Odds ratio and 95% CIs summarized the interquartile change for continuous predictors. To capture the nonlinear relationship between continuous predictors and HT groups, continuous predictors were entered into the model using restricted cubic spline transformation (with 3 knots). Multicollinearity was assessed using a variance inflation factor (VIF).³⁹ All statistical analyses were performed using R v. 3.5.6 software (R Foundation for Statistical Computing, Vienna, Austria). We built our model based on previous knowledge and biological plausibility.

Results

In this study, the mean age of 199 patients was 56.4 ± 11 years, and 105 (52.8%) were female. The mean HT treatment duration was 11.1 ± 6.4 years. There were no significant differences between groups in terms of age, gender, family history, and the number of drugs prescribed. The mean HADS-A score was 7.4 ± 4.8 , and the HADS-D score was 6.0 ± 4.0 . The HADS-A score (8.8 ± 5.1 compared to 6.3 ± 4.3 , $p < 0.001$) and HADS-D score (7.1 ± 4.3 compared to 5.0 ± 3.6 , $p = 0.001$) were higher in the uncontrolled HT patients compared to the controlled HT group. The BMI of the resistant HT group was higher than in the controlled HT group (24.9 ± 5.0 compared to 23.2 ± 3.0 , $p = 0.011$). C-reactive protein (CRP) level was higher in the uncontrolled group than in the controlled group (3.3 (0.40–10) mg/L compared to 2.2 (0.12–11) mg/L, $p = 0.045$) (Table 1).

Blood pressure monitoring findings differed between the groups (Table 2). In multivariable analysis, HADS-D score (OR: 1.88, 95% CI: 1.10–3.21, $p = 0.005$) and HADS-A score (OR: 1.89, 95% CI: 1.04–3.45, $p = 0.008$) were independent predictors of resistant HT. In addition, BMI (OR: 1.46, 95% CI: 0.98–2.18, $p = 0.027$) and CRP (OR: 3.06, 95% CI: 1.47–6.38, $p = 0.004$) predicted the presence of resistant HT (Table 3). The main study findings were that higher levels of anxiety and depression, as measured using HADS, were independent predictors of resistant HT. Additionally, higher BMI and CRP levels were associated with resistant HT.

Discussion

This study revealed that patients with uncontrolled HT exhibited higher levels of anxiety and depression compared

to those with controlled HT. In addition, the resistant HT patients had higher BMI and CRP levels. The multivariable analysis confirmed that anxiety and depression scores, BMI, and CRP levels independently predicted resistant HT. These findings suggest that psychological factors and inflammation may contribute to the course of resistant HT.

Hypertension is a common chronic disease that affects public health globally and is one of the most important preventable risk factors for CVDs.⁴⁰ The World Health Organization (WHO) reported in 2015 that approx. 25% of the adult population had HT, and around 40% of cardiovascular deaths were caused secondary to HT.⁴¹ Blacher et al. stated that every 10 mm Hg increase in BP causes increasingly severe CVD complications and increases the risk of death by nearly 20%.⁴² Considering these high mortality and morbidity rates, it can be concluded that uncontrolled and resistant HT represents a more complicated status. Moreover, patients with resistant HT have a twofold increased risk for CVDs than patients without resistant HT, so those with resistant HT are a critical population that needs further evaluation.⁴³

Recently, it has been frequently emphasized that anxiety and depression increase the risk of CVDs and eventually complicate their treatment.^{44,45} Although the etiopathogenesis of resistant HT is heterogeneous, conditions that increase the activity of the sympathetic nervous system, including chronic stress and chronic pain, appear to be particularly responsible factors.⁴⁶ It has been known for more than 50 years that oxidative stress and inflammation have a crucial role in the pathogenesis of HT. Biomarkers of inflammation, including high-sensitivity CRP, numerous cytokines and various products of the complement pathway, are elevated in patients with HT.⁴⁷ Long-term inflammatory responses and pro-inflammatory factors also play a critical role in the pathogenesis of anxiety and depression and are central to HT, while the activation of certain enzymes by stress hormones such as cortisol and inflammatory cytokines is well known. Moreover, genotypic variations contribute to inflammation, which in turn may lead to the development of various diseases.⁴⁸ In this study, CRP was higher in resistant HT patients than in control patients, compatible with the current literature. These findings predicate that chronic inflammation arising from anxiety and depression contributes to the pathogenesis of resistant HT.

The negative effects of dietary habits and being overweight are well known in HT.⁴⁹ In this study, BMI was significantly higher in resistant HT patients compared to the control group, which also shows that it has a deleterious effect on controlling HT in the normal range.

The relationship between psychosocial stress and HT is complex, with multiple mechanisms involved. The 2 main mechanisms are behavioral responses and pathophysiological responses. Maladaptive behavioral responses include smoking, poor activity and dietary habits thought to contribute to resistant HT over time.⁴⁴ Physiological

Table 1. Baseline clinical and laboratory characteristics of patients

Variable	Study population					
	overall (n = 199)	group 1 (n = 108)	group 2 (n = 91)	p-value	test value	
Age [years]	56 (35–81)	57.5 (36–81)	55 (35–78)	0.242*	U: 4441	
Female sex, %	52.8	54	60	0.413 [‡]	χ ² : 0.724	
Diabetes, %	12.6	11	13	0.676 [‡]	χ ² : 0.034	
Duration of HT [years]	11.1 ±6.4	11.7 ±6	10.5 ±6	0.159 [#]	t: 1.095	
Smoking, %	11.1	12	10	0.665 [‡]	χ ² : 0.182	
Dyslipidemia, %	18.6	20	18	0.756 [‡]	χ ² : 0.443	
Family history of HT	18	17	18	0.592 [‡]	χ ² : 0.524	
CV disease, %	10	9	11	0.653 [‡]	χ ² : 0.163	
HADS-Anxiety score	7 (0–20)	6 (0–18)	9 (0–20)	0.001*	U: 3511	
HADS-Depression score	5 (0–17)	5 (0–17)	7 (0–16)	<0.001*	U: 3493	
C-reactive protein [mg/dL]	2.7 (0.12–11)	2.2 (0.12–11)	3.3 (0.40–10)	0.045*	U: 4102	
Hemoglobin [g/dL]	13 (8–16)	13 (8–16.5)	14 (10.2–16.6)	0.444*	U: 4604	
Fasting glucose [mg/dL]	98 (83–242)	100 (83–242)	97 (83–213)	0.520*	U: 4654	
Total cholesterol [mg/dL]	217 ±46	214 ±50	220 ±39	0.280 [#]	t: 1.095	
LDL cholesterol [mg/dL]	126 (31–257)	121 (31–257)	131 (41–257)	0.123*	U: 4249	
HDL cholesterol [mg/dL]	39 (16–59.8)	39 (16–59.8)	39 (16–59.3)	0.941*	U: 4884	
Triglyceride [mg/dL]	180 (93–603)	185 (99–603)	171 (93–392)	0.252*	U: 4450	
GFR [mL/min]	58 (40–100)	56 (40–98)	60 (40–100)	0.163*	U: 4349	
BMI [kg/m ²]	23.4 (16–39)	22.7 (16.3–35.7)	23.8 (16.3–39)	0.040*	U: 4082	
Medications, %	aspirin	8.8	10.2	7.4	0.603 [‡]	χ ² : 1.470
	statin	13.6	13.9	12	0.685 [‡]	χ ² : 1.724
	ACE-inhibitors	41.7	38	44.4	0.407 [‡]	χ ² : 1.363
	ARB	29.1	26.9	29.2	0.763 [‡]	χ ² : 0.027
	CCB	34.2	34.3	33.3	0.100 [‡]	χ ² : 0.001
	β-blocker	15.6	18.5	13	0.262 [‡]	χ ² : 1.553
	alfa-adrenergic receptor blocker	9	6.5	10.2	0.325 [‡]	χ ² : 1.887
	diuretic	78.4	60.2	100	<0.001 [‡]	χ ² : 46.218
combined pill	61.8	60.2	63.9	0.670 [‡]	χ ² : 0.264	

Normally distributed continuous variables are presented as mean ± standard deviation (M ±SD). Categorical variables are presented as percentage (%). Non-normally distributed variables are presented as median (Me) (interquartile range (IQR)). group 1 – patients with regulated blood pressure; group 2 – resistant hypertensive patients; HT – hypertension; HADS – Hospital Anxiety and Depression Scale; CV – cardiovascular; BMI – body mass index; GFR – glomerular filtration rate; LDL – low-density lipoprotein; HDL – high-density lipoprotein; ACE – angiotensin converting enzyme; ARB – angiotensin II receptor blocker; CCB – calcium channel blocker; * Mann–Whitney U test; # Student’s t-test; [‡]Pearson’s χ² test.

Table 2. 24-hour blood pressure monitoring findings in the patients

Variable	Group 1 (n = 108)	Group 2 (n = 91)	p-value	test value
Mean daytime systolic	116 (95–170)	160 (108–172)	<0.001*	U: 1731
Mean daytime diastolic	75 (62–123)	97 (67–112)	<0.001*	U: 1954
Mean night systolic	70 (55–115)	140 (94–150)	<0.001*	U: 1680
Mean night diastolic	105 (74–148)	85 (60–101)	<0.001*	U: 1850

Non-normally distributed variables are presented as median (Me) (interquartile range (IQR)). group 1 – patients with regulated blood pressure; group 2 – resistant hypertensive patients; * Mann–Whitney U test.

pathways, such as the hypothalamus–pituitary–adrenal (HPA) axis, sympathetic activation, vagal withdrawal, and immune responses, mediate the pathophysiological response.⁴⁹ The HPA axis releases corticotropin-releasing factor (CRF) from the hypothalamus, and subsequently,

adrenocorticotrophic hormone (ACTH) is released into the systemic circulation and reaches the adrenal cortex. Glucocorticoid synthesis is stimulated by the adrenal cortex, which ultimately contributes to the development of HT.⁵⁰ The sympathetic nervous system is also thought

Table 3. Association of depression and anxiety with resistant hypertension (HT) tested using multivariable binary logistic regression

Variable	Predictors of patients with resistant HT			
	univariable analysis		multivariable analyzes	
	OR (95% CI)	p-value	OR (95% CI)	p-value
Model 1			Nagelkerke R ² = 0.243	
HADS-Depression score (from 3 to 8.5)	1.99 (1.26–3.15)	0.002	1.88 (1.10–3.21)	0.005
BMI (from 20.9 to 26.5)	1.30 (0.91–1.86)	0.040	1.46 (0.98–2.18)	0.027
CRP (from 1.4 to 5.6)	3.00 (1.56–5.79)	0.001	3.06 (1.47–6.38)	0.004
Age (from 47 to 66)	0.73 (0.46–1.17)	0.115	0.63 (0.37–1.07)	0.218
Male sex	1.28 (0.73–2.23)	0.395	1.46 (0.78–2.74)	0.239
Model 2			Nagelkerke R ² = 0.237	
HADS-Anxiety score (from 3 to 11)	2.18 (1.26–3.75)	0.002	1.89 (1.04–3.45)	0.008
BMI (from 20.9 to 26.5)	1.30 (0.91–1.86)	0.031	1.47 (1.00–2.17)	0.046
CRP (from 1.4 to 5.6)	3.00 (1.56–5.79)	0.001	3.19 (1.58–6.46)	0.003
Age (from 47 to 66)	0.73 (0.46–1.17)	0.115	0.67 (0.39–1.14)	0.183
Male sex	1.28 (0.73–2.23)	0.395	1.50 (0.80–2.82)	0.208

HADS – Hospital Anxiety and Depression Scale; OR – odds ratio; 95% CI – 95% confidence interval; CRP – C-reactive protein; BMI – body mass index.

to play a vital role in the pathophysiological response of HT to stress. Furthermore, decreased vagal tone is thought to be a reliable indicator of new-onset HT, and fluctuations in vagal tone can be as imperative to psychology-related BP increases as sympathetic nerves and the HPA systems. The role of the parasympathetic system in recovery and restoration is also essential, and those who cannot relax under chronic stress are more likely to develop premature coronary events.⁵¹ Overall, individuals with hyperactive HPA and sympathetic systems, and decreased vagal tone, aggravated by chronic stress, are at greater risk of developing HT.

Most disorders have a different pathophysiological basis, though concomitant depression and anxiety may be seen in all patients attending the clinic and presenting with fluctuating symptoms. Furthermore, psychiatric symptoms can serve as prodromal indicators of a particular condition.⁵² It is thought that emotional and psychosocial stress takes on an important role in HT development, and BP is negatively affected by anxiety and depression.⁵³ On the other hand, patients experience emotional deterioration after HT diagnosis. As such, evaluating emotional status would be beneficial for detecting resistance to HT treatment. Accordingly, it can be asserted that emotional status assessment, even after resistant HT development, would be beneficial to prevent HT progression and provide a response to treatment. In parallel with our study, Lane et al. demonstrated that depression is an independent predictor of uncontrolled HT.¹⁶ Indeed, anxiety and depression levels were higher in patients with resistant HT than in control patients, and both were independent predictors of HT. In this respect, if there is no identifiable secondary cause, anxiety and depression play a critical role in uncontrolled development of HT.

Our study may shed light on better defining emotional disturbances that have a negative impact on the course

of chronic diseases in future large-scale studies. A general overview of the pathogenesis, biochemical markers, preclinical evidence, and translational research on anxiety and depression, which may be common in chronic diseases, could provide insight into the discovery of new therapeutic targets. In resistant HT management, it may be essential to address psychological and lifestyle factors, such as weight management and inflammation, as suggested by these findings.

Healthcare providers should consider screening for anxiety and depression in patients with HT, as these conditions may contribute to poor BP control. Furthermore, implementing strategies to address psychological lifestyle factors, such as weight management and inflammation reduction, may be vital in managing resistant HT.

Limitations of the study

First, we could not establish a causative relationship between depression and uncontrolled HT due to the cross-sectional study design. More studies and clinical trials are necessary to determine the effects of depression and anxiety on uncontrolled HT. Second, the HADS questionnaire assessed depression and anxiety, and a psychiatrist did not evaluate the scores. Third, we were unable to collect reliable information on adherence to the HT treatment used. Blood pressure levels and antihypertensive treatment benefits may affect BP control in HT patients, and our results may be biased for this reason.

Conclusions

The study found that high anxiety and depression scores were independent predictors for true resistant HT in patients with uncontrolled BP. Thus, we can use the HADS

score to assess risks in HT patients with uncontrolled BP. Emotional status is mostly neglected by medical doctors in general practice, although it might be the basis of uncontrolled but treatable HT. This oversight may cause undesirable outcomes and waste time dedicated to HT. Therefore, it is essential to screen for anxiety and depression in primary healthcare facilities while diagnosing and during follow-up in patients with arterial HT to identify high-risk groups, improve treatment strategies and prevent future adverse events.

Supplementary data

The supplementary materials are available at <https://doi.org/10.5281/zenodo.7916433>. The package contains the following files:

Supplementary Fig. 1. HADS-A was positively correlated with mean daytime systolic blood pressure ($p < 0.001$, $r = -0.235$).

Supplementary Fig. 2. HADS-A was positively correlated with mean daytime systolic blood pressure ($p = 0.001$, $r = -0.227$).

Supplementary Table 1. Mann–Whitney U, χ^2 and Student's t-test of presented statistical values.

Supplementary Table 2. Mann–Whitney U test values.

Supplementary Table 3. Multivariable binary logistic regression analysis and Nagelkerke R^2 values.

Supplementary Table 4. Shapiro–Wilk test results.

ORCID iDs

Handan Duman  <https://orcid.org/0000-0002-9519-8739>
 Hanan Duman  <https://orcid.org/0000-0002-1441-7320>
 Meltem Puşuroğlu  <https://orcid.org/0000-0002-1970-3262>
 Ahmet Seyda Yılmaz  <https://orcid.org/0000-0003-3864-4023>

References

- Forouzanfar MH, Alexander L, Anderson HR, et al. Global, regional, and national comparative risk assessment of 79 behavioural, environmental and occupational, and metabolic risks or clusters of risks in 188 countries, 1990–2013: A systematic analysis for the Global Burden of Disease Study 2013. *Lancet*. 2015;386(10010):2287–2323. doi:10.1016/S0140-6736(15)00128-2
- Van Dyne JR. Iproniazid in the treatment of resistant hypertension: A preliminary report on twenty intractable cases. *J Am Geriatr Soc*. 1960;8(6):454–462. doi:10.1111/j.1532-5415.1960.tb00410.x
- Psaty BM, Lumley T, Furberg CD, et al. Health outcomes associated with various antihypertensive therapies used as first-line agents: A network meta-analysis. *JAMA*. 2003;289(19):2534. doi:10.1001/jama.289.19.2534
- Williams B, Mancia G, Spiering W, et al. 2018 ESC/ESH Guidelines for the management of arterial hypertension. *Eur Heart J*. 2018;39(33):3021–3104. doi:10.1093/eurheartj/ehy339
- Yılmaz MB. Temporal changes in the epidemiology of diabetes mellitus in Turkey: A systematic review and meta-analysis. *Arch Turk Soc Cardiol*. 2018. doi:10.5543/tkda.2018.15679
- Daugherty SL, Powers JD, Magid DJ, et al. Incidence and prognosis of resistant hypertension in hypertensive patients. *Circulation*. 2012;125(13):1635–1642. doi:10.1161/CIRCULATIONAHA.111.068064
- Datta BK, Ansa BE, Husain MJ. An analytical model of population level uncontrolled hypertension management: A care cascade approach. *J Hum Hypertens*. 2022;36(8):726–731. doi:10.1038/s41371-021-00572-x
- Cohen BE, Edmondson D, Kronish IM. State of the art review: Depression, stress, anxiety, and cardiovascular disease. *Am J Hypertens*. 2015; 28(11):1295–1302. doi:10.1093/ajh/hpv047
- Tanaka M, Bohár Z, Vécsei L. Are kynurenines accomplices or principal villains in dementia? Maintenance of kynurenine metabolism. *Molecules*. 2020;25(3):564. doi:10.3390/molecules25030564
- Tajti J, Szok D, Csáti A, Szabó Á, Tanaka M, Vécsei L. Exploring novel therapeutic targets in the common pathogenic factors in migraine and neuropathic pain. *Int J Mol Sci*. 2023;24(4):4114. doi:10.3390/ijms24044114
- Chojdak-Lukasiewicz J, Dziadkowiak E, Zimny A, Paradowski B. Cerebral small vessel disease: A review. *Adv Clin Exp Med*. 2021;30(3):349–356. doi:10.17219/acem/131216
- Battaglia S, Cardellicchio P, Di Fazio C, Nazzi C, Fracasso A, Borgomaneri S. Stopping in (e)motion: Reactive action inhibition when facing valence-independent emotional stimuli. *Front Behav Neurosci*. 2022; 16:998714. doi:10.3389/fnbeh.2022.998714
- Carrera-González MDP, Cantón-Habas V, Rich-Ruiz M. Aging, depression and dementia: The inflammatory process. *Adv Clin Exp Med*. 2022;31(5):469–473. doi:10.17219/acem/149897
- Chen C. Recent advances in the study of the comorbidity of depressive and anxiety disorders. *Adv Clin Exp Med*. 2022;31(4):355–358. doi:10.17219/acem/147441
- FiDanci İ, Aksoy H, Ayhan Başer D, Cankurtaran M. Esansiyel Hipertansiyon Tanılı Hastalarda Anksiyete veya Depresyon Görülme Sıklıklarının Değerlendirilmesi: Retrospektif Çalışma. *Kahramanmaraş Sütçü İmam Üniversitesi Tıp Fakültesi Dergisi*. 2022;17(3):72–76. doi:10.17517/ksutfd.960125
- Lane D, Carroll D, Ring C, Beevers DG, Lip GYH. The prevalence and persistence of depression and anxiety following myocardial infarction. *Br J Health Psychol*. 2002;7(1):11–21. doi:10.1348/135910702169321
- Ruo B, Rumsfeld JS, Hlatky MA, Liu H, Browner WS, Whooley MA. Depressive symptoms and health-related quality of life: The Heart and Soul Study. *JAMA*. 2003;290(2):215. doi:10.1001/jama.290.2.215
- Rutledge T, Reis VA, Linke SE, Greenberg BH, Mills PJ. Depression in heart failure. *J Am Coll Cardiol*. 2006;48(8):1527–1537. doi:10.1016/j.jacc.2006.06.055
- Yadoğan Ü. Hipertansiyon Hastalarında Anksiyete Bozukluğu. *Konuralp Tıp Dergisi*. 2012;4(2):1–5. <https://dergipark.org.tr/tr/pub/ktd/issue/10303/126402>. Accessed October 15, 2022.
- Hackett ML, Yapa C, Parag V, Anderson CS. Frequency of depression after stroke: A systematic review of observational studies. *Stroke*. 2005;36(6):1330–1340. doi:10.1161/01.STR.0000165928.19135.35
- Johnson HM. Anxiety and hypertension: Is there a link? A literature review of the comorbidity relationship between anxiety and hypertension. *Curr Hypertens Rep*. 2019;21(9):66. doi:10.1007/s11906-019-0972-5
- Polishchuk OY, Tashchuk VK, Barchuk NI, Amelina TM, Hrechko SI, Trefanenko IV. Anxiety and depressive disorders in patients with arterial hypertension. *Wiad Lek*. 2021;74(3 cz 1):455–459. PMID:33813449.
- Duman H, Bahçeci İ, Çinier G, Duman H, Bakırcı EM, Çetin M. Left ventricular hypertrophy is associated with increased sirtuin level in newly diagnosed hypertensive patients. *Clin Exp Hypertens*. 2019; 41(6):511–515. doi:10.1080/10641963.2018.1510946
- Tanaka M, Szabó Á, Spekker E, Polyák H, Tóth F, Vécsei L. Mitochondrial impairment: A common motif in neuropsychiatric presentation? The link to the tryptophan–kynurenine metabolic system. *Cells*. 2022;11(16):2607. doi:10.3390/cells11162607
- Török N, Maszlag-Török R, Molnár K, et al. Single nucleotide polymorphisms of indoleamine 2,3-dioxygenase 1 influenced the age onset of Parkinson's disease. *Front Biosci (Landmark Ed)*. 2022;27(9):265. doi:10.31083/j.fbl2709265
- Agita A, Alsagaff MT. Inflammation, immunity, and hypertension. *Acta Med Indones*. 2017;49(2):158–165. PMID:28790231.
- Lee EC, Hong DY, Lee DH, et al. Inflammation and rho-associated protein kinase-induced brain changes in vascular dementia. *Biomedicine*. 2022;10(2):446. doi:10.3390/biomedicine10020446
- Sfera A, Hazan S, Kozlakidis Z, Klein C. Microbiota-derived psychedelics: Lessons from COVID-19. *Adv Clin Exp Med*. 2023;32(4):395–399. doi:10.17219/acem/159477
- Sherbourne CD. Comorbid anxiety disorder and the functioning and well-being of chronically ill patients of general medical providers. *Arch Gen Psychiatry*. 1996;53(10):889. doi:10.1001/archpsyc.1996.01830100035005
- Lee E, Park E. Self-care behavior and related factors in older patients with uncontrolled hypertension. *Contemporary Nurse*. 2017;53(6): 607–621. doi:10.1080/10376178.2017.1368401

31. Oliveras A, De La Sierra A. Resistant hypertension: Patient characteristics, risk factors, co-morbidities and outcomes. *J Hum Hypertens*. 2014;28(4):213–217. doi:10.1038/jhh.2013.77
32. Şahinarslan A. Consensus paper on the evaluation and treatment of resistant hypertension by the Turkish Society of Cardiology. *Anatol J Cardiol*. 2020;24(3):137–152. doi:10.14744/AnatolJCardiol.2020.74154
33. Kulach A, Stachowiak P, Prasal M, et al. A questionnaire-based, multicenter registry of resistant and pseudo-resistant arterial. *Wiad Lek*. 2019;72(10):1866–1871. PMID:31978136.
34. Pathan MK, Cohen DL. Resistant hypertension: Where are we now and where do we go from here? *IBPC*. 2020;13:83–93. doi:10.2147/IBPC.S223334
35. Bjelland I, Dahl AA, Haug TT, Neckelmann D. The validity of the Hospital Anxiety and Depression Scale. *J Psychosom Res*. 2002;52(2):69–77. doi:10.1016/S0022-3999(01)00296-3
36. Özdemir Ö, Akyüz A, Doruk H. Geriatrik Hipertansif Hastaların İlaç Tedavisine Uyumluluğu. *Bakırköy Tıp Dergisi*. 2016;12(4):195–201. doi:10.5350/BTDMJB201612404
37. Wang L, Li N, Heizhati M, et al. Association of depression with uncontrolled hypertension in primary care setting: A cross-sectional study in less-developed northwest China. *Int J Hypertens*. 2021;2021:6652228. doi:10.1155/2021/6652228
38. Aydemir O. Validity and reliability of Turkish version of Hospital Anxiety and Depression Scale [in Turkish]. *Türk Psikiyatri Derg*. 1997;8:280–287. https://www.researchgate.net/publication/284678404_VValidity_and_Reliability_of_Turkish_Version_of_Hospital_Anxiety_and_Depression_Scale. Accessed November 15, 2022.
39. Wang H, Peng J, Wang B, et al. Inconsistency between univariate and multiple logistic regressions. *Shanghai Arch Psychiatry*. 2017;29(2):124–128. doi:10.11919/j.issn.1002-0829.217031
40. Pedretti RFE, Hansen D, Ambrosetti M, et al. How to optimize the adherence to a guideline-directed medical therapy in the secondary prevention of cardiovascular diseases: A clinical consensus statement from the European Association of Preventive Cardiology. *Eur J Prev Cardiol*. 2023;30(2):149–166. doi:10.1093/eurjpc/zwac204
41. Go AS, Mozaffarian D, Roger VL, et al. Heart disease and stroke statistics: 2014 update. A report from the American Heart Association. *Circulation*. 2014;129(3):e28–e292. doi:10.1161/01.cir.0000441139.02102.80
42. Blacher J, Levy BI, Mourad JJ, Safar ME, Bakris G. From epidemiological transition to modern cardiovascular epidemiology: Hypertension in the 21st century. *Lancet*. 2016;388(10043):530–532. doi:10.1016/S0140-6736(16)00002-7
43. Daugherty SL, Powers JD, Magid DJ, et al. Incidence and prognosis of resistant hypertension in hypertensive patients. *Circulation*. 2012;125(13):1635–1642. doi:10.1161/CIRCULATIONAHA.111.068064
44. Meng R, Yu C, Liu N, et al. Association of depression with all-cause and cardiovascular disease mortality among adults in China. *JAMA Netw Open*. 2020;3(2):e1921043. doi:10.1001/jamanetworkopen.2019.21043
45. Ladwig KH, Baumert J, Marten-Mittag B, et al. Room for depressed and exhausted mood as a risk predictor for all-cause and cardiovascular mortality beyond the contribution of the classical somatic risk factors in men. *Atherosclerosis*. 2017;257:224–231. doi:10.1016/j.atherosclerosis.2016.12.003
46. Doroszko A, Janus A, Szahidewicz-Krupska E, Mazur G, Derkacz A. Resistant hypertension. *Adv Clin Exp Med*. 2016;25(1):173–183. doi:10.17219/acem/58998
47. Xiao L, Harrison DG. Inflammation in hypertension. *Can J Cardiol*. 2020;36(5):635–647. doi:10.1016/j.cjca.2020.01.013
48. Tanaka M, Tóth F, Polyák H, Szabó Á, Mándi Y, Vécsei L. Immune influencers in action: Metabolites and enzymes of the tryptophan–kynurenine metabolic pathway. *Biomedicines*. 2021;9(7):734. doi:10.3390/biomedicines9070734
49. Castro I, Waclawovsky G, Marcadenti A. Nutrition and physical activity on hypertension: Implication of current evidence and guidelines. *Curr Hypertens Rev*. 2015;11(2):91–99. doi:10.2174/1573402111666150429170302
50. Tanaka M, Vécsei L. Editorial of Special Issue “Crosstalk between Depression, Anxiety, and Dementia: Comorbidity in Behavioral Neurology and Neuropsychiatry.” *Biomedicines*. 2021;9(5):517. doi:10.3390/biomedicines9050517
51. Spruill TM, Butler MJ, Thomas SJ, et al. Association between high perceived stress over time and incident hypertension in black adults: Findings from the Jackson Heart Study. *J Am Heart Assoc*. 2019;8(21):e012139. doi:10.1161/JAHA.119.012139
52. Tanaka M, Szabó Á, Vécsei L. Integrating armchair, bench, and bedside research for behavioral neurology and neuropsychiatry: Editorial. *Biomedicines*. 2022;10(12):2999. doi:10.3390/biomedicines10122999
53. Szcześniak M, Furmańska J, Konieczny K, Widecka K, Rachubińska K. Dimensions of neurotic personality and its selected predictors in individuals with arterial hypertension. *Psychiatr Pol*. 2019;53(4):901–914. doi:10.12740/PP/100373

Efficacy of intravitreal injections of melphalan in the treatment of retinoblastoma vitreous seeding

Krzysztof Cieřlik^{A–F}, Anna Rogowska^{B,E,F}, Małgorzata Danowska^{B,E–F}, Wojciech Hautz^{C–F}

Department of Ophthalmology of the Children’s Memorial Health Institute, Warsaw, Poland

A – research concept and design; B – collection and/or assembly of data; C – data analysis and interpretation; D – writing the article; E – critical revision of the article; F – final approval of the article

Advances in Clinical and Experimental Medicine, ISSN 1899–5276 (print), ISSN 2451–2680 (online)

Adv Clin Exp Med. 2024;33(2):119–125

Address for correspondence

Krzysztof Cieřlik
E-mail: okoiooczko@gmail.com

Funding sources

None declared

Conflict of interest

None declared

Received on May 15, 2022

Reviewed on April 5, 2023

Accepted on May 15, 2023

Published online on June 1, 2023

Abstract

Background. The introduction of intravitreal injections of melphalan (IVIM) has significantly improved the efficacy of retinoblastoma treatment and the prognosis for eye preservation.

Objectives. To evaluate the results of using IVIM to treat retinoblastoma vitreous seeding.

Materials and methods. This was a clinical, retrospective, single-center study. Twenty-six children (27 eyes) who met all of the following inclusion criteria qualified for the study: 1) active vitreous seeding at the time of retinoblastoma diagnosis; 2) IVIM performed between 1 January 2017 and 30 September 2020; and 3) a minimum follow-up period of 12 months since the last IVIM. Doses of 20–40 µg melphalan per injection were used.

Results. The eye observation period from the last IVIM to the last ophthalmic examination averaged 32.41 months (median 30.00; range 13.00–56.00). Success (no active tumors in the vitreous body) was achieved in 24 eyes (88.9%), and a doubtful result (recurrence in the retina with a difficult-to-determine etiology) in 2 eyes (7.4%). In 1 eye (3.7%), despite treatment, active tumors were still present in the vitreous body. Out of all 27 eyes, 4 eyeballs were removed, but the direct cause of enucleation was not vitreous seeding. There were no complications in the form of intraocular inflammation, extraocular retinoblastoma or distant metastases. There was 1 case of anterior uveitis and 1 case of cataract.

Conclusions. The IVIM is a highly effective and safe form of treatment for retinoblastoma vitreous seeding.

Key words: therapy, retinoblastoma, injection, melphalan, intravitreal

Cite as

Cieřlik K, Rogowska A, Danowska M, Hautz W. Efficacy of intravitreal injections of melphalan in the treatment of retinoblastoma vitreous seeding. *Adv Clin Exp Med.* 2024;33(2):119–125. doi:10.17219/acem/166180

DOI

10.17219/acem/166180

Copyright

Copyright by Author(s)

This is an article distributed under the terms of the Creative Commons Attribution 3.0 Unported (CC BY 3.0) (<https://creativecommons.org/licenses/by/3.0/>)

Background

The introduction of intravitreal injections of melphalan (IVIM or, more generally, intravitreal chemotherapy (IVitC)) has significantly improved the efficacy of retinoblastoma treatment and the prognosis for eye preservation.^{1,2}

For decades, in many cases of retinoblastoma vitreous seeding (Fig. 1,2), even in patients with good visual acuity, the treatment of choice was enucleation or external beam radiotherapy, which had serious side effects. When active retinoblastoma seeding is present in the vitreous body, IVIM allows therapeutic concentrations of the chemotherapeutic agent to be achieved in the vitreous chamber.³ No other treatment is as effective in eradicating retinoblastoma seeds from the vitreous body as IVitC. The use of systemic chemotherapy, intra-arterial chemotherapy (IAC)

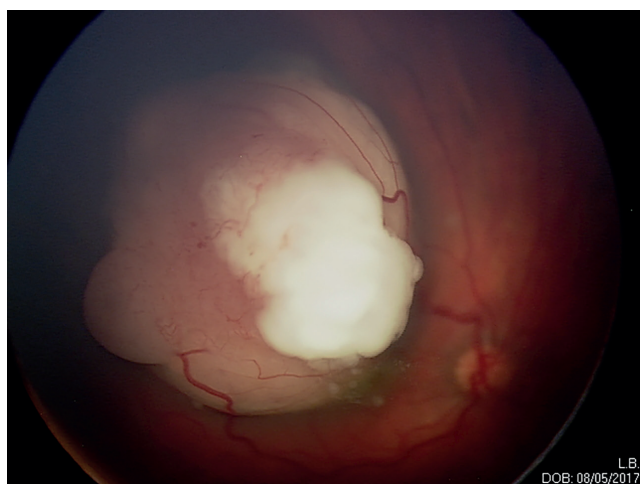


Fig. 1. Retinoblastoma before treatment. Visible perforation of the internal limiting membrane in the form of a characteristic nonvascularized “cap” on the main tumor mass. Spreading to the vitreous body can be observed below

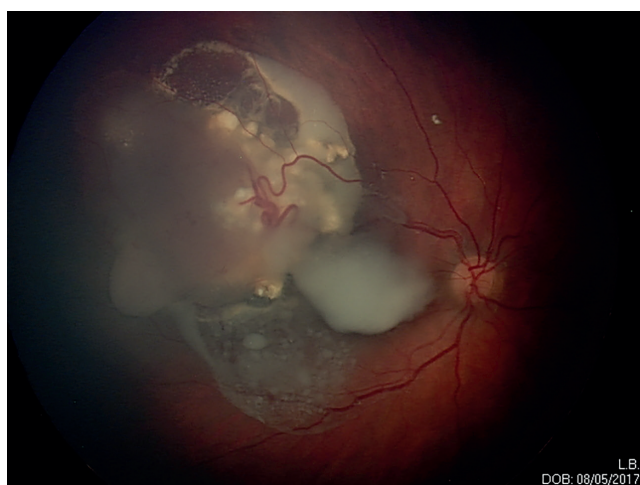


Fig. 2. The same eye after 2 intra-arterial chemotherapy (IAC) treatments. Despite the high efficacy of IAC in the treatment of retinoblastoma (retinal tumors and subretinal spreading), seeding in the vitreous body remains active. The use of intravitreal injections of melphalan (IVIM) is necessary

or periocular chemotherapy does not make it possible to achieve adequate concentrations of chemotherapeutics in this compartment because of the blood–retina barrier and the lack of blood vessels in the normal vitreous body.¹

For decades, when treating retinoblastoma, there was a concern that intravitreal injections might carry the risk of extraocular spreading of the tumor due to needle penetration of the sclera. It was not until the pioneering work of researchers in Japan that melphalan was identified as a highly effective chemotherapeutic agent against retinoblastoma cells. Effective and safe concentrations of this drug for ocular tissues were determined, and it was introduced into intra-arterial and intravitreal therapy.^{1,4–6} Further research on the safety of IVIM and dissemination of the treatment is largely due the research by Munier.^{2,3}

Objectives

The aim of this study was to determine the efficacy and safety of IVIM in the treatment of retinoblastoma vitreous seeding in patients treated at our center.

Materials and methods

This study was approved by the Ethics Committee of the Children’s Memorial Health Institute (Warsaw, Poland; approval No. 1/KBE/2022). The study was a retrospective analysis of clinical data.

Setting and participants

The study group included all patients from the Department of Ophthalmology at our center who fulfilled all 3 of the following inclusion criteria: 1) active vitreous seeding at the time of retinoblastoma diagnosis; 2) treatment with IVIM between January 1, 2017 and September 30, 2020; and 3) a follow-up period of at least 12 months since the last IVIM.

Indications and dosages of IVIM therapy

In each patient, the indication for the 1st course of IVIM was the presence of retinoblastoma in the vitreous body. The IVIM was started before the completion of primary retinoblastoma treatment (systemic or IAC). If the 1st course of IVIM failed, the eye was eligible for a 2nd course of IVIM and simultaneously for other forms of therapy, if needed (IAC or local treatment). None of the eyes qualified for a 3rd course of IVIM. A prerequisite for completion of a given course of IVIM was the absence of an active tumor in the vitreous body at the 1st follow-up examination, which was at the latest 6 weeks after the last IVIM.

The number of IVIMs and the injection dose varied between patients and differed between the 1st and eventual

2nd courses of IVIM. It depended on the severity of retinoblastoma seeding in the vitreous body at the time of qualification for IVIM and the response to IVIM therapy. Dust-like seeds localized in 1 quadrant of the vitreous body were an indication to schedule fewer injections (1 or 2 IVIMs) and use a lower single dose (20 µg or 25 µg). Seeding consisting of spheres or larger tumor fragments or those occupying 2 or more quadrants were indications to schedule more injections (3 or more) and use a higher single dose (30 µg). Some patients received different doses in successive injections (IVIM was started with higher doses that were then reduced to minimize toxicity). Individual injections were planned at intervals of 1–2 weeks.

Criteria for assessing the success of IVIM therapy

The efficacy of IVIM was assessed in follow-up examinations under general anesthesia. Patients underwent follow-up sessions every 1–2 months in the 1st year after treatment, then every 2–6 months.

We considered the IVIM therapy to be successful if there were no active tumors in the vitreous body and no active tumors on the retina originating from the vitreous body. We considered the IVIM therapy to be a failure in the case of the presence of active retinoblastoma in the vitreous body (recurrence or tumor not responding to treatment) or the appearance of new active tumors on the retina originating from the vitreous. We did not consider the therapy to be a failure in the case of the presence of an active retinal tumor originating from the retina or in the case of enucleation if it was performed for reasons other than an active tumor in the vitreous body or an active tumor on the retina originating from the vitreous body. We considered the presence of an active retinal tumor of difficult-to-determine etiology to be a doubtful result (i.e., it was not possible to exclude its origin from seeding in the vitreous body).

IVIM surgical technique

At the time of qualification for IVIM, a seed-free quadrant was chosen as the injection site. The most frequently chosen location was the 11 o'clock meridian. The skin of the eyelids was cleaned with a solution of 10% povidone-iodine (PI) and then the conjunctival sac was cleaned with with 5% PI eye drops for 1 min. The needle insertion site was planned 2.0–3.5 mm from the corneal limbus (depending on the child's age). An injection of 20–40 µg of melphalan in a volume of 0.02–0.04 mL was performed with a 30G × ½" needle (0.3 × 13 mm). The injection was followed by applying cryotherapy at the injection site during needle withdrawal or a subconjunctival injection of 0.005 µg of melphalan in a volume of 0.005 mL. Finally, the conjunctival sac was rinsed with AquaPro injection solution.

During the study period, we used the following melphalan preparations, subject to availability: Melphalan

Tillomed 50 mg, Aspen Melphalan 50 mg, or Mederan Melphalan 50 mg.

Systemic or intra-arterial chemotherapy

All patients who qualified for the study were administered systemic chemotherapy (VEC – vincristine, etoposide and carboplatin), intra-arterial chemotherapy or a combination of both, as primary treatment for retinoblastoma. Systemic chemotherapy, as standard, consisted of 6 cycles of VEC administered at 3-week intervals. The IAC, as standard, consisted of 3 courses of melphalan, topotecan and carboplatin at intervals of 3–4 weeks. The VEC+IAC combination consisted of 2 courses of VEC followed by 3 courses of IAC.

Participants

Twenty-seven eyes of 26 children (15 boys and 11 girls) were eligible for the study (1 child had IVIM administered to both eyes). The mean age at retinoblastoma diagnosis was 28.04 months (median 26.00; range 2.00–83.00). Bilateral retinoblastoma was diagnosed in 9 patients, and unilateral retinoblastoma was diagnosed in 17 children. All patients were Caucasian (relatively low amounts of pigment in the eye tissues).

At the time of diagnosis, the eyes were classified according to the International Classification for Retinoblastoma, as modified by Shields, into the following groups: A – 0 eyes, B – 0 eyes, C – 7 eyes, D – 15 eyes, and E – 5 eyes.⁷ Retinoblastoma seeding in the vitreous body found at the time of diagnosis was retrospectively classified according to Munier's classification into the following groups: dust – 12 eyes, spheres – 8 eyes, clouds – 3 eyes, and no data – 4 eyes.³ The eye observation period from the last IVIM to the last ophthalmic examination averaged 32.41 months (median 30.00; range 13.00–56.00).

First course of IVIM

All patients were administered a 1st course of IVIM to treat retinoblastoma seeding in the vitreous body. The mean number of injections during the 1st course of IVIM was 3.41 (median: 3.00, range: 1.00–8.00). The single doses of melphalan used in the 1st course of IVIM were 20 µg – 42 injections (46.2%), 25 µg – 19 injections (20.9%), 30 µg – 29 injections (31.9%), and 40 µg – 1 injection (1.1%). The mean cumulative dose of melphalan per eye in the 1st course of IVIM was 83.33 µg (median: 80.00, range: 30.00–200.00).

Second course of IVIM

If the 1st course of IVIM failed, a 2nd course of IVIM was administered. The mean number of injections during the 2nd course of IVIM was 2.83 (median: 3.00, range: 2.00–4.00).

The single doses of melphalan used in the 2nd course of IVIM were 20 µg – 4 injections (23.5%), 25 µg – 5 injections (29.4%) and 30 µg – 8 injections (47.1%). The mean cumulative dose of melphalan per eye in the 2nd course of IVIM was 74.17 µg (median: 67.50, range: 55.0–120.00).

Systemic or intra-arterial chemotherapy

During the 1st IVIM cycle, the following were used as primary treatments for retinoblastoma: systemic chemotherapy only – 3 eyes, IAC only – 9 eyes and VEC+IAC combination – 15 eyes. During the 2nd IVIM cycle, the following were administered: IAC only – 4 eyes, and neither IAC nor systemic chemotherapy – 2 eyes.

Results

The results of IVIM treatment (after the 1st and 2nd courses of IVIM combined) are shown in Table 1. The eye classified in the treatment failure group had active seeding in the vitreous body at the time of enucleation, despite 6 IVIMs, and a subretinal recurrence. Seeding in the vitreous body was not the direct cause of any enucleations.

Table 1. Results of IVIM treatment (after the 1st and 2nd course of IVIM combined)

Result of treatment	Number of eyes	Enucleations
Success	24 eyes (88.9%)	1
Doubtful	2 eyes (7.4%)	2
Failure	1 eye (3.7%)	1

IVIM – intravitreal injections of melphalan.

Results of the 1st course of IVIM

The 1st course of IVIM was successful in 20 eyes (74.1% of 27 eyes). No form of retinoblastoma recurrence was found in 16 eyes (59.3% of 27 eyes). In 4 eyes (14.8% of 27 eyes), a recurrence was found on or under the retina, probably not originating from the vitreous body (one of those eyes was later removed due to a recurrence anterior to the ora serrata).

Failure of the 1st course of IVIM was observed in 7 eyes (25.9% of 27 eyes). No adequate response was found in 1 eye (3.7% of 27 eyes); the tumor remained active in the vitreous body, and there was a recurrence under the retina, which was the immediate cause of eye removal. Recurrence in the vitreous body was found in 4 eyes (14.8% of 27 eyes). A retinal recurrence, probably originating from the vitreous body, was found in 2 eyes (7.4% of 27 eyes).

The time to recurrence in the vitreous body from the last IVIM injection (4 eyes after the 1st course of IVIM) averaged 11.50 months (median: 5.00, range: 2.00–34.00).

The time to retinal recurrence from the last IVIM (2 eyes after the 1st course of IVIM), probably originating from

persistent retinal cells in the vitreous body, was, on average, 5 months (4 months and 6 months).

Results of the 2nd course of IVIM

Six eyes were eligible for a 2nd course of IVIM. After it, no recurrence was observed in 4 eyes. A difficult-to-interpret result was reported in 2 eyes. One of those eyes was removed 1 month after completion of the 2nd course of IVIM due to a lack of retinal tumor response to IAC. The short follow-up period for this eye makes it impossible to determine the efficacy of the 2nd course of IVIM. The 2nd of those eyes, 1 month after completion of the 2nd course of IVIM, had a recurrence on the retina with a difficult-to-determine etiology, and was removed after a further 7 months due to a recurrence near the main tumor mass (this recurrence did not originate from the vitreous body).

Complications after IVIM

One patient developed anterior uveitis the day after IVIM, which was probably due to the administration of melphalan under the conjunctiva as a form of prevention of local spreading of retinoblastoma through the injection site. In 2 patients, sharply demarcated, semicircular in shape, retinal and choroidal atrophy was found on the fundus around the IVIM insertion site on the periphery of the retina near the ora serrata. One patient was diagnosed with a cataract 21 months after the last IVIM injection. No patient was diagnosed with intraocular inflammation, extraocular spreading of retinoblastoma, or distant metastases. None of the patients died.

Discussion

Numerous factors can significantly influence the effectiveness of IVIM treatment of retinoblastoma seeding in the vitreous body: IVIM procedure technique, number of IVIM injections and individual injection doses, diameter of the seeds in the vitreous body, concomitant treatment (IAC and systemic chemotherapy), diameter of the eyeball, presence of posterior vitreous detachment, time interval between IVIM injections, sensitivity of cells with a given genetic mutation to melphalan, and type of melphalan preparation used.^{1,3,8–11}

Based on the results of the therapy of our previously treated patients and the group of patients discussed here, it seems that a single IVIM dose of 20 µg is too low. The initial response of the seeding in the vitreous body is very good, and the tumors become invisible, but within a few months, recurrences in the vitreous body appear. As recommended by Munier, the 20 µg dose should be reserved for the smallest eyeballs because it allows the therapeutic concentration of melphalan to be achieved in only a small volume of the vitreous chamber.¹² Our study was conducted at a time when

we tried to decrease the single dose of 30 µg melphalan to lower doses of 25 µg or 20 µg to reduce retinal toxicity, but we did see an increase in the number of recurrences of retinoblastoma in the vitreous body, which we had not observed before in patients with the 30 µg dose. Liao et al. published a comparison of 2 groups of patients receiving doses of 25 µg or 30 µg, finding no statistically significant difference in retinal toxicity between these groups based on the results of electroretinography (ERG) tests.¹³ Currently, the dose we use most frequently is 30 µg. In the case of massive seeding in the vitreous body and a high risk of perioperative extraocular spreading (seeding occupying a very large part of the vitreous body), we start with an initial dose of up to 40 µg and reduce subsequent doses to 30 µg.

Another issue is the number of IVIM injections. From 2012, in the early days of IVIM at our center, we administered only 1 dose of melphalan – 30 µg. After a very good initial response to treatment, we observed recurrences in the vitreous body at a later time. Currently, based on the results of our study and the literature, we use a dose of 30 µg for retinoblastoma seeding in the vitreous body, repeated a minimum of 3 times if “dust” (according to Munier’s classification) is present, 4–5 times if “spheres” are present, and up to 8 times if large retinoblastoma fragments detached from the main tumor mass are found.³ The interval between injections is 1–2 weeks.

Late recurrences originating from persistent retinal cells in the vitreous body are a major problem.^{1,14,15} In our study, the longest follow-up period after which recurrence was observed was almost 3 years (34 months). After such a long period, ophthalmological screenings become less frequent, and tumors can grow significantly in the interval between examinations, necessitating not only the administration of IVIM but often renewed IAC as well. It is, therefore, extremely important to dose the drugs appropriately (number of injections and single dosages) to avoid late recurrence of retinoblastoma in the vitreous body or on the retinal surface. Berry et al. described a relationship between the occurrence of more severe IVIM toxicity of the retina and a lower rate of recurrence in the vitreous body, as well as a lower rate of secondary enucleation.¹⁴

Despite the use of relatively low doses of melphalan in IVIM during the analyzed period, active seeding in the vitreous body alone was not the direct cause of any enucleation in our patient group. In the event of recurrence of a retinoblastoma in the vitreous body, we performed a 2nd course of IVIM. The only eye classified in the treatment failure group was enucleated because of a subretinal recurrence and not because of seeding in the vitreous body.

Causes of retinoblastoma seeding in the vitreous body may include perforation of the internal limiting membrane (ILM) in the form of a characteristic hypovascularized “cap” on the retinal surface (Fig. 1), large size of the endophytic tumor, and the use of certain therapeutic methods, such as laser photocoagulation and transpupillary thermotherapy.^{3,12}

Prophylactic administration of IVIM should be considered if the above risk factors for vitreous seeding are present. Based on experience, it appears that a dose of 20 µg is insufficient, even as a preventative measure. In the case of the above risk factors, we currently administer 2 injections of 30 µg IVIM.

Munier’s “dust, spheres and clouds” classification could possibly be enhanced with a “high risk of seeding” point referring to a condition in which ILM puncture occurs or a large endophytic tumor is found without obvious seeding in the vitreous body.

Any active retinoblastoma seeds in the vitreous cavity at the time of diagnosis, therapy or follow-up should be an indication to plan more IVIM. At our center, the decision to plan IVIM is most often made at the time of diagnosis because later, after IAC or systemic chemotherapy, retinoblastoma seeds usually disappear from the vitreous body; however, if not treated with IVIM, they will most often reoccur.

A space with an increased concentration of melphalan is created around the needle in the vitreous body when melphalan is administered.^{3,8} For this reason, retinal atrophy is observed at the puncture site, but at the same time, the risk of retinoblastoma spreading beyond the eyeball through this site is low. We have noted that the area of pigment regrouping at the puncture site has a semi-circular shape and a very clear boundary. It appears that this may be due to reflux of melphalan along the needle remaining in the vitreous body (in children with thick gel consistency) and partial displacement of the injected drug through the hole created by the needle in the base of the vitreous body into the space between the vitreous body and the retina. If this actually occurs, as described above, the risk of extraocular spreading of the retinoblastoma through the injection orifice should be relatively low. It is likely that the focus of choroidal atrophy around the insertion site is a result of the higher concentration of the chemotherapeutic agent at this site.

We perform cryotherapy at the injection site during the 1st course of IVIM when viable tumor cells in the vitreous are most abundant, as well as during subsequent rounds of treatment if we believe there is still an increased risk of extraocular spreading. There are no studies that support the effectiveness of IVIM injection site cryotherapy in preventing extraocular spreading. Cryotherapy induces tissue necrosis around the needle track, which may impair postoperative wound healing and paradoxically facilitate spreading.

In the past, instead of cryotherapy at the injection site, we used a subconjunctival injection of melphalan. We stopped performing this procedure because of the single complication of anterior uveitis described above. This complication appears to have occurred due to an unintentional overdosing of melphalan administered under the conjunctiva. To perform subconjunctival injections safely, a separate puncture with a 2nd syringe and needle

is needed. The subconjunctival dose we used was 0.005 μg in a volume of 0.005 mL.

During IVIM, we administer melphalan into the vitreous chamber in a very small volume of fluid (30 μg of melphalan in 0.03 mL) in order to minimize the possibility of reflux outside the eyeball and an increase in intraocular pressure, with all its consequences.

The IVIM is planned before the completion of systemic or intra-arterial chemotherapy so that IVIM is administered during the period of the lowest tumor activity. The administration of a course of systemic chemotherapy or IAC after the 1st IVIM injection reduces the possibility of extraocular spreading. Starting IVIM treatment before systemic chemotherapy or IAC would pose a higher risk of extraocular spreading due to the large number of viable tumor cells.

There are various techniques for administering IVIM. One technique, promoted by Munier, includes paracentesis of the anterior chamber and aspiration of the same volume of fluid that is then injected into the vitreous chamber. Melphalan is then administered in a relatively large volume of fluid into the anterior vitreous body to the area immediately behind the lens. When the needle is withdrawn, cryotherapy is applied at the injection site, and the eye is shaken to distribute the drug evenly.³ Yu et al. proposed a more precise method of administering melphalan into the area of the retinoblastoma seeding in the vitreous body using an indirect ophthalmoscope.¹⁵ The technique used in our center is similar to standard intravitreal injections of anti-VEGF preparations, taking into account the specificity of retinoblastomas. There are no studies proving superior efficacy or safety of any of the IVIM techniques. Our IVIM technique is easier, cheaper and faster, and significantly reduces the number of manipulations performed on the eye and the risk of mechanical or toxic damage to the lens. Compared to the techniques described by Suzuki et al., Munier, Francis et al., and Yu et al., we use the smallest volume of injected fluids.^{1,3,8,15,16} In the course of any IVIM technique, care should be taken when performing ultrasound before the procedure to ensure that the needle does not enter the retrohyaloid space created after the rapid regression of a large tumor because then the administration of a standard dose of melphalan may cause retinal atrophy in the entire area under the detached vitreous body. A similar complication can arise from unintentional insertion of the needle tip into Cloquet's canal.

At our center, we do not perform eyeball shaking with tweezers immediately after IVIM to distribute melphalan throughout the vitreous body (some authors recommend such shaking).^{1,3} It is not recommended after injections of other agents, such as anti-VEGF for example. Our observations of the fluorescence of intravitreal topotecan indicate a relatively rapid (within minutes) diffusion of this drug into the vitreous chamber. There are no published studies indicating the superior efficacy of the treatment

of retinoblastoma seeding with IVIM combined with ocular shaking compared to IVIM without shaking.

We do not use IVIM to treat solid tumors of the retina, as proposed by other authors.^{9,14} This is because we have observed a lack of noticeable changes in solid retinal tumors after treatment with IVIM during ophthalmoscopic examination.

Limitations of the study


There are 2 main limitations to this study. First, the nature of qualifying eyes into appropriate groups when assessing treatment outcomes is partially subjective. Second, the follow-up period for the regression of tumors in the vitreous body was relatively short.


Conclusions


The IVIM is a highly effective and safe form of treatment for retinoblastoma vitreous seeding. It enables the preservation of eyes in patients for whom, in the past, the only effective treatment was external radiotherapy or enucleation.

ORCID iDs

Krzysztof Cieřlik  <https://orcid.org/0000-0002-8322-4987>

Anna Rogowska  <https://orcid.org/0000-0002-6370-7180>

Małgorzata Danowska  <https://orcid.org/0000-0002-8215-0939>

Wojciech Hautz  <https://orcid.org/0000-0003-2065-8646>

References

- Suzuki S, Aihara Y, Fujiwara M, Sano S, Kaneko A. Intravitreal injection of melphalan for intraocular retinoblastoma. *Jpn J Ophthalmol*. 2015;59(3):164–172. doi:10.1007/s10384-015-0378-0
- Munier FL, Gaillard MC, Balmer A, et al. Intravitreal chemotherapy for vitreous disease in retinoblastoma revisited: From prohibition to conditional indications. *Br J Ophthalmol*. 2012;96(8):1078–1083. doi:10.1136/bjophthalmol-2011-301450
- Munier FL. Classification and management of seeds in retinoblastoma [Ellsworth Lecture, Ghent, Belgium, August 24th 2013]. *Ophthalmic Genet*. 2014;35(4):193–207. doi:10.3109/13816810.2014.973045
- Kaneko A, Suzuki S. Eye-preservation treatment of retinoblastoma with vitreous seeding. *Jpn J Clin Oncol*. 2003;33(12):601–607. PMID:14769836.
- Inomata M, Kaneko A. Chemosensitivity profiles of primary and cultured human retinoblastoma cells in a human tumor clonogenic assay. *Jpn J Cancer Res*. 1987;78(8):858–868. PMID:3115934.
- Ueda M, Tanabe J, Inomata M, Kaneko A, Kimura T. Study on conservative treatment of retinoblastoma: Effect of intravitreal injection of melphalan on the rabbit retina [in Japanese]. *Nippon Ganka Gakkai Zasshi*. 1995;99(11):1230–1235. PMID:8533651.
- Shields CL, Mashayekhi A, Au AK, et al. The international classification of retinoblastoma predicts chemoreduction success. *Ophthalmology*. 2006;113(12):2276–2280. doi:10.1016/j.ophtha.2006.06.018
- Francis JH, Brodie SE, Marr B, Zabor EC, Mondesire-Crumpl, Abramson DH. Efficacy and toxicity of intravitreal chemotherapy for retinoblastoma: Four-year experience. *Ophthalmology*. 2017;124(4):488–495. doi:10.1016/j.ophtha.2016.12.015
- Abramson DH, Ji X, Francis JH, Catalanotti F, Brodie SE, Habib L. Intravitreal chemotherapy in retinoblastoma: Expanded use beyond intravitreal seeds. *Br J Ophthalmol*. 2019;103(4):488–493. doi:10.1136/bjophthalmol-2018-312037
- Francis JH, Habib LA, Abramson DH. Vitreous disease in retinoblastoma. *Adv Ophthalmol Optom*. 2017;2(1):177–195. doi:10.1016/j.yaoo.2017.03.008

11. Hsieh T, Liao A, Francis JH, et al. Comparison of efficacy and toxicity of intravitreal melphalan formulations for retinoblastoma. *PLoS One*. 2020;15(7):e0235016. doi:10.1371/journal.pone.0235016
12. Munier FL, Beck-Popovic M, Chantada GL, et al. Conservative management of retinoblastoma: Challenging orthodoxy without compromising the state of metastatic grace. "Alive, with good vision and no comorbidity." *Prog Retin Eye Res*. 2019;73:100764. doi:10.1016/j.preteyeres.2019.05.005
13. Liao A, Hsieh T, Francis JH, et al. Toxicity and efficacy of intravitreal melphalan for retinoblastoma: 25 µg vs 30 µg. *Retina*. 2021;41(1):208–212. doi:10.1097/IAE.0000000000002782
14. Berry JL, Kim ME, Pefkianaki M, et al. Intravitreal melphalan for retinoblastoma: The impact of toxicity on recurrence and ultimate globe salvage. *Ocul Oncol Pathol*. 2020;6(6):388–394. doi:10.1159/000509080
15. Yu MD, Dalvin LA, Welch RJ, Shields CL. Precision intravitreal chemotherapy for localized vitreous seeding of retinoblastoma. *Ocul Oncol Pathol*. 2019;5(4):284–289. doi:10.1159/000491432
16. Yousef YA, Al Jboor M, Mohammad M, et al. Safety and efficacy of intravitreal chemotherapy (melphalan) to treat vitreous seeds in retinoblastoma. *Front Pharmacol*. 2021;12:696787. doi:10.3389/fphar.2021.696787

Oligoclonal gammopathy: An analysis of 253 cases

Kajetan Karaszewski^{1,B–D}, Marcin Jasiński^{1,2,B,D,E}, Anna Waszczuk-Gajda^{1,A,E,F},
Anna Rodziewicz-Lurzyńska^{3,B,E}, Olga Ciepela^{4,A,B,E}, Wiesław Wiktor Jędrzejczak^{1,A,D–F}

¹ Department of Hematology, Transplantation and Internal Medicine, Medical University of Warsaw, Poland

² Doctoral School, Medical University of Warsaw, Poland

³ Central Laboratory, University Clinical Center of the Medical University of Warsaw, Poland

⁴ Department of Laboratory Medicine, Medical University of Warsaw, Poland

A – research concept and design; B – collection and/or assembly of data; C – data analysis and interpretation;

D – writing the article; E – critical revision of the article; F – final approval of the article

Advances in Clinical and Experimental Medicine, ISSN 1899–5276 (print), ISSN 2451–2680 (online)

Adv Clin Exp Med. 2024;33(2):127–134

Address for correspondence

Marcin Jasiński

E-mail: marcin.jasinski@wum.edu.pl

Funding sources

None declared

Conflict of interest

None declared

Received on December 4, 2022

Reviewed on April 16, 2023

Accepted on May 18, 2023

Published online on June 21, 2023

Cite as

Karaszewski K, Jasiński M, Waszczuk-Gajda A, Rodziewicz-Lurzyńska A, Ciepela O, Jędrzejczak WW. Oligoclonal gammopathy: An analysis of 253 cases. *Adv Clin Exp Med.* 2024;33(2):127–134. doi:10.17219/acem/166297

DOI

10.17219/acem/166297

Copyright

Copyright by Author(s)

This is an article distributed under the terms of the Creative Commons Attribution 3.0 Unported (CC BY 3.0) (<https://creativecommons.org/licenses/by/3.0/>)

Abstract

Background. Oligoclonal gammopathy (OG) is a rare disorder of the lymphoid system that is characterized by the presence of at least 2 distinct monoclonal proteins in a patient's serum or urine. The biological and clinical characteristics of this disease are as yet poorly understood.

Objectives. The study aimed to assess whether there are significant differences between patients with OG regarding the developmental history (i.e., OG diagnosed at the first presentation compared to OG that has developed in patients with an original monoclonal gammopathy) and the number of monoclonal proteins (2 compared to 3). Moreover, we attempted to determine when secondary oligoclonality develops following the original diagnosis of monoclonal gammopathy.

Materials and methods. Patients were analyzed with regard to their age at diagnosis, sex, serum monoclonal proteins, and underlying hematological disorders. Multiple myeloma (MM) patients were additionally evaluated for their Durie–Salmon stage and cytogenetic alterations.

Results. Patients with triclonal gammopathy (TG: $n = 29$) did not differ significantly from patients with biclonal gammopathy (BG: $n = 223$) ($p = 0.81$) in terms of age at diagnosis and the dominant diagnosis (MM was the most common diagnosis (65.0% and 64.7%, respectively)). In both cohorts, myeloma patients were mainly classified to the Durie–Salmon stage III. In the TG cohort, there was a higher proportion of males (69.0%) than among patients with BG (52.5%). Oligoclonality developed at various times after diagnosis (up to 80 months in the investigated cohort). However, the occurrence of new cases was higher during the initial 30-month period following the diagnosis of monoclonal gammopathy.

Conclusions. There are only small differences between patients with primary compared to secondary OG, between BG and TG, and most patients have a combination of IgGκ+IgGλ. Oligoclonality could develop at any time after the diagnosis of monoclonal gammopathy, but it happens more frequently during the first 30 months, with advanced myeloma being the most prevalent underlying disorder.

Key words: immunofixation, multiple myeloma, oligoclonal gammopathy, biclonal gammopathy, triclonal gammopathy

Background

Oligoclonal gammopathy (OG) is a clinical condition characterized by the production of at least 2 separate monoclonal components (M-proteins) detectable in serum or urine. Their presence might be the result of the proliferation of more than 1 clone of pathological plasma cells, or the result of the production of distinct proteins by 1 specific clone.^{1,2} Despite the seemingly low probability of the first alternative, it has already been confirmed by the analyses of mutational profiles that 2 distinct populations of neoplastic plasma cells may exist in an individual patient.^{1,3} Most of the previously published literature concerns biclonal gammopathy (BG). However, the term ‘triclonal gammopathy’ (TG) is also used.^{4,5} Other names, such as ‘biclonal paraproteinemia’ or ‘double gammopathy’ have already been relegated to history.¹ However, pathologists might refer to the manifestation of biclonal gammopathy as ‘double gammopathy manifestation’.²

At least 2 distinct monoclonal proteins can be identified in 1–6% of gammopathies.^{6–8} The specific types of gammopathy include biclonal gammopathy of undetermined significance (BGUS),⁶ together with asymptomatic and symptomatic multiple myeloma (MM). The last one likely develops from a previously diagnosed monoclonal gammopathy of undetermined significance (MGUS)⁴ and other plasma cell dyscrasia, such as light chain amyloidosis. However, the spectrum of hematologic diagnoses identified in patients with OG is not limited to plasma cell dyscrasias. Other underlying abnormalities include lymphoid malignancies (e.g., chronic lymphocytic leukemia, diffuse large B-cell lymphoma or follicular lymphoma) or myeloid malignancies (e.g., acute myeloid leukemia, acute prolymphocytic leukemia or myelodysplastic syndrome).⁶

According to the published data, the clinical picture and response to therapy in patients with biclonal myeloma are similar to those observed in patients with monoclonal myeloma.^{2,9} However, it is still unknown whether the presence of 2nd or further monoclonal proteins affects the incidence or aggressiveness of potential relapse. Based on these results, authors have recommended identical treatment approaches for both groups of patients.⁹

Unfortunately, most of the data on biclonal and triclonal gammopathies come from case reports.^{10–13} Hence, more research is still needed on this subject to determine if there are any specific differences between the conditions.

Objectives

This study aimed to assess the differences between patients in whom OG was recognized during initial diagnosis (further termed as ‘primary OG’) and the remaining patients who had OG diagnosed later (‘secondary OG’).

In secondary OG, we evaluated the time at which the abnormality developed. Then, we evaluated the underlying hematopoietic disorders and possible differences between biclonal and triclonal gammopathies. Moreover, we assessed whether there are differences in the contribution of various monoclonal proteins as indicators of biclonality and triclinality.

Materials and methods

Study design

In this retrospective study, we searched a database of a large, 1000-bed hospital Serum Protein Electrophoresis (SPEP) Laboratory for results containing at least 2 distinct peaks of monoclonal proteins verified with immunofixation (OG). Their presence was the only inclusion criterion in our study. Next, we extracted clinical data from the hospital records of the patients to be included in the study.

Setting

The analysis concerned the results of serum immunofixation of patients who had this test performed during the period from January 2017 to December 2020, and relevant clinical data from all available patient records of those who met the criterion of OG. Data were collected from January 2021 to November 2021.

Participants

We identified 253 patients who met the criterion of OG (137 males and 116 females, 54.2% and 45.8%, respectively) and subsequently analyzed their hospital records. Then, we identified a group of 13 patients with primary OG, that is OG at initial presentation prior to any treatment. The remaining 240 patients had secondary OG, in whom the 2nd peak of monoclonal protein developed later during observation and/or treatment.

Variables

The data available for this study included the patient’s age and sex (available for all patients, $n = 253$), types of monoclonal proteins (2 or more) detectable in the patient’s serum (available for all patients diagnosed during the 4-year period from January 2017 to December 2020 ($n = 253$)), the type of hematopoietic disorder they were diagnosed with (available for $n = 154$ (60.9%)), the date of diagnosis (available for $n = 86$ (34%), the period from 2005 to 2020), Durie–Salmon stage for myeloma patients (available for $n = 69$ (27.3%)), and specific cytogenetic alterations ($n = 16$ (6.3%)).

Data sources

All included data were collected exclusively from the mentioned sources, namely laboratory results and patient hospital records.

Study size

The patients were chosen as participants of the study only based on the results of immunofixation. No other criteria were used for the selection of the participants. The study size of 253 was chosen to maximize the chances of identifying primary OG patients (the smaller portion of the overall cohort) and to minimize the period of observation (4 years).

Quantitative variables

Quantitative variables were analyzed and compared in terms of means, medians and 95% confidence intervals (95% CIs).

Statistical analyses

Comparative analyses were performed using age to segregate the patients. The arranged cohorts were compared with the use of Welch's t-test, with a statistical significance threshold of $p < 0.05$. The normal distribution of the data in the analyzed cohorts was verified using Shapiro–Wilk test, with a threshold of $p < 0.05$ necessary to reject the hypothesis of normality.

Results

Among 253 subjects, 223 patients had 2 distinct M-proteins detectable in serum. In addition, 29 patients had confirmed TG, and 1 patient presented with 4 distinct M-proteins. Cohort sizes and further information are presented in Fig. 1. In the BG patients, the following combinations of M-proteins were the most common: IgG κ +IgG λ (n = 77), IgG λ +IgM κ (n = 21), IgG κ +IgM λ (n = 19), IgG κ +IgM κ (n = 16), IgG κ +IgA κ (n = 14), IgG λ +IgA κ (n = 13), IgG λ +IgA λ (n = 10), IgG λ +IgM λ (n = 8), IgM κ +IgM λ

(n = 8), IgG κ +IgA λ (n = 7), and IgG κ +IgG λ +IgM κ (n = 7), without regard to which M-protein was dominant. The remaining combinations of monoclonal proteins (n = 53) were considered miscellaneous to the analysis (the incidence of each combination did not exceed 5 cases). These particular combinations often included less common M-proteins, such as free light chains (κ or λ), free heavy chains (IgG, IgA or IgE), or immunoglobulins (IgE λ or IgD λ).

In TG, the following combinations were found: IgG κ +IgG λ +IgM κ (n = 7), IgG κ +IgG λ +IgM λ (n = 2), IgG κ +IgG λ +free κ chain (n = 2), IgG κ +IgA κ +IgM λ (n = 2), IgG λ +IgA κ +free λ chain (n = 2), IgG λ +IgA κ +IgA λ (n = 1), IgG κ +IgA κ +IgA λ (n = 1), IgG κ +IgG λ +IgA κ (n = 1), IgG κ +IgG λ +IgA λ (n = 1), IgG κ +IgG λ +free κ chain (n = 1), IgG κ +IgG λ +free λ chain (n = 1), IgG λ +IgA κ +free κ chain (n = 1), IgG λ +IgA λ +free λ chain (n = 1), IgG κ +IgM κ +free κ chain (n = 1), IgG κ +IgM κ +free λ chain (n = 1), IgG κ +IgM κ +IgM λ (n = 1), IgG κ +IgD λ +free λ chain (n = 1), IgG κ +IgM κ +free IgG heavy chain (n = 1), and IgG κ +IgM λ +free IgG heavy chain (n = 1), without regard to which M-protein was dominant.

Interestingly, free light chains were found in 29 combinations (n = 18 with λ and n = 11 with κ), 12 of which were found among patients with TG (n = 29). The patient with 4 distinct M-proteins also had a detectable free light chain band.

The distribution of M-protein types with their categorization into dominant and secondary M-proteins is shown in Table 1. Analogous results, selectively for TG cases, are shown in Table 2. An individual case of OG with 4 distinct monoclonal proteins displayed the combination of IgG λ +free λ chain+IgG κ +IgM λ .

The patients with primary OG (n = 13) were analyzed separately for the types of M-proteins they produced, which were as follows: IgG κ +IgG λ (n = 3), IgG κ +IgG κ (n = 1), IgG λ +IgA λ (n = 1), IgG κ +IgM κ (n = 1), IgG κ +IgA heavy chain (n = 1), IgG κ +IgA λ (n = 1), IgG λ +IgM κ (n = 1), IgG λ +IgA κ +free light chain λ (n = 1), IgG λ +IgM κ +free light chain λ (n = 1), IgG λ +IgA λ +free light chain λ (n = 1), and IgG κ +IgA λ +free light chain κ (n = 1). The occurrence of IgG κ +IgG λ 3 times among these patients corresponded to the high incidence of this combination of M-proteins in the entire cohort (77 cases, >30% of all combinations) in comparison to other combinations. However, 4 out of 13 patients with primary OG had a specific combination of 2 immunoglobulins + free light chain. There were only 12 such combinations in the entire cohort.

We further investigated whether there is a specific time preference for the development of secondary oligoclonality after the initial diagnosis of monoclonal gammopathy (Fig. 2). As shown, the curve is biphasic, with faster development of biconality during the first 30 months after the diagnosis and a slower rate at later timepoint. However, there is no specific timepoint in which the risk of oligoclonality development is increased compared to other timepoints, or a time when it no longer occurs.

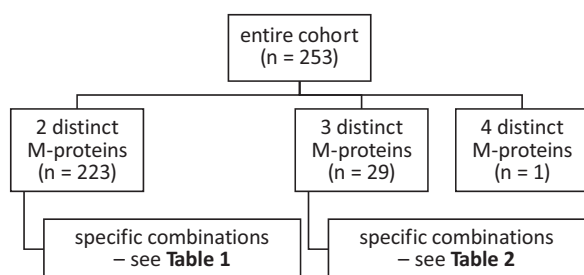


Fig. 1. Sample sizes depending on the number of monoclonal proteins detected with immunofixation

Table 1. Distribution of the most common combinations of monoclonal proteins in the entire cohort (n = 253) regarding dominant and secondary M-proteins

Combination of monoclonal proteins	Incidence
IgGκ+IgGλ	57
IgGλ+IgGκ	20
IgGλ+IgMκ	15
IgMκ+IgGλ	6
IgGκ+IgMλ	14
IgMλ+IgGκ	5
IgGκ+IgMκ	9
IgMκ+IgGκ	7
IgGκ+IgAκ	7
IgAκ+IgGκ	7
IgAκ+IgGλ	7
IgGλ+IgAκ	6
IgGλ+IgAλ	6
IgAλ+IgGλ	4
IgGλ+IgMλ	6
IgMλ+IgGλ	2
IgMκ+IgMλ	8
IgMλ+IgMκ	–
IgAλ+IgGκ	5
IgGκ+IgAλ	2

In each combination, the dominant protein is written first, followed by the secondary protein. Apart from included combinations, there were miscellaneous combinations of M-proteins. These combinations often included free light chains (κ or λ), free heavy chains (IgG, IgA or IgE) and immunoglobulins (IgEλ or IgDλ) as components.

The development of oligoclonality occurred on average after 28.8 months (95% CI: 21.3–36.3 months). Notably, approx. 75% of cases occurred within 30 months, a cutoff point chosen to separate different phases of the Kaplan–Meier curve.

Among the patients with an available diagnosis (n = 154), there were 133 patients with BG, 20 patients with TG and 1 patient with 4 M-proteins. In BG patients, it was possible to distinguish subgroups solely with plasma and lymphoplasma cell dyscrasia (n = 111), and classify these patients based on another accompanying disorder (n = 22). Furthermore, in the subgroup of patients with another disorder, it was possible to distinguish those with lymphoid (n = 11), myeloid (n = 8), other neoplasia (n = 1), and non-neoplastic accompanying diseases (n = 2). However, the subgroup with plasma cell dyscrasia included MM (n = 86 (64.7%)), OG of uncertain significance (n = 11), MM + amyloidosis (n = 7), Waldenström's macroglobulinemia (MWalden) (n = 4), light chain deposition disease (n = 1), amyloid light-chain (AL) amyloidosis (n = 1), and plasmacytic leukemia (n = 1). Interestingly, OG with other lymphoid malignancies included chronic lymphocytic leukemia (CLL) (n = 4), marginal zone lymphoma (MZL)

Table 2. Clinical and laboratory characteristics of the patients with triclonal gammopathy (n = 29)

Patient No.	Monoclonal proteins detected with immunofixation	Diagnosis
1	IgGκ+IgGλ+IgMκ	unknown
2	IgAκ+IgGλ+free λ chain	MM
3	IgGλ+IgMκ+IgGκ	AML
4	IgGλ+IgAλ+IgAκ	unknown
5	IgAκ+IgAλ+IgGκ	unknown
6	IgMλ+IgAκ+IgGκ	CLL
7	IgGκ+IgGλ+IgMλ	MM
8	IgGλ+IgMκ+IgGκ	MM
9	IgGλ+IgGκ+IgMκ	unknown
10	IgMκ+IgGκ+IgGλ	unknown
11	IgMκ+IgGκ+IgGλ	unknown
12	IgMκ+IgGκ+IgGλ	unknown
13	IgG heavy chain+IgMκ+IgGκ	splenic lymphoma
14	IgGλ+free λ chain+IgMκ	MM
15	free λ chain+IgGλ+IgAκ	MM
16	IgGκ+IgAκ+IgMλ	SLL
17	free λ chain+IgGλ+IgAλ	MM
18	IgGκ+IgG heavy chain+IgMλ	MM
19	IgGκ+IgDλ+free λ chain	MM
20	IgMκ+IgMλ+IgGκ	MWalden
21	IgAκ+free κ chain+IgGκ	unknown
22	IgGλ+IgGκ+free κ chain	unknown
23	IgGκ+IgGλ+IgAλ	MDS
24	IgMκ+free κ chain+IgGλ	MM
25	IgAκ+IgGκ+IgGλ	MM
26	IgGκ+free κ chain+IgGλ	MM
27	IgGκ+free κ chain+IgGλ	MM
28	IgGκ+IgGλ+free λ chain	MM
29	IgGκ+IgGλ+IgMλ	glomerulonephritis

MM – multiple myeloma; AML – acute myeloid leukemia; CLL – chronic lymphocytic leukemia; SLL – small lymphocytic lymphoma; MWalden – Waldenström's macroglobulinemia; MDS – myelodysplastic syndrome.

(n = 3), diffuse large B-cell lymphoma (DLBCL) (n = 2), small lymphocytic lymphoma (SLL) (n = 1), and mantle cell lymphoma (MCL) (n = 1). Oligoclonal gammopathy cases with myeloid malignancy included acute myeloid leukemia (AML) (n = 5), myelodysplastic syndrome (MDS) (n = 2) and chronic myeloid leukemia (CML) (n = 1). There was also a case of OG with adenocarcinoma (n = 1). Finally, there were individual cases of OG patients with primary autoimmune thrombocytopenia and autoimmune hemolytic anemia (Fig. 3).

Among 20 patients with TG and available diagnoses, there were 14 cases of plasma cell dyscrasias, including MM (n = 13 (65%)) and MWalden (n = 1). There were also 3 cases of lymphoid neoplasias: CLL (n = 1), SLL (n = 1) and splenic lymphoma (n = 1); 2 cases of myeloid neoplasias: AML (n = 1)

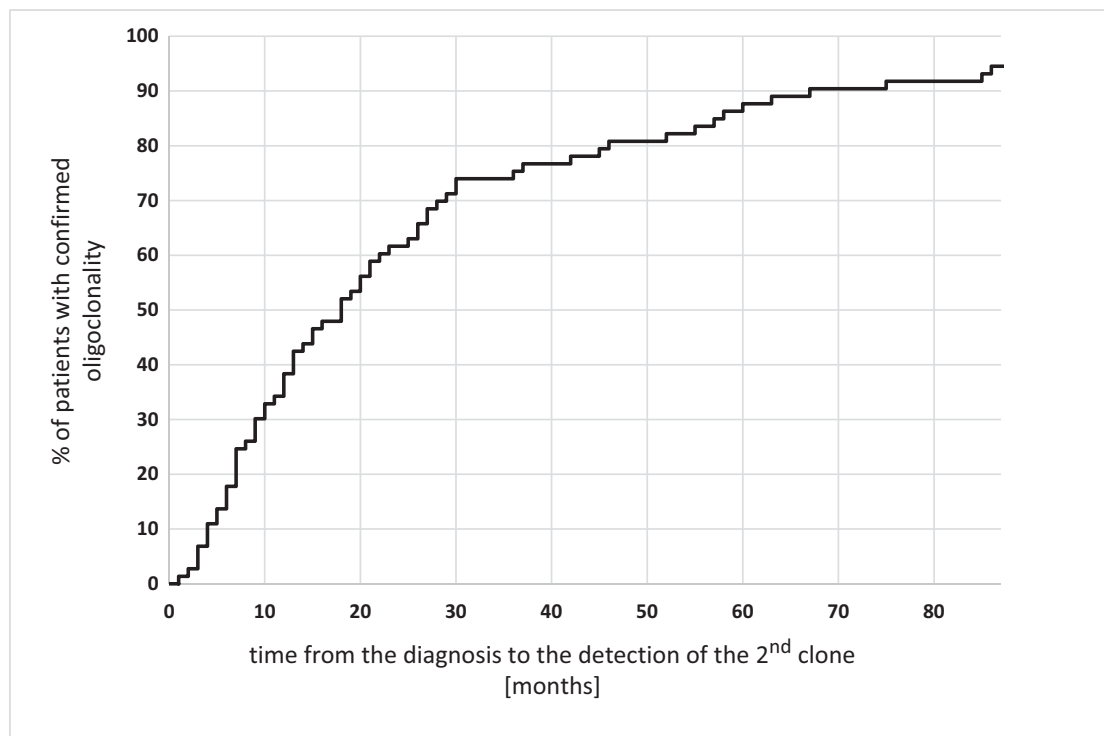


Fig. 2. Kaplan–Meier curve illustrating the amount of time required to detect a 2nd clone using immunofixation in patients with secondary oligoclonal gammopathy (OG) after the diagnosis (n = 73; the date of diagnosis available). Every event is defined as the detection of the 2nd clone in the serum of a single patient (the detection of OG). The figure presents cumulative data, and no data have been censored during this analysis. Therefore, the total number of events for every time interval is 73

time (months)	5	10	15	20	25	30	35	40	45	50	55	60	65	70	75	80
cumulative number of events	10	24	34	41	46	54	54	56	58	59	61	64	65	66	67	67
total number of events	73	73	73	73	73	73	73	73	73	73	73	73	73	73	73	73

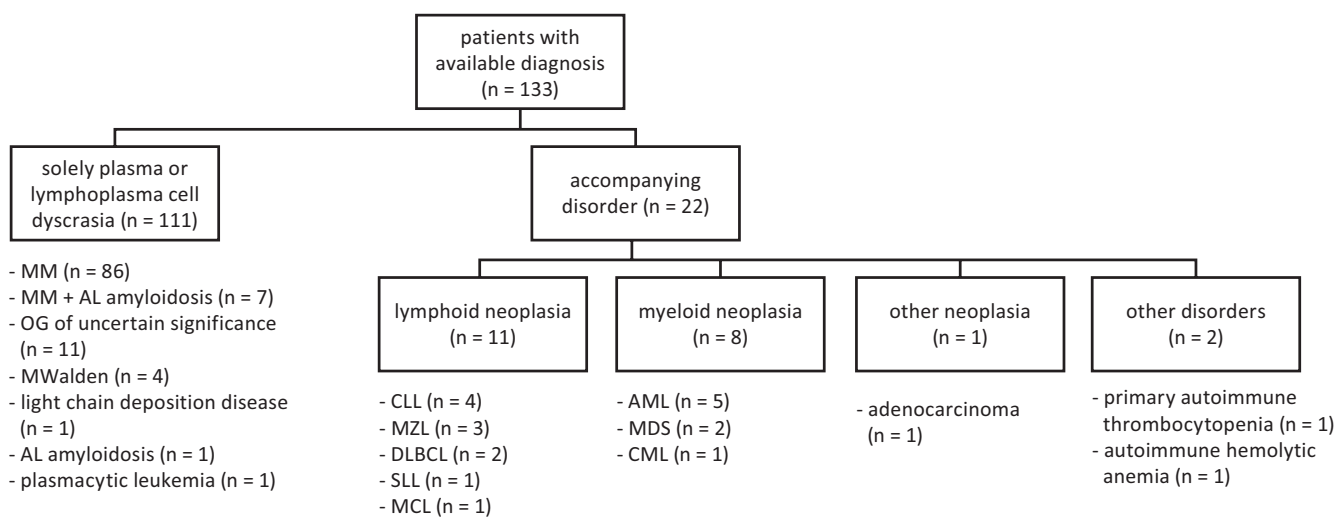


Fig. 3. The spectrum of established diagnoses in patients with biconal gammopathy (BG) (n = 133)

MM – multiple myeloma; AL – amyloid light-chain; OG – oligoclonal gammopathy; MWalden – Waldenström’s macroglobulinemia; CLL – chronic lymphocytic leukemia; MZL – marginal zone lymphoma; DLBCL – diffuse large B-cell lymphoma; SLL – small lymphocytic lymphoma; MCL – mantle cell lymphoma; AML – acute myeloid leukemia; MDS – myelodysplastic syndrome; CML – chronic myeloid leukemia.

and MDS (n = 1); and 1 case of OG resulting from a non-neoplastic disorder, namely glomerulonephritis with vasculitis.

The patient with 4 distinct M-proteins was diagnosed with chronic myelomonocytic leukemia (CMML), a unique diagnosis throughout the entire cohort.

Diagnoses were available for all patients with primary OG (n = 13) and in all cases, plasma cell or lymphoplasma

cell dyscrasia was detected, where the most common was MM (n = 11 (84.6%)). Among them, there was 1 case of MM + amyloidosis and 1 MM + light chain deposition disease. The remaining diagnoses were MWalden and OG of uncertain significance.

Regarding the age at diagnosis (data available for n = 86), the patients with primary OG (n = 12) were significantly

Table 3. Comparison of biclonal and triclonal gammopathies

Compared variables	Biclonal gammopathy	Triclonal gammopathy
Cohort size, n	223	29
Sex (males compared to females)	52.5% compared to 47.5%	69.0% compared to 31.0%
Age at diagnosis [years]	61.6 (95% CI: 59.4–63.8)	63.2 (95% CI: 55.9–70.6)
Most common diagnosis	MM (64.7%)	MM (65.0%)
Durie–Salmon stage (MM)	mainly IIIA and IIIB	mainly IIIA and IIIB
Laboratory findings	<ul style="list-style-type: none"> – IgGκ+IgGλ as the most common combination of monoclonal proteins (>30%) – combinations often include IgG, followed by IgM and IgA – free light chains as distinct proteins occur rarely (17/223) 	<ul style="list-style-type: none"> – high diversity of combinations – all combinations include IgG, often IgM or IgA – free light chains as distinct proteins occur often (12/29)

95% CI – 95% confidence interval; MM – multiple myeloma; Ig – immunoglobulin.

older (mean: 70.8, 95% CI: 66.4–75.3, median: 70.5) than the patients with secondary OG (n = 74) (mean: 60.3, 95% CI: 58.1–62.5, median: 62) (p = 0.0004, Welch's t-test), and the data were normally distributed in both cohorts (p = 0.578 and p = 0.584, respectively, Shapiro–Wilk test). However, no difference in age was observed between patients with TG (n = 26) (mean: 63.2, 95% CI: 55.9–70.6, median: 63.5) and BG (n = 60) (mean: 61.6, 95% CI: 59.4–63.8, median: 63.0) (p = 0.81). A comparative analysis of patients with BG and TG is shown in Table 3.

Notably, 11 out of 13 patients (84.6%) with primary OG were males, while in patients with secondary OG (n = 240), the occurrence of both sexes was similar (126 males and 114 females, 52.5% and 47.5%, respectively). Interestingly, in the TG cohort, there were 20 males (69.0%) and 9 females (31.0%). The patient with 4 detectable monoclonal proteins was also male.

The analysis of Durie–Salmon stages in OG myeloma patients (data available for n = 69 (27.3%)) revealed the following results: IA – n = 6, I – n = 1, IB – n = 0, IIA – n = 12, II – n = 2, IIB – n = 3, IIIA – n = 25, III – n = 0, IIIB – n = 20. Therefore, the majority of patients developed oligoclonality in the advanced stages of myeloma, sometimes years after the primary diagnosis of monoclonal gammopathy. Conversely, in patients with primary OG (data available for n = 6), 2 patients were classified to stage IA, 2 patients to IIA, 1 to IIIA, and 1 to IIIB. For myeloma patients with 3 detectable clones, Durie–Salmon staging was available for 8 out of 13 cases. The results were as follows: 1 patient with IA, 1 patient with IIA, 3 patients with IIIA, and 3 patients with IIIB stage. While no statistical comparison was possible with these numbers, the data did not reveal major differences between the BG and TG cohorts.

The cytogenetic analysis was only performed in 16 out of 253 patients but revealed 10 individuals with karyotype abnormalities, as follows: t(4,14) in 2 patients and del(17) + del(1), IGH/FGFR3 fusion with rearrangements of IGH, t(11,14), hyperdiploid, del(17p–), deletion of TP53, monosomy of 17p, and partial monosomy of 17p + partial deletion of TP53, each in 1 patient. Among patients with

primary OG, cytogenetic alterations were not found. Finally, the patient with monosomy of chromosome 17p had 3 detectable M-proteins in serum.

Discussion

This study analyzed the problem of secondary OG and provided a comparison of BG and TG for the first time. We observed that the development of both biclonality and triclinality is frequently a late event in the evolution of MGUS, often observed when MGUS progresses to MM. Furthermore, most cases of so-called primary OG had symptomatic MM. It suggests that they underwent an evolution from monoclonal gammopathy during undiagnosed disease and not as a primary event. Furthermore, our data suggest that the spectrum of both biclonality and triclinality is very large and every theoretically possible combination of M-proteins may be observed.

We failed to associate any specific event in a disease course (transformation, treatment, progression, remission, stabilization) with the development of oligoclonality (the detection of the 2nd or subsequent clone). Therefore, we performed a time analysis with the Kaplan–Meier curve (Fig. 2). Some studies postulate potential emerging factors of OG, such as autologous hematopoietic stem cell transplantation.⁶ However, there are no prospective cohort studies that have analyzed this aspect of the disease. Therefore, the etiology of OG remains unknown and no contributing factors have been identified.

There are 2 major possible mechanisms for developing oligoclonality. One possibility is that 2 or more clonally different plasma cell dyscrasias co-occur in the same patient. The other is that BG and TG represent an evolution of the primary clone with subclones derived from cells that underwent additional mutational events. Recent analysis with next-generation sequencing has revealed that aberrations in the TP53 signaling pathway are responsible for the occurrence of multiple, synchronous primary cancers.¹⁴ Moreover, and specifically for OG, the cases of 2 (or more)

monoclonal immunoglobulins that contain distinct light chains (κ and λ) might be considered truly biclonal, since no molecular mechanism of changing light chain expression has been described so far.¹⁵ Such a statement has already been made by some authors³ and our study reveals numerous cases of oligoclonal gammopathies where M-proteins include immunoglobulins with different light chains. This phenomenon seems to occur too frequently to be just a coincidence without any underlying mutational background. Lastly, polymerase chain reaction (PCR) and immunofluorescence (IF) analyses of clonal relationship in patients with BG imply that 2 independent clones can coexist synchronously in individual patients, even when the clones produce immunoglobulins with the same type of light chain (κ and λ).¹⁶

We failed to identify major differences between primary and secondary OG, except for primary OG patients of more advanced age. The similarities between both groups (primary compared to secondary OG) have been observed regarding the dominant diagnosis. In both groups, MM or MM + comorbidities were the dominant diagnoses, which remains consistent with earlier findings.⁴ We have also failed to identify significant differences between patients with biclonal compared to triclonal gammopathies when comparing age, underlying disorder and the dominant combinations of monoclonal proteins that are present. In the only other analysis of TG concerning 6 cases, there were 2 cases of MWalden, 1 case of non-Hodgkin lymphoma, 1 case of polycythemia vera, and 2 cases without any hematopoietic disease.¹⁷ However, the same analysis revealed that 64.6% of TGs were detected in lymphoproliferative diseases, based on all known cases.¹⁷ The IgG occurred the most often in combinations of monoclonal proteins in all groups. This is not surprising, since this serum protein is also detectable in the majority of monoclonal gammopathy cases (followed by IgM and IgA).^{4,18} The additional 3rd M-protein in patient serum was often a free light chain. Furthermore, free light chains tended to be detectable as a part of a triclonal combination (12/29), as opposed to biclonal combinations (17/223). The reasons for the presence of additional free light chains in patients with TG (especially the patients with primary OG) remain unknown, and this phenomenon requires further research and clarification.

Other publications concerning TG are limited to case reports, for example, IgM κ +IgG κ +IgA κ ,^{4,19} IgG κ +IgG λ +IgA λ ,⁵ IgG κ +IgG λ +IgM λ ,²⁰ or IgA κ +IgG κ +IgM κ .²¹ The case of IgA κ + free κ light chain + free λ light chain has also been reported.²² However, our analysis shows that 29/253 (11.4%) cases represent TG, suggesting that the magnitude of the phenomenon is larger than expected.

While data concerning cytogenetic alterations are limited (10 out of 16 tested patients), they only identified changes that have already been found in MM cases.²³ However, they appear to be quite common in OG cases.

Limitations

The main limitation of the study was the availability of clinical data, such as diagnoses. The lack of data resulted from the fact that OG is a rare disorder. Moreover, we did not identify any comprehensive disease mechanism underlying OG.


Conclusions


The diagnosis of patients with primary OG is more often established in males in older age (approx. 10 years older) than in patients with secondary OG. The detection of secondary OG often (in approx. 75% of cases) occurs up to 30 months after the initial diagnosis. Moreover, there are laboratory and clinical findings that are specific to patients with primary OG and TG cases. Despite the findings of this study, OG remains a poorly understood disorder and more research, especially prospective studies, is necessary to support these conclusions. It will take more time for the detailed pathogenesis of the disease to be established.

ORCID iDs

Marcin Jasiński  <https://orcid.org/0000-0002-7519-9507>

Anna Waszczuk-Gajda  <https://orcid.org/0000-0001-5626-1750>

Olga Ciepiela  <https://orcid.org/0000-0002-3694-4076>

Wiesław Wiktor Jędrzejczak  <https://orcid.org/0000-0002-6813-3331>

References

- Kyle RA, Robinson RA, Katzmann JA. The clinical aspects of biclonal gammopathies. *Am J Med.* 1981;71(6):999–1008. doi:10.1016/0002-9343(81)90326-0
- Sharma S, Gupta P, Aggarwal R, Malhotra P, Minz RW, Bansal F. Demystifying biclonal gammopathy: A pathologist's perspective. *Lab Med.* 2019;50(4):357–363. doi:10.1093/labmed/lmz006
- Ando K, Yaguchi M, Okabe S, Miyazawa K, Ohyashiki K. IgA-lambda/IgG-kappa biclonal myeloma in which two clones proliferated in individual sites. *Intern Med.* 2000;39(2):170–175. doi:10.2169/internalmedicine.39.170
- Kyle RA, Rajkumar SV. Monoclonal gammopathy of undetermined significance. *Clin Lymphoma Myeloma.* 2005;6(2):102–114. doi:10.3816/CLM.2005.n.036
- Aksungar FB, Ayer M, Serteser M, Coskun A, Unsal I. A triclonal gammopathy in a relapsing multiple myeloma patient, detected by immunosubtraction method. *Ann Clin Biochem.* 2014;51(5):606–610. doi:10.1177/0004563213512801
- Mullikin TC, Rajkumar SV, Dispenzieri A, et al. Clinical characteristics and outcomes in biclonal gammopathies. *Am J Hematol.* 2016;91(5):473–475. doi:10.1002/ajh.24319
- Österborg A, Mellstedt H. Monoclonal and biclonal immunoglobulin-producing disorders. *Eur J Haematol.* 2009;43(S51):11–18. doi:10.1111/j.1600-0609.1989.tb01486.x
- Bakta IM, Sutarka IN. Biclonal gammopathy in multiple myeloma: A case report. *Gan To Kagaku Ryoho.* 2000;27(Suppl 2):544–548. PMID:10895208.
- Jurczyszyn A, Gozzetti A, Gdula-Argasińska J, et al. Similar survival outcomes in patients with biclonal versus monoclonal myeloma: A multi-institutional matched case-control study. *Ann Hematol.* 2017;96(10):1693–1698. doi:10.1007/s00277-017-3084-9
- Nikolova-Vlahova MK, Kamburova M, Hristova J, et al. Biclonal myeloma in renal failure. *Cent Eur J Immunol.* 2020;45(1):122–124. doi:10.5114/ceji.2020.94714

11. Banerjee A. A rare case of multiple myeloma with biclonal gammopathy. *J Clin Diagn Res*. 2016;10(12):BD03–BD04. doi:10.7860/JCDR/2016/22466.8984
12. Kancharla P, Patel E, Hennrick K, Ibrahim S, Goldfinger M. A rare presentation of biclonal gammopathy in multiple myeloma with simultaneous extramedullary involvement: A case report. *Case Rep Oncol*. 2019;12(2):537–542. doi:10.1159/000499902
13. Coen M, Bornand A, Samii K, Koegler F, Serratrice J. Gastrointestinal amyloidosis in biclonal gammopathy. *Clin Lymphoma Myeloma Leuk*. 2021;21(7):e606–e610. doi:10.1016/j.clml.2021.02.015
14. Kong Y, Li J, Lin H, Liang X, Zhou X. Landscapes of synchronous multiple primary cancers detected by next-generation sequencing. *FEBS Open Bio*. 2022;12(11):1996–2005. doi:10.1002/2211-5463.13491
15. González D, Van Der Burg M, García-Sanz R, et al. Immunoglobulin gene rearrangements and the pathogenesis of multiple myeloma. *Blood*. 2007;110(9):3112–3121. doi:10.1182/blood-2007-02-069625
16. Tschumper RC, Dispenzieri A, Abraham RS, Henderson KJ, Jelinek DF. Molecular interrogation of biclonal multiple myeloma for clonal relatedness. *Blood*. 2012;120(21):2928. doi:10.1182/blood.V120.21.2928.2928
17. Guastafierro S, Sica A, Parascandola RR, et al. Clinical significance of serum triple monoclonal components: A report of 6 cases and a review of the literature. *Leuk Res*. 2014;38(2):166–169. doi:10.1016/j.leukres.2013.10.020
18. García-García P, Enciso-Alvarez K, Diaz-Espada F, Vargas-Nuñez JA, Moraru M, Yebra-Bango M. Biclonal gammopathies: Retrospective study of 47 patients. *Rev Clin Esp (Barc)*. 2015;215(1):18–24. doi:10.1016/j.rceng.2014.07.004
19. Grosbois B, Jégo P, De Rosa H, et al. Triclonal gammopathy and malignant immunoproliferative syndrome [in French]. *Rev Med Interne*. 1997;18(6):470–473. doi:10.1016/S0248-8663(97)80618-2
20. Tirelli A, Guastafierro S, Cava B, Lucivero G. Triclonal gammopathy in an extranodal non-Hodgkin lymphoma patient. *Am J Hematol*. 2003;73(4):273–275. doi:10.1002/ajh.10338
21. Murata T, Fujita H, Harano H, et al. Triclonal gammopathy (IgAk, IgGk, and IgMk) in a patient with plasmacytoid lymphoma derived from a monoclonal origin. *Am J Hematol*. 1993;42(2):212–216. doi:10.1002/ajh.2830420213
22. Myrlande M, Vikram P. Triclonal gammopathy in a patient with smoldering plasma cell myeloma (PCM). *Arch Hematol Case Rep Rev*. 2021;6(1):13–17. doi:10.17352/ahcrr.000032
23. Castaneda O, Baz R. Multiple myeloma genomics: A concise review. *Acta Med Acad*. 2019;48(1):57. doi:10.5644/ama2006-124.242

Effect of passive ankle movement in the sitting position on the symptoms of chronic venous insufficiency with long-term observation

Bartosz Radosław Wnuk^{1,A,B,D–F}, Damian Ziaja^{2,3,A,B,D–F}, Michał Buczek^{4,A,B,D–E}, Krzysztof Ziaja^{5,A,D–F}, Marcin Banyś^{6,A,C,D}

¹ Department of Rehabilitation, Faculty of Health Sciences in Katowice, Medical University of Silesia, Poland

² Department of General and Vascular Surgery, Angiology and Phlebology, Medical University of Silesia, Katowice, Poland

³ Department of Physiotherapy, School of Health Science, Medical University of Silesia, Katowice, Poland

⁴ Department of General and Vascular Surgery, Angiology and Phlebology, Upper Silesian Medical Center, Katowice, Poland

⁵ Hospital Megrez LLC, Tychy, Poland

⁶ MIDMED LLC, Katowice, Poland

A – research concept and design; B – collection and/or assembly of data; C – data analysis and interpretation;

D – writing the article; E – critical revision of the article; F – final approval of the article

Advances in Clinical and Experimental Medicine, ISSN 1899–5276 (print), ISSN 2451–2680 (online)

Adv Clin Exp Med. 2024;33(2):135–141

Address for correspondence

Bartosz Radosław Wnuk
E-mail: bwnuk@sum.edu.pl

Funding sources

National Centre for Research and Development
– NCBiR (grant No. NCBiR-POIR.01.01.01-00-1910/15).

Conflict of interest

None declared

Received on December 29, 2022

Reviewed on March 27, 2023

Accepted on May 9, 2023

Published online on June 1, 2023

Cite as

Wnuk BR, Ziaja D, Buczek M, Ziaja K, Banyś M. Effect of passive ankle movement in the sitting position on the symptoms of chronic venous insufficiency with long-term observation.

Adv Clin Exp Med. 2024;33(2):135–141.

doi:10.17219/acem/166046

DOI

10.17219/acem/166046

Copyright

Copyright by Author(s)

This is an article distributed under the terms of the Creative Commons Attribution 3.0 Unported (CC BY 3.0) (<https://creativecommons.org/licenses/by/3.0/>)

Abstract

Background. Chronic venous insufficiency (CVI) is the most common vascular disease. One major risk factor for its development is either long-term sitting or standing in the same position and the nature of the work performed.

Objectives. This study aims to assess the effectiveness of passive ankle movement in the sitting position performed using the Bella Vena robot for the symptoms of CVI with long-term observation.

Materials and methods. A group of 58 patients (mean age: 59.69 ± 14.59 years) with CVI in CEAP (Clinical (C), Etiological (E), Anatomical (A), and Pathophysiological (P)) classification categories 2 and 3, and a group of 37 (mean age: 51.49 ± 14.86 years) healthy volunteers performing sedentary work for at least 6 h during the working day were enrolled into the study. The total duration of observation lasted 8 months (8 visits), during which the following parameters were assessed at the beginning and end of this period: pain intensity (according to the visual analogue scale (VAS)), level of saturation on the toe, pulse rate, and lower limb Doppler ultrasound evaluation of reflux parameters.

Results. The exercises used in people with CVI resulted in a significant reduction ($p \leq 0.01$) in the occurrence of symptoms. Among all respondents, after 8 months of exercise, a significant reduction in pain level according to the VAS of the lower limbs, an improvement in saturation at the toe level, and a reduction in venous reflux was recorded ($p \leq 0.05$).

Conclusions. Home exercises with the use of an automatic exercise rehabilitation device alleviated significant symptoms in patients with CVI and improved the calf muscle pump.

Key words: chronic venous insufficiency, home exercises, calf muscle pump

Background

Chronic venous insufficiency (CVI) is a common health problem which may cause significant morbidity and mortality. It develops when the venous pressure is increased and blood return is impaired. Several mechanisms may result in blood flow impairment, including incompetent valves (superficial or deep veins), perforating veins, venous obstruction, or a combination of these mechanisms. This leads to general or local venous hypertension, mainly while standing or ambulating, contributing to macro- or micro-circulatory hemodynamic impairments and local tissue ischemia.^{1,2} Prolonged standing or sitting are important risk factors of CVI; therefore, it is very important during initial and regular check-ups in people who do this kind of work to control the state of the venous system of the lower limbs. At the same time, employees in such workplaces should be informed about the health effects of prolonged sitting and standing and possible preventive measures.³ Occupational leg symptoms, especially leg swelling, are associated with feelings of tiredness and heaviness of the legs and leg pain. Hence, reducing leg swelling is important in preventing the development of CVI.

The calf muscle pump is also important for venous competence – it is called the peripheral heart. Through contraction of the calf muscles, the veins are squeezed, and the blood is pumped upward with the help of one-way valves.⁴ Numerous authors report satisfying results of the use of supervised training to activate the calf pump through planned dorsal and plantar flexion of the foot in patients treated for CVI.^{5,6} In Polish health service, no procedures are used embracing physiotherapy in patients suffering from CVI; that is why we offer the Bella Vena platform for people who work in the sitting position.

Objectives

This study aimed to assess the effectiveness of passive ankle movement in the sitting position with the use of the Bella Vena robot for the symptoms of CVI over a long-term observation. The influence of passive ankle movement on blood flow from the lower extremities, measured by the duration of valvular reflux and the circumference of the shins, was also examined.

Materials and methods

The trial was conducted in accordance with the guidelines proposed by the institution supervising the trial, which approved the clinical trial protocol, and the institution intermediating the trial for the National Centre for Research and Development. The study had permission to start clinical trials from the President of the Office for

Registration of Medicinal Products, Medical Devices, and Biocidal Products (approval No. U.D.WM.DNB.83.2018 issued on November 19, 2018). This study has been approved by the Bioethics Committee of the Medical University of Silesia in Katowice (approval No. MIDMED/BV/2017, resolution No. 48/2017), and each participant received and signed a consent form to participate in the study. The study was conducted in accordance with the Declaration of Helsinki of 1975, as revised in 2008.

In the beginning, the study included 102 participants. Seven people did not qualify for the study (3 men and 4 women), so 95 patients met the inclusion criteria for the study. They were divided into 2 groups: 1) CVI group – 58 patients (16 men and 42 women) with CVI and a CEAP (Clinical (C), Etiological (E), Anatomical (A), and Pathophysiological (P)) classification of 2 and 3; and 2) control group – 37 healthy volunteers (20 men and 17 women) performing work in a sitting position for at least 6 h during each working day.

The selection of the study group was deliberate. Members of the group were recruited via traditional post (an invitation letter). The median age of group participants was 51–63 years, the body mass 73–74 kg and the body mass index (BMI) 25.31–27.49 kg/m² (Table 1). This group of patients had symptoms of CVI and had not been previously treated with mechanical rehabilitation devices.

The exclusion criteria consisted of deep vein thrombosis of the lower extremities, thrombosis of the superficial vein system in the lower extremities, acute inflammation in the venous system of the lower extremities without thrombosis, inflammation of all joints of the lower limbs, pregnancy and breastfeeding, plaster casts preventing movement in the ankle, knee and hip joints, inability to adopt the appropriate body position to use the device (contractures in the joints, lack of mobility of the joints), cardiovascular diseases, commission of the attending physician not to use this type of device, other diseases that prevent the use of the device in accordance with the instructions for use, a severe general condition of the patient, or insufficient physical and mental abilities of the patient to independently operate the product (unless it was operated under the constant supervision of the caregiver).

Parameter measurements

The total duration of observation was 8 months (8 visits), and the following parameters were assessed at the beginning and end of this period: assessment of pain intensity – according to the VAS, level of saturation on the toes, pulse rate, lower limb Doppler ultrasound evaluation of reflux (right popliteal vein, left popliteal vein, right small saphenous vein outlet, left small saphenous vein outlet, right great saphenous vein outlet, left great saphenous vein outlet, right femoral vein, and left femoral vein), measurement of the right and left shin circumference using a measuring tape, and subjective patient assessment regarding

Table 1. Demographic and biometric data of the respondents

Variable	Both groups (n = 95)	CVI group (n = 58)	Control group (n = 37)
Age [years]			
Min	25	25	25
Q1	46	50	40
Me	58	63	51
Q3	69	70	62
Max	83	83	78
Body height [cm]			
Min	149	149	158
Q1	160	159	165
Me	166	164.5	171
Q3	173	170	177
Max	187	185	187
Body mass [kg]			
Min	50	56	50
Q1	66	67	66
Me	73	73	74
Q3	84	85	80
Max	125	125	107
BMI [kg/m ²]			
Min	18.98	19.61	18.98
Q1	23.89	24.65	22.84
Me	26.71	27.49	25.31
Q3	29.35	30.18	27.04
Max	41.44	41.44	36.17

Min – minimum; Max – maximum; Me – median; Q1 – 1st quartile; Q3 – 3rd quartile; BMI – body mass index; CVI – chronic venous insufficiency.

the degree of reflux (scale 0–4). Doppler ultrasound examination with color flow imaging was performed after 15 min of adaptation of the patient with the SonoScape S8 portable ultrasonograph (SonoScape Medical Corp, Shenzhen, China) and linear probe (frequency 5–7.5 MHz). The examination was performed in a sitting position.

Reflux was assessed after the transducer was placed at the great saphenous vein (Vena saphena magna) mouth level after the cough test. The assessment of reflux in the popliteal vein was performed at the exit of the small saphenous vein by pressing the calf muscle. All ultrasound examinations were performed by 1 doctor who was authorized to conduct this type of examination and could correctly interpret the examination results.^{7,8}

The case report form (CRF) contained data on the occurrence of edema of the legs, skin cyanosis, muscle cramps (involuntary contractions), leg heaviness, patients bedridden or using wheelchair (i.e., immobilized patients), residual movements in the shoulder girdle, and other symptoms. Subsequent visits, except for the 1st one, encompassed the same questions, physical examination and imaging test. The visits took place every 4–5 weeks.

Intervention

To improve the quality of life of patients in the study groups, the Bella Vena device forced movement in the ankle joint to activate the calf pump. The Bella Vena device is an automated platform for exercising the lower limbs by forcing the heel–toe–heel movement of the foot at a properly selected foot inclination angle and speed of movement. The user places both feet on the exercising platform and then activates the device using the infrared (IR) remote control. Thanks to the properly designed movement of the platform that simulates gait, the Bella Vena device gives the possibility of training in the form of foot movement, activating the calf muscles. The so-called calf pump improves the outflow of blood from the lower limbs. While the device is operating, movement is forced in the ankle joints by the appropriate tilting of the training platform on which the feet are placed. The direct current DC motor installed in the Bella Vena device works in accordance with the values programmed in the microcomputer's memory – number of repetitions, speed of movement and angle of the platform. The mechanical structure of the device is responsible for the platform's inclination angle. The pendulum movement of the platform is possible thanks to a specially designed drive transmission system from the engine to the movable part of the platform. The operation of the device was selected in such a way as not to exceed the motion limits for the ankle joint, including the limit of the ankle flexion angle, since excessive movement can damage the joint. The device is powered by the 230 V mains through the alternating current/direct current (AC/DC) adapter that reduces the voltage supplied the device to a value that is safe for humans – 24 V DC. The Bella Vena device allows to exercise 2 feet at the same time or only 1 – left or right, depending on the user's needs. The casing of the Bella Vena device is made entirely of aluminum, while inside there is a DC motor with electronics controlling the motor operation and a drive transmission system. The study subjects used the device once a day for 30 min, and the frequency of the platform swing was 1 swing per second. The swing angle was 23°. During the 8 months of physical therapy at home, patients also had the opportunity for a telephone consultation with the physical therapist supervising this form of treatment. The device, before it was transferred for testing with the participation of patients, was subjected to a safety test for selected points of the PN-EN 60601 standard for medical devices by the Institute of Medical Technology and Apparatus in Zabrze (Poland) and KOMAG in Gliwice (Poland), where tests were carried out to obtain the International Protection Rating (IP) degree. The physical parameters of the device were selected in such a way that the device would be suitable for 90% of the population. The device is intended for people with a maximum weight of 120 kg. The components of the device in the form of electronics, motor, power supply, and construction were selected for this purpose. For people over 120 kg, a modified version

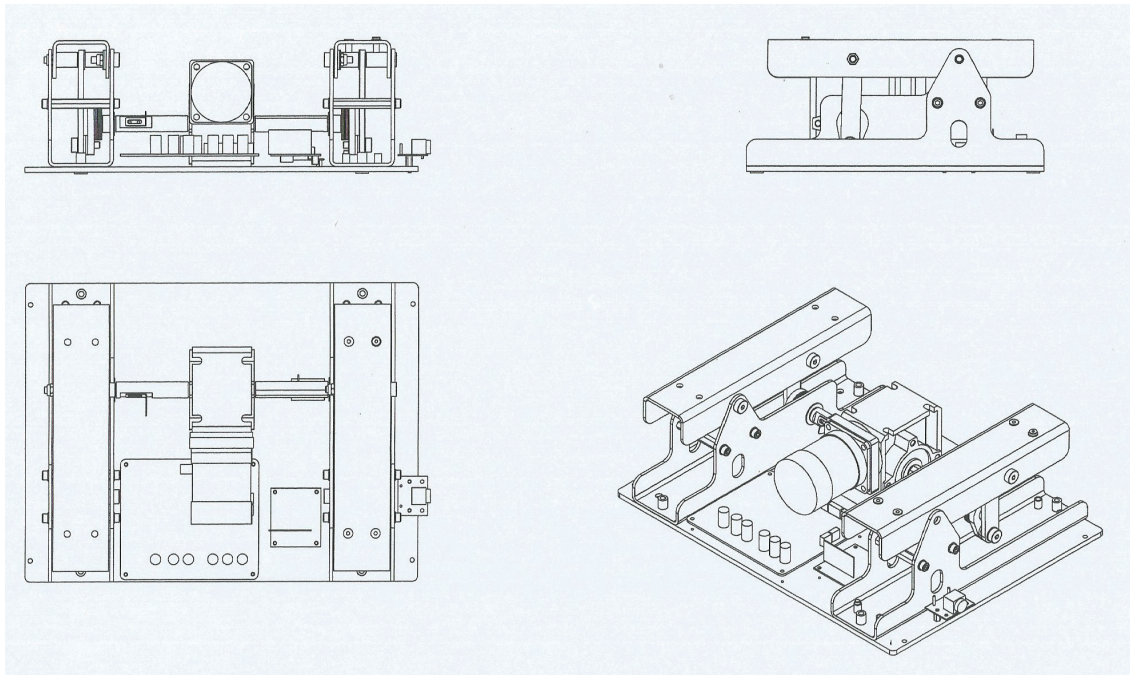


Fig. 1. Diagram of the Belle Vena device – internal view

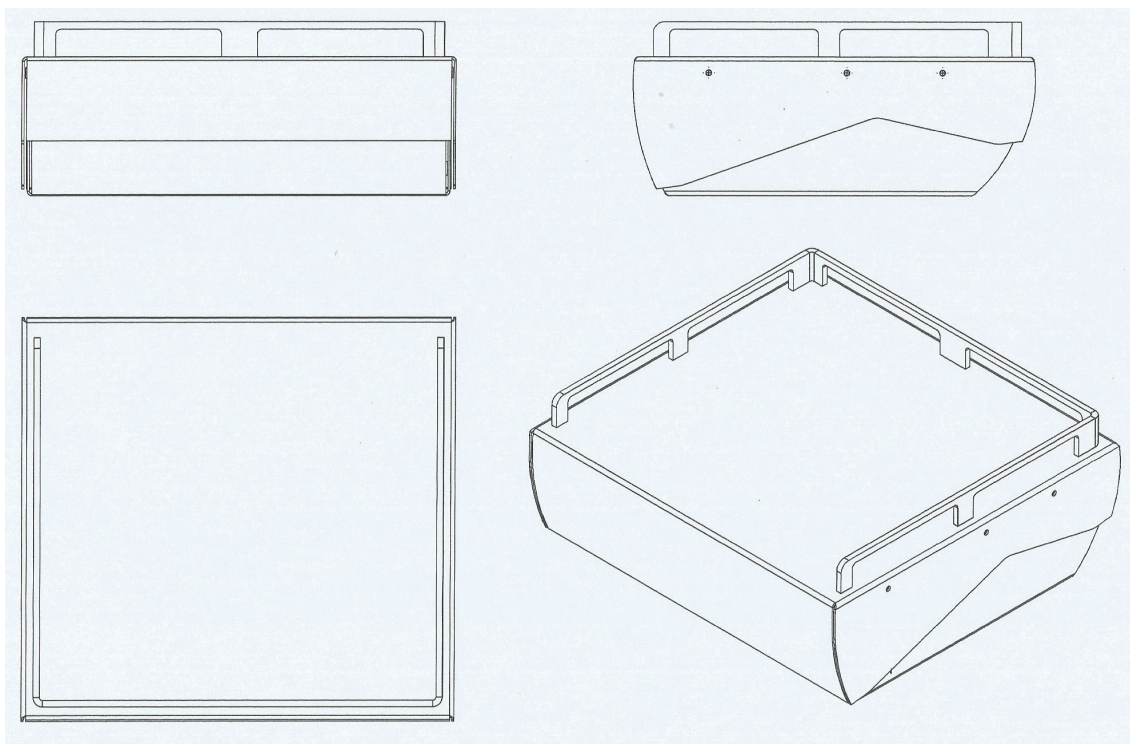


Fig. 2. Diagram of the Belle Vena device – external view

of the device was created, the so-called HD (heavy duty) version, where the appropriate design and electronics can cope with the increased weight of the lower limbs (Fig. 1,2).

Statistical analyses

To select an adequate statistical test to compare the studied groups, the Shapiro–Wilk normality test was used for

all the tested variables; the distribution was not normal ($p < 0.05$). Following the above analysis, the nonparametric Wilcoxon test (continuous variables) and the McNemar test (nominal variables) were used. Moreover, the basic descriptive statistics were calculated: the percentage frequency of occurrence (nominal variables), median, and 1st and 3rd quartile (Q1, Q3). The results at a $p \leq 0.05$ were considered statistically significant.

Results

The difference in body weight of the studied groups was not statistically significant. In the group of people with CVI, the BMI was higher than in the control group (Table 1).

There was a statistically significant reduction of edema in 28.42% of the whole study population and of night cramps in 35.79%, while 29.47% of subjects reported a reduction in leg heaviness. Regarding cyanosis of the skin and problems with walking, no statistically significant differences were observed ($p > 0.05$; Table 2).

The exercises used in the group of people with CVI have resulted in a significant alleviation ($p \leq 0.001$) between the 1st and the last follow-up visit regarding edema of the legs, night muscle cramps, leg heaviness, and other problems. In the control group, in terms of other symptoms, a significant improvement was noted for 21.62% of the respondents (Table 2).

In all respondents, after 8 months of exercise, a significant reduction in pain level of the lower limbs according to the VAS, an improvement in saturation at the toe level, and a reduction in venous reflux was recorded. The reduction in venous reflux during the examination of the Doppler ultrasound in the control group was not statistically significant except for the right popliteal vein, right femoral vein and left femoral vein. The reduction in venous reflux during the examination of the Doppler ultrasound in the group with CVI was statistically significant for the right popliteal vein, left popliteal vein, right small saphenous vein outlet, right femoral vein, and left femoral vein ($p > 0.05$; Table 3). The differences in the measurement of the circumference of the right and left shin in the control group and CVI group were statistically insignificant ($p > 0.05$; Table 3).

The statistical analysis of the difference in reflux values during the subjective assessment of the patient with a scale of 0–4 was significant in the CVI group and both groups ($p > 0.05$; Table 3).

Discussion

The CVI is not a disease that directly threatens the patient’s life, but it significantly reduces the everyday comfort of life. The chronic nature and severity of symptoms make normal functioning in society difficult, and in extreme cases impossible. The analysis of the obtained results indicated a significant alleviation of the symptoms of CVI in all 58 patients with CVI symptoms and healthy volunteers in long-term follow-up. The attenuation in subjective symptoms was associated with a reduction in venous reflux in the group with CVI. The alleviation of these symptoms confirms the positive effect of the calf pump on the venous system through the mechanical effect of the platform forcing movement in the ankle joint.

The veins of the lower extremity include the superficial and deep veins, which are defined by their respective relationships to the muscular fascia. The deep veins of the lower extremities primarily drain muscles and are encompassed by muscular fascia. Venous return from the lower extremities is vitally dependent on the action of the foot, calf and thigh muscle pumps, with approx. 90% of venous return attributed to these muscle structures during ambulation. Among these pumps, the calf muscle pump plays the pivotal role, reflected in the fact that it has the largest capacitance and generates the highest pressure, with an ejection fraction (EF) of approx. 65% in healthy subjects.^{9,10} Calf muscle pump failure is a therapeutic target

Table 2. Values of study variables – symptoms

V1. Occurrence of symptoms		V8. Both groups (n = 95)		V8. CVI group (n = 58)		V8. Control group (n = 37)		V8. Both groups (n = 95)		V8. CVI group (n = 58)		V8. Control group (n = 37)	
		yes	no	yes	no	yes	no	McNemar test (df = 1)	p-value	McNemar test (df = 1)	p-value	McNemar test (df = 1)	p-value
		%	%	%	%	%	%						
Edema of the legs	yes	15.79	28.42	24.14	37.93	2.70	13.51	17.633	<0.001	20.045	<0.001	0.125	0.728
	no	3.16	52.63	0.00	37.93	8.11	75.68						
Skin cyanosis	yes	1.05	4.21	1.72	6.90	0.00	0.00	2.25	0.134	2.25	0.134	–	–
	no	0.00	94.74	0.00	91.38	0.00	100.00						
Night muscle cramps	yes	11.58	35.79	12.07	44.83	10.81	21.62	26.694	<0.001	24.038	<0.001	2.5	0.114
	no	2.11	50.53	0.00	43.10	5.41	62.16						
Leg heaviness	yes	17.89	29.47	18.97	43.10	16.22	8.11	23.310	<0.001	20.346	<0.001	1.333	0.248
	no	1.05	51.58	1.72	36.21	0.00	75.68						
Walking problems	yes	9.47	7.37	6.90	12.07	13.51	0.00	0.9	0.343	1.778	0.182	0.00	1.00
	no	3.16	80.00	3.45	77.59	2.70	83.78						
Another symptoms	yes	2.11	26.32	1.72	29.31	2.70	21.62	58.368	<0.001	34.225	<0.001	4.00	0.045
	no	2.11	69.47	1.72	67.24	2.70	72.97						

CVI – chronic venous insufficiency.

Table 3. Values of study variables

Parameters	Both groups (n = 95)		CVI group (n = 58)		Control group (n = 37)		Both groups (n = 95)		CVI group (n = 58)		Control group (n = 37)	
	V1	V8	V1	V8	V1	V8	Wilcoxon test	p-value	Wilcoxon test	p-value	Wilcoxon test	p-value
	Me (Q1–Q3)	Me (Q1–Q3)	Me (Q1–Q3)	Me (Q1–Q3)	Me (Q1–Q3)	Me (Q1–Q3)						
VAS [cm]	5.0 (2.0–5.0)	1.5 (0.0–3.0)	5.0 (2.5–5.0)	1.5 (0.0–3.0)	4.0 (2.0–5.0)	1.5 (0.0–3.0)	7.463	<0.001	5.857	<0.001	4.649	<0.001
Saturation on the toe [%]	98.0 (97.0–99.0)	99.0 (98.0–99.0)	98.0 (97.0–99.0)	98.0 (98.0–99.0)	98.0 (97.0–99.0)	99.0 (98.0–99.0)	3.953	<0.001	2.361	0.018	3.309	<0.001
Pulse rate [bpm]	67.0 (63.0–72.0)	69.0 (66.0–71.0)	68.0 (63.0–74.0)	70.0 (67.0–72.0)	67.0 (63.0–71.0)	67.0 (65.0–69.0)	1.793	0.073	1.668	0.095	0.508	0.612
Doppler of reflux (velocity) [cm/s]												
Right popliteal vein	0.2 (0.0–0.3)	0.1 (0.0–0.2)	0.2 (0.0–0.4)	0.1 (0.0–0.2)	0.0 (0.0–0.2)	0.0 (0.0–0.1)	4.838	<0.001	4.308	<0.001	2.201	0.028
Left popliteal vein	0.2 (0.0–0.3)	0.1 (0.0–0.2)	0.2 (0.0–0.3)	0.1 (0.0–0.2)	0.0 (0.0–0.2)	0.0 (0.0–0.1)	4.004	<0.001	3.782	<0.001	1.392	0.164
Right small saphenous vein outlet	0.0 (0.0–0.0)	0.0 (0.0–0.1)	0.0 (0.0–0.0)	0.0 (0.0–0.1)	0.0 (0.0–0.0)	0.0 (0.0–0.0)	1.043	0.297	2.108	0.035	1.400	0.161
Left small saphenous vein outlet	0.0 (0.0–0.0)	0.0 (0.0–0.1)	0.0 (0.0–0.0)	0.0 (0.0–0.1)	0.0 (0.0–0.0)	0.0 (0.0–0.0)	0.197	0.844	1.090	0.276	1.303	0.193
Right great saphenous vein outlet	0.0 (0.0–0.1)	0.0 (0.0–0.1)	0.0 (0.0–0.1)	0.0 (0.0–0.1)	0.0 (0.0–0.0)	0.0 (0.0–0.0)	1.441	0.150	0.937	0.349	1.274	0.203
Left great saphenous vein outlet	0.0 (0.0–0.0)	0.0 (0.0–0.1)	0.0 (0.0–0.1)	0.0 (0.0–0.1)	0.0 (0.0–0.0)	0.0 (0.0–0.0)	0.107	0.915	0.429	0.668	0.889	0.374
Right femoral vein	0.2 (0.0–0.4)	0.1 (0.0–0.2)	0.2 (0.0–0.4)	0.1 (0.0–0.2)	0.0 (0.0–0.3)	0.0 (0.0–0.1)	4.574	<0.001	4.019	<0.001	2.374	0.018
Left femoral vein	0.2 (0.0–0.3)	0.1 (0.0–0.2)	0.2 (0.0–0.3)	0.1 (0.0–0.2)	0.1 (0.0–0.3)	0.0 (0.0–0.1)	3.790	<0.001	2.490	0.013	2.971	0.003
Right shin circumference [cm]	38.0 (36.0–40.0)	38.0 (36.2–39.5)	39.0 (37.0–40.0)	38.0 (36.5–39.8)	37.0 (36.0–39.0)	37.0 (36.0–38.0)	1.472	0.141	1.406	0.160	0.423	0.673
Left shin circumference [cm]	38.0 (36.0–40.0)	38.0 (36.0–39.5)	39.0 (37.0–40.5)	38.0 (36.5–39.8)	37.0 (36.0–39.0)	37.0 (36.0–38.0)	1.665	0.096	1.177	0.239	0.825	0.409
Degree of reflux (scale 0–4)	0.0 (0.0–0.0)	0.0 (0.0–0.0)	0.0 (0.0–0.0)	0.0 (0.0–0.0)	0.0 (0.0–0.0)	0.0 (0.0–0.0)	3.408	<0.001	3.180	0.001	–	–

VAS – visual analogue scale; CVI – chronic venous insufficiency; Me – median; Q1 – 1st quartile; Q3 – 3rd quartile.

in the treatment of CVI. Evidence suggests that isotonic exercises may be an effective method of increasing the hemodynamic performance of the calf muscle pump.^{11,12}

Calf-muscle pumping is the primary mechanism to promote blood return from the lower limbs to the heart. During exercise, the calf muscles (gastrocnemius and soleus) contract and compress the deep intramuscular veins, which increases the venous pressure and the blood flow from the deep venous system to the heart. The efficacy of this mechanism depends on talocrural mobility, venous competence and contraction strength of the calf muscles.¹³

To improve venous circulation, researchers have tested different training periods – from 6 weeks to 18 months. Training was planned every day or several times a week, with a duration of each session from 15 min to 1 h. The exercises were performed in the form of walking and stretching and resistance exercises.^{14–19} The higher frequency of ankle pump exercises (APE) can effectively promote venous blood return and has anticoagulant effects in the prophylaxis of deep vein thrombosis.^{20,21} Based on a study of 29 patients after total hip arthroplasty, Nakayama et al. reported that APE at 60 times/min were more effective than that at 40 or 80 times/min.²²

So far, no studies have been conducted on training the calf muscles in a sitting position in the form of passive exercises in this group of patients. The purpose of the Bella Vena device is to activate the calf pump by imitating the physiological movement in the ankles (60 times/min). The 8-month period of exercises, despite the unfavorable sitting position, had a positive effect on the venous system. People working in a standing posture are at a significantly greater risk for CVI than those working in a prolonged sitting posture. Ambulatory venous pressure while sitting is about 60–80 mm of water, as opposed to 20 mm while walking, and the number is only slightly higher (about 100 mm) while standing.^{23,24}

The innovation of the Bella Vena device is its availability and ease of use at home. The intention of the authors was that anyone in need could use this device at home and exercise several times a day. The objective of the designers was to create a device available to everyone. The Bella Vena device should not be compared to highly technologically advanced robots, but treated as a complement to daily physiotherapy.

In our study, the regularity of training was supervised during monthly visits and telephone consultations by physical therapists. This supervision ensured control of training and gave the opportunity to submit comments on the prototype of the device during its operation. The device itself is easy to use and enables performance of home exercises according to the patient's physical condition.

Limitations of the study

In this study, venous reflux was assessed, but it was not examined how it affects the level of muscle strength and range of motion in the joints, which is important in improving the gait function. Only subjective symptoms of venous insufficiency and the level of venous reflux were assessed. There are no publications in the available literature concerning the use of mechanical devices for supervised passive exercises of the ankle joint at home. For these reasons, the authors could not compare their results with the data of other authors.

Conclusions

Home exercises with the use of a prototype of the Bella Vena device for exercising the lower limb with CVI can improve the calf pump in a group of patients undergoing long-term observation. Such exercises employing an automatic exercise rehabilitation device alleviate the significant symptoms of CVI. Further research must be concentrated on expanding the technological capabilities of the device, which will allow patients to fully engage in exercises based on biofeedback.

ORCID iDs

Bartosz Radosław Wnuk  <https://orcid.org/0000-0002-2574-6955>
 Damian Ziaja  <https://orcid.org/0000-0002-1592-3997>
 Michał Buczek  <https://orcid.org/0000-0003-2584-8801>
 Krzysztof Ziaja  <https://orcid.org/0000-0003-2230-5860>

References

- Eberhardt RT, Raffetto JD. Chronic venous insufficiency. *Circulation*. 2014;130(4):333–346. doi:10.1161/CIRCULATIONAHA.113.006898
- Tew GA, Michaels J, Crank H, Middleton G, Gumber A, Klonizakis M. Supervised exercise training as an adjunctive therapy for venous leg ulcers: Study protocol for a randomised controlled trial. *Trials*. 2015;16(1):443. doi:10.1186/s13063-015-0963-z
- Łastowiecka-Moras E. Standing and sitting postures at work and symptoms of venous insufficiency: Results from questionnaires and a Doppler ultrasound study. *Int J Occup Saf Ergon*. 2021;27(4):963–969. doi:10.1080/10803548.2020.1834232
- Youn YJ, Lee J. Chronic venous insufficiency and varicose veins of the lower extremities. *Korean J Intern Med*. 2019;34(2):269–283. doi:10.3904/kjim.2018.230
- Orr L, Klement KA, McCrossin L, et al. A systematic review and meta-analysis of exercise intervention for the treatment of calf muscle pump impairment in individuals with chronic venous insufficiency. *Ostom Wound Manag*. 2017;63(8):30–43. doi:10.25270/owm.2017.08.3043
- Silva KLS, Figueiredo EAB, Lopes CP, et al. The impact of exercise training on calf pump function, muscle strength, ankle range of motion, and health-related quality of life in patients with chronic venous insufficiency at different stages of severity: A systematic review. *J Vasc Bras*. 2021;20:e20200125. doi:10.1590/1677-5449.200125
- Thorisson HM, Pollak JS, Scoutt L. The role of ultrasound in the diagnosis and treatment of chronic venous insufficiency. *Ultrasound Q*. 2007;23(2):137–150. doi:10.1097/01.ruq.0000277035.82208.bf
- Khilnani NM. Duplex ultrasound evaluation of patients with chronic venous disease of the lower extremities. *Am J Roentgenol*. 2014;202(3):633–642. doi:10.2214/AJR.13.11465
- Black CM. Anatomy and physiology of the lower-extremity deep and superficial veins. *Tech Vasc Interv Radiol*. 2014;17(2):68–73. doi:10.1053/j.tvir.2014.02.002
- Meissner MH. Lower extremity venous anatomy. *Semin Interv Radiol*. 2005;22(03):147–156. doi:10.1055/s-2005-921948
- Williams KJ, Ayekoloye O, Moore HM, Davies AH. The calf muscle pump revisited. *J Vasc Surg Venous Lymphat Disord*. 2014;2(3):329–334. doi:10.1016/j.jvsv.2013.10.053
- Araujo DN, Ribeiro CT, Maciel AC, Bruno SS, Fregonezi GA, Dias FA. Physical exercise for the treatment of non-ulcerated chronic venous insufficiency. *Cochrane Database Syst Rev*. 2016;2016(12):CD010637. doi:10.1002/14651858.CD010637.pub2
- O'Brien J, Edwards H, Finlayson K, Kerr G. Understanding the relationships between the calf muscle pump, ankle range of motion and healing for adults with venous leg ulcers: A review of the literature. *Wound Pract Res*. 2012;20(2):80–85. <https://eprints.qut.edu.au/54223/>
- Kan YM. Hemodynamic effects of supervised calf muscle exercise in patients with venous leg ulceration: A prospective controlled study. *Arch Surg*. 2001;136(12):1364. doi:10.1001/archsurg.136.12.1364
- O'Brien J, Edwards H, Stewart I, Gibbs H. A home-based progressive resistance exercise programme for patients with venous leg ulcers: A feasibility study. *Int Wound J*. 2013;10(4):389–396. doi:10.1111/j.1742-481X.2012.00995.x
- Tew GA, Gumber A, McIntosh E, et al. Effects of supervised exercise training on lower-limb cutaneous microvascular reactivity in adults with venous ulcers. *Eur J Appl Physiol*. 2018;118(2):321–329. doi:10.1007/s00421-017-3772-0
- Szewczyk MT, Jawień A, Cwajda-Białasik J, Cierzniańska K, Mościcka P, Hancke E. Randomized study assessing the influence of supervised exercises on ankle joint mobility in patients with venous leg ulcerations. *Arch Med Sci*. 2010;6:956–963. doi:10.5114/aoms.2010.19308
- Sharifi M, Bay RC, Karandish K, Emrani F, Snyder R, D'Silva S. The randomized, controlled ATLANTIS trial of aquatic therapy for chronic venous insufficiency. *J Vasc Surg Venous Lymphat Disord*. 2021;9(4):961–970. doi:10.1016/j.jvsv.2020.10.016
- Yang D, Vandongen YK, Stacey MC. Effect of exercise on calf muscle pump function in patients with chronic venous disease. *Br J Surg*. 2003;86(3):338–341. doi:10.1046/j.1365-2168.1999.00993.x
- Li T, Yang S, Hu F, Geng Q, Lu Q, Ding J. Effects of ankle pump exercise frequency on venous hemodynamics of the lower limb. *Clin Hemorheol Microcirc*. 2020;76(1):111–120. doi:10.3233/CH-200860
- Li H, Zhang W, Lu Q, et al. Which frequency of ankle pump exercise should be chosen for the prophylaxis of deep vein thrombosis? *Inquiry*. 2022;59:004695802211059. doi:10.1177/00469580221105989
- Nakayama T, Tsukada S, Hiyama T, Yamada T, Hirasawa N. Impact of active ankle movement frequency on velocity of lower limb venous flow following total hip arthroplasty. *Adv Orthop*. 2016;2016:7683272. doi:10.1155/2016/7683272
- Sudoł-Szopińska I, Bogdan A, Szopiński T, Panorska AK, Kołodziejczak M. Prevalence of chronic venous disorders among employees working in prolonged sitting and standing postures. *Int J Occup Saf Ergon*. 2011;17(2):165–173. doi:10.1080/10803548.2011.11076887
- Bahk JW, Kim H, Jung-Choi K, Jung MC, Lee I. Relationship between prolonged standing and symptoms of varicose veins and nocturnal leg cramps among women and men. *Ergonomics*. 2012;55(2):133–139. doi:10.1080/00140139.2011.582957

Olfaction-associated quality of life: Polish adaptation and validation of a Questionnaire of Olfactory Disorders (QOD-PL) in patients with chronic rhinosinusitis

Katarzyna Resler^{1,A–F}, Anna Oleszkiewicz^{2,3,A,C–F}, Marcin Frączek^{1,A,B,D–F}, Monika Morawska-Kochman^{1,B,D,F}, Anna Resler^{4,B,D,F}, Tomasz Zatoński^{1,D–F}, Thomas Hummel^{3,A,C–F}

¹ Department and Clinic of Otolaryngology, Head and Neck Surgery, Wrocław Medical University, Poland

² Institute of Psychology, University of Wrocław, Poland

³ Clinic of Smell and Taste, Department of Otorhinolaryngology, Medical Faculty Carl-Gustav Carus, Technische Universität Dresden, Germany

⁴ Faculty of Physiotherapy, University School of Physical Education in Wrocław, Poland

A – research concept and design; B – collection and/or assembly of data; C – data analysis and interpretation;

D – writing the article; E – critical revision of the article; F – final approval of the article

Advances in Clinical and Experimental Medicine, ISSN 1899–5276 (print), ISSN 2451–2680 (online)

Adv Clin Exp Med. 2024;33(2):143–150

Address for correspondence

Katarzyna Resler

E-mail: katarzyna.resler@umw.edu.pl

Funding sources

None declared

Conflict of interest

None declared

Received on November 3, 2022

Reviewed on April 12, 2023

Accepted on July 24, 2023

Published online on September 7, 2023

Cite as

Resler K, Oleszkiewicz A, Frączek M, et al. Olfaction-associated quality of life: Polish adaptation and validation of a Questionnaire of Olfactory Disorders (QOD-PL) in patients with chronic rhinosinusitis. *Adv Clin Exp Med.* 2024;33(2):143–150. doi:10.17219/acem/169978

DOI

10.17219/acem/169978

Copyright

Copyright by Author(s)

This is an article distributed under the terms of the Creative Commons Attribution 3.0 Unported (CC BY 3.0) (<https://creativecommons.org/licenses/by/3.0/>)

Abstract

Background. The focus on health-related quality of life (HRQOL) in medical research is becoming more and more intensive, with attention being paid to the patient's subjective feelings and assessment of one's health status. Smell disorders can significantly impact human life. The Questionnaire of Olfactory Disorders (QOD) is a self-monitoring questionnaire that provides subjective information about olfactory disorders.

Objectives. This study aimed to check the reliability and validation of the Polish version of QOD (QOD-PL) for use in patients with olfactory impairment in Poland.

Materials and methods. A total of 158 patients (76 females, mean age (M_{age}) 45.97 ± 16.37 years), suffering from chronic rhinosinusitis (CRS), whose olfactory function was measured using the Sniffin' Sticks test (SST), were studied. All patients completed 3 validated questionnaires: Importance of Olfaction (IO), Sino-Nasal Outcome Test–22 (SNOT-22) and QOD-PL.

Results. Internal consistency and test-retest reliability of the entire QOD-PL scale were good (Cronbach's $\alpha = 0.88$). The convergent validity of the QOD-PL and its subscales correlated with IO and SNOT-22. The life quality statements in the QOD-PL (QOD-PL-LQ) score, its negative statements, and the mean score for VAS scales were significantly and positively correlated with all symptoms measured with SNOT-22 and none of the IO scales.

Conclusions. The QOD-PL is a reliable, valid and important tool for assessing HRQOL in patients with olfactory disorders. However, it is important to note that not all of its subscales can be considered and interpreted separately.

Key words: quality of life, questionnaire, olfaction disorders, smell, patient-reported outcome measures

Background

The focus on the health-related quality of life (HRQOL) in medical research is increasing, with attention being paid to the patient's subjective feelings and assessment of one's health status. The patient's self-assessment plays an essential role in the treatment process and the effectiveness of the undertaken therapy.^{1,2} Smell disorders can significantly impact human life,^{3,4} yet olfactory dysfunction is consistently undervalued by patients and disregarded by physicians.^{5,6} When the sense of smell is impaired or completely absent, food intake is disrupted, and the critical alarm system toward environmental hazards such as gas leakages or spoiled foods becomes dysfunctional. Furthermore, human social communication becomes impaired when the sense of smell is not functioning.⁷ People affected by smell loss (anosmics) are more likely to suffer from psychological problems such as depression. It is estimated that this affects 1 in 4 patients with olfactory disorders.^{8,9}

The growing interest in olfaction-related quality of life (QoL) resulted in a dedicated measurement tool – the Questionnaire of Olfactory Disorders (QOD).³ It is a self-monitoring questionnaire that provides subjective information about olfactory disorders. Furthermore, QOD has been shown to have greater specificity in assessing olfaction-related QoL as compared to other instruments, such as the 36-item Short Form Health Survey (SF-36).¹⁰ Monitoring the consequences of olfactory disorders is of particular importance now, in the post-COVID era, when many people struggle with post-infection anosmia. Furthermore, the COVID-19 pandemic has drawn global attention to the large-scale problem of sudden olfactory loss^{11,12} and the associated reduction in QoL.¹³ Therefore, there is an urgent need to monitor changes in the sense of smell and the severity of these changes in daily life by means of a questionnaire since the loss of smell is a non-specific symptom, and the use of objective tests is problematic.

Objectives

Since QOD is not available in Polish and has no normative data for the Polish population, the present study aimed to check the reliability and validation of the Polish version of QOD (QOD-PL; Supplementary file available at <https://doi.org/10.5281/zenodo.8263258>) for use in patients with olfactory impairment in Poland.

Materials and methods

Participants

A total of 158 people participated in the study, of which 115 were in the study group and were patients with chronic rhinosinusitis (CRS), while the remaining 43 healthy

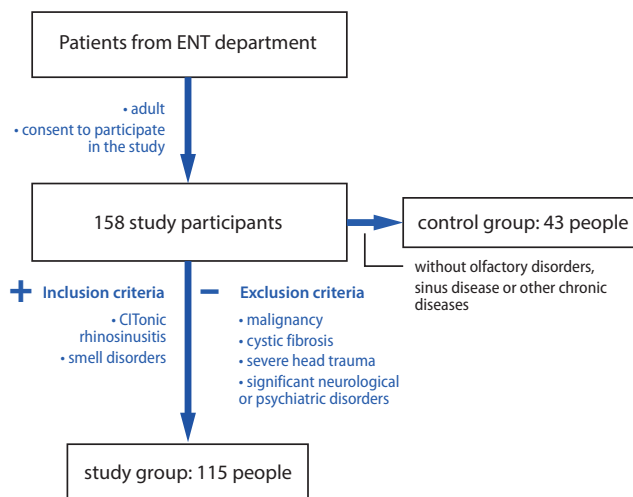


Fig. 1. Recruitment strategy

subjects (without olfactory disorders, sinus disease or other chronic diseases) were in the control group. The study participants were recruited at the Department of Otolaryngology, Head and Neck Surgery of the University Hospital in Wrocław, Poland. The diagnosis was established based on the medical history and a clinical examination, including nasal endoscopy, and complemented with diagnostic imaging – computed tomography (CT) of the sinuses. Patients with malignancy, cystic fibrosis, severe head trauma, or significant neurological or psychiatric disorders were excluded (Fig. 1). Based on the subject's olfactory performance quantified with the Sniffin' Sticks battery (SST test),¹⁴ we categorized them as functionally anosmic (<16 points) or hyposmic (<30.75 points). The parosmia assessment was based on a QOD-PL questionnaire only.

Procedure

Patients included in the study completed 3 questionnaires: 1) QOD-PL, 2) Importance of Olfaction (IO) test¹⁵ and 3) Sino-Nasal Outcome Test – 22 (SNOT-22).¹⁶ The patients completed the QOD-PL twice (test and re-test) at intervals of a minimum of 14 days, prior to surgery or after significant modifications in treatment. The original English version of the QOD questionnaire was translated and adapted to Polish according to internationally accepted guidelines.^{17,18} Two native speakers of Polish who were also fluent in English and familiar with Polish culture translated the original English version of the QOD questionnaire into Polish. A 3rd independent expert compared the 2 translated versions, reaching a consensus. A sequentially coherent version was re-translated into English by 2 native speakers of English who were also experts in Polish and familiar with the country's culture. The translated questionnaire was then compared with the English original. The process was repeated until a consensus was reached, and a final version of the Polish QOD-PL questionnaire was created. Similar to the original QOD questionnaire, the Polish adaptation

Table 1. Items and score method of the questionnaire on olfactory disorders QOD-PL

QOD-PL items		Items	Score method [points]
1. Parosmia statement	QOD-PL-Parosmia	1–4	agree = 3, partly agree = 2, partly disagree = 1, disagree = 0
2. Quality of life statement	QOD-PL-PS	19, 22	agree = 0, partly agree = 1, partly disagree = 2, disagree = 3
	QOD-PL-NS	5–8, 10, 12, 13, 15–17, 20, 21, 24–26, 28, 29	agree = 3, partly agree = 2, partly disagree = 1, disagree = 0
3. Socially desired statements	QOD-PL-SS	11, 18, 27	agree = 3, partly agree = 2, partly disagree = 1, disagree = 0
		9, 14, 23	agree = 0, partly agree = 1, partly disagree = 2, disagree = 3
4. VAS	QOD-VAS	VAS1-VAS5	Scored from 0 to 10 points; the score for each question is chosen individually by the patient based on their own assessment.

VAS – visual analogue scale; QOD-PL – Polish adaptation of QOD questionnaire; QOD-PL-PS – quality of life positive statement; QOD-PL-NS – quality of life negative statement; QOD-PL-SS – socially desired statements; QOD-VAS – Visual Analogue Scale of QOD-PL.

(QOD-PL) consists of 2 parts. The 1st part contains 29 statements divided into 3 subscales: life quality statements (LQ, QOD-PL-LQ), “socially desirable” responses (Sincerity statements, QOD-PL-SS) and parosmia assessment (Parosmia statements, QOD-PL-Parosmia), as shown in Table 1. The 2nd part of the test consists of 5 visual analogue scales (QOD-PL-VAS; Supplementary file available at <https://doi.org/10.5281/zenodo.8263258>). The QOD-PL-LQ expresses the patient’s complaints related to olfactory disorders. They consist of 19 statements – 17 “negative” (so-called negative statements (QOD-PL-NS) and 2 “positive statements” (QOD-PL-PS). For each statement, the respondent gives one answer by marking respectively: “agree”, “partially agree”, “partially disagree”, or “disagree”. Each response is assigned 3, 2, 1, or 0 points, respectively, for NS and reverse scoring for PS. The total score for the Quality of Life (LQrv) assessment can reach 57 points. The LQrv converts to a QoL score. Higher scores indicate a more significant deterioration in the QoL. Statements from the SS subscale indicate whether patients provide the expected information and how reliable their indicated responses are in relation to this. Low scores indicate a tendency to give socially desirable answers. Points for the parosmia assessment are assigned analogously to the QoL-NS. High scores indicate parosmia. The part of the VAS of the questionnaire assesses difficulties with smell using 5 VAS. These relate to how annoying the smell difficulties are (1), how often patients are aware of how annoying the smell difficulties are (1), how often the patients are aware of them (2), to what extent they are affected at their work (3) and on their leisure time (4) and private life (5). The summary and scoring key for QOD-PL are shown in Table 1.

The IO questionnaire by Croy et al. aims to determine the differences in the subjective perception of the sense of smell among patients.¹⁵ The form consists of 20 statements to which one response must be indicated on a 4-point scale from “completely agree” to “completely disagree”. Accordingly, 6 statements each form 3 subscales: Association (IO-Ass), Application (IO-App) and Consequence (IO-Con). The other 2 belong to the Aggravation subscale. The questionnaire’s authors demonstrated its usefulness for normosmia, hyposmia and anosmia.

Sino-Nasal Outcome Test – 22 (SNOT-22),¹⁶ the commonly used questionnaire for the assessment of QoL in rhinosinusitis, was obtained from the author with permission to use it.¹⁹ The first version of this questionnaire was published in 2002 as SNOT-20 by Piccirillo et al.²⁰ It was then modified in 2009 by Hopkins et al. and named SNOT-22.¹⁶ This tool is used to assess the severity of symptoms and complaints in CRS and their impact on the patient’s HRQoL. The SNOT-22 covers a wide range of health problems, including physical problems, functional limitations and emotional consequences resulting from persistent complaints. The questionnaire consists of 22 statements to which responses are assigned on a 5-point scale: 0 – no problem, 1 – a very minor problem, 2 – a minor problem, 3 – a moderate problem, 4 – a severe problem, and 5 – worst possible problem. The maximum possible score is 110 points. The higher the sum of the scores obtained, the more significant the complaints of CRS are and the greater the negative impact on the patient’s QoL. In the 2nd part of the questionnaire, the respondent is asked to mark 5 of the listed complaints that have the greatest impact on their health. DeConde et al. distinguished 5 domains in the SNOT-22 questionnaire. Three of them are specific to sinus complaints (i.e., rhinological symptoms, extra-nasal symptoms and ear-facial symptoms) and 2 general domains related to HRQoL – psychological and sleep disturbance domains.²¹ When comparing the questionnaires with each other and assuming that the validated questionnaire is working properly, positive correlations are expected between QOD-PL and SNOT-22; it can be assumed that the relationship between QOD-PL and IO will be inversely proportional or neutral.

Statistical analyses

Data were analyzed using IBM SPSS v. 26 software (IBM Corp., Armonk, USA) with the level of significance set to $\alpha = 0.01$ to correct for multiple comparisons and reduce the risk of false positive results (type I errors). The internal consistency of the QOD and its subscales was assessed using Cronbach’s α coefficient, and the values of 0.70–0.95²² were considered satisfactory. Data distribution was confirmed

Table 2. Descriptive statistics for demographical information and Sniffin' Sticks scores across the 3 groups. Numbers in brackets denote standard deviation (SD)

Variable	Functional anosmia	Hyposmia	Normosmia
Number of participants, n	47	47	64
Women, n	20	19	37
Age [years]	54.5 (±13.9)	49.9 (±15.4)	36.8 (±14.3)
Odor threshold	1.0 (±0.4)	4.4 (±2.8)	10.1 (±2.3)
Odor discrimination	1.2 (±2)	9.4 (±2)	11.9 (±1.5)
Odor identification	1.8 (±2.5)	10.3 (±2)	12.8 (±1.8)
TDI	3.9 (±4.3)	24.1 (±4.5)	34.7 (±3.2)

TDI – total score of the Sniffin' Sticks test (threshold + discrimination + identification).

to differ from normality, as indicated by the significant result of the Kolmogorov–Smirnov test ($p < 0.01$). Therefore, we used non-parametric tests. Intergroup differences in age were assessed utilizing the Kruskal–Wallis test. The test-retest reliability examined the absolute agreement between the measurements with the two-way mixed intraclass correlation coefficient (ICC). The convergent validity of the QOD-PL was assessed by examining the correlation between its scores with the SNOT-22 and IO questionnaire scores and the SST test for olfactory dysfunction, using the Spearman's rho (r_s) partial correlation coefficient (controlling for rhinological symptoms measured with SNOT-22). Finally, the discriminative validity of the QOD-PL was evaluated by comparing its scores between subgroups of patients with different olfactory functions (anosmics, hyposmics and normosmics) using the Kruskal–Wallis test as well as between patients with CRS compared to healthy controls utilizing the Mann–Whitney U test.

Ethical considerations

The ethics review board of Wroclaw Medical University approved the study design and consent approach (approval No. KB – 259/2017). The study was conducted in accordance with the Declaration of Helsinki on Biomedical Studies Involving Human Subjects. Informed written consent was obtained from all participants, who were volunteers and were aware of the study's aim, design and clinical implications.

Results

Participants

A total of 158 subjects aged between 19 and 87 years participated in this study (median age (M_{age}) = 45.97 ± 16.37 years, 76 women), of whom 115 subjects were patients with CRS (without/with nasal polyps; M_{age} = 49.4 ± 15.4 years, 51 women). The control group was 43 healthy subjects (M_{age} = 36.7 ± 15.4 years, 25 women).

Sex was distributed independently from olfactory performance ($\chi^2 = 4.1$, $p = 0.13$). There was a significant effect

of the group on age ($H(2) = 37.5$, $p < 0.001$), suggesting that the anosmic and hyposmic groups were significantly older than the normosmic group ($p < 0.001$) but not different from each other ($p = 0.618$). All 43 healthy subjects' SST scores fell into the range of normosmia (≥ 30.75 points).²³ Descriptive statistics for the 3 groups are summarized in Table 2.

The reliability of the entire QOD-PL scale was good (Cronbach's $\alpha = 0.88$). Reliability of the QOD-PL-NS was excellent, as reflected by Cronbach's $\alpha = 0.94$, yet the reliability of QOD-PL-PS was poor with Cronbach's $\alpha = 0.50$ (for QOD-LQ jointly Cronbach's $\alpha = 0.88$ suggesting overall good reliability), reliability of QOD-PL-SS was poor with Cronbach's $\alpha = 0.53$, and QOD-PL-Parosmia Cronbach's $\alpha = 0.70$ suggested satisfactory reliability, while VAS scales presented good reliability with Cronbach's $\alpha = 0.86$. The ICCs and the results of the paired samples t-tests are summarized in Table 3.

Table 3. Interclass correlation of the QOD-PL and its subscales

QOD-PL items	ICC	
	ICC	p-value
QOD-LQ	0.97	<0.001
QOD-PL-NS	0.82	<0.001
QOD-PL-PS	0.96	<0.001
QOD-PL-SS	0.82	<0.001
QOD-PL-Parosmia	0.88	<0.001
QOD-PL-VAS	0.96	<0.001

ICC – intra-class correlation; QOD-PL – Polish adaptation of QOD questionnaire; QOD-LQ – life quality statement; QOD-PL-PS – quality of life positive statement; QOD-PL-NS – quality of life negative statement; QOD-PL-SS – socially desired statements; QOD-VAS – Visual Analogue Scale of QOD-PL.

Correlation between QOD-PL and IO and SNOT-22

The convergent validity of the QOD-PL and its subscales were correlated with IO and SNOT-22. The QOD-PL-LQ score, its negative statements and the mean score for VAS scales were significantly and positively correlated with all symptoms measures with SNOT-22 and none of the IO scales (Table 4). QOD-PL-PS and QOD-PL-SS were not

Table 4. Spearman's rho correlation coefficients and the significance level for the relationship between QOD-PL, IO and SNOT-22

Items of the questionnaires		QOD-PL-NS	QOD-PL-PS	QOD-LQ	QOD-PL-SS	QOD-PL-Parosmia	QOD-PL-VAS
IO-Ass	r_s	-0.08	0.23	0.01	0.14	-0.02	0.02
	p	0.33	0.01	0.89	0.07	0.86	0.82
IO-App	r_s	-0.01	0.16	0.04	0	0.06	0.04
	p	0.88	0.05	0.58	1	0.43	0.63
IO-Con	r_s	-0.13	0.13	-0.07	0.07	-0.02	-0.06
	p	0.10	0.12	0.36	0.42	0.78	0.43
Rhinological symptoms	r_s	0.66	-0.02	0.67	0.08	0.52	0.59
	p	<0.001	0.77	<0.001	0.34	<0.001	<0.001
Extra-nasal symptoms	r_s	0.54	-0.02	0.54	-0.01	0.49	0.47
	p	<0.001	0.77	<0.001	0.93	<0.001	<0.001
Ear/facial symptoms	r_s	0.45	0.02	0.47	0.07	0.46	0.36
	p	<0.001	0.77	<0.001	0.40	<0.001	<0.001
Psychological dysfunction	r_s	0.50	0.03	0.52	0.04	0.43	0.46
	p	<0.001	0.86	<0.001	0.63	<0.001	<0.001
Sleep dysfunction	r_s	0.60	0.04	0.61	0.02	0.49	0.47
	p	<0.001	0.57	<0.001	0.81	<0.001	<0.001

QOD-PL – Polish adaptation of QOD questionnaire; QOD-PL-PS – quality of life positive statement; QOD-PL-NS – quality of life negative statement; QOD-PL-SS – socially desired statements; QOD-VAS – Visual Analogue Scale of QOD-PL; r_s – Spearman's rho correlation coefficient; p – p-value of the significant result; IO – Importance of Olfaction questionnaire: IO-Ass – Association, IO-App – Application, IO-Con – Consequence. Values in bold are statistically significant.

related to IO or SNOT-22. Statistical coefficients and the level of significance are summarized in Table 4.

The discriminant validity was assessed by examining the intergroup differences in QOD-The PL scores for subjects with anosmia, hyposmia and normosmia. We found significant intergroup differences for the total QOD-LQ score and its negative statements (QOD-PL-NS) and VAS scales. The questionnaire also differentiated subjects with normosmia from both groups exhibiting olfactory deficits in terms of parosmia symptoms. Positive and sincerity statements did not yield any differences between subjects with anosmia, hyposmia and normosmia. However, healthy controls scored lower than CRS patients in the QOD-PL-NS (mean rank (M_{rank}) = 94.5 compared to M_{rank} = 39.3, U = 744, p < 0.001, respectively), QOD-PL-LQ (M_{rank} = 94 compared to M_{rank} = 40.7, U = 805.5, p < 0.001), QOD-PL-Parosmia (M_{rank} = 87.9 compared to M_{rank} = 57.1, U = 1510, p < 0.001), and QOD-PL-VAS (M_{rank} = 97.2 compared to M_{rank} = 48.3, U = 1130.5, p < 0.001); and healthy controls scored higher than CRS patients in QOD-PL-SS (M_{rank} = 87.9 compared to M_{rank} = 76.4, U = 2834, p < 0.001), corroborating the comparison between anosmic, hyposmic and normosmic groups (Fig. 2).

Subjects with CRS diagnosis

There were no significant sex-related differences in any of the QOD-PL subscales (all p > 0.13). Age was positively related to QOD-PL-NS (r_s = 0.22, p = 0.006) and

QOD-PL-Parosmia (r_s = 0.25, p = 0.001), suggesting that olfaction-related complaints and parosmia increase with age. On the contrary, the QOD-PL-PS score was negatively related to age (r_s = -0.16, p = 0.049), indicating worse coping with olfactory loss in older subjects. Examination of the relationships between QOD-PL scores and olfactory performance while controlling for rhinological symptoms revealed a significant negative relationship between QOD-LQ scores (driven by the QOD-PL-NS subscale), indicating that stronger complaints were recorded with the questionnaire (i.e., higher QOD-PL scores), the poorer olfactory performance was measured with the SST test. The QOD-PL-VAS was negatively associated with odor identification, suggesting that lower scores on the QOD-PL-VAS related to the lower ability to name odorants. No relationship was found between the QOD-PL-PS, QOD-PL-SS and QOD-PL-Parosmia and olfactory performance. Spearman's rho correlation coefficients are presented in Table 5.

Discussion

The results of our study showed that the QOD-PL had good reliability and accuracy, making this questionnaire in our translation a reliable and valid tool for otolaryngological assessments of the QoL. Moreover, a poorer smell-related QoL (QOD-PL) correlated with scores on the more objective SST test. In the next steps of the tool's development, QOD-PL should be included in clinical trials to see

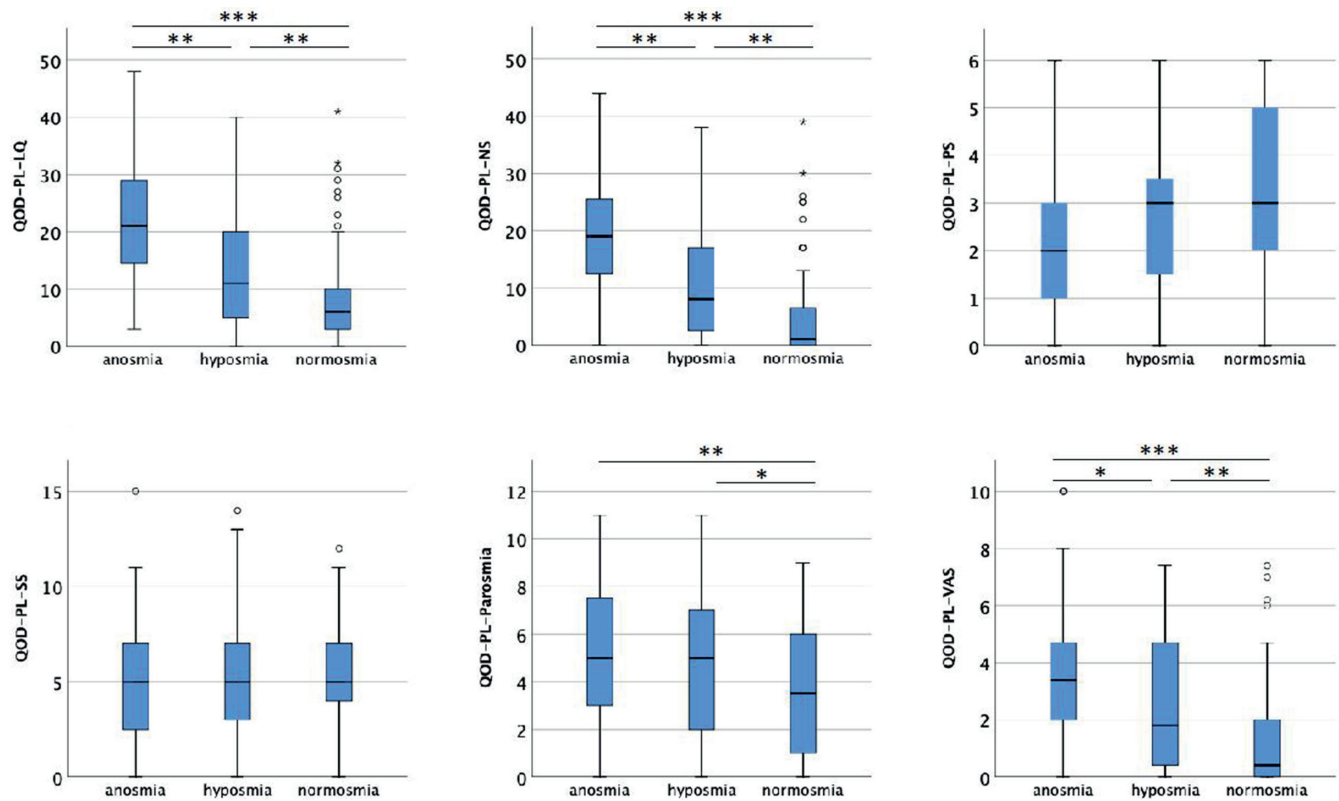


Fig. 2. The discriminant validity of the Polish adaptation of a Questionnaire of Olfactory Disorders (QOD-PL) was assessed as a function of olfactory performance. Black thick horizontal lines mark the median, boxes mark the distribution of scores from 25th–75th percentiles, and whiskers mark the 0–25th and 75th–100th percentiles. Dots represent outliers (as defined using SPSS software, no outliers were excluded)

*** $p < 0.001$; ** $p < 0.01$; * $p < 0.05$.

Table 5. Spearman's rho partial correlation coefficients for the relationships between olfactory performance and QOD-PL scores controlling for rhinological symptoms (SNOT-22)

QOD-PL item		Odor threshold	Odor discrimination	Odor identification
QOD-LQ	r_s	-0.23	-0.29	-0.30
	p	0.004	<0.001	<0.001
QOD-PL-NS	r_s	-0.27	-0.32	-0.34
	p	<0.001	<0.001	<0.001
QOD-PL-PS	r_s	0.21	0.17	0.18
	p	0.01	0.04	0.02
QOD-PL-SS	r_s	0.04	0.14	0.14
	p	0.60	0.09	0.08
QOD-PL-Parosmia	r_s	-0.04	-0.06	-0.02
	p	0.61	0.45	0.79
QOD-PL-VAS	r_s	-0.14	-0.17	-0.21
	p	0.09	0.04	0.008

QOD-PL – Polish adaptation of QOD questionnaire; QOD-PL-PS – quality of life positive statement; QOD-PL-NS – quality of life negative statement; QOD-PL-SS – socially desired statements, QOD-VAS – Visual Analogue Scale of QOD-PL, r_s – Spearman's rho correlation coefficient, p – p-value of the significant result. Values in bold are statistically significant.

if an improvement in the QoL (as measured with QOD-PL) follows various interventions, including surgical. However, this component was not part of this study.

We observed relatively lower psychometrical values for the QOD-PL-PS. The questionnaire authors obtained similar values for Cronbach's α coefficients for the QOD-PS

components at 0.054,³ while a slightly higher value of Cronbach's α for this component (0.69) was obtained by the authors of the questionnaire's adaptation into Greek.¹⁰ Following other research groups, it is possible to use only the negative scale (QOD-NS),^{24,25} with the partial omission of the positive scale, and this should not have

significant consequences for the reliability of the results, but we suggest empirically testing it in Poland.

A comparison of QOD-PL and SNOT-22 scores in the same group of patients showed statistically significant correlations between smell-related QoL and all domains of the SNOT-22 questionnaire, i.e., rhinological symptoms, extra-nasal symptoms, ear/facial symptoms, psychological dysfunction, and sleep dysfunction. In conclusion, as CRS disease severity-related QoL deteriorates, olfactory-related QoL declines. Therefore, the expected relationship between QOD-PL and SNOT-22 proves the external validity of QOD-PL in the Polish population.

A comparison of QOD-PL and IO scores showed no significant correlation. This may be explained by the fact that functional anosmic patients, compared to normosmic subjects, both healthy and CRS patients, place statistically significantly less importance on using the sense of smell during daily activities.^{26,27} This simultaneously indicates a successful adaptation of these patients to the disorders of the sense of smell. At the same time, normosmic patients tend to exaggerate the importance of the sense of smell. This may be due to the sudden, temporary deterioration of the ability to smell due to the severity of the CRS lesions, which is associated with a lack of adaptation to the changes and, consequently, a lack of acceptance of the loss of smell.²⁶ Hence, the IO questionnaire alone should not be used to monitor olfactory impairment.

Limitations

The study included patients with the same cause of olfactory disorders, and it would be worthwhile in the future to test the questionnaire's performance for different reasons of disorders.

Conclusions

The QOD-PL is a reliable, valid and important tool for assessing HRQOL in patients with olfactory disorders. However, when the subgroups of this questionnaire are considered separately, the negative statement domain of QOD-PL can be analyzed independently and the positive statements part of the QOD-PL should not be considered individually for any interpretation. Nevertheless, to the authors' knowledge, it is the only tool currently available in the Polish population to assess the QoL and to measure problems related to olfactory impairment.

ORCID iDs

Katarzyna Resler  <https://orcid.org/0000-0002-1399-5524>
 Anna Oleszkiewicz  <https://orcid.org/0000-0003-2217-1858>
 Marcin Frączek  <https://orcid.org/0000-0003-0181-122X>
 Monika Morawska-Kochman  <https://orcid.org/0000-0001-6551-7535>
 Anna Resler  <https://orcid.org/0000-0001-9297-6198>
 Tomasz Zatoński  <https://orcid.org/0000-0003-3043-4806>
 Thomas Hummel  <https://orcid.org/0000-0001-9713-0183>

Reference

- Kanakubo A, Mizuno M, Asano Y, Inoue Y. Acceptability to making a self-assessment using a tablet computer and health-related quality of life in ambulatory breast cancer patients. *Asia Pac J Oncol Nurs*. 2022;9(2):105–112. doi:10.1016/j.apjon.2021.12.011
- Soler ZM, Smith TL, Alt JA, Ramakrishnan VR, Mace JC, Schlosser RJ. Olfactory-specific quality of life outcomes after endoscopic sinus surgery. *Int Forum Allergy Rhinol*. 2016;6(4):407–413. doi:10.1002/alr.21679
- Frasnelli J, Hummel T. Olfactory dysfunction and daily life. *Eur Arch Otorhinolaryngol*. 2005;262(3):231–235. doi:10.1007/s00405-004-0796-y
- Thomas AJ, Mace JC, Ramakrishnan VR, et al. Quality of life and olfaction changes observed with short-term medical management of chronic rhinosinusitis. *Int Forum Allergy Rhinol*. 2020;10(5):656–664. doi:10.1002/alr.22532
- Landis BN. Ratings of overall olfactory function. *Chem Senses*. 2003;28(8):691–694. doi:10.1093/chemse/bjg061
- Welge-Luessen A, Hummel T, Stojan T, Wolfensberger M. What is the correlation between ratings and measures of olfactory function in patients with olfactory loss? *Am J Rhinol*. 2005;19(6):567–571. PMID:16402642.
- Hummel T, Nordin S. Olfactory disorders and their consequences for quality of life. *Acta Otolaryngol*. 2005;125(2):116–121. doi:10.1080/00016480410022787
- Croy I, Hummel T. Olfaction as a marker for depression. *J Neuro*. 2017;264(4):631–638. doi:10.1007/s00415-016-8227-8
- Mattos JL, Schlosser RJ, DeConde AS, et al. Factor analysis of the questionnaire of olfactory disorders in patients with chronic rhinosinusitis: QOD-NS Factor Analysis. *Int Forum Allergy Rhinol*. 2018;8(7):777–782. doi:10.1002/alr.22112
- Simopoulos E, Katotomichelakis M, Gouveris H, Tripsianis G, Livaditis M, Danielides V. Olfaction-associated quality of life in chronic rhinosinusitis: Adaptation and validation of an olfaction-specific questionnaire. *Laryngoscope*. 2012;122(7):1450–1454. doi:10.1002/lary.23349
- Moein ST, Hashemian SM, Mansourafshar B, Khorram-Tousi A, Tabarsi P, Doty RL. Smell dysfunction: A biomarker for COVID-19. *Int Forum Allergy Rhinol*. 2020;10(8):944–950. doi:10.1002/alr.22587
- Parma V, Ohla K, Veldhuizen MG, et al. More than smell: COVID-19 is associated with severe impairment of smell, taste, and chemesthesis. *Chem Senses*. 2020;45(7):609–622. doi:10.1093/chemse/bjaa041
- Coelho DH, Reiter ER, Budd SG, Shin Y, Kons ZA, Costanzo RM. Quality of life and safety impact of COVID-19 associated smell and taste disturbances. *Am J Otolaryngol*. 2021;42(4):103001. doi:10.1016/j.amjoto.2021.103001
- Hummel T, Sekinger B, Wolf SR, Pauli E, Kobal G. 'Sniffin' Sticks': Olfactory performance assessed by the combined testing of odor identification, odor discrimination and olfactory threshold. *Chem Senses*. 1997;22(1):39–52. doi:10.1093/chemse/22.1.39
- Croy I, Buschhüter D, Seo HS, Negoias S, Hummel T. Individual significance of olfaction: Development of a questionnaire. *Eur Arch Otorhinolaryngol*. 2010;267(1):67–71. doi:10.1007/s00405-009-1054-0
- Hopkins C, Gillett S, Slack R, Lund VJ, Browne JP. Psychometric validity of the 22-Item Sinonasal Outcome Test. *Clin Otolaryngol*. 2009;34(5):447–454. doi:10.1111/j.1749-4486.2009.01995.x
- Guillemin F, Bombardier C, Beaton D. Cross-cultural adaptation of health-related quality of life measures: Literature review and proposed guidelines. *J Clin Epidemiol*. 1993;46(12):1417–1432. doi:10.1016/0895-4356(93)90142-N
- Beaton DE, Bombardier C, Guillemin F, Ferraz MB. Guidelines for the process of cross-cultural adaptation of self-report measures. *Spine (Phila Pa 1976)*. 2000;25(24):3186–3191. doi:10.1097/00007632-200012150-00014
- Office of Technology Management of Washington University in St. Louis. Sino-Nasal Outcome Test (SNOT). Available translations. St. Louis, USA: Washington University of St. Louis; 2023. <https://sinonasaltest.wustl.edu/sino-nasal-outcome-test-snot/available-translations-2>. Accessed April 6, 2023.
- Piccirillo JF, Merritt MG, Richards ML. Psychometric and clinimetric validity of the 20-Item Sino-Nasal Outcome Test (SNOT-20). *Otolaryngol Head Neck Surg*. 2002;126(1):41–47. doi:10.1067/mhn.2002.121022

21. DeConde AS, Mace JC, Bodner T, et al. SNOT-22 quality of life domains differentially predict treatment modality selection in chronic rhinosinusitis. *Int Forum Allergy Rhinol.* 2014;4(12):972–979. doi:10.1002/alr.21408
22. Tavakol M, Dennick R. Making sense of Cronbach's alpha. *Int J Med Educ.* 2011;2:53–55. doi:10.5116/ijme.4dfb.8dfd
23. Oleszkiewicz A, Schriever VA, Croy I, Hähner A, Hummel T. Updated Sniffin' Sticks normative data based on an extended sample of 9139 subjects. *Eur Arch Otorhinolaryngol.* 2019;276(3):719–728. doi:10.1007/s00405-018-5248-1
24. Chiesa-Estomba CM, Lechien JR, Calvo-Henríquez C, et al. Translation and validation of the short version of the Questionnaire of Olfactory Disorders–Negative Statements to Spanish. *Am J Otolaryngol.* 2021;42(1):102775. doi:10.1016/j.amjoto.2020.102775
25. Mattos JL, Schlosser RJ, Storck KA, Soler ZM. Understanding the relationship between olfactory-specific quality of life, objective olfactory loss, and patient factors in chronic rhinosinusitis. *Int Forum Allergy Rhinol.* 2017;7(7):734–740. doi:10.1002/alr.21940
26. Murr J, Hummel T, Ritschel G, Croy I. Individual significance of olfaction: A comparison between normosmic and dysosmic people. *Psychosomatics.* 2018;59(3):283–292. doi:10.1016/j.psym.2017.11.009
27. Croy I, Landis BN, Meusel T, Seo HS, Krone F, Hummel T. Patient adjustment to reduced olfactory function. *Arch Otolaryngol Head Neck Surg.* 2011;137(4):377. doi:10.1001/archoto.2011.32

Tasquinimod enhances the sensitivity of ovarian cancer cells to cisplatin by regulating the Nur77-Bcl-2 apoptotic pathway

Ying Lin^{1,A,B,D–F}, Ya-Qiong Liu^{2,A–D,F}, Ke-An Zhu^{1,B,C,E,F}, Meng-Qi Hu^{1,B–D,F}, Zhao Li^{1,B–D,F}, Xiao-Jia Min^{1,A,B,E,F}

¹ Department of Gynecology, The First Affiliated Hospital of Hunan Normal University, Changsha, China

² Department of Gynecology and Obstetrics, Guangzhou Women and Children's Medical Center, Guangzhou Medical University, China

A – research concept and design; B – collection and/or assembly of data; C – data analysis and interpretation;

D – writing the article; E – critical revision of the article; F – final approval of the article

Advances in Clinical and Experimental Medicine, ISSN 1899–5276 (print), ISSN 2451–2680 (online)

Adv Clin Exp Med. 2024;33(2):151–161

Address for correspondence

Xiao-Jia Min

E-mail: Minminjia2022@163.com

Funding sources

This work was supported by the Clinical Medical Technology Innovation Guide Project of Hunan Province (grant No. 2020SK50905).

Conflict of interest

None declared

Received on September 30, 2022

Reviewed on December 5, 2022

Accepted on May 9, 2023

Published online on July 28, 2023

Cite as

Lin Y, Liu YQ, Zhu KA, Hu MQ, Li Z, Min XJ. Tasquinimod enhances the sensitivity of ovarian cancer cells to cisplatin by regulating the Nur77-Bcl-2 apoptotic pathway.

Adv Clin Exp Med. 2024;33(2):151–161.

doi:10.17219/acem/166044

DOI

10.17219/acem/166044

Copyright

Copyright by Author(s)

This is an article distributed under the terms of the Creative Commons Attribution 3.0 Unported (CC BY 3.0) (<https://creativecommons.org/licenses/by/3.0/>)

Abstract

Background. Resistance to cisplatin (DDP) in ovarian cancer therapy has been a major clinical barrier. Drug-resistant cancers have been shown to downregulate the proapoptotic protein B-cell lymphoma-2 (Bcl-2) to inhibit apoptosis. Therefore, we explored whether tasquinimod could modulate resistance to DDP through apoptotic pathways.

Objectives. We aimed to explore the relationship between tasquinimod, Nur77-Bcl-2 apoptosis pathway and sensitivity of the ovarian carcinoma cell line SKOV3 and the DDP-resistant strain SKOV3/DDP cells to DDP.

Materials and methods. First, SKOV3 and SKOV3/DDP cells were treated with 2 µg/mL DDP or 40 µM tasquinimod. Western blot and quantitative real-time polymerase chain reaction (qPCR) were then used to analyze the expression of histone deacetylase 4 (HDAC4), Nur77, Bcl-2 (BH3 domain-specific), and caspase-3. Flow cytometry, scratch-wound assay and immunofluorescence were used to detect apoptosis, migration rate, and related expression of Nur77 and Bcl-2 (BH3 domain-specific). Subsequently, 5×10^7 SKOV3 or SKOV3/DDP cells cultured with 2 µg/mL DDP were injected into 4-week-old female BALB/c nude mice. Then, the mice were administered 4 mg/kg DDP and 50 mg/kg tasquinimod every 3 days. Finally, the changes in tumor diameter and weight were measured.

Results. After treatment of SKOV3 and SKOV3/DDP cells with tasquinimod, cell migration and HDAC4 expression levels were significantly reduced, while Nur77 expression was increased. Tasquinimod treatment enhanced the expression of Nur77 and caspase-3, and cells transfected with si-Nur77 showed the opposite result. Transfection of si-Nur77 reduced the expression of caspase-3 and Nur77 in the SKOV3/DDP cells that were treated with both DDP and tasquinimod. After injection of SKOV3/DDP cells into the mice, the tumor diameter, mass and in vivo HDAC4 level were significantly decreased by tasquinimod. Meanwhile, the levels of Nur77 and Bcl-2 (BH3 domain-specific) were increased.

Conclusions. Tasquinimod upregulated the Nur77/Bcl-2 pathway to induce apoptosis in SKOV3/DDP cells and enhanced the anti-tumor effect of DDP in SKOV3/DDP xenografts. Therefore, tasquinimod can be expected to find clinical applications in enhancing DDP resistance.

Key words: ovarian cancer, resistance to cisplatin (DDP), tasquinimod, Nur77-Bcl-2 pathway

Background

Ovarian cancer is considered one of the deadliest gynecological malignancies worldwide,¹ with most patients presenting at an advanced stage due to a lack of formal screening and early detection methods.² Currently, the standard treatment for ovarian cancer is chemotherapy and cytoreductive surgery,^{3,4} with the initial adjuvant treatment being platinum-based drugs such as cisplatin (DDP) or carboplatin.¹ Cisplatin interferes with DNA repair mechanisms by cross-linking DNA purine bases, thus inducing apoptosis in cancer cell.⁵ Although DDP has been for decades a key chemotherapeutic drug for treating patients with different forms of tumors, drug resistance is a major clinical barrier.⁶

Cancer cells often evade apoptosis by upregulating the anti-apoptotic protein B-cell lymphoma 2 (Bcl-2), while drug-resistant cancers downregulate or inactivate proapoptotic proteins to inhibit apoptosis.⁷ The level of Bcl-2 increases in DDP-resistant ovarian cancer cell lines compared with non-resistant cells,⁸ and the overexpression of Bcl-2 increases the cell growth and apoptosis inhibition of DDP-induced SKOV3 cells.⁹

It is widely known that Bcl-2 exposes its Bcl-2 (BH3 domain-specific) after binding to orphan nuclear receptor 4A1 (Nur77),¹⁰ resulting in the conversion of the original anti-apoptotic effect to a proapoptotic effect.¹¹ This interaction with Nur77 is mediated by the N-terminal ring region of Bcl-2, and this action is required for the apoptosis of cancer cells that is induced by many anti-tumor drugs.¹⁰ In ovarian cancer tissue microarrays, the expression of Nur77 was significantly reduced in platinum-resistant tumors.¹² While Nur77 binds Bcl-2 to induce its conformational change and exposes its BH3 domain, resulting in the proapoptotic effect of Bcl-2,¹⁰ this effect has not been investigated in DDP-resistant ovarian cancer.

Interestingly, histone deacetylase 4 (HDAC4) binds to the transcriptional regulatory region of the *Nur77* gene.¹³ Deacetylation of histones occurs through HDAC, which is abnormal in many types of cancer,^{14,15} and histone acetylation significantly affects the transcription of target genes.¹³ Moreover, HDAC4 can regulate tumorigenesis by remodeling the chromatin structure and controlling protein entry onto DNA.¹⁴ Additionally, HDAC inhibitors enhance radiation-induced cell death and reduce DNA double-strand breaks, leading to increased apoptosis,¹⁴ which suggests that HDAC may play a role in the disease process.^{14,15}

Tasquinimod is an analog of the HDAC inhibitor BML-210.¹⁶ It prevents HDAC4-dependent recruitment of MEF2 to DNA, thereby increasing the expression of the target gene *Nur77*.^{17,18} Tasquinimod, a quinoline 3-carboxamide derivative, has shown structural similarity to kynurenic acid (KYNA), an endogenous tryptophan metabolite,^{15,20} and is primarily considered an anti-cancer drug.¹⁹ Therefore, it is reasonable to speculate that the lack of Nur77 can convert the anti-apoptotic function of Bcl-2 to proapoptotic.

Objectives

There is currently no research regarding the effect of tasquinimod on the DDP sensitivity of ovarian cancer cell lines. Therefore, this study aims to explore the relationship between tasquinimod, the Nur77-Bcl-2 apoptosis pathway and the DDP sensitivity of ovarian cancer cell lines.

Materials and methods

Cell culture and treatment

First, the normal human ovarian epithelial cell IOSE80 was obtained from Shanghai Huiying Biotech (Shanghai, China), and the ovarian carcinoma cell line SKOV3 and the DDP-resistant strain SKOV3/DDP cells were produced by American Type Culture Collection (ATCC; Manassas, USA). The IOSE80,²¹ SKOV3²² and SKOV3/DDP²³ cells were cultured in Roswell Park Memorial Institute (RPMI)-1640 medium containing 10% fetal bovine serum (FBS) at 37°C with 5% CO₂.⁴ The cells were passaged at a ratio of 1:3 to 1:4, and they were in the log phase for subsequent experiments.

The cells were divided into 11 groups and then treated as follows: 1) SKOV3 group – SKOV3 cells without treatment; 2) SKOV3+tasquinimod group – SKOV3 cells treated with 40 μM tasquinimod²⁴; 3) SKOV3/DDP group – SKOV3/DDP cells without any treatment; 4) SKOV3/DDP+tasquinimod group – SKOV3/DDP cells treated with 40 μM tasquinimod; 5) SKOV3+DDP group – SKOV3 cells treated with 2 μg/mL DDP²³; 6) SKOV3/DDP+DDP group – SKOV3/DDP cells treated with 2 μg/mL DDP; 7) SKOV3/DDP+DDP+tasquinimod group – SKOV3/DDP cells treated with 2 μg/mL DDP and 40 μM tasquinimod.

The last 4 groups were treated with tasquinimod or DDP after being transfected with expression vectors according to the manufacturer's protocol. The negative siRNA (si-NC) or Nur77 siRNA (si-Nur77) (Shanghai GenePharma Co., Ltd., Shanghai, China) was transfected into SKOV3/DDP cells using Lipofectamine® 2000 (Invitrogen, Thermo Fisher Scientific, Waltham, USA).^{8,25} The transfected cell groups were as follows: 8) SKOV3/DDP+DDP+si-NC group – SKOV3/DDP cells cultured with 2 μg/mL DDP after being transfected with si-NC; 9) SKOV3/DDP+DDP+tasquinimod+si-NC group – SKOV3/DDP cells cultured with 40 μM tasquinimod and 2 μg/mL DDP after being transfected by si-NC; 10) SKOV3/DDP+DDP+si-Nur77 group – SKOV3/DDP cells cultured with 2 μg/mL DDP after transfection with si-Nur77; and 11) SKOV3/DDP+DDP+tasquinimod+si-Nur77 group – SKOV3/DDP cells cultured with 2 μg/mL DDP and 40 μM tasquinimod after being transfected with si-Nur77. All groups cultured with 40 μM tasquinimod or 2 μg/mL DDP were treated for 24 h.

Animals

The SKOV3 or SKOV3/DDP cells (5×10^7) were subcutaneously injected into 4-week-old female BALB/c nude mice.^{26,27} To explore the role of tasquinimod, we divided the nude mice into 3 groups, namely SKOV3+DDP, SKOV3/DDP+DDP and SKOV3/DDP+DDP+tasquinimod. The SKOV3+DDP group was subcutaneously injected with 5×10^7 SKOV3 cells after being treated with 2 $\mu\text{g}/\text{mL}$ DDP for 48 h, and then 4 mg/kg DDP was injected every 3 days. The SKOV3/DDP+DDP group was subcutaneously injected with 5×10^7 SKOV3/DDP cells after being cultured with 2 $\mu\text{g}/\text{mL}$ DDP for 48 h, and then 4 mg/kg DDP was injected every 3 days. The SKOV3/DDP+DDP+tasquinimod group was subcutaneously injected with 5×10^7 SKOV3/DDP cells after being cultured with 2 $\mu\text{g}/\text{mL}$ DDP for 48 h, then 4 mg/kg DDP and 50 mg/kg tasquinimod were injected every 3 days. All mice were sacrificed, and tumor lesions were excised after 5 weeks. Next, images of mice and tumors were obtained from Shanghai Laboratory Animal Research Center (Shanghai, China), which was approved by China Medical University Animal Care and Use Committee, and complied with national criteria on experimental procedures on animals.

Cell Counting Kit-8 (CCK-8)

The cells (logarithmic phase) were seeded at a density of 2.5×10^3 into a well for 24 h. The CCK-8 reagent (NU679; Dojindo Laboratories, Rockville, USA) was added to the wells and then incubated for 1 h at 37°C.²⁸ The absorbance of the sample at 450 nm was detected using a microplate reader, and each group was tested 3 times.

Scratch-wound assay²⁹

Cells were seeded at a density of 1×10^5 cells/well on 1% gelatin-coated six-well plates (Corning, Cambridge, USA). The linear wounds were scratched using a sterile pipette tip. The monolayers were then washed with phosphate-buffered saline (PBS) to clear away floating cells. After 24 h or 48 h of incubation with RPMI-1640 media, cell migration was assessed using inverted biological microscope (model DSZ2000X; Cnmicro, Beijing, China). All experiments were performed independently in triplicate. Each group was tested 3 times.

Detection of cell apoptosis by flow cytometry

Collected cells were washed once with PBS and treated with Annexin V-FITC Apoptosis Detection Kit (KGA108; Nanjing KeyGen Biotech, Nanjing, China).³⁰ Briefly, the binding buffer was used to suspend cells; then, Annexin V-FITC and propidium iodide were added for 10 min

in the dark. A flow cytometer (A00-1-1102; Beckman Coulter, Brea, USA) was used to analyze apoptosis.³¹ Each group was tested 3 times.

Immunofluorescence

The distribution and level of Nur77³² and Bcl-2 (BH3 domain-specific)³³ were detected with immunofluorescence (IF) staining. Cells were fixed in 4% paraformaldehyde for 15 min, washed with PBS and permeabilized with 0.1% Triton X-100. Next, bovine serum albumin (BSA) was used to block the non-specific antigens at room temperature, and an anti-Nur77 antibody (#3960s; Cell Signaling Technology, Danvers, USA) or an anti-Bcl-2 antibody (ab32445; Abcam, Waltham, USA) was applied overnight at 4°C. After washing with PBS, secondary anti-rabbit IgG (H+L) antibodies were applied. Finally, the nucleus was visualized with 4',6-diamidino-2-phenylindole (DAPI), and cells were observed under a fluorescence microscope (model BA210T; Motic, Xiamen, China). Each group was tested 3 times.

Quantitative real-time polymerase chain reaction (qPCR)

Total RNA (cells or tissues) was separated using the TRIzol method. RevertAid™ First Strand cDNA Synthesis Kit (CW2569; Beijing Comwin Biotech, Beijing, China) was used to transcribe cDNA.³⁴ Primer sequences of β -actin, HDAC4 and Nur77 were purchased from Sangon Biotech (Shanghai, China) (Table 1).³⁵ Next, a fluorescent quantitative PCR instrument (PikoReal™; Thermo Fisher Scientific) was used to measure gene expression.³⁶ The $2^{-\Delta\Delta\text{CT}}$ method was applied to assess the relative mRNA level³⁷ concerning β -actin. Each group was tested 4 times.

Table 1. The primer sequence

Primer ID	5'-3'
β -actin-F	ACCCTGAAGTACCCCATCGAG
β -actin-R	AGCACAGCCTGGATAGCAAC
HDAC4-F	CTTGTGGGTTACTGGCTCA
HDAC4-R	TCCAACGAGCTCCAAACTCC
Nur77-F	CCTGGTGTAAGCTTTGGTATGGA
Nur77-R	GCCTTGCCAACCCACATTAT

Western blot

Total protein was obtained by centrifuging each sample at 10,000 g for 10 min at 4°C. Then, a bicinchoninic acid (BCA) protein kit was used to measure the protein level.³⁸ Sodium dodecyl sulfate-polyacrylamide gel electrophoresis (SDS-PAGE) (12%) was used to separate total proteins with 100 mV power. Proteins were then transferred to a polyvinylidene difluoride (PVDF) membrane at 300 mA power.

Then, a 5% nonfat skim milk powder-Tween 0.1% solution was applied to block membranes. Antibodies against HDAC4 (668381-Ig, 1:3000; Proteintech, San Diego, USA), Nur77 (12235-1-AP, 1:1000; Proteintech), caspase-3 (#9661, 1:1000; Cell Signaling Technology, Danvers, USA), Bcl-2 (BH3 domain-specific) (AP1303a, 1:1000; Abcepta Biotech Ltd. Co., Suzhou, China), PCNA (10205-2-AP, 1:5000; Proteintech), and β -actin (66009-1-Ig, 1:5000; Proteintech) were added. Samples were washed, and the secondary antibody HRP goat anti-mouse IgG (SA00001-1, 1:5000; Proteintech) or HRP goat anti-rabbit IgG (SA00001-2, 1:6000; Proteintech) was applied to the membrane. The protein samples were assessed using chemiluminescence imaging system.³⁹ The internal reference was PCNA or β -actin.⁴⁰ Each group was tested 4 times.

Statistical analyses

GraphPad Prism 9 (GraphPad Software, San Diego, USA) was used for statistical analysis.⁴¹ The data were presented as the mean \pm standard deviation ($M \pm SD$), and the data normality distribution was assessed with the Shapiro–Wilk test.⁴² The homogeneity of variance was tested with the F test of Student's *t*-test between the 2 groups.⁴² The Brown–Forsythe test was utilized to evaluate the homogeneity of variance between multiple groups.⁴³ Following data normality and homogeneity testing, the differences between the 2 groups were analyzed using unpaired Student's *t*-test.⁴² When the hypothesis of normality was satisfied, but the homogeneity of variance was unsatisfied, the differences between the 2 groups were analyzed using the Mann–Whitney U-test.^{44,45} When the hypothesis of normality was satisfied, the difference between multiple groups was analyzed with one-way analysis of variance (ANOVA).⁴⁶ The Tukey–Kramer post hoc test comparisons were completed if the main effects of ANOVA were statistically significant.⁴⁷

In the Shapiro–Wilk test, $p > 0.1$ demonstrated that the data conform to a normal distribution. In the F-test of Student's *t*-test and Brown–Forsythe test, $p > 0.05$

illustrated that the variance was uniform. In the Mann–Whitney U test, unpaired Student's *t*-test or one-way ANOVA test, $p < 0.05$ illustrated significant differences between the groups. No outlying data were excluded, and data were analyzed blindly. The statistical methods, results and sample size related to the figures are shown in Supplementary Tables 1–7.

Results

Expression of HDAC4 in ovarian cancer cells

To determine whether there is a difference in HDAC4 expression in different ovarian cancer cells, we examined IOSE80, SKOV3 and SKOV3/DDP cell lines. We found that HDAC4 expression in SKOV3 cells was higher than that in IOSE80 cells, and the HDAC4 level was higher in the SKOV3/DDP cells than in SKOV3 cells (Fig. 1A,B). These results illustrated that ovarian cancer resistance to DDP may be regulated by HDAC4.

Effect of tasquinimod on growth inhibition of SKOV3 or SKOV3/DDP cells

To further analyze the HDAC4 function in DDP resistance in ovarian cancer, we treated SKOV3 and SKOV3/DDP cells with 40 μ M tasquinimod (HDAC4 inhibitor). Cell viability was significantly decreased after the cells were treated with tasquinimod for 24 h or 48 h (Fig. 2A,B). Furthermore, cell mobility was negatively correlated with the addition of tasquinimod. The relative scratch width in the SKOV3+tasquinimod and SKOV3/DDP+tasquinimod groups decreased when compared to both the SKOV3 and SKOV3/DDP groups after 48 h, respectively (Fig. 3). Furthermore, we found that the HDAC4 level in SKOV3/DDP cells significantly decreased under the influence of tasquinimod, while the Nur77 level significantly increased 48 h later (Fig. 2C). These results showed that tasquinimod affected the growth inhibition rate of SKOV3 or SKOV3/DDP cells.

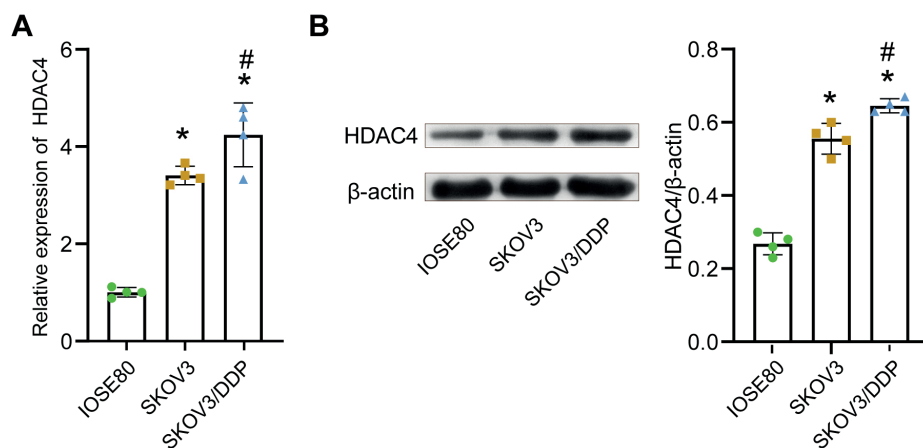


Fig. 1. Expression of histone deacetylase 4 (HDAC4) in IOSE80, SKOV3 and SKOV3/DDP cells. HDAC4 level was measured with quantitative real-time polymerase chain reaction (qPCR) (A) and western blot (B) ($n = 4$ for qPCR and western blot (both biological replicates)). Comparisons were made using the one-way analysis of variance (ANOVA) test. In the one-way ANOVA test, $p < 0.05$ illustrated significant differences between the data (* $p < 0.05$ compared to IOSE80; # $p < 0.05$ compared to SKOV3). Data are presented as mean \pm standard deviation ($M \pm SD$). The scatter point represents the value of a single sample. The details of statistical methods, results and sample size are listed in Supplementary Table 1

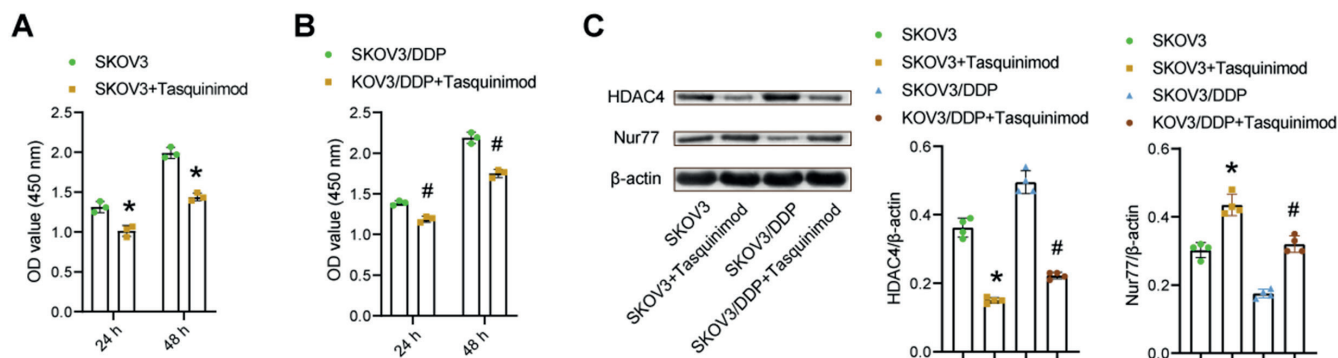


Fig. 2. Tasquinimod effect on growth inhibition rate of SKOV3 or SKOV3/DDP cells. Cell Counting Kit-8 (CCK-8) was applied to assess SKOV3 cells (A) and SKOV3/DDP cell viability (B) (n = 3 for CCK-8). Comparisons were made using the Student's t-test. The histone deacetylase 4 (HDAC4) and Nur77 expression was measured with western blot after cells were treated with 0.01 mmol/L tasquinimod (C) (n = 4 for quantitative real-time polymerase chain reaction (qPCR) and western blot (both biological replicates)). Comparisons were made using the one-way analysis of variance (ANOVA) test. In the unpaired t-test of Student's t-test or one-way ANOVA test, p < 0.05 illustrated significant differences between the data (* p < 0.05 compared to SKOV3; # p < 0.05 compared to SKOV3/DDP). Data are presented as mean ± standard deviation (M ±SD). The scatter point represents the value of a single sample. The details of statistical methods, results and sample size are listed in Supplementary Table 2

OD – optical density.

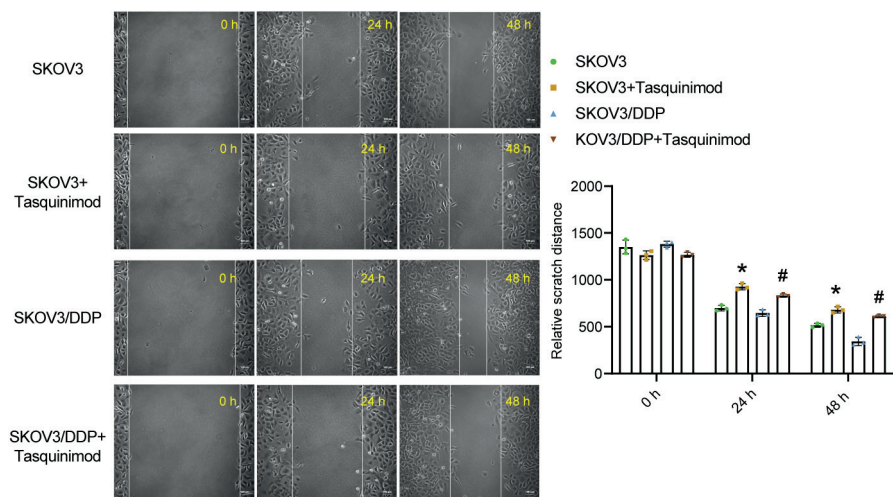


Fig. 3. Tasquinimod effect on growth inhibition rate of SKOV3 or SKOV3/DDP cells. The scratch-wound assay was utilized to measure the scratch width (* p < 0.05 compared to SKOV3; # p < 0.05 compared to SKOV3/DDP; n = 3 for scratch-wound assay (both biological replicates)). Comparisons were made using the one-way analysis of variance (ANOVA) test, with p < 0.05 illustrating significant differences between the groups (* p < 0.05 compared to SKOV3; # p < 0.05 compared to SKOV3/DDP). Data are presented as mean ± standard deviation (M ±SD). The scatter point represents the value of a single sample

Tasquinimod increased the sensitivity of SKOV3/DDP cells to DDP

Taking into consideration the influence of tasquinimod on the growth inhibition rate of SKOV3 or SKOV3/DDP, we treated cells with DDP to investigate whether tasquinimod could improve cell sensitivity to DDP. Cell viability in the SKOV3/DDP+DDP+tasquinimod group was significantly decreased compared to the SKOV3/DDP+DDP group (Fig. 4A). Furthermore, the relative scratch distance of the SKOV3/DDP+DDP+tasquinimod group was lower than that of the SKOV3/DDP+DDP group (Fig. 4B). Moreover, the apoptosis rate in the SKOV3/DDP+DDP+tasquinimod group was significantly increased when compared to the SKOV3/DDP+DDP group (Fig. 4C). After 48 h, the western blot demonstrated that the expression of capase-3 in the SKOV3/DDP+DDP+tasquinimod group significantly increased compared with the SKOV3/DDP+DDP group (Fig. 4D). These data demonstrate that

tasquinimod increased cell sensitivity to DDP while inhibiting growth and promoting apoptosis.

Tasquinimod affected the Nur77 apoptosis pathway of DDP-treated SKOV3/DDP cells

To further verify the effect of tasquinimod on the Nur77-Bcl-2 apoptotic pathway in DDP-treated SKOV3/DDP cells, we detected related mRNA and protein expression. We observed increased Nur77 and Bcl-2 (BH3 domain-specific) and decreased total Bcl-2 in SKOV3/DDP cells after the administration of tasquinimod (Fig. 5A,B). The treatment with tasquinimod induced abundant Nur77 expression in the cytoplasm (Fig. 5C). Immunofluorescence and western blot detected increased Nur77 and Bcl-2 (BH3 domain-specific), which were mainly localized in the cytoplasm (Fig. 5D,E). These results confirmed that tasquinimod affected the Nur77-Bcl-2 apoptotic pathway of SKOV3/DDP cells.

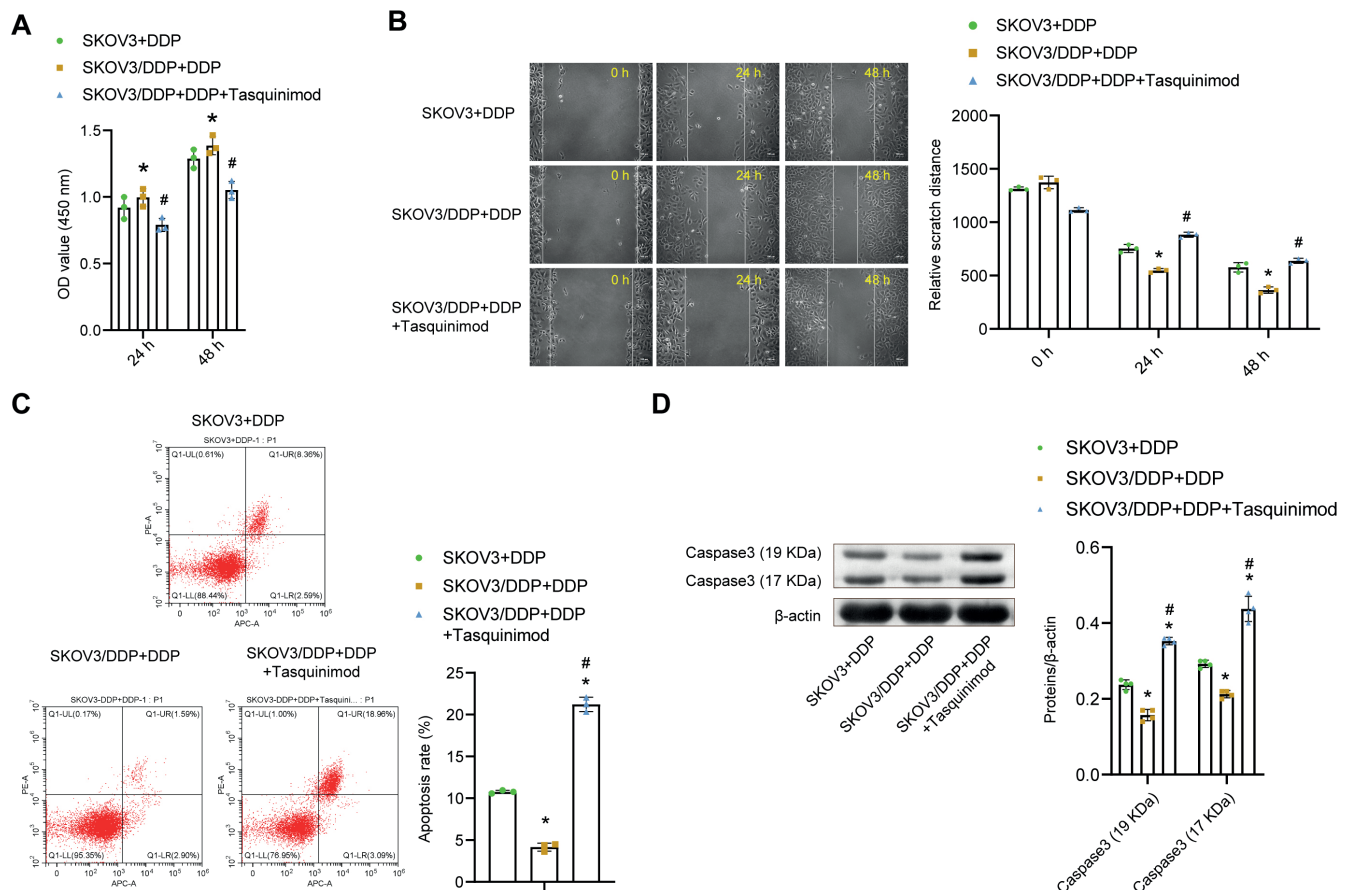


Fig. 4. Tasquinimod increased the sensitivity of SKOV3/DDP cells to cisplatin (DDP). SKOV3 and SKOV3/DDP cell viability was assessed using Cell Counting Kit-8 (CCK-8) (A). The scratch-wound assay was applied to measure the scratch width within 24 h and 48 h (B). In SKOV3 and SKOV3/DDP cells, apoptosis was analyzed with flow cytometry (C). The caspase-3 content was measured with western blot (D) ($n = 3$ for CCK-8, scratch-wound assay and flow cytometry; $n = 4$ for western blot (both biological replicates)). Comparisons were made using the one-way analysis of variance (ANOVA) test. In the one-way ANOVA test, $p < 0.05$ illustrated significant differences between the data (* $p < 0.05$ compared to SKOV3+DDP; # $p < 0.05$ compared to SKOV3/DDP+DDP). Data were presented as mean \pm standard deviation (M \pm SD). The scatter point represented the value of a single sample. The details of statistical methods, results and sample size are listed in Supplementary Table 4

OD – optical density.

Tasquinimod induced apoptosis of DDP-resistant ovarian cancer strains by upregulating the Nur77 apoptosis pathway

Next, we determined the relationship between tasquinimod, Nur77 and apoptosis. After the transfection of si-Nur77 into SKOV3/DDP cells, Nur77 expression was significantly decreased, indicating that the transfection with si-Nur77 was successful. Furthermore, compared with the SKOV3/DDP+DDP+tasquinimod+si-NC group, caspase-3 and Nur77 expression in the SKOV3/DDP+DDP+DDP+tasquinimod+si-Nur77 group was significantly lower (Fig. 6A,B). Flow cytometry results also showed that apoptosis in the SKOV3/DDP+DDP+si-Nur77 group decreased compared to the SKOV3/DDP+DDP+DDP+tasquinimod+si-NC group (Fig. 6C). The effect of tasquinimod was reversed by the si-Nur77 transfection. This indicates that tasquinimod upregulates the Nur77 apoptosis pathway to induce apoptosis in drug-resistant ovarian cancer strains.

Tasquinimod enhanced the anti-tumor effect of DDP in xenografts

To determine the influence of tasquinimod in vivo, we subcutaneously injected SKOV3/DDP cells into nude mice and performed DDP and tasquinimod treatment once the tumor diameter reached 5 mm. The results showed that both tumor volume and diameter gradually increased after subcutaneous injection of SKOV3/DDP cells. The tumor diameter and weight of the SKOV3/DDP+DDP+DDP+tasquinimod group significantly decreased when compared to the SKOV3/DDP+DDP group (Fig. 7A–C). Moreover, western blot results demonstrated that the expression of HDAC4 in the SKOV3/DDP+DDP+DDP+tasquinimod group decreased significantly when compared to the SKOV3/DDP+DDP group, while the levels of Nur77 and Bcl-2 (BH3 domain-specific) demonstrated the opposite (Fig. 7D). These data indicate that tasquinimod enhanced the anti-tumor effect of DDP in xenografts.

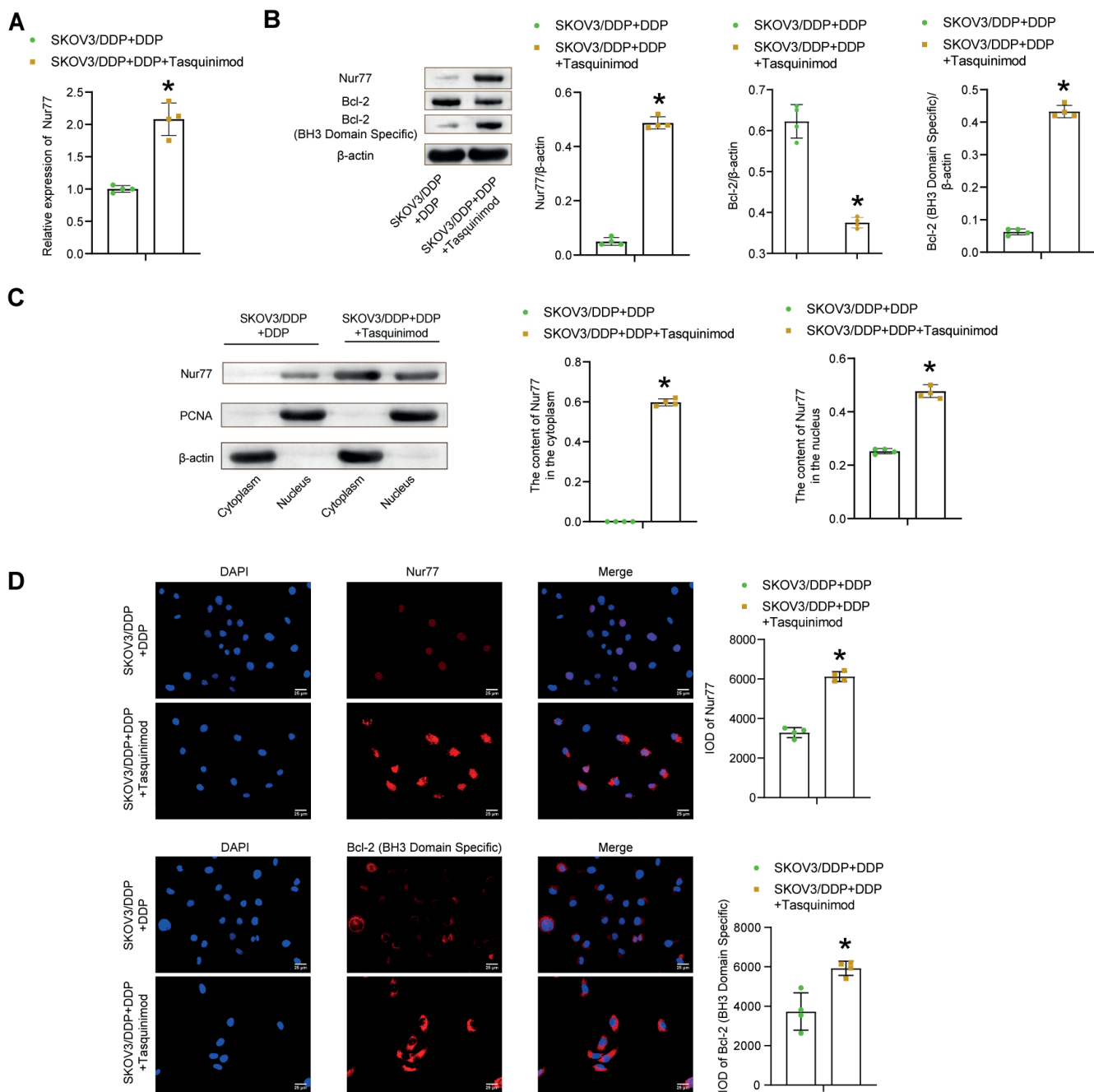


Fig. 5. Tasquinimod affected the Nur77 apoptosis pathway of cisplatin (DDP)-treated ovarian cancer cells. Nur77 expression was detected using quantitative real-time polymerase chain reaction (qPCR) (A) and western blot (B). Nur77, B-cell lymphoma-2 (Bcl-2) and Bcl-2 (BH3 domain-specific) content was detected with western blot (B). Nur77 distribution in cytoplasm or nucleus was detected with western blot (C). Nur77 and Bcl-2 (BH3 domain-specific) distribution were probed with immunofluorescence (IF) (D) (n = 3 for IF; n = 4 for western blot (both biological replicates)). Comparisons were made using the Mann–Whitney U test or Student’s t-test. In the unpaired t-test of Student’s t-test or Mann–Whitney U test, p < 0.05 illustrated significant differences between the data (* p < 0.05 compared to SKOV3/DDP+DDP). Data were presented as mean \pm standard deviation (M \pm SD). The scatter point represented the value of a single sample. The details of statistical methods, results and sample size are listed in Supplementary Table 5

Discussion

Cisplatin resistance is an important factor in the high mortality of ovarian cancer.⁴⁸ It is currently a first-line chemotherapy agent for platinum-sensitive ovarian cancer that damages DNA or activates endoplasmic reticulum (ER) stress pathways.⁴⁹ The upregulation of anti-apoptotic pathways is thought to play a crucial role in ovarian cancer drug

resistance.⁷ Therefore, we attempted to influence the apoptosis pathway by regulating HDAC4 expression in order to overcome ovarian cancer drug resistance. In this study, we investigated the effect of tasquinimod on the DDP resistance of SKOV3 and SKOV3/DDP cells, and the association of tasquinimod with the Nur77-Bcl-2 apoptotic pathway. Subsequently, we studied the anti-tumor effect of tasquinimod on DDP in xenografts. We found that HDAC4

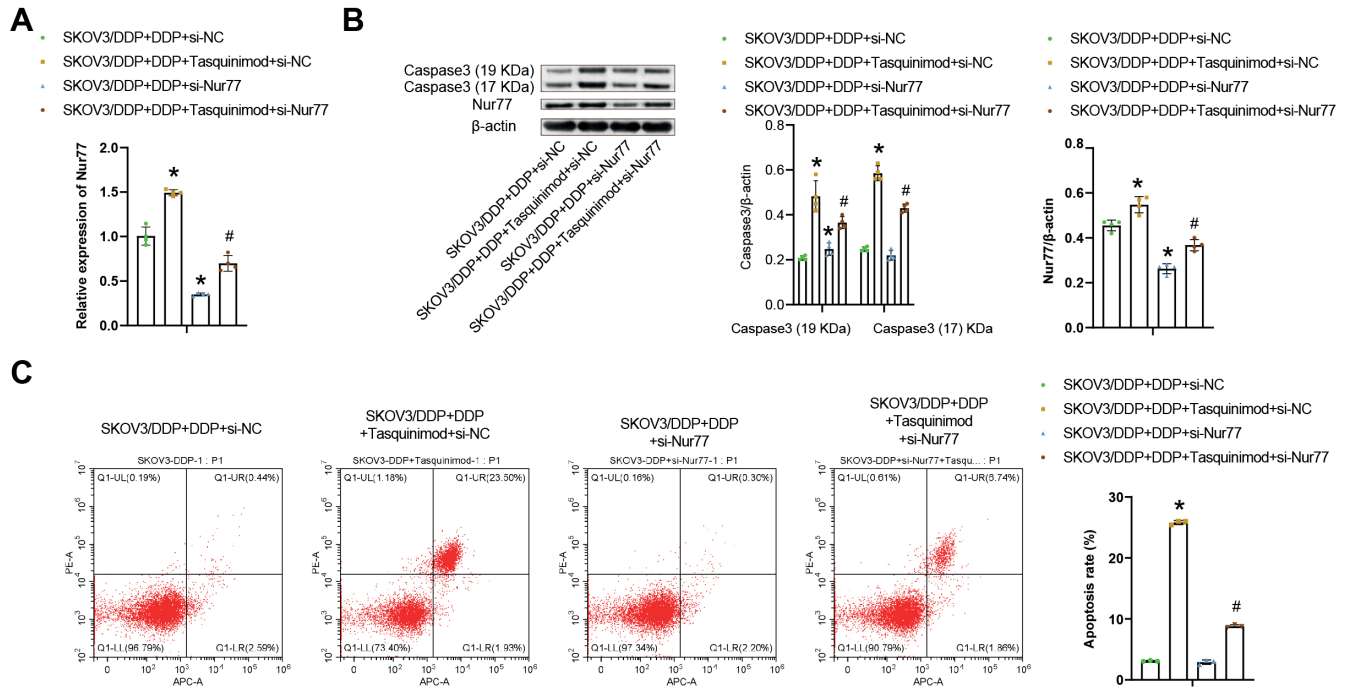


Fig. 6. Tasquinimod induced apoptosis of ovarian cancer drug-resistant strains by upregulating the Nur77 apoptosis pathway. Quantitative real-time polymerase chain reaction (qPCR) was used to measure the Nur77 content (A). Nur77 and caspase-3 content were detected using western blot (B). SKOV3/DDP cell apoptosis was analyzed with flow cytometry (C) ($n = 3$ for flow cytometry; $n = 4$ for qPCR and western blot (both biological replicates)). Comparisons were made using the one-way analysis of variance (ANOVA) test, with $p < 0.05$ illustrating significant differences between the data (* $p < 0.05$ compared to SKOV3/DDP+DDP+si-NC; # $p < 0.05$ compared to SKOV3/DDP+DDP+tasquinimod+si-NC). Data are presented as mean \pm standard deviation (M \pm SD). The scatter point represented the value of a single sample. The details of statistical methods, results and sample size are listed in Supplementary Table 6

may play a role in regulating ovarian cancer resistance to DDP. After tasquinimod (HDAC4 inhibitor) treatment, ovarian cancer cells showed increased sensitivity to DDP, inhibited growth and increased apoptosis. Tasquinimod upregulated the Nur77-Bcl-2 pathway to induce apoptosis in drug-resistant ovarian cancer cell strains and enhanced the anti-tumor effect of DDP in SKOV3/DDP xenografts.

The HDAC4 is upregulated in a subset of recurrent tumors, including epithelial ovarian cancer (EOC),^{50,51} demonstrating the clinical relevance of the current study.⁵² In particular, HDAC4 was overexpressed in EOC and was connected with poor overall survival of all examined ovarian cancer patients.^{53,54} The HDAC4 also formed protein complexes with HIF1 α that could modulate chemoresistance through protein phosphorylation, translocation and degradation in SKOV3 cells.⁵⁴ We found that HDAC4 level was higher in SKOV3 cells than in IOSE80, and the HDAC4 level was higher in SKOV3/DDP cells than in SKOV3 cells. These results demonstrated that HDAC4 may regulate ovarian cancer resistance to DDP.

Therefore, we treated SKOV3 and SKOV3/DDP cells with tasquinimod. Tasquinimod targets the tumor microenvironment to overcome tumor-associated immunosuppression while inhibiting angiogenesis, metastasis and tumor growth.^{55,56} The inhibitory effects of tasquinimod on tumor-infiltrating immunosuppressive myeloid cells, particularly M2-polarized tumor-associated macrophages (TAMs), have also been observed.^{57,58} Consistently, we found that

tasquinimod, an analog of the HDAC inhibitor, increased cell sensitivity to cisplatin, inhibited growth and promoted apoptosis. Based on this, we hypothesized that the apoptotic pathway regulated by HDAC was related to DDP sensitivity. Previous studies have shown that tasquinimod upregulated the Nur77-Bcl-2 pathway^{59,60} to induce apoptosis in drug-resistant ovarian cancer strains and enhance the anti-tumor effect of DDP in SKOV3/DDP cell xenografts.^{61,62}

A key step in the mitochondrial apoptosis pathway of Nur77 is the interaction of Nur77 with Bcl-2, which induces a conformational change of Bcl-2 and switched Bcl-2 from pro-survival to pro-apoptosis.⁶³ While the growth-promoting role of Nur77 appears to depend on its nuclear role, the death role of Nur77 involved its translocation from the nucleus to the cytoplasm.^{64,65} For example, the death effect of BI1071 was also dependent on the expression of Bcl-2, and BI1071 induced the interaction of Nur77 and Bcl-2.^{11,66} We found increased expression of Nur77 and Bcl-2 (BH3 domain-specific), which were mainly localized in the cytoplasm after tasquinimod induction. Moreover, tasquinimod enhanced the anti-tumor effect of DDP in xenografts.

As a widely used chemotherapy drug in the treatment of breast cancer, DDP has shown good results. However, the development of drug resistance during treatment often leads to treatment failure. Finding new drugs that could be used in clinical resistance is an urgent need, as it could improve the clinical benefits to patients. We found that tasquinimod enhanced the sensitivity of ovarian cancer

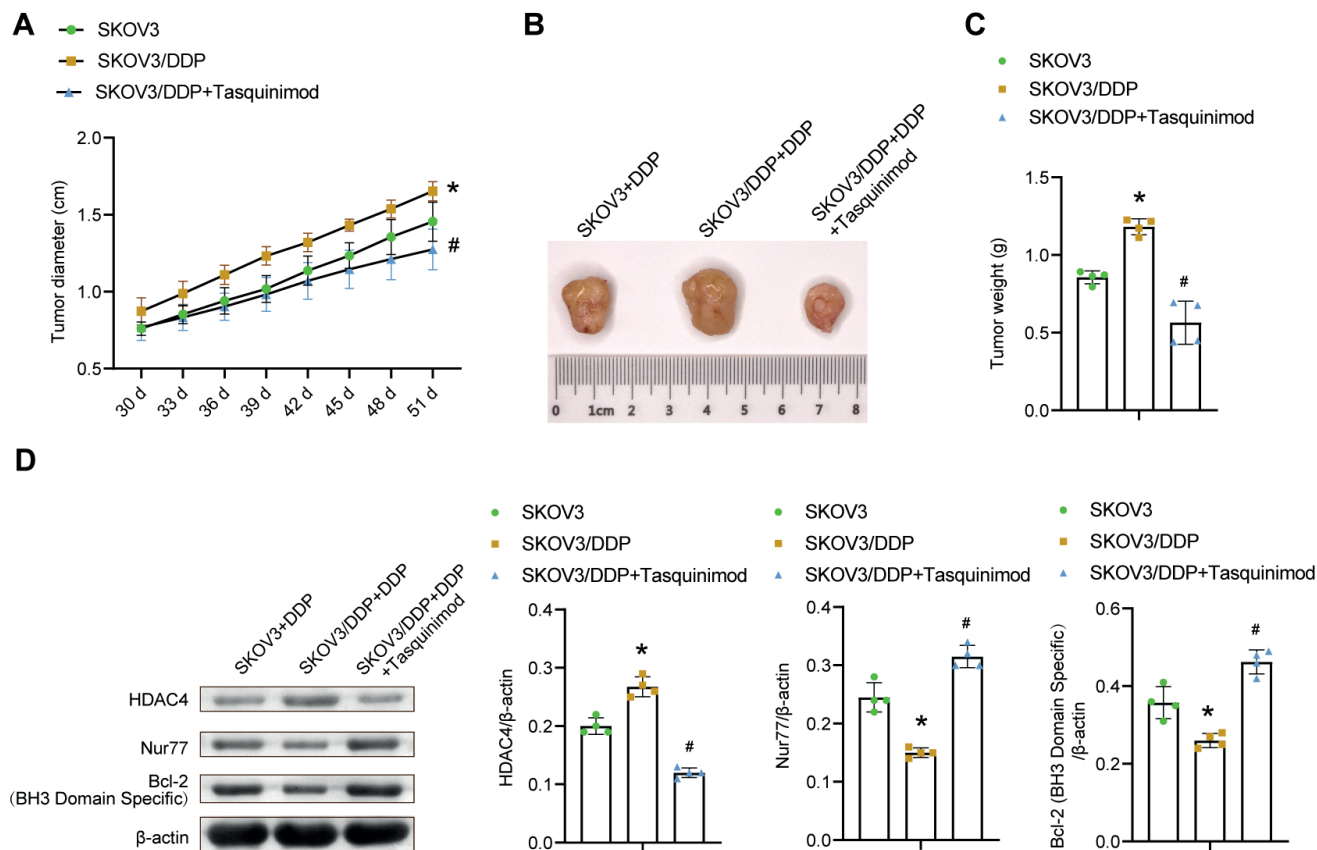


Fig. 7. Tasquinimod enhanced the anti-tumor effect of cisplatin (DDP) in xenografts. Changes in tumor volume of mice (A), typical images of tumors (B) and changes in tumor weight (C) were all measured. The expression changes of histone deacetylase 4 (HDAC4), Nur77 and B-cell lymphoma-2 (Bcl-2) (BH3 domain-specific) were measured using western blot (n = 4 for western blot, statistics of tumor volume/weight (both biological replicates)). Comparisons were made using the one-way analysis of variance (ANOVA) test, with p < 0.05 illustrating significant differences between the data (* p < 0.05 compared to SKOV3+DDP; # p < 0.05 compared to SKOV3/DDP+DDP). Data are presented as mean \pm standard deviation (M \pm SD). The bar chart showed the M for each group of samples. The error bar represented SD. The scatter point represented the value of a single sample. The details of statistical methods, results and sample size are listed in Supplementary Table 7

cells to DDP by regulating the Nur77-Bcl-2 apoptotic pathway. In future research, it may be necessary to further expand the study sample in order to investigate the effect of tasquinimod (in terms of dose and time) to achieve relief of clinical drug resistance.

Limitations

First, there was a lack of in vivo ovarian cancer staging studies, which is important as the expression of HDAC4/Nur77/Bcl-2 may vary at different tumor stages. Second, we did not explore the relationship between the therapeutic effect of tasquinimod on disease and its dose. We used only a single concentration for exploration in the experiments herein. Third, we did not investigate the relationship between polymorphisms and tasquinimod due to limitations of time and funds.

Conclusions

We found that HDAC4 plays a role in regulating ovarian cancer resistance to DDP. After treatment with

tasquinimod, the sensitivity of ovarian cancer cells to DDP was increased, and the apoptosis rate was decreased. At the molecular level, tasquinimod upregulated the Nur77-Bcl-2 pathway to induce apoptosis in drug-resistant ovarian cancer strains. In vivo mouse studies showed that tasquinimod enhanced the anti-tumor effect of DDP in SKOV3/DDP xenografts. In conclusion, tasquinimod increased the sensitivity of ovarian cancer cells to DDP by regulating the Nur77-Bcl-2 apoptotic pathway.

Supplementary data

The supplementary materials are available at <https://doi.org/10.5281/zenodo.8134377>. The package contains the following files:

Supplementary Table 1. The details of statistical methods, results and sample size for Fig. 1.

Supplementary Table 2. The details of statistical methods, results and sample size for Fig. 2.

Supplementary Table 3. The details of statistical methods, results and sample size for Fig. 3.

Supplementary Table 4. The details of statistical methods, results and sample size for Fig. 4.


Supplementary Table 5. The details of statistical methods, results and sample size for Fig. 5.

Supplementary Table 6. The details of statistical methods, results and sample size for Fig. 6.


Supplementary Table 7. The details of statistical methods, results and sample size for Fig. 7.

ORCID iDs

Ying Lin  <https://orcid.org/0000-0002-0599-1734>

Ya-Qiong Liu  <https://orcid.org/0009-0009-7124-3556>

Ke-An Zhu  <https://orcid.org/0009-0009-6656-6385>

Meng-Qi Hu  <https://orcid.org/0009-0005-4139-5832>

Zhao Li  <https://orcid.org/0009-0007-9448-6484>

Xiao-Jia Min  <https://orcid.org/0000-0001-8093-0969>

References

- Gralewska P, Gajek A, Marczak A, Rogalska A. Participation of the ATR/CHK1 pathway in replicative stress targeted therapy of high-grade ovarian cancer. *J Hematol Oncol.* 2020;13(1):39. doi:10.1186/s13045-020-00874-6
- Budiana ING, Angelina M, Pemayun TGA. Ovarian cancer: Pathogenesis and current recommendations for prophylactic surgery. *J Turkish German Gynecol Assoc.* 2019;20(1):47–54. doi:10.4274/jtgga.galenos.2018.2018.0119
- Liu HD, Xia BR, Jin MZ, Lou G. Organoid of ovarian cancer: Genomic analysis and drug screening. *Clin Transl Oncol.* 2020;22(8):1240–1251. doi:10.1007/s12094-019-02276-8
- Wang JY, Lu AQ, Chen LJ. LncRNAs in ovarian cancer. *Clin Chim Acta.* 2019;490:17–27. doi:10.1016/j.cca.2018.12.013
- Dasari S, Tchounwou PB. Cisplatin in cancer therapy: Molecular mechanisms of action. *Eur J Pharmacol.* 2014;740:364–378. doi:10.1016/j.ejphar.2014.07.025
- Chen SH, Chang JY. New insights into mechanisms of cisplatin resistance: From tumor cell to microenvironment. *Int J Mol Sci.* 2019;20(17):4136. doi:10.3390/ijms20174136
- Lopez A, Reyna DE, Gitego N, et al. Co-targeting of BAX and BCL-XL proteins broadly overcomes resistance to apoptosis in cancer. *Nat Commun.* 2022;13(1):1199. doi:10.1038/s41467-022-28741-7
- Wang J, Zhou JY, Zhang L, Wu GS. Involvement of MKP-1 and Bcl-2 in acquired cisplatin resistance in ovarian cancer cells. *Cell Cycle.* 2009;8(19):3191–3198. doi:10.4161/cc.8.19.9751
- Xu L, Xie Q, Qi L, et al. Bcl-2 overexpression reduces cisplatin cytotoxicity by decreasing ER-mitochondrial Ca²⁺ signaling in SKOV3 cells. *Oncol Rep.* 2017;39(3):985–992. doi:10.3892/or.2017.6164
- Lin B, Kolluri SK, Lin F, et al. Conversion of Bcl-2 from protector to killer by interaction with nuclear orphan receptor Nur77/TR3. *Cell.* 2004;116(4):527–540. doi:10.1016/S0092-8674(04)00162-X
- Banta KL, Wang X, Das P, Winoto A. B cell lymphoma 2 (Bcl-2) residues essential for Bcl-2's apoptosis-inducing interaction with Nur77/Nor-1 orphan steroid receptors. *J Biol Chem.* 2018;293(13):4724–4734. doi:10.1074/jbc.RA117.001101
- Wilson AJ, Liu AY, Roland J, et al. TR3 modulates platinum resistance in ovarian cancer. *Cancer Res.* 2013;73(15):4758–4769. doi:10.1158/0008-5472.CAN-12-4560
- Hu Y, French SW, Chau T, et al. RAR β acts as both an upstream regulator and downstream effector of miR-22, which epigenetically regulates NUR77 to induce apoptosis of colon cancer cells. *FASEB J.* 2019;33(2):2314–2326. doi:10.1096/fj.201801390R
- Tsai C, Liu W, Hsu F, et al. Targeting histone deacetylase 4/ubiquitin-conjugating enzyme 9 impairs DNA repair for radiosensitization of hepatocellular carcinoma cells in mice. *Hepatology.* 2018;67(2):586–599. doi:10.1002/hep.29328
- Tanaka M, Spekker E, Szabó Á, Polyák H, Vécsei L. Modelling the neurodevelopmental pathogenesis in neuropsychiatric disorders: Bioactive kynurenes and their analogues as neuroprotective agents. In celebration of 80th birthday of Professor Peter Riederer. *J Neural Transm.* 2022;129(5–6):627–642. doi:10.1007/s00702-022-02513-5
- Irwin JJ, Shoichet BK. ZINC: A free database of commercially available compounds for virtual screening. *J Chem Inf Model.* 2005;45(1):177–182. doi:10.1021/ci049714+
- Jayathilaka N, Han A, Gaffney KJ, et al. Inhibition of the function of class IIa HDACs by blocking their interaction with MEF2. *Nucl Acids Res.* 2012;40(12):5378–5388. doi:10.1093/nar/gks189
- Wang C, Liu G, Dou G, et al. Z-ligustilide selectively targets AML by restoring nuclear receptors Nur77 and NOR-1-mediated apoptosis and differentiation. *Phytomedicine.* 2021;82:153448. doi:10.1016/j.phymed.2020.153448
- Boros F, Vécsei L. Progress in the development of kynurenine and quinoline-3-carboxamide-derived drugs. *Exp Opin Investig Dugs.* 2020;29(11):1223–1247. doi:10.1080/13543784.2020.1813716
- Martos D, Tuka B, Tanaka M, Vécsei L, Telegdy G. Memory enhancement with kynurenic acid and its mechanisms in neurotransmission. *Biomedicines.* 2022;10(4):849. doi:10.3390/biomedicines10040849
- Li Y, Zhou J, Wang J, Chen X, Zhu Y, Chen Y. Mir-30b-3p affects the migration and invasion function of ovarian cancer cells by targeting the CTHRC1 gene. *Biol Res.* 2020;53(1):10. doi:10.1186/s40659-020-00277-4
- Zhang X, Liu G, Qiu J, Zhang N, Ding J, Hua K. E2F1-regulated long non-coding RNA RAD51-AS1 promotes cell cycle progression, inhibits apoptosis and predicts poor prognosis in epithelial ovarian cancer. *Sci Rep.* 2017;7(1):4469. doi:10.1038/s41598-017-04736-z
- Cao Y, Xie X, Li M, Gao Y. CircHIPK2 contributes to DDP resistance and malignant behaviors of DDP-resistant ovarian cancer cells both in vitro and in vivo through circHIPK2/miR-338-3p/CHTOP ceRNA pathway. *Onco Targets Ther.* 2021;14:3151–3165. doi:10.2147/OTT.S291823
- Olsson A, Björk A, Vallon-Christersson J, Isaacs JT, Leanderson T. Tasquinimod (ABR-215050), a quinoline-3-carboxamide anti-angiogenic agent, modulates the expression of thrombospondin-1 in human prostate tumors. *Mol Cancer.* 2010;9(1):107. doi:10.1186/1476-4598-9-107
- Dalby B, Cates S, Harris A, et al. Advanced transfection with Lipofectamine 2000 reagent: Primary neurons, siRNA, and high-throughput applications. *Methods.* 2004;33(2):95–103. doi:10.1016/j.jymeth.2003.11.023
- Zhang Z, Zhu H, Hu J. CircRAB11FIP1 promoted autophagy flux of ovarian cancer through DSC1 and miR-129. *Cell Death Dis.* 2021;12(2):219. doi:10.1038/s41419-021-03486-1
- Miao JT, Gao JH, Chen YQ, Chen H, Meng HY, Lou G. LncRNA ANRIL affects the sensitivity of ovarian cancer to cisplatin via regulation of let-7a/HMGA2 axis. *Biosci Rep.* 2019;39(7):BSR20182101. doi:10.1042/BSR20182101
- Ding K, Li D, Zhang R, Zuo M. Circ_0047339 promotes the activation of fibroblasts and affects the development of urethral stricture by targeting the miR-4691-5p/TSP-1 axis. *Sci Rep.* 2022;12(1):14746. doi:10.1038/s41598-022-19141-4
- Meng X, Gao X, Chen X, Yu J. Umbilical cord-derived mesenchymal stem cells exert anti-fibrotic action on hypertrophic scar-derived fibroblasts in co-culture by inhibiting the activation of the TGF β 1/Smad3 pathway. *Exp Ther Med.* 2021;21(3):210. doi:10.3892/etm.2021.9642
- Wang X, Zhang Y, Wuyun K, Gong H. Therapeutic effect and mechanism of 4-phenyl butyric acid on renal ischemia-reperfusion injury in mice. *Exp Ther Med.* 2021;23(2):144. doi:10.3892/etm.2021.11067
- Buyandelger B, Bar EE, Hung KS, et al. Histone deacetylase inhibitor MPT0B291 suppresses glioma growth in vitro and in vivo partially through acetylation of p53. *Int J Biol Sci.* 2020;16(16):3184–3199. doi:10.7150/ijbs.45505
- Luchtel RA, Bhagat T, Pradhan K, et al. High-dose ascorbic acid synergizes with anti-PD1 in a lymphoma mouse model. *Proc Natl Acad Sci U S A.* 2020;117(3):1666–1677. doi:10.1073/pnas.1908158117
- Payapilly A, Guilbert R, Descamps T, et al. TIAM1-RAC1 promote small-cell lung cancer cell survival through antagonizing Nur77-induced BCL2 conformational change. *Cell Rep.* 2021;37(6):109979. doi:10.1016/j.celrep.2021.109979
- Zhang J, Liu Z, Dong Y. miR-127-5p targets JAM3 to regulate ferroptosis, proliferation, and metastasis in malignant meningioma cells. *Dis Markers.* 2022;2022:6423237. doi:10.1155/2022/6423237
- Fan QL, Wang JW, Zhang SL, Liu T, Zhao J, You SP. Phenylethanol glycosides protect myocardial hypertrophy induced by abdominal aortic constriction via ECE-1 demethylation inhibition and PI3K/PKB/eNOS pathway enhancement. *Evid Based Complement Alternat Med.* 2020;2020:2957094. doi:10.1155/2020/2957094

36. Scheffler JM, Sparber F, Tripp CH, et al. LAMTOR2 regulates dendritic cell homeostasis through FLT3-dependent mTOR signalling. *Nat Commun*. 2014;5(1):5138. doi:10.1038/ncomms6138
37. Al Haq AT, Tseng HY, Chen LM, Wang CC, Hsu HL. Targeting prooxidant MnSOD effect inhibits triple-negative breast cancer (TNBC) progression and M2 macrophage functions under the oncogenic stress. *Cell Death Dis*. 2022;13(1):49. doi:10.1038/s41419-021-04486-x
38. Msaouel P, Malouf GG, Su X, et al. Comprehensive molecular characterization identifies distinct genomic and immune hallmarks of renal medullary carcinoma. *Cancer Cell*. 2020;37(5):720–734.e13. doi:10.1016/j.ccell.2020.04.002
39. Park Y, Park J, Hwang HJ, et al. Nonsense-mediated mRNA decay factor UPF1 promotes aggresome formation. *Nat Commun*. 2020;11(1):3106. doi:10.1038/s41467-020-16939-6
40. Li P, Xu J, Rao HM, et al. Mechanism of apoptosis induction by mycoplasma nuclease MGA_0676 in chicken embryo fibroblasts. *Front Cell Infect Microbiol*. 2018;8:105. doi:10.3389/fcimb.2018.00105
41. Brynjolfsson SF, Sigurgrimsdottir H, Einarsdottir ED, et al. Detailed multiplex analysis of SARS-CoV-2 specific antibodies in COVID-19 disease. *Front Immunol*. 2021;12:695230. doi:10.3389/fimmu.2021.695230
42. Yudovich D, Bäckström A, Schmiderer L, Žemaitis K, Subramaniam A, Larsson J. Combined lentiviral- and RNA-mediated CRISPR/Cas9 delivery for efficient and traceable gene editing in human hematopoietic stem and progenitor cells. *Sci Rep*. 2020;10(1):22393. doi:10.1038/s41598-020-79724-x
43. Venâncio C, Félix L, Almeida V, et al. Acute ketamine impairs mitochondrial function and promotes superoxide dismutase activity in the rat brain. *Anesth Analg*. 2015;120(2):320–328. doi:10.1213/ANE.0000000000000539
44. Fay MP, Proschan MA. Wilcoxon–Mann–Whitney or t-test? On assumptions for hypothesis tests and multiple interpretations of decision rules. *Statist Surv*. 2010;4:1–39. doi:10.1214/09-SS051
45. Zimmerman DW, Zumbo BD. Parametric alternatives to the Student t-test under violation of normality and homogeneity of variance. *Percept Mot Skills*. 1992;74(3):835–844. doi:10.2466/pms.1992.74.3.835
46. Wang X, Wang Z, Tang D. Aerobic exercise improves LPS-induced sepsis via regulating the Warburg effect in mice. *Sci Rep*. 2021;11(1):17772. doi:10.1038/s41598-021-97101-0
47. Meah VL, Backx K, Cockcroft JR, Shave RE, Stöhr EJ. Left ventricular mechanics in late second trimester of healthy pregnancy. *Ultrasound Obstet Gynecol*. 2019;54(3):350–358. doi:10.1002/uog.20177
48. Zhang Y, Dong Y, Fu H, et al. Multifunctional tumor-targeted PLGA nanoparticles delivering Pt(IV)/siBIRC5 for US/MRI imaging and overcoming ovarian cancer resistance. *Biomaterials*. 2021;269:120478. doi:10.1016/j.biomaterials.2020.120478
49. Rabik CA, Dolan ME. Molecular mechanisms of resistance and toxicity associated with platinating agents. *Cancer Treat Rev*. 2007;33(1):9–23. doi:10.1016/j.ctrv.2006.09.006
50. Mrkvicova A, Chmellarova M, Peterova E, et al. The effect of sodium butyrate and cisplatin on expression of EMT markers. *PLoS One*. 2019;14(1):e0210889. doi:10.1371/journal.pone.0210889
51. Smith HJ, Straughn JM, Buchsbaum DJ, Arend RC. Epigenetic therapy for the treatment of epithelial ovarian cancer: A clinical review. *Gynecol Oncol Rep*. 2017;20:81–86. doi:10.1016/j.gore.2017.03.007
52. Fan Q, Li L, Wang TL, Emerson RE, Xu Y. A novel ZIP4-HDAC4-VEGFA axis in high-grade serous ovarian cancer. *Cancers*. 2021;13(15):3821. doi:10.3390/cancers13153821
53. Zhou L, Xu X, Liu H, et al. Prognosis analysis of histone deacetylases mRNA expression in ovarian cancer patients. *J Cancer*. 2018;9(23):4547–4555. doi:10.7150/jca.26780
54. Zhang X, Qi Z, Yin H, Yang G. Interaction between p53 and Ras signaling controls cisplatin resistance via HDAC4- and HIF-1 α -mediated regulation of apoptosis and autophagy. *Theranostics*. 2019;9(4):1096–1114. doi:10.7150/thno.29673
55. Raymond E, Dalglish A, Damber JE, Smith M, Pili R. Mechanisms of action of tasquinimod on the tumour microenvironment. *Cancer Chemother Pharmacol*. 2014;73(1):1–8. doi:10.1007/s00280-013-2321-8
56. Leimkühler NB, Gleitz HFE, Ronghui L, et al. Heterogeneous bone-marrow stromal progenitors drive myelofibrosis via a druggable alarmin axis. *Cell Stem Cell*. 2021;28(4):637–652.e8. doi:10.1016/j.stem.2020.11.004
57. Murdoch C, Muthana M, Coffelt SB, Lewis CE. The role of myeloid cells in the promotion of tumour angiogenesis. *Nat Rev Cancer*. 2008;8(8):618–631. doi:10.1038/nrc2444
58. Sawant A, Deshane J, Jules J, et al. Myeloid-derived suppressor cells function as novel osteoclast progenitors enhancing bone loss in breast cancer. *Cancer Res*. 2013;73(2):672–682. doi:10.1158/0008-5472.CAN-12-2202
59. Tu X, Chen X, Zhang D, et al. Optimization of novel oxidative DIMs as Nur77 modulators of the Nur77-Bcl-2 apoptotic pathway. *Eur J Med Chem*. 2021;211:113020. doi:10.1016/j.ejmech.2020.113020
60. Thompson J, Winoto A. During negative selection, Nur77 family proteins translocate to mitochondria where they associate with Bcl-2 and expose its proapoptotic BH3 domain. *J Exp Med*. 2008;205(5):1029–1036. doi:10.1084/jem.20080101
61. Zhong Y, Le F, Cheng J, et al. Triptolide inhibits JAK2/STAT3 signaling and induces lethal autophagy through ROS generation in cisplatin-resistant SKOV3/DDP ovarian cancer cells. *Oncol Rep*. 2021;45(5):69. doi:10.3892/or.2021.8020
62. Hu H, Zhu S, Tong Y, Huang G, Tan B, Yang L. Antitumor activity of triptolide in SKOV3 cells and SKOV3/DDP in vivo and in vitro. *Anticancer Drugs*. 2020;31(5):483–491. doi:10.1097/CAD.0000000000000894
63. Kolluri SK, Zhu X, Zhou X, et al. A short Nur77-derived peptide converts Bcl-2 from a protector to a killer. *Cancer Cell*. 2008;14(4):285–298. doi:10.1016/j.ccr.2008.09.002
64. Lee SO, Andey T, Jin UH, Kim K, Sachdeva M, Safe S. The nuclear receptor TR3 regulates mTORC1 signaling in lung cancer cells expressing wild-type p53. *Oncogene*. 2012;31(27):3265–3276. doi:10.1038/onc.2011.504
65. Peng SZ, Chen XH, Chen SJ, et al. Phase separation of Nur77 mediates celastrol-induced mitophagy by promoting the liquidity of p62/SQSTM1 condensates. *Nat Commun*. 2021;12(1):5989. doi:10.1038/s41467-021-26295-8
66. Chen X, Cao X, Tu X, et al. BI1071, a novel Nur77 modulator, induces apoptosis of cancer cells by activating the Nur77-Bcl-2 apoptotic pathway. *Mol Cancer Ther*. 2019;18(5):886–899. doi:10.1158/1535-7163.MCT-18-0918

Oridonin attenuates apoptosis and NLRP3 inflammasome activation in IL-4-stimulated human bronchial epithelial cells in an in vitro pediatric asthma model

Weiwei Wang^{A,B,D,F}, Dan Ming^{A–D}

Department of Pediatrics, Tianjin Hospital, China

A – research concept and design; B – collection and/or assembly of data; C – data analysis and interpretation; D – writing the article; E – critical revision of the article; F – final approval of the article

Advances in Clinical and Experimental Medicine, ISSN 1899–5276 (print), ISSN 2451–2680 (online)

Adv Clin Exp Med. 2024;33(2):163–170

Address for correspondence

Weiwei Wang
E-mail: tjyywww@sina.com

Funding sources

None declared

Conflict of interest

None declared

Received on August 30, 2022
Reviewed on December 23, 2022
Accepted on May 16, 2023

Published online on July 24, 2023

Abstract

Background. Asthma is a chronic illness that causes recurrent inflammation and airway constriction. The primary risk factors for asthma development are exposure to environmental allergens and house dust mites, which can trigger deoxyribonucleic acid (DNA) damage. Oxidative stress can also cause DNA impairments and plays a crucial role in the progression of human immunological disorders.

Objectives. The aim of the study was to evaluate the effects of oridonin (ORD) on proliferation, inflammation and apoptosis in interleukin 4 (IL-4)-stimulated human bronchial epithelial (16HBE) cells.

Materials and methods. Proliferation was assessed using a 5-Bromo-2-deoxyuridine (BrdU) assay, while acridine orange (AO), ethidium bromide (EB), propidium iodide, and 4',6'-diamidino-2-phenylindole (DAPI) measured apoptosis. The protein expression levels of apoptosis-associated speck-like protein containing a C-terminal caspase recruitment domain (ASC), cleaved caspase-1, and nucleotide-binding domain and leucine-rich repeat protein 3 (NLRP3) were detected with western blot.

Results. The results established that IL-4 stimulation markedly decreased ($p < 0.05$) the proliferation of 16HBE cells, while the administration of ORD increased their proliferation. Apoptosis and DNA damage were enhanced in the IL-4-stimulated group, whereas ORD exhibited anti-apoptotic activity. Moreover, the treatment with ORD significantly reduced ($p < 0.05$) the IL-4-induced expression of cleaved caspase-1, ASC and NLRP3 proteins.

Conclusions. The findings suggest that NLRP3 is a direct target for ORD-mediated anti-inflammatory actions in injured 16HBE cells. Therefore, ORD may be a novel therapy against NLRP3-related disorders, including pediatric asthma (PA).

Key words: apoptosis, oridonin, NLRP3 inflammasome, inflammation, pediatric asthma

Cite as

Wang W, Ming D. Oridonin attenuates apoptosis and NLRP3 inflammasome activation in IL-4-stimulated human bronchial epithelial cells in an in vitro pediatric asthma model. *Adv Clin Exp Med.* 2024;33(2):163–170. doi:10.17219/acem/166253

DOI

10.17219/acem/166253

Copyright

Copyright by Author(s)
This is an article distributed under the terms of the Creative Commons Attribution 3.0 Unported (CC BY 3.0) (<https://creativecommons.org/licenses/by/3.0/>)

Background

Asthma is a chronic inflammatory syndrome that causes recurrent inflammation and narrowing of the airways.¹ Pediatric asthma (PA) is a persistent inflammatory respiratory disease characterized by inflammation and airway hyper-responsiveness and alterations.² Despite substantial developments in treatment strategies, the increasing occurrence of PA has become a burden to human mental and physical health due to its substantial prevalence and related juvenile death.^{3,4} The elevated incidence of asthma has been ascribed to numerous risk factors, including genetics, house dust mites, allergens, environmental pollution, and childhood obesity.^{5,6}

Reports have shown that chronic airway inflammation stimulates airway restoration, which is accompanied by generation of excessive extracellular matrix (ECM).⁷ Furthermore, it is well documented that a central pathological feature of asthma involves stimulated inflammatory cells that produce several pro-inflammatory cytokines to induce hypersecretion of mucus in the affected airway.⁸ Accordingly, potential drugs that can prevent mucus discharge, ECM production and airway inflammation may be effective in PA treatment. Although effective, enduring corticosteroid usage in youngsters leads to hormone resistance and toxic effects.⁹ Therefore, it is vital to understand the multifaceted molecular mechanisms of PA to improve future therapies.

Oridonin (ORD) is a bioactive ent-kaurane diterpenoid isolated from the aromatic plant *Rabdosia rubescens*, which has been comprehensively employed in the Chinese traditional medicine.¹⁰ Accumulating evidence propose that ORD exerts apoptotic and anti-proliferative activities in numerous malignant cells, including mammary, colorectal, and liver cancer cells.^{11–13} Studies unveiled that ORD triggered apoptosis in several tumor cells such as acute gliomas, leukemia, melanoma cells, and prostate, and these in vitro trials have exposed that ORD prompts cell death, recovers the phagocytosis, and prevents cell cycle progress.^{14,15} In ancient times, ORD was used as a remedy for many inflammatory disorders.¹⁶ Previously, ORD has been documented to constrain MAPK/NF- κ B stimulation to suppress the generation of pro-inflammatory cytokines.¹⁷ Furthermore, ORD has demonstrated protective anti-inflammatory action in neuroinflammation, colitis and sepsis.^{18–20}

However, the principal mechanisms through which ORD interacts with its targets remain unidentified. Recently, it has been shown that nucleotide-binding domain and leucine-rich repeat protein 3 (NLRP3) is a direct target for ORD-mediated anti-inflammatory action.²¹ The NLRP3 inflammasome is a complex of multiple proteins including NLRP3, caspase-1 and apoptosis-associated speck-like protein containing a C-terminal caspase recruitment domain (ASC).²² The activation of the complex stimulates caspase-1 and initiates the cleavage and production

of cytokines, exhibiting profound action in inflammation and immunity. However, the protective role and the underlying mechanisms of ORD against cell apoptosis in bronchial epithelial cells remain unknown.

Objectives

The current study explored the mechanisms underlying interleukin 4 (IL-4)-induced human bronchial epithelial (16HBE) cell injury and assessed the protective actions of ORD. Specifically, the study investigated the regulatory effects of ORD on apoptosis and IL-4-induced deoxyribonucleic acid (DNA) damage to identify an innovative approach to PA treatment.

Materials and methods

Chemicals

Oridonin (empirical formula: $C_{20}H_{28}O_6$ and molecular weight (MW): 364.43 g/mol; Thermo Fisher Scientific, Waltham, USA), with a purity $\geq 98\%$, confirmed with high-performance liquid chromatography (HPLC), was initially dissolved in dimethyl sulfoxide (DMSO) to prepare a 20-mM stock solution, and stored at -20°C for further use. Other chemicals, including RPMI-1640 media, fetal bovine serum (FBS), antibiotics, phosphate-buffered saline (PBS), 5-Bromo-2-deoxyuridine (BrdU), acridine orange (AO), ethidium bromide (EB), 4',6-diamidino-2-phenylindole (DAPI), DMSO, terminal deoxynucleotidyl transferase dUTP nick end labeling (TUNEL), and sodium dodecyl-sulfate (SDS), were acquired from Thermo Fisher Scientific. The antibodies for western blot examination were procured from Beyotime Biotechnology (Haimen, China).

Cell culture

The 16HBE cells (Shanghai Aiyuan Biotechnology Co., Ltd., Shanghai, China) were cultured in RPMI-1640 medium containing FBS (10%) and 1% of antibiotics, and incubated at 37°C and 5% CO_2 in a moistened chamber. The 16HBE cells were arbitrarily stratified into 4 groups: 16HBE control cells, 16HBE cells + ORD (20 $\mu\text{M}/\mu\text{L}$), 16HBE cells + IL-4 (100 ng/ μL), and 16HBE cells + IL-4 (100 ng/ μL) + ORD (20 $\mu\text{M}/\mu\text{L}$).

Cell proliferation assay

Proliferation was estimated in 16HBE cells using the BrdU technique. Concisely, cells were seeded onto 96-well plates and grown in a culture medium containing IL-4 in the presence or absence of ORD. The BrdU (10 μL) was added separately to all wells after 48 h, and the plates were incubated for 4 h. Afterward, treated

cells were incubated with BrdU for 60 min. Wells were washed 3 times with PBS, a substrate solution (200 μ L) was added to each well for 25 min, and sulfuric acid was added to the wells in the final step. The optical density (OD) was determined for each well at 490 nm, and the relative rate of cell proliferation was calculated as a percentage of the control. Three independent replicates were performed in each group.

Analysis of apoptosis with acridine orange and ethidium bromide double staining

Morphological and nuclear changes were assessed in treated 16HBE cells with AO and EB double staining.²³ The 16HBE cells were grown in a medium spiked with IL-4, with or without ORD, and kept for 1 day. Each group of cells had a mixture of AO and EB added, and were incubated at room temperature in the dark for 20 min. Cells were then washed using PBS to remove unbound AO and EB, and viewed under a fluorescence microscope (Nikon Eclipse TS100; Nikon Corp., Tokyo, Japan).

Cell apoptosis assay

The 16HBE cells were grown in a medium supplemented with IL-4 in the presence or absence of ORD for 24 h and then treated with 5% cigarette smoke extract (CSE) for 1 h. The cells were fixed with cold methanol and acetone (1:1) for 5 min, then incubated with DAPI and propidium iodide (PI) solution for 10 min. The apoptotic morphology of the cells was observed using fluorescence microscope (Nikon Eclipse TS100). For quantification, the 16HBE cells were washed with cold PBS buffer and harvested, and the number of stained cells was counted and expressed as a percentage of apoptotic cells. Three independent trials were performed to determine the mean apoptosis rate.

Western blot study

The 16HBE cells were cultured for 1 day in a medium spiked with IL-4 in the presence or absence of ORD (20 μ M). The cells were then lysed in an ice-cold lysis

buffer containing protease inhibitors and used for a western blot assay. Cellular protein content was measured using a Pierce™ BCA Protein Assay Kit (Pierce Chemical, Dallas, USA). Briefly, the proteins were electrophoretically dispersed and transferred to a polyvinylidene difluoride (PVDF) film. Afterward, the film was blocked overnight at 4°C and then incubated overnight at 4°C with primary antibodies (1:100 dilutions); secondary antibodies (1:1000) were added subsequently. Glyceraldehyde 3-phosphate dehydrogenase (GAPDH) was used as an internal control. Protein visualization employed an Odyssey imaging system (LI-COR Biosciences, Lincoln, USA).

Statistical analyses

The data from each group were statistically analyzed using GraphPad Prism v. 8.0.1 (GraphPad Software, San Diego, USA) and Statistical Package for Social Sciences (SPSS) v. 25 software (IBM Corp., Armonk, USA). The Shapiro–Wilk test determined the normality of data distribution. Comparisons between groups (control, n = 6; ORD, n = 6; IL-4-induced, n = 6; and IL-4+ORD, n = 6) utilized one-way analysis of variance (ANOVA) followed by Tukey's post hoc test. The Kruskal–Wallis test generated p-values because the sample size was small. The continuous data are presented as mean \pm standard deviation (M \pm SD), and differences were considered statistically significant for p < 0.05.

Results

All variables had a normal distribution. Table 1 presents the comparison of the variables between the groups.

The influence of oridonin on IL-4-induced 16HBE cell proliferation

To examine the effects of ORD on PA, we evaluated the proliferation of IL-4-treated 16HBE cells using an in vitro model (Fig. 1), with BrdU used as a marker. Proliferation was marginally elevated in the ORD group, whereas

Table 1. Comparison of the groups

Variables	Control (n = 6)	ORD (n = 6)	IL-4 inducer (n = 6)	IL-4+ORD (n = 6)	p-value*	Welch's p-value
AO/EB	5.23 \pm 0.39	6.90 \pm 0.52	80.18 \pm 6.13	51.10 \pm 3.9	<0.001	<0.001
ASC	1.00 \pm 0.07	0.74 \pm 0.05	1.73 \pm 0.13	0.89 \pm 0.06	<0.001	<0.001
Cleaved caspase-5	1.00 \pm 0.07	0.83 \pm 0.06	1.60 \pm 0.12	0.99 \pm 0.076	<0.001	<0.001
DAPI	9.35 \pm 0.71	9.40 \pm 0.71	83.28 \pm 6.37	53.52 \pm 4.09	<0.001	<0.001
MTT	100.01 \pm 7.61	99.97 \pm 7.61	49.12 \pm 3.76	77.26 \pm 5.91	<0.001	<0.001
NLRP3	1.00 \pm 0.076	0.41 \pm 0.031	1.49 \pm 0.111	0.67 \pm 0.049	<0.001	<0.001
PI	6.20 \pm 0.47	7.03 \pm 0.53	91.10 \pm 6.97	49.73 \pm 3.80	<0.001	<0.001

AO/EB – acridine orange/ethidium bromide; ASC – C-terminal caspase recruitment domain; DAPI – 4',6-diamidino-2-phenylindole; MLRP3 – nucleotide-binding domain and leucine-rich repeat protein 3; PI – propidium iodide; ORD – oridonin; IL-4 – interleukin 4; * based on Kruskal–Wallis test. Data are presented as mean \pm standard deviation (M \pm SD).

it declined considerably in the IL-4-treated cells compared to the control cells ($p < 0.05$, Fig. 1). Moreover, the supplementation of the IL-4-treated 16HBE cells with ORD markedly enhanced proliferation compared to the IL-4-treated 16HBE cells without ORD ($p < 0.05$).

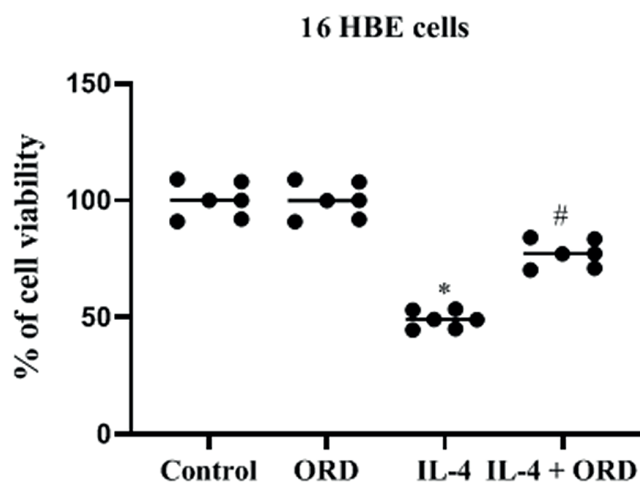


Fig. 1. Oridonin (ORD) ameliorates human bronchial epithelial (16HBE) cell proliferation. 16HBE cell relative proliferation was determined using the 5-Bromo-2-deoxyuridine (BrdU) method. The figure presents spectrofluorometric quantification of apoptosis. The results were statistically analyzed using one-way analysis of variance (ANOVA) followed by the Tukey's test for post hoc analysis

* $p < 0.05$, # $p < 0.01$ compared to the control cells; ORD – oridonin; IL-4 – interleukin 4.

The influence of oridonin on IL-4-induced 16HBE cell apoptosis

We explored the apoptotic activity of ORD on 16HBE cells using AO and EB (Fig. 2A), DAPI (Fig. 3A), and PI (Fig. 4A) assays. Control 16HBE cells and ORD-treated cells showed no substantial variation in apoptosis or DNA damage. Conversely, the administration of ORD attenuated IL-4-induced apoptosis and DNA damage in 16HBE cells (Fig. 2B, 3B, 4B).

Oridonin inhibited NLRP3 inflammasome activation in IL-4-stimulated 16HBE cells

The western blot analysis was used to assess NLRP3 inflammasome activation. The results demonstrated that ORD did not markedly alter protein expression levels of ASC, cleaved caspase-1, or NLRP3 in control 16HBE cells (Fig. 5A). However, IL-4 stimulation significantly increased ($p < 0.05$) the cleaved caspase-1 (Fig. 5B), ASC (Fig. 5C) and NLRP3 protein levels (Fig. 5D), which were suppressed by ORD (Fig. 5A–D).

Discussion

Asthma is recognized as a highly prevalent lethal clinical condition that causes a substantial health and economic burden.¹ The characteristic hallmarks of bronchial

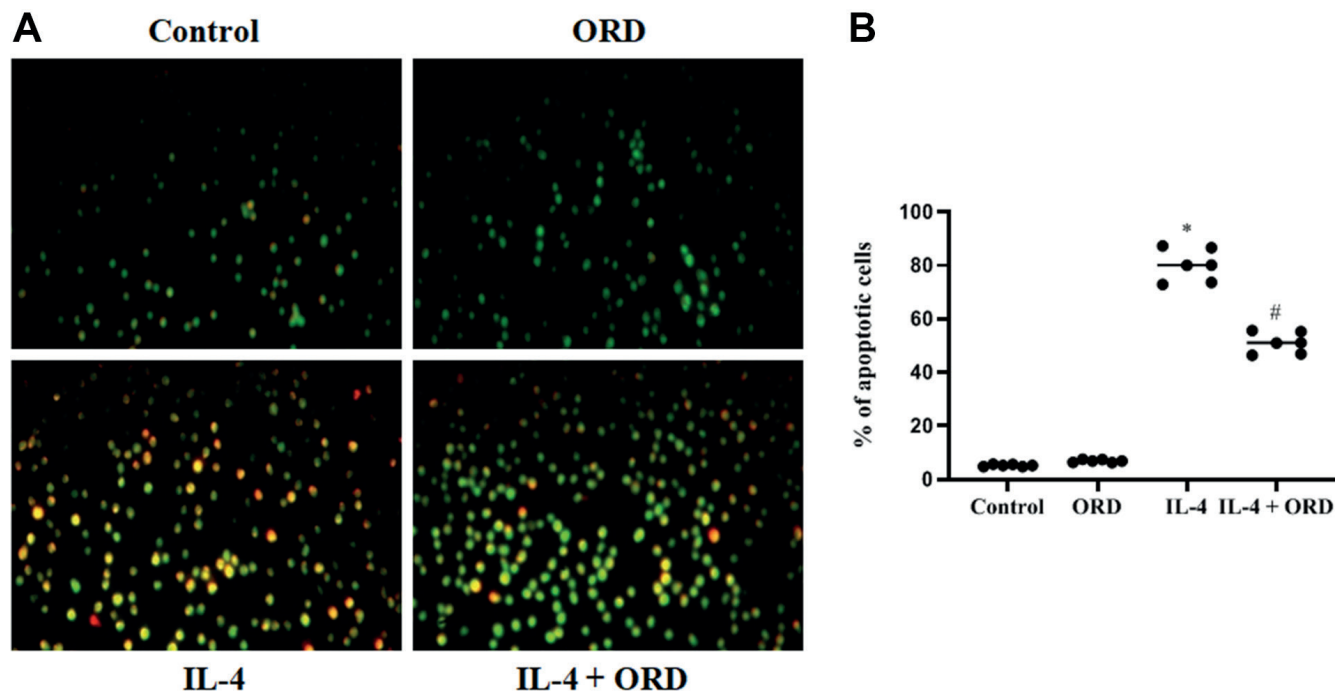


Fig. 2. Oridonin (ORD) inhibits apoptosis on human bronchial epithelial (16HBE) cells, as evidenced by acridine orange/ethidium bromide (AO/EB) staining. A. The apoptosis was evaluated using dual AO/EB staining and viewed with fluorescence microscopy. Effects of ORD on the percentage of cells display apoptotic morphology; B. Quantification of apoptosis in the spectrofluorometry. The results were statistically analyzed using one-way analysis of variance (ANOVA) followed by the Tukey's test for post hoc analysis

* $p < 0.05$, # $p < 0.01$ compared to the control cells; IL-4 – interleukin 4.

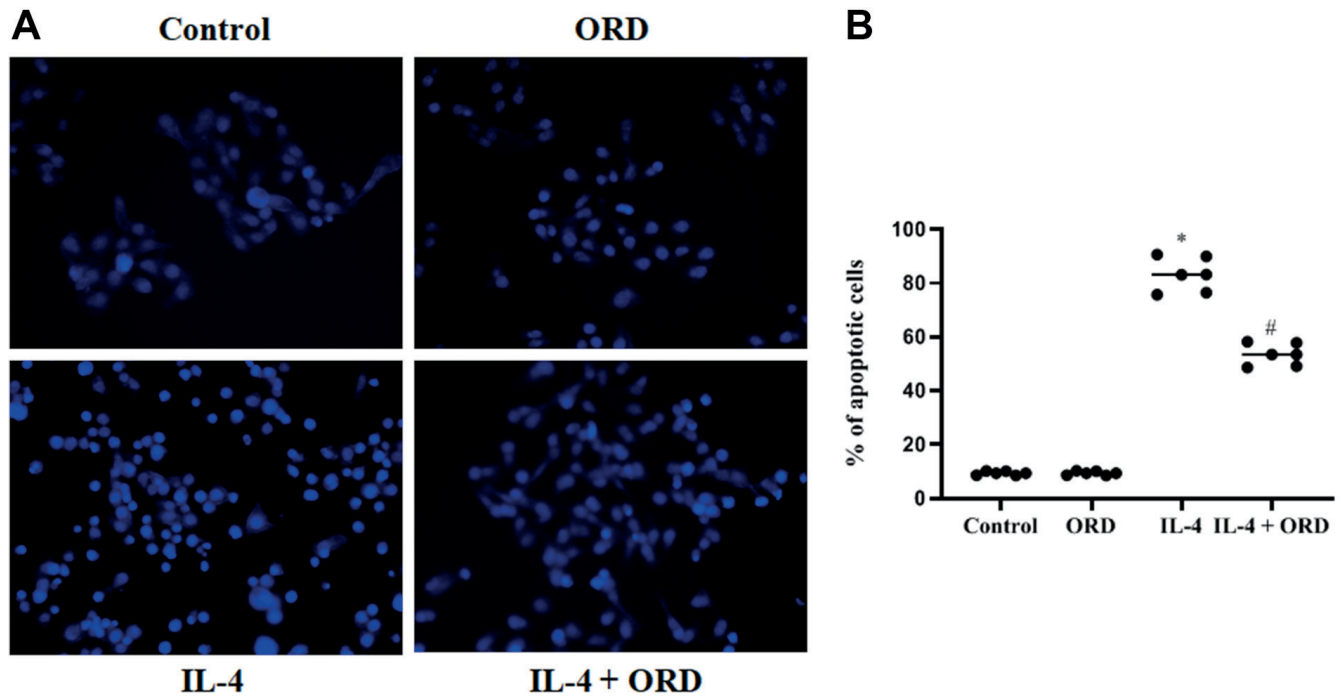


Fig. 3. Oridonin (ORD) mitigates apoptosis on human bronchial epithelial (16HBE) cells, as visualized using 4',6-diamidino-2-phenylindole (DAPI) staining. A. The apoptosis was evaluated using staining with DAPI and viewed with fluorescence microscopy. Effects of ORD on the percentage of cells display apoptotic morphology; B. Quantification of apoptosis in the spectrofluorometry. The results were statistically analyzed using one-way analysis of variance (ANOVA) followed by the Tukey's test for post hoc analysis

* $p < 0.05$, # $p < 0.01$ compared to the control cells; IL-4 – interleukin 4.

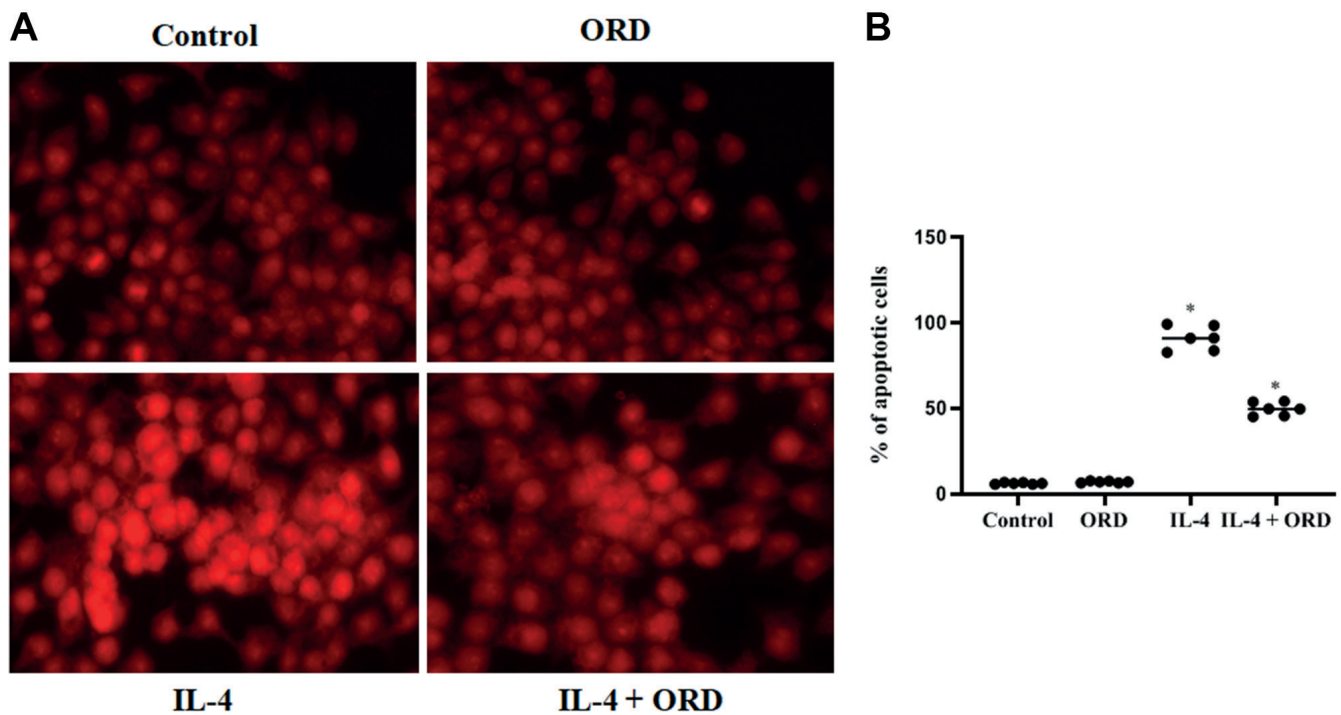


Fig. 4. Oridonin (ORD) reduces apoptosis on human bronchial epithelial (16HBE) cells, as confirmed using terminal deoxynucleotidyl transferase-mediated dUTP nick end labeling (TUNEL) assay. A. The apoptosis was assessed using a TUNEL assay and observed with a fluorescence microscope. Effects of ORD on the percentage of cells display apoptotic cell morphology; B. Quantification of apoptosis in the spectrofluorometry. The results were statistically analyzed using one-way analysis of variance (ANOVA) followed by the Tukey's test for post hoc analysis

* $p < 0.05$ compared to the control cells; IL-4 – interleukin 4.

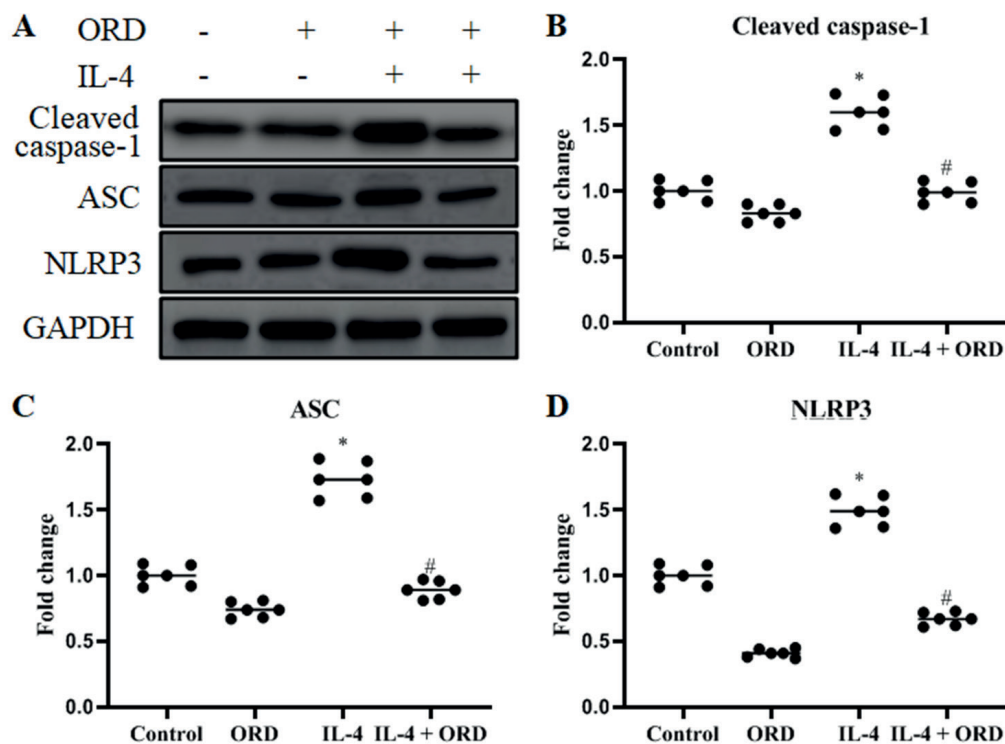


Fig. 5. Western blot analysis of vascular cleaved caspase-1, apoptosis-associated speck-like protein (ASC) and NLR family pyrin domain containing 3 (NLRP3). A. Representative bands of cleaved caspase-1, ASC and NLRP3 proteins; B. Cleaved caspase-1 protein expression measured in various cohorts; C. ASC marker expression quantified in different cohorts; D. NLRP3 protein levels quantified in various cohorts. The results were statistically analyzed using one-way analysis of variance (ANOVA) followed by the Tukey's test for post hoc analysis

* $p < 0.05$, # $p < 0.01$ compared to the control cells; ORD – oridonin; IL-4 – interleukin 4; GAPDH – glyceraldehyde 3-phosphate dehydrogenase.

asthma are airway stenosis, as a consequence of airway restoration, restricted airflow, inflammation, and airway hyper-responsiveness.^{1,2} Many reports have demonstrated that airway remodeling is central to PA pathogenesis.²⁻⁴ As such, remedies that counter the formation of airway alterations represent an opportunity to develop an innovative PA therapy. Therefore, exploring the anti-inflammatory properties of putative anti-asthmatic drugs is essential. The current study examined for the first time the anti-inflammatory activity of ORD as an anti-asthmatic natural substitute. Its molecular actions in airway remodeling pathogenesis, mostly on airway epithelial cell apoptosis, were scrutinized using IL-4-stimulated 16HBE cells in an in vitro asthma model.

The reparative effects of short-chain fatty acids (SCFAs) were studied by incubating cells with IL-4, IL-13 or house dust mite extract, and SCFA. Short-chain fatty acid affected zonular occludin-1 (ZO-1), MAPK signaling pathway expression and IL-4-induced cytokine production.²⁴ The current study demonstrated the effects of ORD on IL-4-stimulated 16HBE cells as an in vitro model of PA by evaluating proliferation using the BrdU technique. It was found that 16HBE cell proliferation was somewhat increased in the ORD group but decreased in the IL-4 treated cells. Additionally, ORD supplementation increased the proliferative growth of IL-4-stimulated 16HBE cells compared to 16HBE cells without ORD. These findings show that IL-4 stimulation significantly reduced proliferation of 16HBE cells used as an in vitro cell line model.

Immune cells release mediators such as the type 2 cytokines IL-4 and IL-13, which are associated with allergies, as well as reactive oxygen species (ROS) and proteases

that play a role in epithelial destruction.²⁵ The present study determined the effects of ORD on IL-4-stimulated 16HBE cells by exploring its apoptotic activity using AO and EB, PI, and DAPI assays. The ORD-treated cells showed no substantial variation in apoptosis and DNA damage compared to the untreated controls. However, the administration of ORD attenuated IL-4-induced apoptosis and DNA damage in 16HBE cells. These findings indicate that IL-4 stimulation considerably augmented apoptosis.

In the current study, the western blot analysis demonstrated that ORD inhibited NLRP3 inflammasome activation in IL-4-stimulated 16HBE cells. The western blot results showed that in control 16HBE cells, ORD had no appreciable impact on the levels of ASC, cleaved caspase-1 or NLRP3 protein expression. However, IL-4 stimulation increased the levels of ASC, cleaved caspase-1 and NLRP3 proteins, which ORD inhibited. From this, we concluded that IL-4 stimulation significantly augmented inflammation and apoptosis of the 16HBE cells. Furthermore, ORD treatment markedly increased cell proliferation, reduced apoptosis and inhibited IL-4-induced inflammation in 16HBE cells, indicating protection against IL-4-stimulated cellular damage. These outcomes are consistent with previous reports and confirm IL-4-stimulated inflammatory impairment in 16HBE cells.^{26,27} Moreover, the supplementation with ORD had no negative impact on the 16HBE cells relative to IL-4 stimulation, which suggests that ORD is safe for bronchial epithelial cells and safe for the treatment of asthma.

Several reports have documented that ORD possesses anti-cancer, anti-inflammatory and apoptosis-modulatory

activities.^{13–15} Previously, ORD has been administered in various inflammatory disorders.¹⁶ Many studies revealed that ORD exerts protective actions in numerous disorders, including sepsis, colitis and neuroinflammation.^{18–20} Also, ORD has been shown to inhibit MAPK/NF- κ B activation by suppressing pro-inflammatory cytokine production.¹⁷ Thus, the healing action of ORD on IL-4-stimulated 16HBE cells is perhaps attributed to its anti-inflammatory and anti-apoptotic effects.

In asthma, bronchial epithelial cell impairment is firmly connected to cellular inflammation. The Chinese traditional medicine *Rabdosia rubescens* is frequently consumed as a remedy for inflammatory diseases.¹⁰ However, its unknown mechanism of action restricts its medical usage. Here, we established that ORD, the main active constituent of *Rabdosia rubescens*, openly or covalently links to NLRP3 and has substantial anti-inflammatory properties in vitro, suggesting that ORD can be employed as an innovative therapeutic against NLRP3-stimulated disorders.

The current research demonstrated that IL-4 remarkably augmented NLRP3 inflammasome activation in 16HBE cells, while ORD treatment marginally reduced ASC, cleaved caspase-1 and NLRP3 protein expression. Such a marginal response may be due to stimulation of the NLRP3 inflammasome in 16HBE control cells, which negates the requirement for ORD to have a substantial influence. Conversely, ORD intensely reduced excessive activation of the NLRP3 inflammasome in IL-4-stimulated cells, indicating that ORD protects 16HBE cells by inhibiting NLRP3 inflammasome signaling.

Excessive stimulation of the NLRP3 inflammasome has a crucial role in inflammation and allergic airway disorders, including PA.²¹ Hyperexpression of ASC, cleaved caspase-1 and NLRP3 occurred in lipopolysaccharide (LPS)-stimulated HBE cells.²² Previous studies have suggested that ORD could prevent MAPK and NF- κ B stimulation and attenuate inflammasome-induced cytokine generation, including tumor necrosis factor alpha (TNF- α) and IL-6.^{17,28} The current findings indicate that ORD targets NLRP3 to exert its anti-inflammatory effects.

Limitations

A few restrictions must be taken into account when evaluating our results. By utilizing destructive techniques for particular time points, and conducting experiments using inflammatory and apoptotic markers, such as fluorescein-labeled dyes, it is possible to determine the impact of ORD on 16HBE cells and determine more mechanisms of action of ORD as an anti-asthmatic natural substitute. Even though its molecular actions in airway remodeling pathogenesis occur mostly through airway epithelial cells, apoptosis was scrutinized using IL-4-stimulated 16HBE cells as an in vitro asthma model in this study.

Conclusions

One of the signs of immune-mediated respiratory illnesses, such as asthma, is a compromised epithelium, which frequently causes increased sensitivity to inhaled substances and exacerbates these airway disorders. We demonstrated, for the first time, that ORD helped restore the barrier functions of IL-4-stimulated 16HBE cells, which may be mediated by downregulating the expression of NLRP3. In summary, ORD alleviated cellular proliferation and exhibited anti-apoptotic activity in IL-4-induced 16HBE cell impairments by suppressing NLRP3 inflammasome signaling pathways. These findings indicate that ORD may be a potential anti-asthmatic agent and contribute to its well-known anti-inflammatory activities.

Supplementary data

The supplementary materials are available at <https://doi.org/10.5281/zenodo.7927638>. The package contains the following files:

Supplementary Table 1. Results of normality tests as presented in Fig. 1.

Supplementary Table 2. Results of normality tests as presented in Fig. 2.


Supplementary Table 3. Results of normality tests as presented in Fig. 3.

Supplementary Table 4. Results of normality tests as presented in Fig. 4.

Supplementary Table 5. Results of normality tests as presented in Fig. 5B–D.

ORCID iDs

Weiwei Wang  <https://orcid.org/0000-0002-3919-5277>

Dan Ming  <https://orcid.org/0000-0001-8041-3566>

References

1. Sleiman PMA, Flory J, Imielinski M, et al. Variants of *DENND1B* associated with asthma in children. *N Engl J Med*. 2010;362(1):36–44. doi:10.1056/NEJMoa0901867
2. Saglani S. A video questionnaire identifies upper airway abnormalities in preschool children with reported wheeze. *Arch Dis Child*. 2005;90(9):961–964. doi:10.1136/adc.2004.071134
3. Akinbami LJ, Moorman JE, Liu X. Asthma prevalence, health care use, and mortality: United States, 2005–2009. *Natl Health Stat Report*. 2011;(32):1–14. PMID:21355352.
4. Okpapi A, Friend AJ, Turner SW. Asthma and other recurrent wheezing disorders in children (acute). *BMJ Clin Evid*. 2012;2012:0300. PMID:24807832.
5. Trasande L, Thurston GD. The role of air pollution in asthma and other pediatric morbidities. *J Allergy Clin Immunol*. 2005;115(4):689–699. doi:10.1016/j.jaci.2005.01.056
6. Kaugars AS. Family influences on pediatric asthma. *J Pediatr Psychol*. 2004;29(7):475–491. doi:10.1093/jpepsy/jsh051
7. Britt RD, Fakh A, Vogel ER, et al. Vitamin D attenuates cytokine-induced remodeling in human fetal airway smooth muscle cells. *J Cell Physiol*. 2015;230(6):1189–1198. doi:10.1002/jcp.24814
8. Zhu T, Zhang W, Wang DX, et al. Rosuvastatin attenuates mucus secretion in a murine model of chronic asthma by inhibiting the gamma-aminobutyric acid type A receptor. *Chin Med J (Engl)*. 2012;125(8):1457–1464. PMID:22613653.

9. Yeo SH, Aggarwal B, Shantakumar S, Mulgirigama A, Daley-Yates P. Efficacy and safety of inhaled corticosteroids relative to fluticasone propionate: A systematic review of randomized controlled trials in asthma. *Exp Rev Respir Med*. 2017;11(10):763–778. doi:10.1080/17476348.2017.1361824
10. Marks LS, DiPaola RS, Nelson P, et al. PC-SPES: Herbal formulation for prostate cancer. *Urology*. 2002;60(3):369–375. doi:10.1016/S0090-4295(02)01913-1
11. Dong Y, Zhang T, Li J, et al. Oridonin inhibits tumor growth and metastasis through anti-angiogenesis by blocking the Notch signaling. *PLoS One*. 2014;9(12):e113830. doi:10.1371/journal.pone.0113830
12. Jin H, Tan X, Liu X, Ding Y. Downregulation of *AP-1* gene expression is an initial event in the oridonin-mediated inhibition of colorectal cancer: Studies in vitro and in vivo. *J Gastroenterol Hepatol*. 2011;26(4):706–715. doi:10.1111/j.1440-1746.2010.06500.x
13. Wang H, Ye Y, Pan SY, et al. Proteomic identification of proteins involved in the anticancer activities of oridonin in HepG2 cells. *Phytomedicine*. 2011;18(2–3):163–169. doi:10.1016/j.phymed.2010.06.011
14. Hsieh TC, Wijeratne EK, Liang JY, Gunatilaka AL, Wu JM. Differential control of growth, cell cycle progression, and expression of NF- κ B in human breast cancer cells MCF-7, MCF-10A, and MDA-MB-231 by ponicedin and oridonin, diterpenoids from the Chinese herb *Rabdosia rubescens*. *Biochem Biophys Res Commun*. 2005;337(1):224–231. doi:10.1016/j.bbrc.2005.09.040
15. Ikezoe T, Yang Y, Bandobashi K, et al. Oridonin, a diterpenoid purified from *Rabdosia rubescens*, inhibits the proliferation of cells from lymphoid malignancies in association with blockade of the NF- κ B signal pathways. *Mol Cancer Ther*. 2005;4(4):578–586. doi:10.1158/1535-7163.MCT-04-0277
16. Ma Z, Hu C, Zhang Y. Therapeutic effect of *Rabdosia rubescens* aqueous extract on chronic pharyngitis and its safety [in Chinese]. *Zhong Nan Da Xue Xue Bao Yi Xue Ban*. 2011;36(2):170–173. PMID:21368429.
17. Xu Y, Xue Y, Wang Y, Feng D, Lin S, Xu L. Multiple-modulation effects of oridonin on the production of proinflammatory cytokines and neurotrophic factors in LPS-activated microglia. *Int Immunopharmacol*. 2009;9(3):360–365. doi:10.1016/j.intimp.2009.01.002
18. Wang S, Zhang Y, Saas P, et al. Oridonin's therapeutic effect: Suppressing Th1/Th17 simultaneously in a mouse model of Crohn's disease. *J Gastroenterol Hepatol*. 2015;30(3):504–512. doi:10.1111/jgh.12710
19. Wang S, Yang H, Yu L, et al. Oridonin attenuates A β 1–42-induced neuroinflammation and inhibits NF- κ B pathway. *PLoS One*. 2014;9(8):e104745. doi:10.1371/journal.pone.0104745
20. Zhao YJ, Lv H, Xu PB, et al. Protective effects of oridonin on the sepsis in mice. *Kaoshiung J Med Sci*. 2016;32(9):452–457. doi:10.1016/j.kjms.2016.07.013
21. He H, Jiang H, Chen Y, et al. Oridonin is a covalent NLRP3 inhibitor with strong anti-inflammasome activity. *Nat Commun*. 2018;9(1):2550. doi:10.1038/s41467-018-04947-6
22. Ahn H, Kang SG, Yoon SI, Kim PH, Kim D, Lee GS. Poly-gamma-glutamic acid from *Bacillus subtilis* upregulates pro-inflammatory cytokines while inhibiting NLRP3, NLRC4 and AIM2 inflammasome activation. *Cell Mol Immunol*. 2018;15(2):111–119. doi:10.1038/cmi.2016.13
23. Kasibhatla S, Amarante-Mendes GP, Finucane D, Brunner T, Bossy-Wetzel E, Green DR. Acridine orange/ethidium bromide (AO/EB) staining to detect apoptosis. *Cold Spring Harb Protoc*. 2006;2006(3):pdb.prot4493. doi:10.1101/pdb.prot4493
24. Richards LB, Li M, Folkerts G, Henricks PAJ, Garssen J, Van Esch BCAM. Butyrate and propionate restore the cytokine and house dust mite compromised barrier function of human bronchial airway epithelial cells. *Int J Mol Sci*. 2020;22(1):65. doi:10.3390/ijms22010065
25. Kany S, Vollrath JT, Relja B. Cytokines in inflammatory disease. *Int J Mol Sci*. 2019;20(23):6008. doi:10.3390/ijms20236008
26. Geng G, Du Y, Dai J, Tian D, Xia Y, Fu Z. KIF3A knockdown sensitizes bronchial epithelia to apoptosis and aggravates airway inflammation in asthma. *Biomed Pharmacother*. 2018;97:1349–1355. doi:10.1016/j.biopha.2017.10.160
27. Zhu C, Zhang L, Liu Z, Li C, Bai Y, Wang L. Atractylenolide III reduces NLRP3 inflammasome activation and Th1/Th2 imbalances in both in vitro and in vivo models of asthma. *Clin Exp Pharmacol Physiol*. 2020;47(8):1360–1367. doi:10.1111/1440-1681.13306
28. Zhao G, Zhang T, Ma X, et al. Oridonin attenuates the release of pro-inflammatory cytokines in lipopolysaccharide-induced RAW264.7 cells and acute lung injury. *Oncotarget*. 2017;8(40):68153–68164. doi:10.18632/oncotarget.19249

Serabelisib regulates GSDMD-mediated pyroptosis, apoptosis and migration of hepatoma cells via the PI3K/Akt/E-cadherin signaling pathway

Ming Li^{A,B,D,F}, Zhao Huang^{B,C,F}, Yuxiang Zhou^{A,B,F}

Second Department of General Surgery, Hunan Children's Hospital, Changsha, China

A – research concept and design; B – collection and/or assembly of data; C – data analysis and interpretation; D – writing the article; E – critical revision of the article; F – final approval of the article

Advances in Clinical and Experimental Medicine, ISSN 1899–5276 (print), ISSN 2451–2680 (online)

Adv Clin Exp Med. 2024;33(2):171–181

Address for correspondence

Ming Li
E-mail: liming8709@aliyun.com

Funding sources

None declared

Conflict of interest

None declared

Acknowledgements

The graphical abstract was prepared using Figdraw software.

Received on August 30, 2022
Reviewed on November 11, 2022
Accepted on May 25, 2023

Published online on July 24, 2023

Cite as

Li M, Huang Z, Zhou Y. Serabelisib regulates GSDMD-mediated pyroptosis, apoptosis and migration of hepatoma cells via the PI3K/Akt/E-cadherin signaling pathway. *Adv Clin Exp Med.* 2024;33(2):171–181. doi:10.17219/acem/166511

DOI

10.17219/acem/166511

Copyright

Copyright by Author(s)
This is an article distributed under the terms of the Creative Commons Attribution 3.0 Unported (CC BY 3.0) (<https://creativecommons.org/licenses/by/3.0/>)

Abstract

Background. Liver cancer is a malignant tumor commonly seen in infants and young children. Serabelisib is a novel and effective phosphoinositide-3-kinase (PI3K α) inhibitor, currently in trials for solid malignancy treatment, such as bladder cancer. However, it is unclear whether serabelisib affects liver cancer.

Objectives. To explore the effects of serabelisib on the proliferation, apoptosis, invasion, and metastasis of HepG2 and HuH-6 cells, and elucidate the relevant molecular mechanisms.

Materials and methods. The HepG2 cells were treated with 2 μ M, 4 μ M or 8 μ M serabelisib, while the 0- μ M group was used as a control. A plate clone formation assay was utilized to measure colony formation ability in each group, a 5-ethynyl-2'-deoxyuridine (EdU) assay examined cell proliferation, a Cell Counting Kit-8 (CCK-8) assay assessed cell viability, flow cytometry measured the cell cycle and apoptosis, JC-1 staining determined mitochondrial membrane potential, and transmission electron microscopy evaluated cell morphology. In addition, gene and protein expression levels of apoptosis markers, epithelial–mesenchymal transition (EMT), Gasdermin D (GSDMD), and the PI3K/protein kinase B (AKT) signaling pathway were measured.

Results. After serabelisib intervention, HepG2 and HuH-6 cells formed fewer colonies, proliferated more slowly, and had reduced viability. The number of HepG2 and HuH-6 cells in the G2 and S phases decreased, apoptosis and the number of apoptotic bodies increased, and mitochondrial membrane potential decreased. Serabelisib treatment also reduced the migration and invasion capacity of the cells. Furthermore, genes and proteins of the PI3K/AKT signaling pathway were downregulated, while those that promote apoptosis and pyroptosis or inhibit EMT were upregulated.

Conclusions. Serabelisib inhibited the PI3K/AKT signaling pathway, thereby inhibiting EMT and promoting apoptosis and pyroptosis in HepG2 and HuH-6 cells.

Key words: PI3K, hepatoblastoma, EMT, pyroptosis, serabelisib

Background

Liver cancer is a common malignant tumor that poses a grave threat to human life.¹ Eighty percent of liver cancers in children and adolescents are primary hepatoblastomas.² Chemotherapy and surgery are the primary treatments for hepatoblastoma,³ with cure dependent on complete excision. However, according to surgical guidelines, 60–80% of patients have nonresectable tumors at diagnosis.⁴ Therefore, researchers seek a pharmacological solution to liver cancer treatment.

Serabelisib (INK-1117, MLN-1117, TAK-117) is a novel, highly selective and effective phosphoinositide-3-kinase (PI3K α) inhibitor administered orally.⁵ The drug is currently being explored for solid malignancy treatment and has shown promising results.⁶ In addition, combining serabelisib with TAK-228 has demonstrated synergistic anti-tumor effects in preclinical bladder cancer models.⁷ Meanwhile, serabelisib pharmacokinetics continue to improve.⁸ However, the effects of serabelisib on liver cancer have not been reported.

The PI3K/protein kinase B (AKT) pathway is a classical signal transduction pathway that promotes proliferation and suppresses apoptosis. It also participates in the growth promotion and proliferation of cancer cells, promotes cellular invasion and metastasis, enhances tumor angiogenesis, and induces apoptosis resistance to chemotherapy and radiotherapy.⁹ Hartmann et al. found that the PI3K/AKT signaling pathway is usually activated in liver cancer, and in vitro PI3K targeting leads to increased apoptosis, which inhibits liver cancer cell proliferation.¹⁰ Furthermore, many substances, such as JTC-801, have been shown to inhibit HepG2 metastasis through the regulation of PI3K/AKT signaling pathway.¹¹

The PI3K/AKT signaling pathway can regulate epithelial–mesenchymal transition (EMT), a process in which epithelial cells lose their characteristics and acquire a mesenchymal phenotype under certain conditions, to reduce tumor aggression.^{12,13} It has been reported that deoxyribonucleic acid (DNA) damage-regulated autophagy modulator 1 (DRAM1) regulates liver cancer cell migration and invasion through the autophagy–EMT pathway,¹⁴ while other studies demonstrated the PI3K/AKT involvement in renal cancer cell pyroptosis.¹⁵ Pyroptosis is a form of cell death that leads to inflammation and further damage to the body.¹⁶ Several studies have found many factors related to pyroptosis, including NLRP3, interleukin (IL)-18, IL-1 β , apoptosis-associated speck-like protein containing a CARD (ASC), and caspase-1. In addition, interactions between caspase-1 and Gasdermin D (GSDMD) can lead to pyroptosis.¹⁷ Therefore, we hypothesized that serabelisib could interfere with HepG2 and HuH-6 pyroptosis through GSDMD regulation of the PI3K/Akt/E-cadherin signaling pathway.

Objectives

The study aimed to assess the effects of serabelisib on the PI3K/AKT signaling pathway in HepG2 and HuH-6 cells by exploring its impact on proliferation, apoptosis, invasion, and metastasis, and to elucidate the relevant molecular mechanisms. This research may provide a novel avenue for liver cancer treatment by establishing a new experimental and theoretical basis for the clinical study of serabelisib in liver cancer.

Materials and methods

Drug treatment

The HepG2, HuH-6, SMMC-7721, and human kidney fibroblast (HKF) cells were purchased from Abiowell (Changsha, China). The cells were digested with 0.25% trypsin solution (C0201; Beyotime Biotechnology, Shanghai, China), and cell suspensions were prepared using Roswell Park Memorial Institute (RPMI) 1640 complete medium (04-001-1ACS; Thermo Fisher Scientific, Waltham, USA). Cells were inoculated on a 6-well plate at approx. 2×10^5 cells per well and cultured overnight in a DH-160I incubator (Shanghai Sanotac Scientific Instruments Co., Ltd., Shanghai, China) at 37°C with saturated humidity and 5% carbon dioxide. The small-molecule inhibitor serabelisib (S8581; Selleckchem, Houston, USA) was dissolved in sterile dimethyl sulfoxide (DMSO) and diluted to the desired concentration. The cells in each group were treated with different drug interventions. Cells in the 0- μ M group were cultured without intervention, cells in the 2- μ M group were cultured with a medium containing 2 μ M of serabelisib, 4 μ M of serabelisib was added to the medium used to culture cells in the 4- μ M group, and the 8- μ M group had 8 μ M of serabelisib added to the medium. For the serabelisib+MK2206 group, 8 μ M of serabelisib and 3 μ M of MK2206 (IM1090; Solarbio, Beijing, China) were added to the medium. The intervention time was 48 h.

Plate clone formation assay

After 24 h of intervention, the cells were digested with a 0.25% trypsin solution and added to high-sugar Dulbecco's modified Eagle's medium (DMEM) (D5796-500mL; Thermo Fisher Scientific) to prepare cell suspensions. Then, the cells were inoculated onto a 6-well plate at a density of 1000 cells per well and shaken thoroughly.¹⁸ Afterwards, they were cultured in an incubator (37°C, 5% CO₂) for 7 days. The colony-forming ability was observed under an inverted biological microscope (model DSZ2000X; Cn-micro, Beijing, China).

5-ethynyl-2'-deoxyuridine assay

After 24 h of intervention, the 5-ethynyl-2'-deoxyuridine (EdU) DNA Proliferation in vitro Detection Kit (C10310; RiboBio, Guangzhou, China) assessed the HepG2 proliferation rate. In brief, the cells were incubated in a medium containing 50 μM of EdU for 24 h, incubated with 1 \times Apollo[®] staining solution and then stained with 1 \times Hoechst33342 solution. Observations were made immediately after staining.

Cell Counting Kit-8 assay

The medium was aspirated, discarded and replaced with 110 μL of Cell Counting Kit-8 (CCK-8) (NU679; Dojindo Molecular Technologies, Rockville, USA) working solution which consisted of 100 μL of high-sugar DMEM and 10 μL of CCK-8 stock solution. Cells were then cultured for another 4 h in a 37°C and 5% CO₂ incubator. Finally, the absorbance of each well was measured at 450 nm using a microplate analyzer (model MB-530; Shenzhen Heales Technology Development Co., Ltd., Shenzhen, China).

Flow cytometry (cell cycle)

The cells were gently suspended and separated into single cells. Then, 1.2 mL of pre-cooled 100% ethanol was added drop by drop until the concentration reached 75%. The mixed solution was stored at 4°C overnight for fixing. The next day, the cells were washed 3 times and incubated with 150 μL of propidium iodide (PI) (MB2920; Dalian Meilunbio, Dalian, China) in the dark at 4°C for 30 min. After incubation, the cells were transferred to the flow testing tube and measured using CytoFLEX A00-1-1102 instrument (Beckman Coulter, Brea, USA).

Flow cytometry (cellular apoptosis)

An apoptosis kit (KGA108; KeyGEN Bio, Nanjing, China) was used to assess cell apoptosis. Each 2 \times 10⁵ aliquot was suspended in 500 μL of binding buffer, and 5 μL of annexin V-fluorescein isothiocyanate (FITC) was added to the cell suspension and mixed well. The mixture was then incubated with 5 μL of PI in the dark at room temperature for 10 min.

JC-1 staining

A mitochondrial membrane potential assay kit with JC-1 (C2006; Beyotime Biotechnology) detected early cell apoptosis. Each 50- μL JC-1 (200 \times) aliquot was diluted with 8 mL of ultra-pure water and mixed to obtain the JC-1 staining working solution. After incubation, the cells were washed twice with JC-1 staining buffer (1 \times) and photographed for observation.

Scratch assay

A flask of cells was digested with trypsin, counted and used to inoculate 6-well plates at 5 \times 10⁵ cells/well. When cells reached 90% confluency, they were scratched with a pipet tip, unattached cells were washed with phosphate-buffered saline (PBS), and serum-free high-sugar DMEM (D5796; Thermo Fisher Scientific) was added. The scratches were photographed and recorded at 0 h and 24 h.

Transwell migration assay

Cell suspensions were prepared using serum-free basal medium, added to the upper chambers of transwell plates (33318035; Corning Inc., Corning, USA) and incubated for 48 h. Then, the cells were immobilized for 20 min in an acetone and methanol solution (Sinopharm, Beijing, China) mixed at a 1:1 ratio. The cells were stained with 0.5% crystal violet (C8470; Solarbio) for 5 min and washed with water. Cells on the external surface were observed and imaged using an inverted microscope (model DSZ2000X; Cnmicro).

Transwell invasion assay

Sixty milliliters of Matrigel solution (356231; Corning) were diluted in 120 μL of serum-free medium, and 60 μL of diluted matrix glue was added to each transwell. The transwells were placed in an incubator (37°C, 60 min) to solidify the gel. Residual liquid was aspirated, 70 μL of a basic medium was added to each transwell, and the basement membrane was hydrated at 37°C for 30 min. The cell suspension was prepared with a basic serum-free medium containing bovine serum albumin (BSA) (5 g/L), and cell density was adjusted to 1 \times 10⁵/mL. After 48 h, the Matrigel glue and cells on the upper compartment were wiped. Finally, the membranes were observed and imaged using an inverted microscope (model DSZ2000X; Cnmicro).

Immunofluorescence

Total ribonucleic acid (RNA) was extracted using TRIzol lysate (15596026; Thermo Fisher Scientific). The protocol included 0.3% Triton permeabilization for 30 min and 5% BSA blocking for 60 min at 37°C. Appropriately diluted primary antibodies, including GSDMD (20770-1-AP, 1:50; Proteintech, Rosemont, USA) and caspase-1 (22915-1-AP, 1:50; Proteintech), were added dropwise at 4°C overnight. Cells were then fixed in 4% paraformaldehyde for 10 min. Nuclei were stained with 4',6-diamidino-2-phenylindole (DAPI) working solution (AWI0331a; Abiowell) at 37°C for 10 min.

Western blot

Total cell protein was extracted using radioimmuno-precipitation (RIPA) lysate (P0013B; Beyotime Biotechnology). Separation gels with concentrations of 10%, 12% and 4.8% were prepared. After closure, membranes were incubated with primary PI3K (4249, 1:1000; Cell Signaling Technology, Danvers, USA), N-cadherin (22018-1-AP, 1:2000; Proteintech), p-AKT (4060, 1:2000; Cell Signaling Technology), E-cadherin (20874-1-AP, 1:5000; Proteintech), cytochrome C (ab184699, 1:5000; Abcam, Cambridge, UK), caspase-9 (#20750, 1:1000; Cell Signaling Technology), caspase-3 (9664, 1:1000; Cell Signaling Technology), B-cell lymphoma 2 (Bcl-2) (12789-1-AP, 1:2000; Proteintech), GSDMD (66387-1-Ig, 1:10000; Proteintech), NLRP3 (19771-1-AP, 1:800; Proteintech), caspase-1 (ab179515, 1:1000; Abcam), ASC (ab180799, 1:1000; Abcam), IL-1 β (16806-1-AP, 1:2000; Proteintech), IL-18 (ab191860, 0.25 μ g/mL; Abcam), and β -actin (66009-1-Ig, 1:5000; Proteintech) antibodies for 90 min. After incubation, the membrane was washed 3 times with PBS Triton X (PBST) solution.

Statistical analyses

All data are expressed as mean \pm standard deviation (M \pm SD). The analysis employed IBM Statistical Package for Social Sciences (SPSS) v. 26.0 software (IBM Corp., Armonk, USA). The Kolmogorov–Smirnov test analyzed data distribution, and all data displayed a normal distribution and homogeneity of variance. The data were analyzed using parametric tests, with one-way analysis of variance (ANOVA) and Tukey's post hoc test used to compare data among the 3 groups. Statistical significance was set at $p < 0.05$.

Results

Screening cell lines

First, we examined the effects of serabelisib on HepG2, HuH-6, SMMC-7721, and HKF cell proliferation. The results of the CCK-8 experiments showed that the proliferation ability of HepG2 cells in the 2- μ M, 4- μ M and 8- μ M groups significantly decreased compared to the 0- μ M group (Fig. 1A). Compared with the 0- μ M group, the proliferation ability of HuH-6 cells was significantly attenuated at 4 μ M and 8 μ M, but not at 2 μ M (Fig. 1B). The proliferation of SMMC-7721 cells was moderated at 2 μ M, 4 μ M and 8 μ M, but not to a statistically significant extent (Fig. 1C). The proliferation of HKF cells was not altered by serabelisib treatment (Fig. 1D). The raw data and analysis are presented in Supplementary Table 1. Serabelisib had no effect on normal HKF cells. Based on these findings, we selected HepG2 and HuH-6 for subsequent experiments.

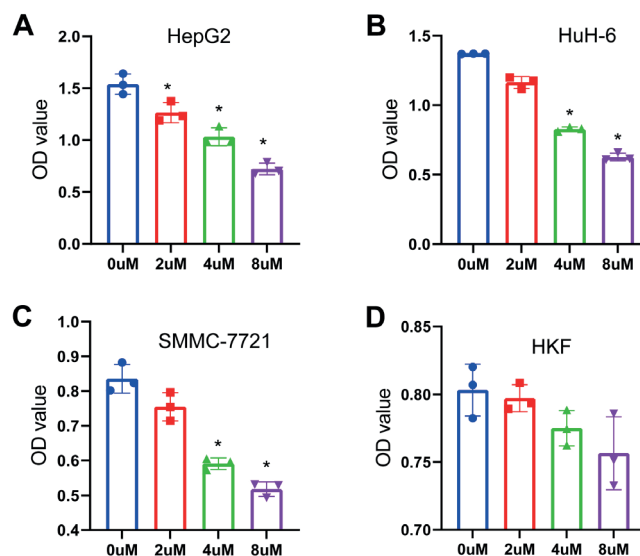


Fig. 1. Serabelisib interfered with the activity of different cells. A. The proliferation of HepG2 cells was detected with Cell Counting Kit-8 (CCK-8) assay 48 h after serabelisib treatment; B. The proliferation of HuH-6 cells was measured using CCK-8 assay 48 h after adding serabelisib; C. The proliferation of SMMC-7721 cells was measured with CCK-8 assay 48 h after adding serabelisib; D. The proliferation of human kidney fibroblasts (HKFs) was measured using CCK-8 assay 48 h after adding serabelisib. The measurement data are expressed as mean \pm standard deviation (M \pm SD). Data between multiple groups were analyzed with one-way analysis of variance (ANOVA) followed by Tukey's post hoc test ($n = 3$)

* $p < 0.05$ compared with the 0- μ M group; OD – optical density.

Serabelisib affected the PI3K/Akt/E-cadherin signaling pathway and pyroptosis

To further understand the effects of serabelisib on cells at the gene and protein levels, western blot was used to detect apoptosis and EMT-related factors in HepG2 and HuH-6 cells. Compared with the 0- μ M group, the intracellular expression levels of PI3K and p-AKT were significantly decreased in the 4- μ M and 8- μ M groups. After serabelisib intervention, the expression of Bcl-2 was decreased, while the expressions of cytochrome C, caspase-9 and caspase-3 were upregulated. Moreover, N-cadherin expression decreased, and E-cadherin expression increased in the drug intervention group, suggesting that serabelisib can affect the expression of apoptosis and EMT-related factors (Fig. 2A). We used immunofluorescence to analyze the fluorescence intensity of caspase-1 and GSDMD, and explore whether serabelisib affects pyroptosis-related factors. The results indicated that caspase-1 and GSDMD fluorescence intensity increased at 4 μ M and 8 μ M compared to the 0- μ M group (Fig. 2B). Western blot was used to detect the expression of pyroptosis-related proteins. The results showed increased pyroptosis-related expression of GSDMD, GSDMD-N, NLRP3, caspase-1, ASC, IL-1 β , and IL-18 (Fig. 2C). All data are presented in Supplementary Table 2.

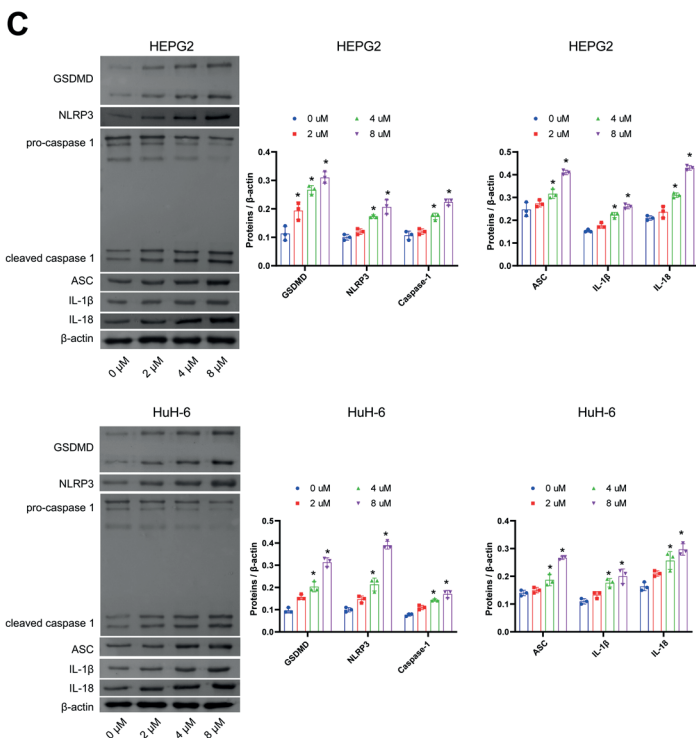
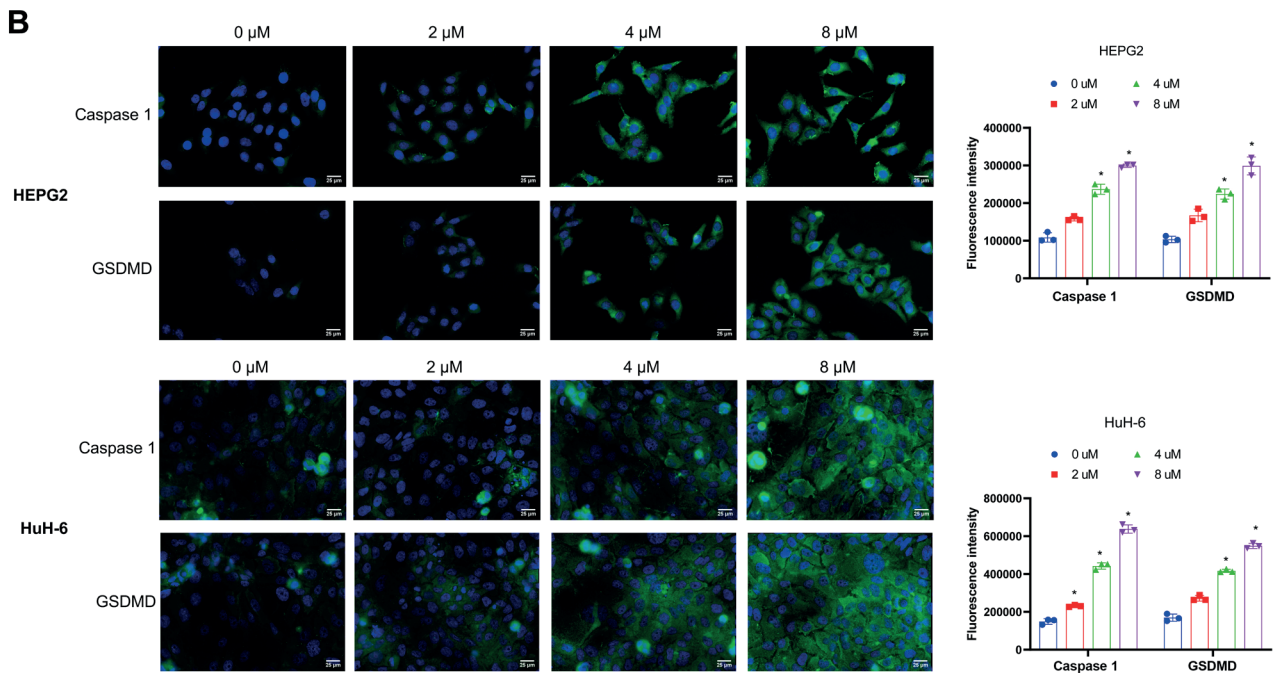
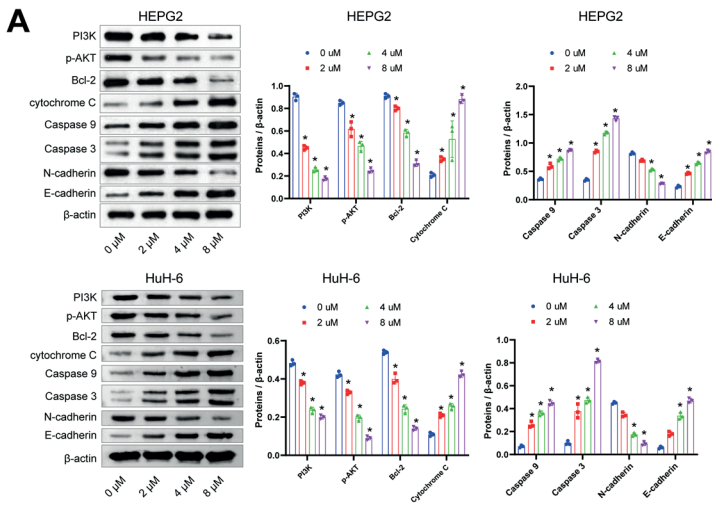


Fig. 2. Serabelisib inhibited pyroptosis of HepG2 and HuH-6 cells. **A.** The protein kinase B (AKT) signaling pathway was detected using western blot; **B.** The fluorescence intensity of caspase-1 and Gasdermin D (GSDMD) when treated with serabelisib; **C.** Western blot measurement of GSDMD, NLRP3, caspase-1, apoptosis-associated speck-like protein containing a CARD (ASC), interleukin (IL)-1β, and IL-18 protein levels. The data are expressed as mean ± standard deviation (M ± SD). Comparisons among multiple groups were analyzed using one-way analysis of variance (ANOVA) (n = 3)

*p < 0.05 compared with the 0-μM group.

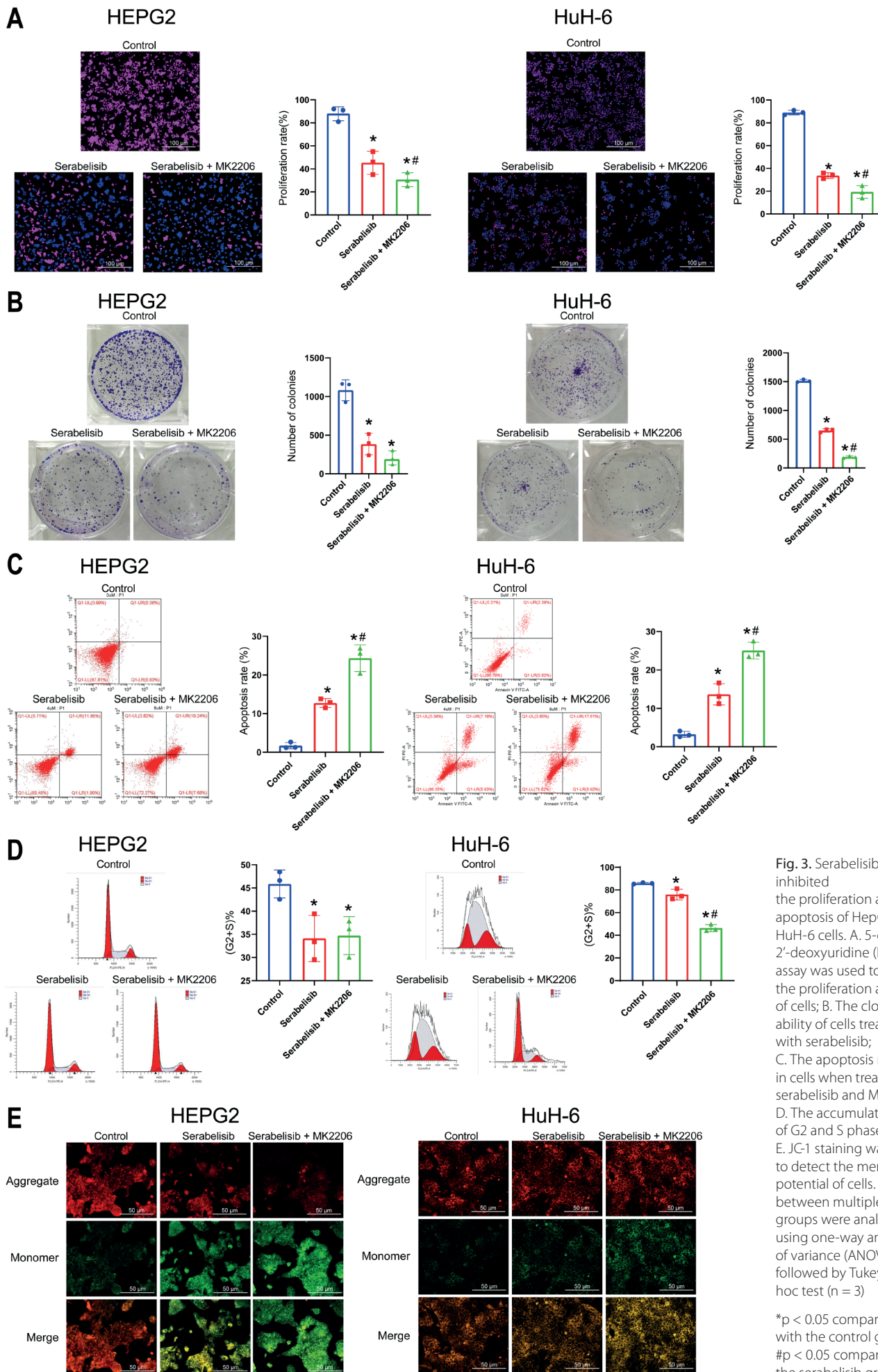


Fig. 3. Serabelisib inhibited the proliferation and apoptosis of HepG2 and HuH-6 cells. A. 5-ethynyl-2'-deoxyuridine (EdU) assay was used to assess the proliferation ability of cells; B. The cloning ability of cells treated with serabelisib; C. The apoptosis rate in cells when treated with serabelisib and MK2206; D. The accumulation of G2 and S phase cells; E. JC-1 staining was used to detect the membrane potential of cells. Data between multiple groups were analyzed using one-way analysis of variance (ANOVA) followed by Tukey's post hoc test ($n = 3$)

* $p < 0.05$ compared with the control group; # $p < 0.05$ compared with the serabelisib group.

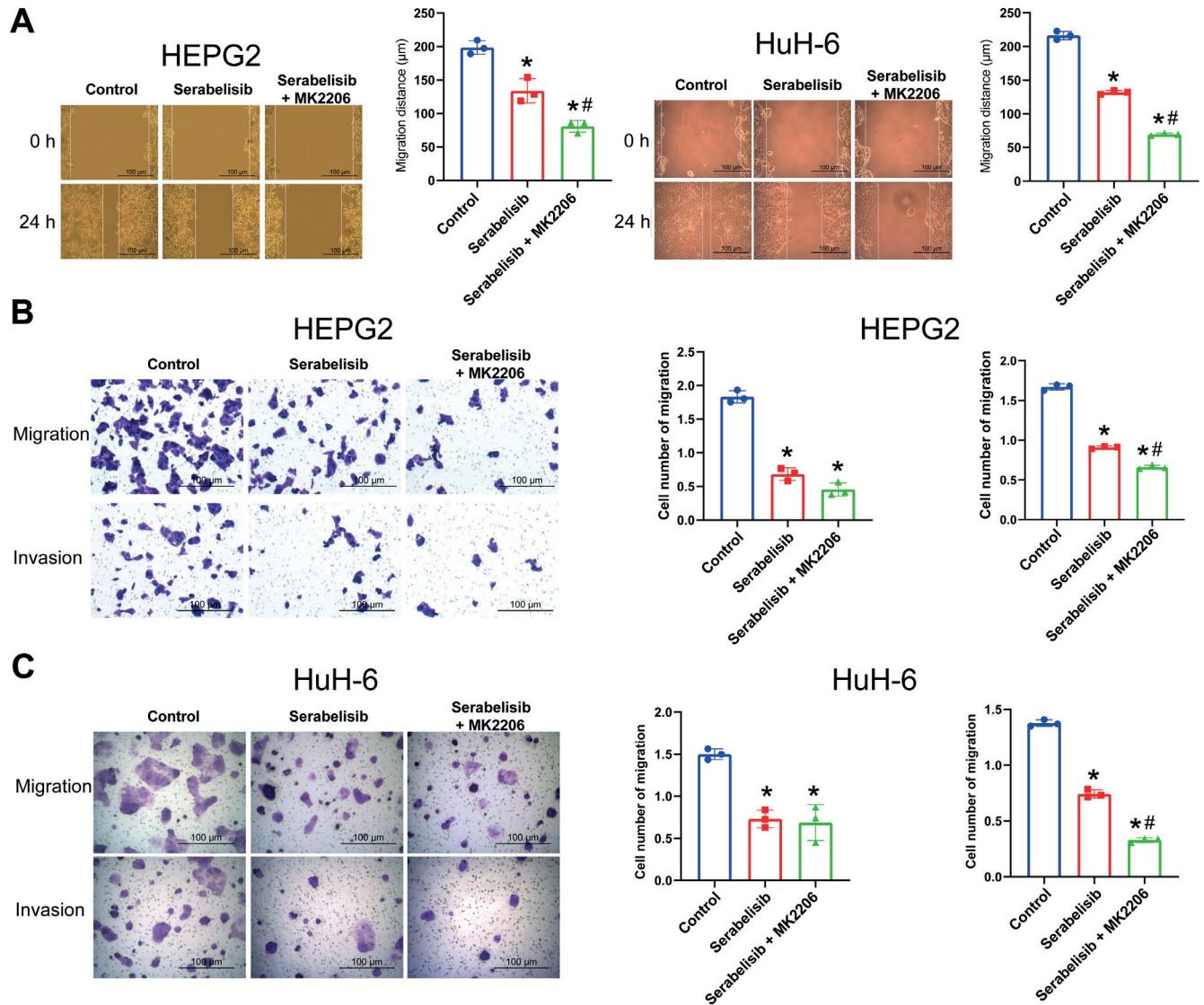


Fig. 4. Serabelisib inhibited HepG2 and HuH-6 migration and invasion. A. The migration of HepG2 and HuH-6 cells after serabelisib and MK2206 treatment; B,C. A transwell assay was used to measure the migration and invasion of HepG2 and HuH-6 cells. The measurement data are expressed as mean ± standard deviation (M ± SD). Data among multiple groups were analyzed with one-way analysis of variance (ANOVA) followed by Tukey’s post hoc test (n = 3)

*p < 0.05 compared with the control group; #p < 0.05 compared with the serabelisib group.

In short, serabelisib affected the PI3K/Akt/E-cadherin signaling pathway and pyroptosis-related protein expression.

Serabelisib affected the proliferation and apoptosis of HepG2 and HuH-6 cells through the PI3K/Akt/E-cadherin signaling pathway

We examined the effects of serabelisib on the proliferation and apoptosis of HepG2 and HuH-6 cells. Plate clone formation and EdU experiments showed that serabelisib reduced the number of cloned colonies and weakened proliferation ability. After adding the AKT signaling pathway

inhibitor MK2206, the colony-forming ability of cells was significantly reduced (Fig. 3A,B). To investigate whether serabelisib can promote apoptosis, flow cytometry examined apoptosis and cell cycle distribution. As shown in Fig. 3C,D, the proportion of apoptotic cells increased, and the proportion of cells in the G2 and S phases decreased after the treatment with serabelisib and MK2206 in HepG2 and HuH-6 cells. Furthermore, serabelisib and MK2206 gradually increased the number of apoptotic cells, and JC-1 changed from a red polymer to a green monomer (Fig. 3E). The data and results are presented in Supplementary Table 3. Briefly, serabelisib and MK2206 can promote apoptosis and inhibit the proliferation of HepG2 and HuH-6 cells.

Serabelisib affected the migration of HepG2 and HuH-6 cells through the PI3K/Akt/E-cadherin signaling pathway

Our findings indicated that serabelisib could affect the proliferation and apoptosis of liver cancer cells through the PI3K/Akt/E-cadherin signaling pathway. The scratch method was employed to explore whether serabelisib could alter HepG2 and HuH-6 migration. Compared with the control group, the horizontal migration ability of the cells in the serabelisib group was reduced, while the horizontal migration ability was significantly reduced in the serabelisib+MK2206 group compared to the serabelisib group (Fig. 4A).

Transwell assays assessed the ability of cells to invade and migrate vertically. As shown in Fig. 4B,C, the migratory and invasive abilities of the cells in the serabelisib group were significantly reduced compared with the control group. Moreover, serabelisib+MK2206 treated cells displayed less migration and invasion capacity than the cells in the serabelisib group. The raw data and results for Fig. 4 are presented in Supplementary Table 4. In summary, serabelisib inhibited migration and invasion of HepG2 and HuH-6 cells.

Serabelisib affected GSDMD-mediated pyroptosis in HepG2 and HuH-6 cells through the PI3K/Akt/E-cadherin signaling pathway

The results indicated that serabelisib affected liver cancer cell migration and invasion. We explored whether serabelisib could affect the pyroptosis of HepG2 and HuH-6 cells using immunofluorescence to detect the pyroptosis-related caspase-1 and GSDMD. Compared with the control group, the fluorescence intensity of caspase-1 and GSDMD increased in the serabelisib group, while the fluorescence intensity increased sharply in the serabelisib+MK2206 group compared to the serabelisib group. These findings indicate that PI3K/Akt/E-cadherin signaling axis inhibition by serabelisib could increase pyroptosis-related gene expression levels (Fig. 5A).

Western blot analysis of the pyroptosis-related pathway showed increased GSDMD, NLRP3, caspase-1, ASC, IL-1 β , and IL-18 protein levels in the serabelisib group compared to the control group. Furthermore, GSDMD, NLRP3, caspase-1, ASC, IL-1 β , and IL-18 significantly increased in the serabelisib+MK2206 group compared with the serabelisib group (Fig. 5B). All raw data and analysis are presented in Supplementary Table 5. The results indicate that PI3K/Akt/E-cadherin inhibition using serabelisib can promote pyroptosis-related gene expression in cells and trigger pyroptosis.

Discussion

Liver cancer originates from abnormal stem cells and hepatic epithelial progenitor cells,¹⁹ and is a malignant embryonic liver tumor commonly found in infants and young children, accounting for around 80% of pediatric liver cancer cases.¹⁹ Currently, liver cancer therapy includes adjuvant chemotherapy, hepatectomy and liver transplantation. Unfortunately, the survival rate is only 60% for high-risk patients.²⁰ Serabelisib is an effective oral selective PI3K α inhibitor currently being explored for clinical use in cancer treatment.²¹ In this study, serabelisib was tested in vitro to assess a range of cell functions. We found that serabelisib promoted apoptosis in a dose-dependent manner. To further explain its mechanism of action, we examined the cellular gene and protein levels.

The PI3K/AKT axis contributes to oncogenic transformation, and its possible mechanisms include stimulation of proliferation, metastasis, and the inhibition of autophagy and senescence.²² Apoptosis is a form of programmed cell death regulated by proteins of the Bcl-2 and caspase families,²³ with *Bcl-2* being an anti-apoptotic gene and an important target for cancer therapy.²⁴ The best biochemical marker recognized for early and late apoptosis detection is cysteine protease activation.²⁵ During apoptosis, caspase-3 acts as an executor and has an important proteolytic function, regulating the final stage of programmed cell death.²⁶ According to reports, lncRNA prostate cancer-associated transcript 1 (PCAT1) interacts with dyskerin pseudouridine synthase 1 to regulate proliferation, invasion and apoptosis in non-small cell lung cancer cells via the vascular endothelial growth factor (VEGF)/AKT/Bcl-2/caspase-9 pathway.²⁷ We found that serabelisib inhibited expression of PI3K, AKT and Bcl-2 in cells, while the expression of cytochrome C, caspase-9 and caspase-3 was elevated. In summary, serabelisib promotes HepG2 and HuH-6 apoptosis by inhibiting the PI3K/AKT signaling pathway.

Tumor metastasis and recurrence are key barriers to a complete liver cancer cure.²⁸ Epithelial–mesenchymal transition is necessary for promoting migration and invasion of tumor cells, and is often characterized by decreased epithelial E-cadherin and increased N-cadherin.^{29,30} The EMT of hepatocellular carcinoma (HCC) is considered crucial in intrahepatic dissemination and distal metastasis.³¹ During EMT, epithelial cells lose their polygonal shape and acquire a fusiform conformation, resulting in enhanced tumor cell motility and invasion abilities.³² In HCC, the protein arginine methyltransferase activates EMT by regulating the PI3K/AKT signaling pathway to promote HCC cell invasion and lung metastasis.³³ In this study, the results indicate that PI3K, p-AKT and E-cadherin expression levels in HepG2 and HuH-6 cells decreased after serabelisib intervention, while the expression of N-cadherin increased, and the effect was dose-dependent.

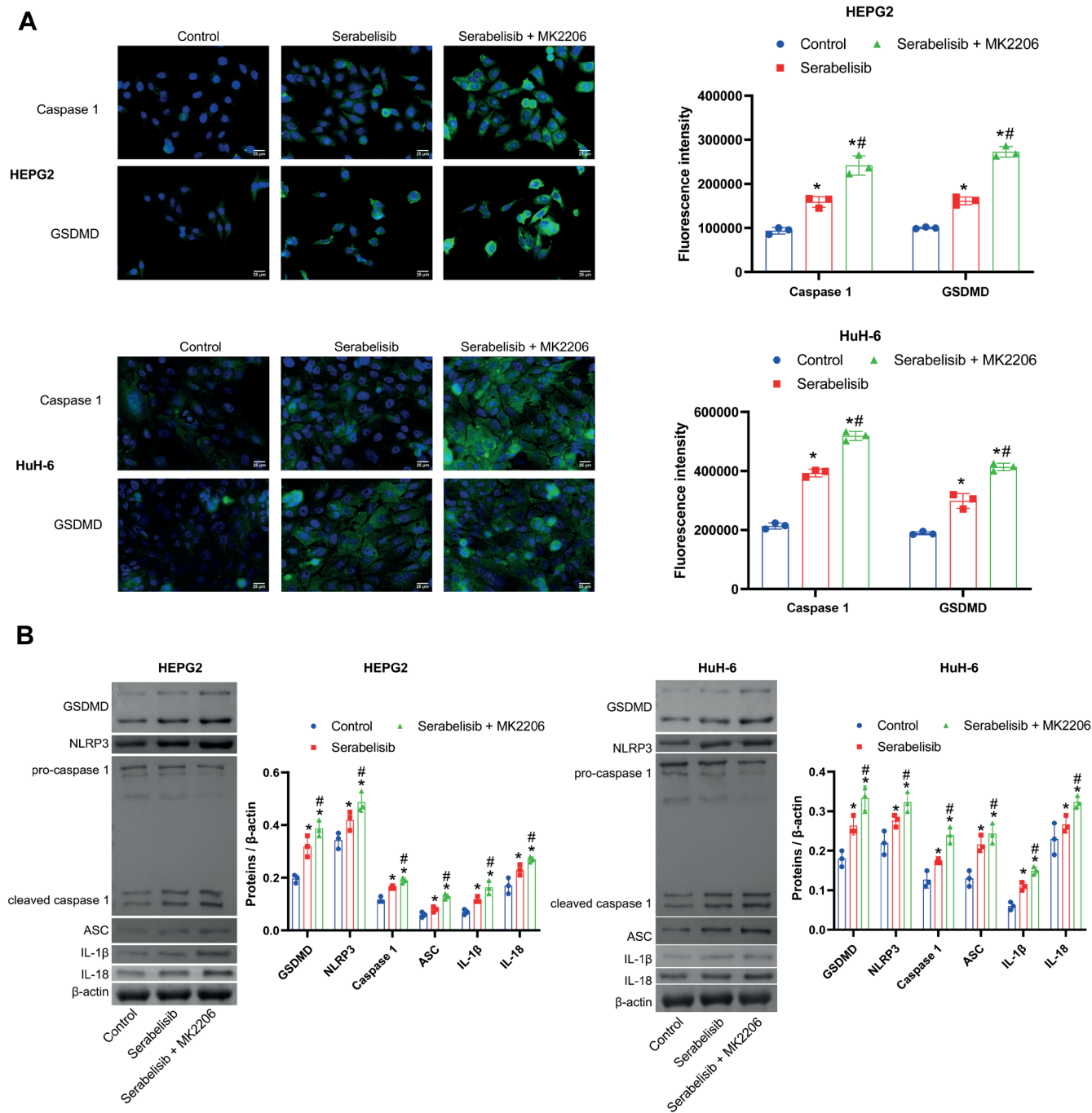


Fig. 5. Serabelisib promoted pyroptosis in HepG2 and HuH-6 cells. **A.** The fluorescence intensity of caspase-1 and Gasdermin D (GSDMD) was measured with immunofluorescence; **B.** The expression levels of pyroptosis-related genes. The data are expressed as mean ± standard deviation (M ±SD). Comparisons among multiple groups were analyzed using a one-way analysis of variance (ANOVA) (n = 3)

*p < 0.05 compared with the control group; #p < 0.05 compared with the serabelisib group; ASC – apoptosis-associated speck-like protein containing a CARD; IL – interleukin.

Limitations

Our future research will focus on investigating the effects of serabelisib on tissue growth in xenotransplantation tumor models. The current study demonstrated that serabelisib inhibited liver cancer development in a dose-dependent manner and explained its

molecular mechanisms, providing a theoretical basis for its formal application in the clinical treatment of liver cancer. However, this study only involved mouse models and did not include a wider population or clinical trials. Therefore, further research is needed to determine the potential and efficacy of serabelisib in treating liver cancer.

Conclusions

Serabelisib inhibited cell migration and invasion by blocking EMT through the PI3K/AKT signaling pathway. Remarkably, GSDMD, a major pyroptosis effector, was repressed by serabelisib. We believe that pyroptosis plays a vital role in liver cancer and is inhibited by serabelisib. Serabelisib inhibited apoptosis and pyroptosis at the gene and protein levels.

Supplementary data

The supplementary materials are available at <https://doi.org/10.5281/zenodo.7964600>. The package contains the following files:

Supplementary Table 1. Proliferation ability of HepG2, HuH-6, SMMC-7721, and HKF cells in the 2- μ M, 4- μ M and 8- μ M groups (for Fig. 1).

Supplementary Table 2. Expression of PI3K/Akt/E-cadherin signaling pathway and pyroptosis (for Fig. 2).


Supplementary Table 3. Proliferation and apoptosis of HepG2 and HuH-6 cells (for Fig. 3).

Supplementary Table 4. Migration of HepG2 and HuH-6 cells through the PI3K/Akt/E-cadherin signaling pathway (for Fig. 4).

Supplementary Table 5. Pyroptosis of GSDMD-mediated HepG2 and HuH-6 cells through the PI3K/Akt/E-cadherin signaling pathway (for Fig. 5).

ORCID iDs

Ming Li  <https://orcid.org/0009-0009-8169-6591>

Zhao Huang  <https://orcid.org/0009-0001-1934-2831>

Yuxiang Zhou  <https://orcid.org/0009-0004-7357-4192>

References

- Lim I, Bondoc A, Geller J, Tiao G. Hepatoblastoma: The evolution of biology, surgery, and transplantation. *Children (Basel)*. 2018;6(1):1. doi:10.3390/children6010001
- Ranganathan S, Lopez-Terrada D, Alaggio R. Hepatoblastoma and pediatric hepatocellular carcinoma: An update. *Pediatr Dev Pathol*. 2020;23(2):79–95. doi:10.1177/1093526619875228
- Yang T, Whitlock RS, Vasudevan SA. Surgical management of hepatoblastoma and recent advances. *Cancers (Basel)*. 2019;11(12):1944. doi:10.3390/cancers11121944
- Trobaugh-Lotrario AD, Meyers RL, O'Neill AF, Feusner JH. Unresectable hepatoblastoma: Current perspectives. *Hepat Med*. 2017;9:1–6. doi:10.2147/HMER.S89997
- Juric D, De Bono JS, LoRusso PM, et al. A first-in-human, phase I, dose-escalation study of TAK-117, a selective PI3K α isoform inhibitor, in patients with advanced solid malignancies. *Clin Cancer Res*. 2017;23(17):5015–5023. doi:10.1158/1078-0432.CCR-16-2888
- Bottino DC, Patel M, Kadakia E, et al. Dose optimization for anticancer drug combinations: Maximizing therapeutic index via clinical exposure-toxicity/preclinical exposure-efficacy modeling. *Clin Cancer Res*. 2019;25(22):6633–6643. doi:10.1158/1078-0432.CCR-18-3882
- Hernández-Prat A, Rodríguez-Vida A, Juanpere-Rodero N, et al. Novel oral mTORC1/2 inhibitor TAK-228 has synergistic antitumor effects when combined with paclitaxel or PI3K α inhibitor TAK-117 in pre-clinical bladder cancer models. *Mol Cancer Res*. 2019;17(9):1931–1944. doi:10.1158/1541-7786.MCR-18-0923
- Patel CG, Rangachari L, Patti M, Griffin C, Shou Y, Venkatakrishnan K. Characterizing the sources of pharmacokinetic variability for TAK-117 (Serabelisib), an investigational phosphoinositide 3-kinase α inhibitor: A clinical biopharmaceutics study to inform development strategy. *Clin Pharmacol Drug Dev*. 2019;8(5):637–646. doi:10.1002/cpdd.613
- Cui X, Liu X, Han Q, et al. DPEP1 is a direct target of miR-193a-5p and promotes hepatoblastoma progression by PI3K/Akt/mTOR pathway. *Cell Death Dis*. 2019;10(10):701. doi:10.1038/s41419-019-1943-0
- Hartmann W, Kuchler J, Koch A, et al. Activation of phosphatidylinositol-3'-kinase/AKT signaling is essential in hepatoblastoma survival. *Clin Cancer Res*. 2009;15(14):4538–4545. doi:10.1158/1078-0432.CCR-08-2878
- Zhao B, Hu T. JTC-801 inhibits the proliferation and metastasis of the Hep G2 hepatoblastoma cell line by regulating the phosphatidylinositol 3-kinase/protein kinase B signalling pathway. *Oncol Lett*. 2018;17(2):1939–1945. doi:10.3892/ol.2018.9780
- Xu W, Yang Z, Lu N. A new role for the PI3K/Akt signaling pathway in the epithelial–mesenchymal transition. *Cell Adh Migr*. 2015;9(4):317–324. doi:10.1080/19336918.2015.1016686
- Georgakopoulos-Soares I, Chartoumpakis DV, Kyriazopoulou V, Zaravinos A. EMT factors and metabolic pathways in cancer. *Front Oncol*. 2020;10:499. doi:10.3389/fonc.2020.00499
- Chen C, Liang Q, Chen H, et al. DRAM1 regulates the migration and invasion of hepatoblastoma cells via autophagy–EMT pathway. *Oncol Lett*. 2018;16(2):2427–2433. doi:10.3892/ol.2018.8937
- Zhang C, Lin T, Nie G, et al. Cadmium and molybdenum co-induce pyroptosis via ROS/PTEN/PI3K/AKT axis in duck renal tubular epithelial cells. *Environ Pollut*. 2021;272:116403. doi:10.1016/j.envpol.2020.116403
- Jia Y, Cui R, Wang C, et al. Metformin protects against intestinal ischemia–reperfusion injury and cell pyroptosis via TXNIP-NLRP3-GSDMD pathway. *Redox Biol*. 2020;32:101534. doi:10.1016/j.redox.2020.101534
- Xu S, Wang J, Zhong J, et al. CD73 alleviates GSDMD-mediated microglia pyroptosis in spinal cord injury through PI3K/AKT/Foxo1 signaling. *Clin Transl Med*. 2021;11(1):e269. doi:10.1002/ctm2.269
- Liu L, Wang J, Sun G, et al. m6A mRNA methylation regulates CTNNB1 to promote the proliferation of hepatoblastoma. *Mol Cancer*. 2019;18(1):188. doi:10.1186/s12943-019-1119-7
- Allan BJ, Parikh PP, Diaz S, Perez EA, Neville HL, Sola JE. Predictors of survival and incidence of hepatoblastoma in the paediatric population. *HPB (Oxford)*. 2013;15(10):741–746. doi:10.1111/hpb.12112
- Zhen N, Gu S, Ma J, et al. CircHMGCS1 promotes hepatoblastoma cell proliferation by regulating the IGF signaling pathway and glutaminolysis. *Theranostics*. 2019;9(3):900–919. doi:10.7150/thno.29515
- Jessen KA, Kessler L, Kucharski J, et al. Abstract 4501: INK117: A potent and orally efficacious PI3K α -selective inhibitor for the treatment of cancer. *Cancer Res*. 2011;71(8 Suppl):4501–4501. doi:10.1158/1538-7445.AM2011-4501
- Aoki M, Fujishita T. Oncogenic roles of the PI3K/AKT/mTOR axis. In: Hunter E, Bister K, eds. *Viruses, Genes, and Cancer*. Current Topics in Microbiology and Immunology. Vol. 407. Cham, Switzerland: Springer International Publishing; 2017:153–189. doi:10.1007/82_2017_6
- Brentnall M, Rodriguez-Menocal L, De Guevara RL, Cepero E, Boise LH. Caspase-9, caspase-3 and caspase-7 have distinct roles during intrinsic apoptosis. *BMC Cell Biol*. 2013;14(1):32. doi:10.1186/1471-2121-14-32
- Ebrahim AS, Sabbagh H, Liddane A, Raufi A, Kandouz M, Al-Katib A. Hematologic malignancies: Newer strategies to counter the BCL-2 protein. *J Cancer Res Clin Oncol*. 2016;142(9):2013–2022. doi:10.1007/s00432-016-2144-1
- Mazumder S, Plesca D, Almasan A. Caspase-3 activation is a critical determinant of genotoxic stress-induced apoptosis. In: Mor G, Alvero AB, eds. *Apoptosis and Cancer*. Totowa, USA: Humana Press; 2008:13–21. doi:10.1007/978-1-59745-339-4_2
- Nichani K, Li J, Suzuki M, Houston JP. Evaluation of caspase-3 activity during apoptosis with fluorescence lifetime-based cytometry measurements and phasor analyses. *Cytometry*. 2020;97(12):1265–1275. doi:10.1002/cyto.a.24207
- Liu SY, Zhao ZY, Qiao Z, Li SM, Zhang WN. LncRNA PCAT1 interacts with DKC1 to regulate proliferation, invasion and apoptosis in NSCLC cells via the VEGF/AKT/Bcl2/caspase-9 pathway. *Cell Transplant*. 2021;30:096368972098607. doi:10.1177/0963689720986071

28. Lu C, Xiangdong T, Wenchen G, et al. Periostin mediates epithelial–mesenchymal transition through the MAPK/ERK pathway in hepatoblastoma. *Cancer Biol Med*. 2019;16(1):89. doi:10.20892/j.issn.2095-3941.2018.0077
29. Fu X, Cui P, Chen F, et al. Thymosin β 4 promotes hepatoblastoma metastasis via the induction of epithelial–mesenchymal transition. *Mol Med Rep*. 2015;12(1):127–132. doi:10.3892/mmr.2015.3359
30. Xie X, Zhu H, Zhang J, et al. Solamargine inhibits the migration and invasion of HepG2 cells by blocking epithelial-to-mesenchymal transition. *Oncol Lett*. 2017;14(1):447–452. doi:10.3892/ol.2017.6147
31. Zucchini-Pascal N, Peyre L, Rahmani R. Crosstalk between beta-catenin and Snail in the induction of epithelial to mesenchymal transition in hepatocarcinoma: Role of the ERK1/2 pathway. *Int J Mol Sci*. 2013;14(10):20768–20792. doi:10.3390/ijms141020768
32. Pastushenko I, Blanpain C. EMT transition states during tumor progression and metastasis. *Trends Cell Biol*. 2019;29(3):212–226. doi:10.1016/j.tcb.2018.12.001
33. Jiang H, Zhou Z, Jin S, et al. PRMT 9 promotes hepatocellular carcinoma invasion and metastasis via activating PI 3K/Akt/GSK-3 β /Snail signaling. *Cancer Sci*. 2018;109(5):1414–1427. doi:10.1111/cas.13598

Use of salusin β for predicting atherosclerosis and components of the metabolic syndrome

Aleksandra Janecka^{1,2,A–D}, Joanna Stefanowicz^{1,2,3,A–C,E,F}

¹ Department of Paediatrics, Haematology and Oncology, Faculty of Medicine, Medical University of Gdansk, Poland

² Department of Paediatrics, Haematology and Oncology, University Clinical Centre, Gdańsk, Poland

³ Faculty of Health Sciences with Institute of Maritime and Tropical Medicine, Medical University of Gdansk, Poland

A – research concept and design; B – collection and/or assembly of data; C – data analysis and interpretation;

D – writing the article; E – critical revision of the article; F – final approval of the article

Advances in Clinical and Experimental Medicine, ISSN 1899–5276 (print), ISSN 2451–2680 (online)

Adv Clin Exp Med. 2024;33(2):183–192

Address for correspondence

Joanna Stefanowicz

E-mail: jstefanowicz@gumed.edu.pl

Funding sources

None declared

Conflict of interest

None declared

Received on August 12, 2022

Reviewed on May 8, 2023

Accepted on May 26, 2023

Published online on June 30, 2023

Abstract

Salusin β is a bioactive peptide, detectable in many tissues and body fluids, first identified nearly 20 years ago. Since then, many studies have been performed to define the role of salusin β , concentrating on its role in atherosclerosis and conditions leading to vascular injury such as hypertension, diabetes and hyperlipidemia, in which salusin β seems to play a proatherogenic role. Previous literature has evaluated salusin as a predictor of atherosclerosis. Herein, we performed online research using 5 databases, namely PubMed, Ovid, Web of Science, Scopus, and Cochrane Library. Inclusion criteria were articles published in the years 2017–2022, concerning the association between salusin β and obesity, atherosclerosis, hypertension, and hyperglycemia. The aim of the review was to provide comprehensive data regarding the latest studies in this area. The latest research confirms that salusin β plays an important role in the development of vascular remodeling, inflammation, hypertension, and atherosclerosis. Additionally, the peptide is associated with hyperglycemia and lipid disorders, and its widespread activity makes it a potential therapeutic target. However, there is a need for additional studies to confirm the potential role of salusin β as a novel target for treatment. Many of the reports were performed in animal models, while research conducted in humans was generally based on small groups of patients and not always compared with healthy controls; studies enrolling children are rare.

Key words: salusin β , atherosclerosis, hypertension, obesity, type 2 diabetes mellitus

Cite as

Janecka A, Stefanowicz J. Use of salusin β for predicting atherosclerosis and components of the metabolic syndrome.

Adv Clin Exp Med. 2024;33(2):183–192.

doi:10.17219/acem/166535

DOI

10.17219/acem/166535

Copyright

Copyright by Author(s)

This is an article distributed under the terms of the Creative Commons Attribution 3.0 Unported (CC BY 3.0)

(<https://creativecommons.org/licenses/by/3.0/>)

Introduction

Salusins are endogenous bioactive peptides first identified by Shichiri et al. in 2003. Salusin α consists of 28 amino acids, and salusin β consists of 20 amino acids. Both peptides are translated from alternative splicing of mRNA from the target of rapamycin 2A (*TOR2A*) gene. Preprosalusin mRNA is ubiquitously expressed and found in many tissues and organs, such as the nervous system, endothelium, muscles, liver, lungs, kidneys, bone marrow, lymph nodes, spleen, thymus, adrenal glands, small intestine, stomach, salivary glands, and testes, and in fluids, such as plasma and urine.¹

It was discovered that when salusins were intravenously administered to rats, they affected cardiac function, causing both rapid bradycardia and hypotension.² However, endogenous salusins play important roles in the development of atherosclerosis and foam cell formation by influencing cholesteryl ester accumulation and acetyl-CoA acetyltransferase 1 (ACAT-1) protein expression.³

Salusin α shows anti-atherogenic effects, as it reduces atherosclerotic plaques, and its expression is decreased in patients with hypertension and lipid disorders.^{4,5} Conversely, salusin β plays a proatherogenic role. The available literature has evaluated salusin α and β as predictors for atherosclerosis, and salusin β seems to be a better indicator of atherosclerosis development than salusin α .⁴

Salusin β has been shown to increase nicotinamide adenine dinucleotide phosphate (NAD(P)H) oxidase activity and reactive oxygen species (ROS) production in cells. It activates the release of inflammatory cytokines, such as interleukin (IL)-1 β , IL-6 and tumor necrosis factor alpha (TNF- α).^{5,6} Inflammation stimulates vascular smooth

muscle cell (VSMC) proliferation and atherosclerotic lesion formation. Furthermore, high glucose levels seem to induce the production of salusin β ,⁷ and increased salusin β expression is observed in conditions that are components of the metabolic syndrome, such as obesity, hypertension, diabetes mellitus (DM)/hyperglycemia, and lipid disorders.

Objectives

The aim of this review was to confirm the hypothesis that salusin β is a good predictor of atherosclerosis and components of the metabolic syndrome, and to provide comprehensive information about the latest studies in this area.

Materials and methods

The research was performed using 5 online databases, namely PubMed, Ovid, Web of Science, Scopus, and Cochrane Library. Only articles published in the years 2017–2022 and those concerning the association between salusin β and atherosclerosis, hypertension, obesity, hyperlipidemia, and hyperglycemia/DM were selected. Only original papers were included, with 33 articles meeting the inclusion criteria. Data were double-checked independently by 2 authors. The process of selection comprised the removal of duplicates, and the elimination by title, abstract and full-text review, following Preferred Reporting Items for Systematic Reviews and Meta-Analyses (PRISMA) guidelines. The selection process is presented in Fig. 1.

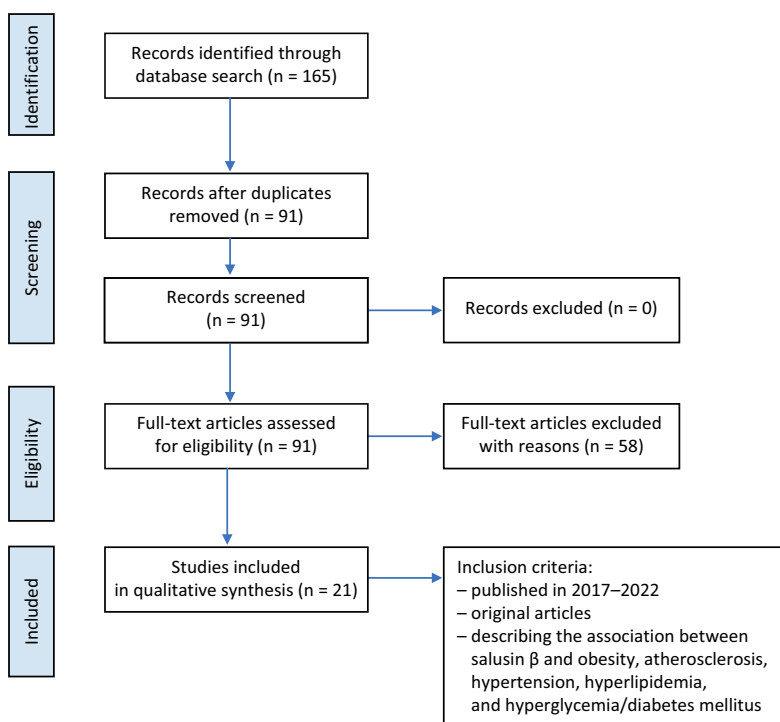


Fig. 1. Study selection process

Results

Contrary to salusin α , the expression of salusin β is increased in patients with atherosclerosis, hypertension and metabolic syndrome. Increased levels of salusin β are observed in patients with cardiovascular disease (CVD) and cerebrovascular disease. Endogenous expression of salusin β is the lowest in the morning. Furthermore, the stimulation of the parasympathetic nervous system and insulin secretion decreases the level of free salusin β .⁸ In the central nervous system, salusin β stimulates or depresses sympathetic and vagal activity depending on the location within the brain. It reduces blood pressure and heart rate in the intermediate dorsal motor nucleus of the vagus.⁶

Salusin β has been shown to stimulate the proliferation of VSMCs and fibroblasts through the activation of immediate response genes such as *c-Myc* and *Fos* in rats and humans. It also activates the release of inflammatory cytokines, including IL-1 β , IL-6 and TNF- α . Consequently, oxidative stress markers increase and monocyte-endothelial adhesion is promoted.⁹ This occurs within lesions of the blood vessel endothelium and in atherosclerosis.

Atherosclerosis

Salusin β is a pro-inflammatory agent. Human umbilical vein endothelial cells (HUVECs) incubated in salusin β increased the production of mRNA and protein levels of IL-6, IL-8, IL-18, and reduced the level of IL-1Ra.¹⁰ Furthermore, salusin β has an influence on the formation of macrophage foam cells. The peptide promotes the growth of atherosclerotic plaques and stimulates the adhesion of monocytes to the endothelium. Salusin β boosts the production of ACAT-1, the enzyme that breaks down fatty acids into acetyl coenzyme A in human monocytes/macrophages. In addition, salusin β encourages the storage of lipid droplets, increases the intracellular cholesterol content and stimulates monocyte adhesion. The proatherogenic role of the peptide was shown by silencing salusin β . The knock-down of the peptide improved cardiac function and cardiovascular remodeling in myocardial infarction-induced heart failure in rats and alleviated cardiac inflammation in diabetic rats.^{2,9}

The relationship between salusin β and atherosclerosis was also confirmed among patients suffering from coronary artery disease (CAD). A study by Awad et al. compared patients undergoing transcatheter therapy, and found that salusin β levels were significantly higher in patients with CVD before therapy compared to healthy controls. Moreover, after therapy, salusin β expression was significantly lower than before the intervention, or when compared to the control group. In addition, patients and controls varied in fasting blood glucose levels, insulin levels, body mass index (BMI), systolic blood pressure (SBP), and lipid profile.¹¹ Salusin β levels were significantly lower in patients with stenosis or dilatation in coronary angiography

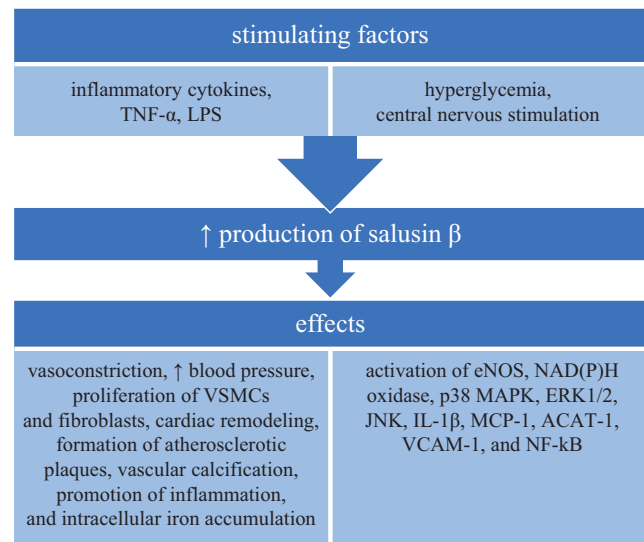


Fig. 2. The role of salusin β in the pathogenesis of atherosclerosis

TNF- α – tumor necrosis factor alpha; LPS – lipopolysaccharides; VSMCs – vascular smooth muscle cells; eNOS – endothelial nitric oxide synthase; NAD(P)H – nicotinamide adenine dinucleotide phosphate; IL – interleukin; ACAT-1 – acetyl-coenzyme A acetyltransferase 1; VCAM-1 – vascular cell adhesion molecule-1; NF- κ B – nuclear factor kappa B.

than in healthy volunteers.^{12,13} A similar finding was observed in patients with slow coronary flow that seemed to be caused by microvascular atherosclerosis.¹⁴

Risk factors of atherosclerosis are similar to abdominal aortic aneurysm (AAA). However, an evaluation of 48 patients with AAA revealed lower salusin β levels compared to 47 healthy controls. The levels of salusin β were also negatively correlated with abdominal aortic diameter.¹⁵ The role of salusin β in the pathogenesis of atherosclerosis is presented in Fig. 2.

Diabetes mellitus

Many studies have confirmed that the serum level of salusin β is increased in DM. High glucose not only increases the level of salusin β mRNA but also upregulates its production by stimulating prosalusin protein expression. In cell culture experiments, the exposure of HUVECs to high glucose reduced proliferation and migration, and the knockdown of salusin β reversed these abilities. Adenosine monophosphate-activated protein kinase (AMPK) participates in the signaling pathway of salusin β .⁷ Parallel overexpression of salusin β in proximal tubular (HK-2) cells from both human and mouse models as well as human retinal capillary endothelial cells incubated in high glucose induced inflammatory cytokines and oxidative stress. In human research, inflammation and apoptosis are activated by ROS-dependent signaling pathways.^{16–19}

In the study performed by Argun et al., the group of patients suffering from type 2 diabetes mellitus (T2DM) had significantly higher levels of salusin β , but only when their

hemoglobin A1C (HbA1C) level was higher than 9%.²⁰ Deyekh et al. also confirmed higher serum salusin β levels in patients with T2DM compared to those with prediabetes or healthy controls, while there was no significant difference in salusin β levels between the prediabetes and control groups. Although each group consisted of 30 persons, a detailed description was not provided.²¹ Additionally, Aldulimya and Alaaraji revealed higher levels of salusin β in women with T2DM than in healthy volunteers, and the levels of salusin β correlated with fasting serum glucose. However, a limitation of this study was the significant difference in age between the examined groups.²² In a study by Wang et al., the level of salusin β was higher in patients with diabetic retinopathy than in healthy controls.¹⁶ Moreover, Yassien et al. revealed a correlation between the mean carotid intima-media thickness and left ventricular hypertrophy.²³ These conclusions suggest that salusin β participates in the development of complications associated with chronic hyperglycemia.

Sipahi et al. reported that the serum levels of salusin β were elevated in patients undergoing hemodialysis compared to healthy controls.²⁴ In patients also suffering from DM, the salusin β /salusin α ratio was higher, and the levels of salusin α were significantly lower. However, there was no evidence of a correlation between salusin β and diabetes in this group of patients.

An opposite outcome was observed in a study performed among diabetic patients with and without diabetic foot.²⁵ Interestingly, among healthy volunteers, salusin β levels were significantly higher than in diabetic patients. Moreover, salusin α was significantly higher in healthy controls, which raises doubts regarding the methodology of the study.

Hypertension

Salusin β is elevated in patients with hypertension, inducing VSMC proliferation and fibrosis within the vascular wall. Moreover, it activates intimal hyperplasia after vascular injury and can trigger vascular constriction. This occurs via the activation of endothelial nitric oxide synthase (eNOS), the release of nitric oxide (NO) and an increase in NAD(P)H oxidase activity. Acute intravenous administration of salusin β increased the mean arterial pressure in spontaneously hypertensive rats (SHRs), while injections of anti-salusin β IgG reduced the mean blood pressure and heart rate. The important role of salusin β in the development of hypertension and the subsequent vascular remodeling was verified by salusin β knockdown, after which the vascular function was augmented in hypertensive rats.^{26–28}

Contrary to patients that normally present with physiological night-time blood pressure reduction, those with newly diagnosed non-dipper hypertension demonstrate elevated levels of salusin β . In addition, salusin β positively correlates with the left ventricle mass index and negatively correlates with diastolic parameters of the left ventricle.

These results were not compared with healthy controls, which is a limitation of the study.²⁹

The interaction between salusin β and hypertension was confirmed in a study performed in patients treated with anti-hypertensive medicines.³⁰ The therapy consisting of felodipine and enalapril was more effective and brought a more relevant reduction of salusin β level than felodipine alone. This is the first study that demonstrated practically this piece of theoretical knowledge.

The correlation between the level of salusin β and hypertension has been confirmed in both adults and children. The study by Kołakowska et al. performed in adolescents revealed that the serum level was significantly higher in patients with essential hypertension when compared to those with white coat hypertension.³¹

Finally, salusin β has an influence on the consequences of hypertension. Ageing SHRs have higher concentrations of the peptide in the hypothalamic paraventricular nucleus, myocardium and mesenteric artery. The knock-down of salusin β improved cardiac function and reduced the levels of p38 MAPK, ERK1/2, JNK, and NAD(P)H, which are likely to be involved in the signaling pathway.³² Furthermore, the level of this peptide is significantly increased in the calcified VSMCs of rats. The calcification has been shown to stimulate the expression of salusin β , and the overexpression of salusin β has been shown to promote spontaneous calcification. This process is probably mediated by ROS and NAD(P)H oxidase. Furthermore, the overexpression of salusin β decreases the levels of Klotho, which is an anti-inflammatory and anti-oxidative stress protein.³³

Obesity/lipid disorders

Previous studies revealed that obesity is another condition that leads to increased serum salusin β levels. In patients with T2DM, salusin β correlated with both BMI and waist circumference, and was significantly higher than in healthy controls.²³ The correlation between salusin β and BMI was also revealed in patients suffering from CVD.¹¹

However, research performed on a group of 75 obese children aged 6–18 years did not confirm this theory.³⁴ No correlation was found between salusin β and BMI, blood pressure, carotid intima-media thickness, and epicardial adipose tissue thickness. There was a negative correlation between salusin α and diastolic blood pressure (DBP). Additionally, in a group of 48 children with Down syndrome, the connection between salusin β and excessive body weight (obesity and overweight) was not proved.³⁵ Nevertheless, physical training decreases the level of serum salusin β in patients with high body weight.

In this regard, moderate- and high-intensity interval training (HIIT) were compared between obese and overweight women. It was revealed that both types of training improved lipid parameters and decreased serum salusin β levels.³⁶

Similar studies were performed among obese or overweight males with a mean age of 11 years. The levels

of salusin β were reduced after 12 weeks of training, with HIIT demonstrating more significant results than aerobic training. Apart from salusin β and α , other parameters also

improved, such as the lipid profile and markers of inflammation.^{37,38} A summary of the studies on salusin β used in this review is included in Table 1.

Table 1. Summary of the studies on salusin β included in the review

No.	Author, year of publication	Title	Subject	Results	Conclusions
Atherosclerosis					
1.	Esfahani et al. (2018) ¹⁰	The effect of salusin- β on expression of pro- and anti-inflammatory cytokines in human umbilical vein endothelial cells	HUVECs	Incubation in salusin β stimulates the production of mRNA and proteins of IL-6, IL-8 and IL-18, and suppresses the production of IL-1Ra.	Salusin β is a proinflammatory agent.
2.	Sipahi et al. (2019) ²⁴	Relationship of salusin-alpha and salusin-beta levels with atherosclerosis in patients undergoing haemodialysis	180 adult patients, 90 healthy controls	The levels of salusin β are higher in patients undergoing hemodialysis. There is a positive correlation between the duration of hemodialysis and salusin β levels. There is no correlation between salusin β and pulse wave analysis. Among patients without DM, the salusin α /salusin β ratio was significantly lower than in the patients also suffering from DM.	Patients undergoing hemodialysis had increased levels of salusin β and an increased salusin α /salusin β ratio.
3.	Wang et al. (2020) ⁴	Salusin- β is superior to salusin- α as a marker for evaluating coronary atherosclerosis	256 patients, 37 healthy controls	Both salusin α and β have substantial impact on SYNTAX scores, but the effect of salusin β is more significant.	There is a connection between salusins and coronary artery injury. Salusin β is superior to salusin α .
4.	Awad et al. (2020) ¹¹	Assessment of serum levels of salusin α and salusin β in cardiovascular disease patients undergoing transcatheter therapy	30 patients with CVD and 30 healthy controls	Before therapy, salusin β levels in patients with CVD are significantly higher than in healthy controls. After therapy, salusin β levels in patients are significantly lower than in the control group and before therapy. The group of CVD patients has higher fasting blood glucose, insulin levels, BMI, SBP, and lipid levels than the control group.	Serum salusin β levels are higher in patients with CVD and decrease after transcatheter therapy.
5.	Xu et al. (2021) ²	Knockdown of salusin- β improves cardiovascular function in myocardial infarction-induced chronic heart failure rats	rats	Knockdown of salusin β increases hemodynamic parameters, lumen diameter of arteries, microvascular density in infarcted area, and decreases the media thickness of arteries, expression of eNOS, ROS and NAD(P)H oxidase, as well as plasma levels of leptin and visfatin.	Salusin β influences endothelial dysfunction, cardiovascular remodeling and cardiac dysfunction in chronic heart failure.
6.	Arkan et al. (2021) ¹³	The importance of circulating levels of salusin- α , salusin- β , and heregulin- β 1 in atherosclerotic coronary arterial disease	113 patients, 55 healthy controls	Serum salusin β levels are lower in patients with CAD than in controls; heregulin- β 1 and hsCRP were significantly different among examined groups.	Salusin β seems to be one of the biomarkers of atherosclerosis.
7.	Akyüz et al. (2019) ¹⁴	Relationship of serum salusin beta levels with coronary slow flow	39 patients, 42 healthy controls	Salusin β is a predictor of CSF.	Salusin β seems to play an important role in the development of CSF.
8.	Yildirim and Kucukosmanoglu (2021) ¹²	Relationship between serum salusin beta levels and coronary artery ectasia	71 patients with CAE and 72 healthy subjects	Mean SBP and DBP values are significantly higher in the CAE group than in the control group, and the mean LVEF is significantly lower. The serum salusin β levels are significantly higher in the CAE group compared to the control group.	Serum salusin β levels are increased in patients with CAE.
9.	Karagöz et al. (2022) ¹⁵	A new insight into pathophysiological mechanism of abdominal aortic aneurysm with novel parameters salusin- β and arterial stiffness	48 patients with AAA and 47 healthy controls	Salusin β levels are significantly lower in patients with AAA. There is a significant negative correlation between salusin β levels and abdominal aorta diameter.	The pathophysiological mechanism of AAA is unclear.

Table 1. Summary of the studies on salusin β included in the review – cont.

No.	Author, year of publication	Title	Subject	Results	Conclusions
Diabetes mellitus					
10.	Sun et al. (2017) ¹⁹	Salusin- β is involved in diabetes mellitus-induced endothelial dysfunction via degradation of peroxisome proliferator-activated receptor gamma	mice	High glucose upregulates the expression of salusin β . Salusin β blockade prevents the overproduction of ROS and inflammatory molecules that are regulated by PPAR γ .	Salusin β takes part in endothelial dysfunction in DM.
11.	Zhao et al. (2017) ⁹	Salusin- β contributes to oxidative stress and inflammation in diabetic cardiomyopathy	rats	Salusin β increases the expression of inflammatory cytokines; high glucose increases the levels of salusin β and prosalusin; knockdown of salusin β reduces the expression of inflammatory cytokines and oxidative stress in cardiomyocytes and left ventricle function, and fails to reduce glucose levels and insulin resistance.	Salusin β induces cardiac inflammation in DM. The knockdown of salusin β improves cardiac function in DM.
12.	Zhu et al. (2017) ⁷	Salusin- β mediates high glucose-induced endothelial injury via disruption of AMPK signaling pathway	HUVECs	HUVECs exposed to high glucose present with the inhibition of proliferation, migration, angiogenesis, as well as retarded cell cycle. The knockdown of salusin β reverses the changes via the AMPK signaling pathway.	Salusin β contributes to endothelial dysfunction, which is related to high glucose by inactivating the AMPK signaling pathway.
13.	Sun et al. (2019) ³³	Salusin- β promotes vascular calcification via nicotinamide adenine dinucleotide phosphate/ reactive oxygen species-mediated klotho downregulation	VSMCs of rats	The levels of salusin β are increased by calcification; the overexpression of salusin β induces calcification and the spontaneous conversion of VSMCs, decreases Klotho protein levels, and increases the expression of oxidative stress molecules.	Salusin β plays an important role in vascular calcification.
14.	Yassien et al. (2020) ²³	Serum salusin- β in relation to atherosclerosis and ventricular dysfunction in patients with T2DM	60 patients, 25 healthy controls	Serum levels of salusin β are higher in patients with DM and positively correlate with obesity, the insulin resistance index, dyslipidemia, carotid intima-media thickness, and left ventricular hypertrophy, and negatively correlate with left ventricular function.	Salusin β levels correlate with left ventricular dysfunction and atherosclerosis in DM.
15.	Deyekh et al. (2020) ²¹	Evaluation of salusin β in patients with prediabetes and T2DM	30 patients with prediabetes, 30 patients with T2DM, 30 healthy volunteers	Serum salusin β levels in patients with T2DM are significantly higher than in the prediabetes group and healthy subjects. There is no significant difference in salusin β levels between prediabetes group and healthy control subjects.	Serum salusin β is increased in T2DM.
16.	Argun et al. (2021) ²⁰	Evaluation of salusin- α and salusin- β levels in patients with T2DM and determination of the impact of severity of hyperglycemia on salusin levels	55 patients, 35 healthy controls	Salusin β positively correlates with fasting glucose and HbA1c levels. The group with HbA1c > 9% has significantly higher levels of salusin β than the group with HbA1c < 9%.	Salusin β levels are higher in patients with DM than in healthy controls and the changes are more significant in those with worse glycemic control.
17.	Wang et al. (2021) ¹⁸	Salusin- β participates in high glucose-induced HK-2 cell ferroptosis in a Nrf-2-dependent manner	human proximal tubular (HK-2) cells	The overexpression of salusin β exacerbates the iron overload triggered by high glucose and the production of ROS and lipid peroxidation. The knockdown of salusin β reverses these effects.	The positive correlation between salusin β and ferroptosis promotes injury of renal tubular cells in DM.
18.	Wang et al. (2021) ¹⁶	Salusin- β mediates high glucose-induced inflammation and apoptosis in retinal capillary endothelial cells via a ROS-dependent pathway in diabetic retinopathy	60 patients, 20 healthy controls	Salusin β levels are higher in patients with DM and significantly higher in patients with diabetic retinopathy, both proliferative and nonproliferative. High glucose increases the levels of salusin β in HRECs. Salusin β increases inflammatory molecules, apoptosis and ROS production; the knockdown of salusin β has the opposite effects.	Salusin β induces inflammation and apoptosis via a ROS-dependent signaling pathway.

Table 1. Summary of the studies on salusin β included in the review – cont.

No.	Author, year of publication	Title	Subject	Results	Conclusions
19.	Chen and Jin (2021) ¹⁷	Downregulation of salusin- β protects renal tubular epithelial cells against high glucose-induced inflammation, oxidative stress, apoptosis and lipid accumulation via suppressing miR-155-5p	mice	Salusin β silencing increases inflammatory factors and oxidative stress, suppresses apoptosis and lipid accumulation in high glucose-induced cells, and reduces the expression of miR-155-5p.	The downregulation of salusin β protects cells against inflammation, oxidative stress, apoptosis, and excessive lipid accumulation that is induced by high glucose.
20.	Sağmak Tartar et al. (2021) ²⁵	Association between dermcidin, salusin- α , salusin- β molecules and diabetic foot infections	40 diabetic patients without DFI, 50 patients with DFI, 40 healthy controls	Salusin β levels were significantly higher in controls than in patients with diabetes. Salusin β levels were higher in DFI than in diabetes without DFI; the difference was not statistically significant. There was a significant difference in dermcidin levels between both groups of patients and between DFI and controls.	Dermcidin seems to be associated with DFI.
21.	Aldulimya and Alaaraji (2021) ²²	Study the association of β -salusin with some anthropometric measurements in Iraqi type II diabetics women	60 women with T2DM and 24 healthy women	β -salusin levels are higher in the patients with T2DM than in healthy controls.	Salusin β level increases in T2DM.
Hypertension					
22.	Ren et al. (2017) ²⁸	Silencing salusin- β attenuates cardiovascular remodeling and hypertension in spontaneously hypertensive rats	rats	Silencing salusin β reduced left ventricular weight, cardiomyocyte hypertrophy, plasma norepinephrine and tyrosine hydroxylase levels, plasma angiotensin II levels, the expression of type 1 receptors of angiotensin in myocardium and mesenteric artery, and prevented media thickness in the arteries of hypertensive rats.	Increased salusin β contributes to the pathogenesis of hypertension and cardiovascular remodeling.
23.	Kolakowska et al. (2018) ³¹	Correlation of salusin beta with hs-CRP and ADMA in hypertensive children and adolescents	58 children with essential hypertension, 30 children with white coat hypertension	Salusin β levels are significantly higher in patients with hypertension and positively correlate with the levels of hs-CRP and ADMA.	Salusin β correlates with hs-CRP and ADMA in hypertensive adolescents.
24.	Li et al. (2019) ³²	Silencing salusin β ameliorates heart failure in aged spontaneously hypertensive rats by ROS-related MAPK/NF- κ B pathways in the paraventricular nucleus	rats	Aging hypertensive rats with heart failure have massively increased salusin β expression. The knockdown of salusin β improves cardiac and vascular functions; there is no result in rats without hypertension. Silencing of salusin β reduces paraventricular nucleus proinflammatory cytokines and ROS levels in aging hypertensive rats with heart failure.	Central salusin β knockdown deteriorates cardiac and vascular functions in ageing hypertensive rats with heart failure via a ROS-related pathway in the hypothalamic PVN.
25.	Alpsoy et al. (2021) ²⁹	Assessment of salusin alpha and salusin beta levels in patients with newly diagnosed dipper and non-dipper hypertension	88 patients	Salusin β levels are higher in patients with non-dipper hypertension.	Increased salusin β may be a predictor of non-dipper hypertension and a poor cardiovascular prognosis.
26.	Pan et al. (2021) ²⁶	Improvement of vascular function by knockdown of salusin- β in hypertensive rats via nitric oxide and reactive oxygen species signaling pathway	rats	Silencing of salusin β enhances vascular relaxation and remodeling, decreases blood pressure and vasoconstriction in hypertension by the activation of eNOS, the release of NO, and the inhibition of NAD(P)H oxidase and ROS.	The knockdown of salusin β improves vascular functions and prevents vasculopathy in hypertension.

Table 1. Summary of the studies on salusin β included in the review – cont.

No.	Author, year of publication	Title	Subject	Results	Conclusions
27.	Sun et al. (2021) ²⁷	A <i>TOR2A</i> gene product: Salusin- β contributes to attenuated vasodilatation of spontaneously hypertensive rats	rats	The intravenous administration of salusin β and anti-salusin β IgG in hypertensive rats has an impact on blood pressure, heart rate and basal vascular tone. The administration of salusin β decreases eNOS activity and NO levels and increases NAD(P)H oxidase activity in hypertensive rats, while anti-salusin β has a reverse impact.	The overexpression of salusin β plays a role in impaired vasodilatation in hypertension by activating NAD(P)H oxidase and inhibiting NO release.
28.	Zhang et al. (2022) ³⁰	Efficacy of felodipine and enalapril in the treatment of essential hypertension with coronary artery disease and the effect on levels of salusin- β , apelin, and <i>PON1</i> gene expression in patients	110 patients with essential hypertension and CAD	Better effectiveness and lower levels of salusin β were observed in patients who were administered felodipine and enalapril than in patients who were administered felodipine alone.	Combination of felodipine and enalapril is more effective in treatment of hypertension with CAD. It decreases the level of salusin β .
Obesity/lipid disorders					
29.	Derviřođlu et al. (2019) ³⁴	Salusin- α levels are negatively correlated with diastolic blood pressure in children with obesity	75 obese children, 101 healthy children	No significant correlation between salusin β and heart rate, SBP, DBP, BMI, carotid intima-media thickness, epicardial adipose tissue thickness, and left ventricular mass index was found; there was a negative correlation between salusin α and DBP.	Salusin α seems to be an earlier predictor of cardiovascular disorders than salusin β in obesity.
30.	Nazari et al. (2020) ³⁶	Effects of two types of moderate- and high-intensity interval training on serum salusin- α and salusin- β levels and lipid profile in women with overweight/obesity	80 women divided in 2 groups according to the type of training, 40 women – control group	Both types of training improved the lipid profile and increased salusin β levels, but in moderate interval training, the changes were more significant.	Moderate intensity interval training is more effective in improving the lipid profile than HIIT.
31.	Stefanowicz-Bielska et al. (2020) ³⁵	Obesity and overweight and accompanying metabolic disorders occur in children with Down syndrome	48 patients with DS (26 girls and 22 boys), aged from 7 to 18 years, divided into 2 groups – 39 with normal weight or underweight and 9 obese or overweight	Higher values of HDL cholesterol were found in patients with normal body mass and underweight than in patients with obesity and overweight ($p = 0.009$). Higher values of uric acid were found in the group of patients with obesity and overweight than in the normal mass and underweight group ($p = 0.012$). The children who are physically active have normal body weight ($p = 0.039$). There was no significant difference in salusin β levels between both groups.	The role of salusin β as an early indicator of metabolic disorders in children with DS was not demonstrated.
32.	Paahoo et al. (2020) ³⁸	Effect of two chronic exercise protocols on pre-atherosclerotic and anti-atherosclerotic biomarkers levels in obese and overweight children	30 obese and overweight boys divided into 2 groups according to the type of training, 15 boys – control group	A significant increase of serum levels of salusin α and NO, and a decrease of serum levels of salusin β , body weight, BMI, and TG/HDL ratio in both training groups, but more significant after HIIT.	Both HIIT and continuous aerobic training have positive impact on cardiometabolic parameters, but HIIT seems to be more effective.
33.	Paahoo et al. (2021) ³⁷	Effectiveness of continuous aerobic versus high-intensity interval training on atherosclerotic and inflammatory markers in boys with overweight/obesity	30 boys divided into 2 groups according to the type of training, 15 boys – control group	Both types of training improved the lipid profile, increased the levels of inflammatory factors and salusin β and increased the salusin ratio; in HIIT, the changes were more significant.	HIIT is more effective in improving the lipid profile and inflammatory factors than aerobic training in obese boys.

T2DM – type 2 diabetes mellitus; eNOS – endothelial nitric oxide synthase; ROS – reactive oxygen species; NAD(P)H – nicotinamide adenine dinucleotide phosphate; CAD – coronary artery disease; CSF – coronary slow flow; PPAR γ – peroxisome proliferator-activated receptor γ ; AMPK – adenosine monophosphate-activated protein kinase; HUVECs – human umbilical vein endothelial cells; VSMCs – vascular smooth muscle cells; HRECs – human retinal capillary endothelial cells; DFI – diabetic foot infections; ADMA – asymmetric dimethylarginine; PVN – paraventricular nucleus; AAA – abdominal aortic aneurysm; DS – Down syndrome; IL – interleukin; BMI – body mass index; hsCRP – high-sensitivity C-reactive protein; LVEF – left ventricular ejection fraction; CAE – coronary artery ectasia; ROS – reactive oxygen species; HbA1c – hemoglobin A1c; IgG – immunoglobulin G; HDL – high-density lipoprotein; TG – triglycerides; HIIT – high-intensity interval training; SBP – systolic blood pressure; DBP – diastolic blood pressure; CVD – cardiovascular disease.

Discussion

Our research encompassed 12 articles based on studies performed on animals or cell culture systems and 21 articles concerning humans; 15 of these included healthy controls, and only 5 articles involved children. Four studies enrolled more than 100 patients, and 11 enrolled more than 50 patients. Therefore, most studies were based on relatively small study groups, which hampers a definitive evaluation. Nonetheless, most of the studies confirmed the thesis that salusin β has a relevant function in atherosclerotic development, and is correlated with components of the metabolic syndrome. Furthermore, Genç Elden et al. demonstrated an association between sudden hearing loss, atherosclerosis and salusin β , and all groups presenting with similar atherosclerotic parameters. The collected material confirmed that salusin β is a prognostic factor in hearing loss. However, the results of the above study did not indicate sufficient evidence for the development of atherosclerosis in the study group, and hence it was not included in the review.³⁹

The analyzed data indicate that there is much that remains to be discovered about salusin β . Preprosalusin mRNA is ubiquitously expressed, being found in many tissues and organs, such as the nervous system, endothelium, muscles, liver, lungs, kidneys, bone marrow, lymph nodes, spleen, thymus, adrenal glands, small intestine, stomach, salivary glands, and testes, as well as in fluids, such as plasma and urine. A significant number of recent studies on salusin β have concentrated on its role in biochemical pathways in hypertension, atherosclerosis, hyperglycemia, and obesity. Currently available data indicate that salusin β could be used in diagnostics of developing atherosclerosis and hypertension, and appears to be a promising novel target for treatment.

Studies performed on animal models provide important knowledge but in a narrow range. Nevertheless, they indicate that salusin β could be a direct target in the treatment of hypertension and heart failure, or an indicator of treatment efficacy. Initial attempts have already been made to use these findings in clinical practice. One promising study on the evaluation of the treatment of hypertension with 110 patients provides interesting and valuable results.³⁰

Recent studies do not directly confirm the connection between elevated levels of salusin β and obesity. However, physical activity in overweight or obese patients brings about a reduction of salusin β and improvement of both lipid profile and inflammatory factors. These data suggest that salusin β could be valuable in the treatment of obesity.

Cohort studies are necessary to confirm the scope and bring us closer to the practical application of salusin β .

Limitations

This review has some limitations. The available literature on salusin β is quite limited and based on a variety of methods, which hinders a systematic review.



The division of included papers into sections was based on the main topics of the studies and seemed to be artificial, as each study contained multiple components and had a high degree of overlap. The aim of this classification was to organize the data. Moreover, research conducted in humans is generally based on small groups of patients.

Conclusions

Recent studies confirm that salusin β plays an important role in the development of vascular remodeling, inflammation, hypertension, and atherosclerosis. Additionally, the peptide is related to hyperglycemia and lipid disorders. The widespread activity of salusin β makes it a potential therapeutic target. However, there is a need for additional studies to confirm the potential role of salusin β as a novel target for treatment.

While it could be useful in the prophylaxis or the treatment of the abovementioned disorders, many reports have been performed in animal models, and those conducted in humans are based on small groups of patients and are not always compared with healthy controls. Studies enrolling children are rare. There is a lack of studies conducted in humans confirming the thesis that salusin β is a good predictor of atherosclerosis and metabolic syndrome, hence further investigations are necessary.

ORCID iDs

Aleksandra Janecka  <https://orcid.org/0000-0002-0276-5301>
 Joanna Stefanowicz  <https://orcid.org/0000-0001-8014-4263>

References

- Shichiri M, Ishimaru S, Ota T, Nishikawa T, Isogai T, Hirata Y. Salusins: Newly identified bioactive peptides with hemodynamic and mitogenic activities. *Nat Med*. 2003;9(9):1166–1172. doi:10.1038/nm913
- Xu Y, Pan Y, Wang X, et al. Knockdown of salusin- β improves cardiovascular function in myocardial infarction-induced chronic heart failure rats. *Oxid Med Cell Longev*. 2021;2021:8896226. doi:10.1155/2021/8896226
- Sun HJ, Zhao MX, Liu TY, et al. Salusin- β induces foam cell formation and monocyte adhesion in human vascular smooth muscle cells via miR155/NOX2/NF κ B pathway. *Sci Rep*. 2016;6(1):23596. doi:10.1038/srep23596
- Wang Y, Wang S, Zhang J, et al. Salusin- β is superior to salusin- α as a marker for evaluating coronary atherosclerosis. *J Int Med Res*. 2020;48(2):30006052090386. doi:10.1177/0300060520903868
- Watanabe T, Sato K, Itoh F, et al. The roles of salusins in atherosclerosis and related cardiovascular diseases. *J Am Soc Hypertens*. 2011;5(5):359–365. doi:10.1016/j.jash.2011.06.003
- Wu LL, Bo JH, Zheng F, et al. Salusin- β in intermediate dorsal motor nucleus of the vagus regulates sympathetic-parasympathetic balance and blood pressure. *Biomedicines*. 2021;9(9):1118. doi:10.3390/biomedicines9091118
- Zhu X, Zhou Y, Cai W, Sun H, Qiu L. Salusin- β mediates high glucose-induced endothelial injury via disruption of AMPK signaling pathway. *Biochem Biophys Res Commun*. 2017;491(2):515–521. doi:10.1016/j.bbrc.2017.06.126
- Fujimoto K, Hayashi A, Kamata Y, et al. Circulating levels of human salusin- β , a potent hemodynamic and atherogenesis regulator. *PLoS One*. 2013;8(10):e76714. doi:10.1371/journal.pone.0076714
- Zhao MX, Zhou B, Ling L, et al. Salusin- β contributes to oxidative stress and inflammation in diabetic cardiomyopathy. *Cell Death Dis*. 2017;8(3):e2690. doi:10.1038/cddis.2017.106

10. Esfahani M, Saidijam M, Najafi R, Goodarzi MT, Movahedian A. The effect of salusin- β on expression of pro- and anti-inflammatory cytokines in human umbilical vein endothelial cells (HUVECs). *ARYA Atheroscler*. 2018;14(1):1–10. doi:10.22122/arya.v14i1.1602
11. Awad A, Ali H, Al-Rufaie M. Assessment of serum levels of salusin α and salusin β in cardiovascular disease patients undergoing transcatheter therapy. *Indian J Med Forensic Med Toxicol*. 2020;14(2):303–308. doi:10.37506/ijfmt.v14i2.2807
12. Yildirim A, Kucukosmanoglu M. Relationship between serum salusin beta levels and coronary artery ectasia. *Acta Cardiol Sin*. 2021;37(2):130–137. doi:10.6515/ACS.202103_37(2).20200910A
13. Arkan A, Atukeren P, Ikitimur B, et al. The importance of circulating levels of salusin- α , salusin- β , and heregulin- β 1 in atherosclerotic coronary arterial disease. *Clin Biochem*. 2021;87:19–25. doi:10.1016/j.clinbiochem.2020.10.003
14. Akyüz A, Aydın F, Alpsoy Ş, Gur DO, Guzel S. Relationship of serum salusin beta levels with coronary slow flow. *Anatol J Cardiol*. 2019;22(4):177–184. doi:10.14744/AnatolJCardiol.2019.43247
15. Karagöz A, Kurt D, Günaydin ZY, et al. A new insight into pathophysiological mechanism of abdominal aortic aneurysm with novel parameters salusin- β and arterial stiffness. *Tex Heart Inst J*. 2022;49(6):e217561. doi:10.14503/THIJ-21-7561
16. Wang H, Zhang M, Zhou H, et al. Salusin- β mediates high glucose-induced inflammation and apoptosis in retinal capillary endothelial cells via a ros-dependent pathway in diabetic retinopathy. *Diabetes Metab Syndr Obes*. 2021;14:2291–2308. doi:10.2147/DMSO.S301157
17. Chen H, Jin G. Downregulation of salusin- β protects renal tubular epithelial cells against high glucose-induced inflammation, oxidative stress, apoptosis and lipid accumulation via suppressing miR-155-5p. *Bioengineered*. 2021;12(1):6155–6165. doi:10.1080/21655979.2021.1972900
18. Wang WJ, Jiang X, Gao CC, Chen ZW. Salusin- β participates in high glucose-induced HK-2 cell ferroptosis in a *Nrf-2*-dependent manner. *Mol Med Rep*. 2021;24(3):674. doi:10.3892/mmr.2021.12313
19. Sun HJ, Chen D, Wang PY, et al. Salusin- β is involved in diabetes mellitus-induced endothelial dysfunction via degradation of peroxisome proliferator-activated receptor gamma. *Oxid Med Cell Longev*. 2017;2017:6905217. doi:10.1155/2017/6905217
20. Argun D, Argun F, Borku Uysal B. Evaluation of salusin- α and salusin- β levels in patients with type 2 diabetes mellitus and determination of the impact of severity of hyperglycemia on salusin levels. *Ir J Med Sci*. 2021;190(4):1403–1411. doi:10.1007/s11845-021-02674-4
21. Deyekh S, Hamzah M, Ateaai J. Evaluation of salusin β in patients with prediabetes and type 2 diabetes mellitus *Medico Legal Update*. 2020;20(1):651–654. doi:10.37506/mlu.v20i1.438
22. Aldulimya BHA, Alaaraji SFT. Study the association of β -salusin with some anthropometric measurements in Iraqi type II diabetics women. *Egypt J Chem*. 2021;64(11):6515–6522. doi:10.21608/ejchem.2021.78221.3830
23. Yassien M, Fawzy O, Mahmoud E, Khidir EG. Serum salusin- β in relation to atherosclerosis and ventricular dysfunction in patients with type 2 diabetes mellitus. *Diabetes Metab Syndr*. 2020;14(6):2057–2062. doi:10.1016/j.dsx.2020.10.025
24. Sipahi S, Genc A, Acikgoz S, et al. Relationship of salusin-alpha and salusin-beta levels with atherosclerosis in patients undergoing haemodialysis. *Singapore Med J*. 2019;60(4):210–215. doi:10.11622/smedj.2018123
25. Sağmak Tartar A, Uğur K, Tuncer Kara K, Akbulut A, Demirdağ K, Aydın S. Association between dermcidin, salusin- α , salusin- β molecules and diabetic foot infections. *Int J Low Extrem Wounds*. 2021;153473462110655. doi:10.1177/15347346211065527
26. Pan Y, Sun S, Wang X, et al. Improvement of vascular function by knockdown of salusin- β in hypertensive rats via nitric oxide and reactive oxygen species signaling pathway. *Front Physiol*. 2021;12:622954. doi:10.3389/fphys.2021.622954
27. Sun S, Zhang F, Pan Y, et al. A *TOR2A* gene product: Salusin- β contributes to attenuated vasodilatation of spontaneously hypertensive rats. *Cardiovasc Drugs Ther*. 2021;35(1):125–139. doi:10.1007/s10557-020-06983-1
28. Ren XS, Ling L, Zhou B, et al. Silencing salusin- β attenuates cardiovascular remodeling and hypertension in spontaneously hypertensive rats. *Sci Rep*. 2017;7(1):43259. doi:10.1038/srep43259
29. Alpsoy S, Dogan B, Ozkaramanli Gur D, et al. Assessment of salusin alpha and salusin beta levels in patients with newly diagnosed dipper and non-dipper hypertension. *Clin Exp Hypertens*. 2021;43(1):42–48. doi:10.1080/10641963.2020.1797086
30. Zhang W, Zhang J, Jin F, Zhou H. Efficacy of felodipine and enalapril in the treatment of essential hypertension with coronary artery disease and the effect on levels of salusin- β , apelin, and *PON1* gene expression in patients. *Cell Mol Biol (Noisy-le-grand)*. 2022;67(6):174–180. doi:10.14715/cmb/2021.67.6.24
31. Kolańska U, Kuroczycka-Saniutycz E, Olański W, Wasilewska A. Correlation of salusin beta with hs-CRP and ADMA in hypertensive children and adolescents. *Curr Pharm Des*. 2018;24(30):3551–3557. doi:10.2174/1381612824666180607124531
32. Li HB, Yu XJ, Bai J, et al. Silencing salusin β ameliorates heart failure in aged spontaneously hypertensive rats by ROS-relative MAPK/NF- κ B pathways in the paraventricular nucleus. *Int J Cardiol*. 2019;280:142–151. doi:10.1016/j.ijcard.2018.12.020
33. Sun H, Zhang F, Xu Y, et al. Salusin- β promotes vascular calcification via nicotinamide adenine dinucleotide phosphate/reactive oxygen species-mediated Klotho downregulation. *Antioxid Redox Signal*. 2019;31(18):1352–1370. doi:10.1089/ars.2019.7723
34. Dervişoğlu P, Elmas B, Kösecik M, İşgüven ŞP, Büyükcavı M, Köroğlu M. Salusin- α levels are negatively correlated with diastolic blood pressure in children with obesity. *Cardiol Young*. 2019;29(10):1225–1229. doi:10.1017/S1047951119001173
35. Stefanowicz-Bielska A, Wierzba J, Stefanowicz J, Owczarzak A, Chamienia A. Obesity and overweight and accompanying metabolic disorders occur in children with Down syndrome. *Acta Med*. 2020;36(4):2473–2479. doi:10.19193/0393-6384_2020_4_384
36. Nazari M, Minasian V, Hovsepian S. Effects of two types of moderate- and high-intensity interval training on serum salusin- α and salusin- β levels and lipid profile in women with overweight/obesity. *Diabetes Metab Syndr Obes*. 2020;13:1385–1390. doi:10.2147/DMSO.S248476
37. Paahoo A, Tadibi V, Behpoor N. Effectiveness of continuous aerobic versus high-intensity interval training on atherosclerotic and inflammatory markers in boys with overweight/obesity. *Pediatr Exerc Sci*. 2021;33(3):132–138. doi:10.1123/pes.2020-0138
38. Paahoo A, Tadibi V, Behpoor N. Effect of two chronic exercise protocols on pre-atherosclerotic and anti-atherosclerotic biomarkers levels in obese and overweight children. *Iran J Pediatr*. 2020;30(2):e99760. doi:10.5812/ijp.99760
39. Genç Elden S, Yılmaz MS, Altındış M, Köroğlu M, Elden H. The role of serum salusin alpha and beta levels and atherosclerotic risk factors in idiopathic sudden hearing loss pathogenesis. *Eur Arch Otorhinolaryngol*. 2022;279(3):1311–1316. doi:10.1007/s00405-021-06804-7